

4 Physical site conditions and data collection



1

2

3

4

5

6

7

8

9

10

CHAPTER 4 CONTENTS

4.1 Bathymetry and morphology	306
4.1.1 General	306
4.1.1.1 Definitions	306
4.1.1.2 Interaction between morphology and bathymetry	307
4.1.2 Bathymetry and morphology related to marine structures	309
4.1.2.1 Introduction	309
4.1.2.2 Sandwaves	310
4.1.2.3 Muddy shorelines: mudflats and saltmarshes	310
4.1.2.4 Beaches	311
4.1.2.5 Coastal dunes	312
4.1.2.6 Cliff and shore platforms	313
4.1.3 Bathymetry and morphology of rivers and estuaries	314
4.1.3.1 General points	314
4.1.3.2 Types of estuary	314
4.1.3.3 Types of river	315
4.1.3.4 Regime theory for rivers	318
4.2 Hydraulic boundary conditions and data collection – marine and coastal waters	319
4.2.1 Wind and pressure conditions	320
4.2.1.1 Use of wind data	320
4.2.1.2 Use of atmospheric pressure data	322
4.2.2 Marine water levels	323
4.2.2.1 Mean sea level	324
4.2.2.2 Tide	324
4.2.2.3 Storm surges	326
4.2.2.4 Wind set-up	326
4.2.2.5 Wave set-up	327
4.2.2.6 Seiches	330
4.2.2.7 Long-period waves	331
4.2.2.8 Tsunamis	332
4.2.2.9 Flood waves	333
4.2.2.10 Sea level rise resulting from climate change	334
4.2.2.11 Sources of water level data	335
4.2.2.12 Design extreme water levels	336
4.2.3 Marine and estuarine currents	340
4.2.3.1 General	340
4.2.3.2 Components of marine and estuarine currents	340
4.2.3.3 Estuarine flow conditions, including basin model and density currents	342
4.2.3.4 Numerical modelling of marine and estuarine currents	346
4.2.4 Wind-sea and swell	347
4.2.4.1 General definitions related to waves, sea-states and wave climate ..	347
4.2.4.2 Representation of regular/random and long-crested/short-crested waves	349
4.2.4.3 Characterisation of wave conditions and wave kinematics	351

4.2.4.4	Statistical properties and distribution of waves in a sea-state	354
4.2.4.5	Spectral description of waves and wave spectra	360
4.2.4.6	Generation of waves in the ocean and on inland waters.	367
4.2.4.7	Transformation of waves in the nearshore and coastal zones.	374
4.2.4.8	Short-term or daily wave climate	385
4.2.4.9	Long-term wave climate – analysis of extreme waves	387
4.2.4.10	Numerical and physical modelling of wave conditions	393
4.2.5	Joint probability of waves and water levels	397
4.2.5.1	Introduction	397
4.2.5.2	The independent and dependent cases.	399
4.2.5.3	Desk study methods of analysis	399
4.2.5.4	Other methods of analysis	402
4.2.5.5	Design with joint waves and water levels.	404
4.3	Hydraulic boundary conditions and data collection – inland waters	405
4.3.1	Hydraulic parameters	405
4.3.1.1	River geometry	405
4.3.1.2	Hydraulic data	406
4.3.2	River discharges and currents	409
4.3.2.1	General	409
4.3.2.2	Hydrology and design discharges	410
4.3.2.3	River discharge and velocity.	412
4.3.2.4	Structure of currents	419
4.3.2.5	Turbulence	425
4.3.2.6	Bed shear stress	426
4.3.2.7	River confluences and bifurcations	428
4.3.3	Flood waves	429
4.3.3.1	General	429
4.3.3.2	Hydrographs (duration/exceedance and rating curves) and stage relationships	429
4.3.3.3	Flood waves and translation waves	431
4.3.4	Ship-induced waves and water movements	434
4.3.4.1	Return current, water level depression, front and stern waves	436
4.3.4.2	Secondary ship waves	440
4.3.4.3	Propeller jet velocities.	440
4.3.5	Modelling of water levels and currents	443
4.3.5.1	Modelling	443
4.3.5.2	Numerical modelling of water levels and currents	443
4.3.5.3	Physical modelling of water levels and currents	446
4.3.5.4	Hybrid modelling of water levels and currents.	448
4.4	Geotechnical investigations and data collection	448
4.4.1	Objectives of geotechnical investigations	449
4.4.2	Procedures for geotechnical investigations	449
4.4.2.1	Preliminary geotechnical investigations.	450
4.4.2.2	Geotechnical investigations for design.	450
4.4.2.3	Controlling and monitoring	451

4.4.3	Key elements of geotechnical investigations.	452
4.4.3.1	Desk studies	452
4.4.3.2	Ground investigations.	452
4.4.3.3	Site visit	458
4.4.3.4	Specific issues related to structure types	458
4.4.3.5	Investigation techniques and equipment.	460
4.4.3.6	Interpretation of results	460
4.4.3.7	Ground investigation report	460
4.4.4	References and standards	460
4.5	Ice conditions	464
4.5.1	Introduction	464
4.5.2	Ice growth	464
4.5.3	Ice formations	464
4.5.4	Typical winter ice action	466
4.5.5	Data collection	467
4.6	References	468

4 Physical site conditions and data collection

Chapter 4 explains how to derive hydraulic and geotechnical **design input conditions** and how to undertake **data collection**.

Key inputs from other chapters

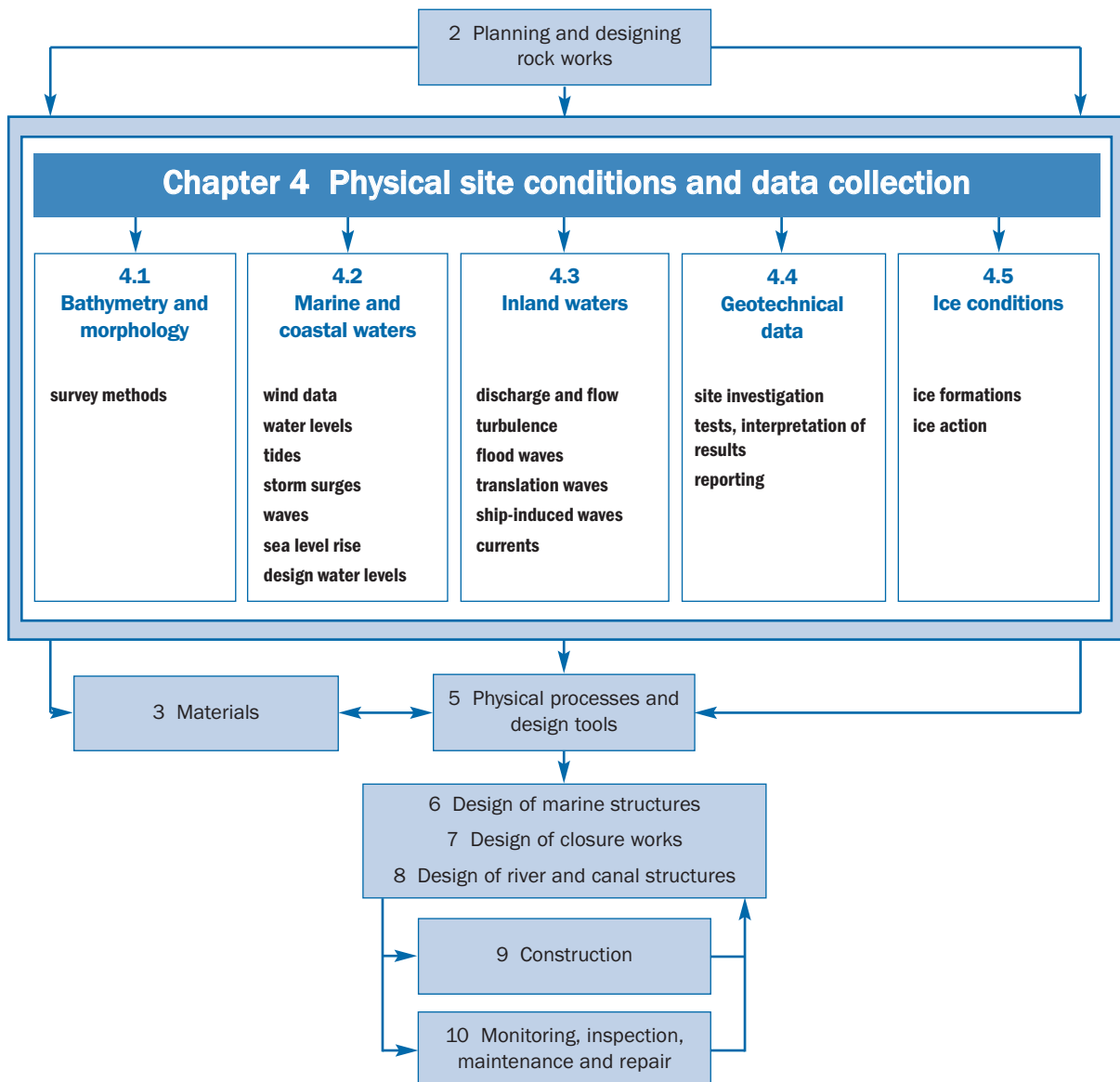
- Chapter 2 ⇨ **project requirements**
- Chapter 3 ⇨ **material properties**.

Key outputs to other chapters

- hydraulic and geotechnical **input conditions** ⇨ Chapter 5
- **physical site conditions** for construction ⇨ Chapter 9
- **physical site conditions** for monitoring ⇨ Chapter 10.

NOTE: The project process is **iterative**. The reader should **revisit Chapter 2** throughout the project life cycle for a reminder of important issues.

This flow chart shows where to find information in the chapter and how it links to other chapters. Use it in combination with the contents page and the index to navigate the manual.



4.1 BATHYMETRY AND MORPHOLOGY

4.1.1 General

4.1.1.1 Definitions

Topography is the description of the geometrical characteristics of the ground surface above water. Three methods are commonly used.

- 1 **Conventional levelling.**
- 2 **Photogrammetry.** In this technique aerial photographs are analysed and the geometry of objects in the photographs is quantified relative to a fixed co-ordinate system. It can normally only be applied to a portion of the ground or a structure visible above the waterline. To maximise the benefits, aerial surveys can be conducted when the water level is low. Conventional levelling checks have suggested that the resolution of photogrammetry is better than ± 90 mm. The initial costs of a photogrammetric survey of an area or a structure can be high relative to a conventional survey, but it may be more economical if several zones are flown together.
- 3 **3D laser scanning.** Laser scanning allows rapid acquisition of 3D data (10 000 points per second) at a relatively high density (approximately 0.1 m point spacing and better). The speed of data acquisition is particularly useful, as the working window within the intertidal zone is relatively limited. The scanner may also be able to provide high-definition digital photographs of the site. Fixed markers, linked to a GPS control network, provide control of the scan. With further filtering and processing of the registered point cloud data, digital terrain models (DTMs) of the structure and profiles can be generated. An additional method of presenting and analysing the data involves combining the 3D scan data with the 2D photography to generate rectified orthophotography.

A wide range of techniques are available, but detailed discussion of this subject is beyond the scope of the manual.

Topographical data are necessary for design and construction. In addition, repeat surveys can be used to inform maintenance requirements (see Section 10.3.4).

Bathymetry is the description of the ground surface below water. It is a major boundary condition for geometric and structural design of rock structures and has a significant influence on the volume of dredging, the volume of rock needed and on the hydraulic loadings. At coastal sites, for example, the water depth can limit wave heights. On charts for navigation purposes the seabed level is defined in relation to the Chart Datum, commonly taken to be the Lowest Astronomical Tide level (LAT) at the site.

The bathymetry of a zone is normally determined by means of a boat equipped with an acoustic sounder, which may be either single-beam (point-by-point process) or multi-beam (profile-by-profile process). A description of bathymetric survey techniques is given in Section 10.3.5.

Bathymetric data comprise series of points, each determined with three co-ordinates: horizontal (x, y) and vertical (z).

Surveying is generally conducted from a boat except in the intertidal and shallow-water zones, where topographical methods may be used. Four parameters are sought:

- the horizontal location (X, Y) of the boat, which is generally obtained by conventional topographic equipment such as differential global positioning system (DGPS), laser and optics

- the water depth (d), measured by the sounder
- the vertical location (Z) of the level of water, which is obtained by standard topographic equipment (such as DGPS, laser or optics), by tide measurement or by referenced scales.

Nowadays, data are digital and particular attention should be paid to the density and spacing of survey lines. They should be sufficiently close to give a fair representation of the bed features and level without excessive cost. Check lines should be run, at right angles to the main survey lines, to highlight any survey errors. Careful quality control of data and daily calibration of equipment are essential.

Morphology is the description of sedimentation and erosion processes occurring at the bed.

Erosion and deposition may cause the bathymetry to change with time. These changes can create difficulties when attempting to determine the bathymetry for design or construction purposes. The rate of morphological change of the bed depends on the rate of sediment transport. High transport rates generally result in relatively rapid changes of the bed. However, these morphological changes are very slow compared with changes in the hydraulic boundary conditions and, except for local scour near structures, may occur over several years or even decades.

The presence of very soft sediments and/or layers of high concentrations of suspended sediments (fluid mud, clay) can cause additional survey problems. Indeed, these softer materials make it difficult to obtain accurate bathymetric measurements because a large part of the signal emitted and reflected is scattered.

Structures covered in this manual generally require data about bathymetry and morphology for their design and construction. For example, the construction of a closure dam, river control works or river-training structures requires overall data about bathymetry and morphology of the estuary or river as well as local data for the construction site. The data should provide information about short-term (eg seasonal) fluctuations and long-term changes and influences. The quantification of these fluctuations will require data from several surveys conducted over an appropriate period of time. Typical seasonal features are:

- monsoons and storms in a marine environment, including estuaries
- flood and dry season for rivers.

4.1.1.2 ***Interaction between morphology and bathymetry***

Morphological and bathymetric studies should include expected long-term changes of the bed level such as those associated with structures along the coast or in an estuary or a river. Local data are required at the construction site itself as well as from the surrounding area. These local data should be more detailed than the overall data. The bed level, for example, should be known with sufficient accuracy before construction can start. Nevertheless, during construction further bathymetric and topographic survey may be necessary to assess modifications to local bathymetry. The interactions between overall and local bathymetry, morphology and hydraulic conditions at a site are shown in Figure 4.1.

The data needed ought to be available from existing maps and charts. Surveys undertaken for the project can provide specific sounding data. Historical records or data collected in earlier surveys may also be used, but their reliability should first be critically examined. Satellite images are another possible source of information. They can be very useful for mapping purposes, for example in identifying the former course of a river or dune frontage, which can give an invaluable insight into the area's morphology.

Special emphasis should be given to morphological data. The characteristics of the sediment need to be studied, as do the type(s) of sediment transport. Samples of the bed material

should be taken to provide data about the size distribution. It is important to take samples at several locations, since the particle size of the bed material may vary considerably from place to place. The bed samples should also help in establishing whether the bed material is cohesive. Cohesion depends on the amount of fine particles, particularly clay, and increases resistance to erosion.

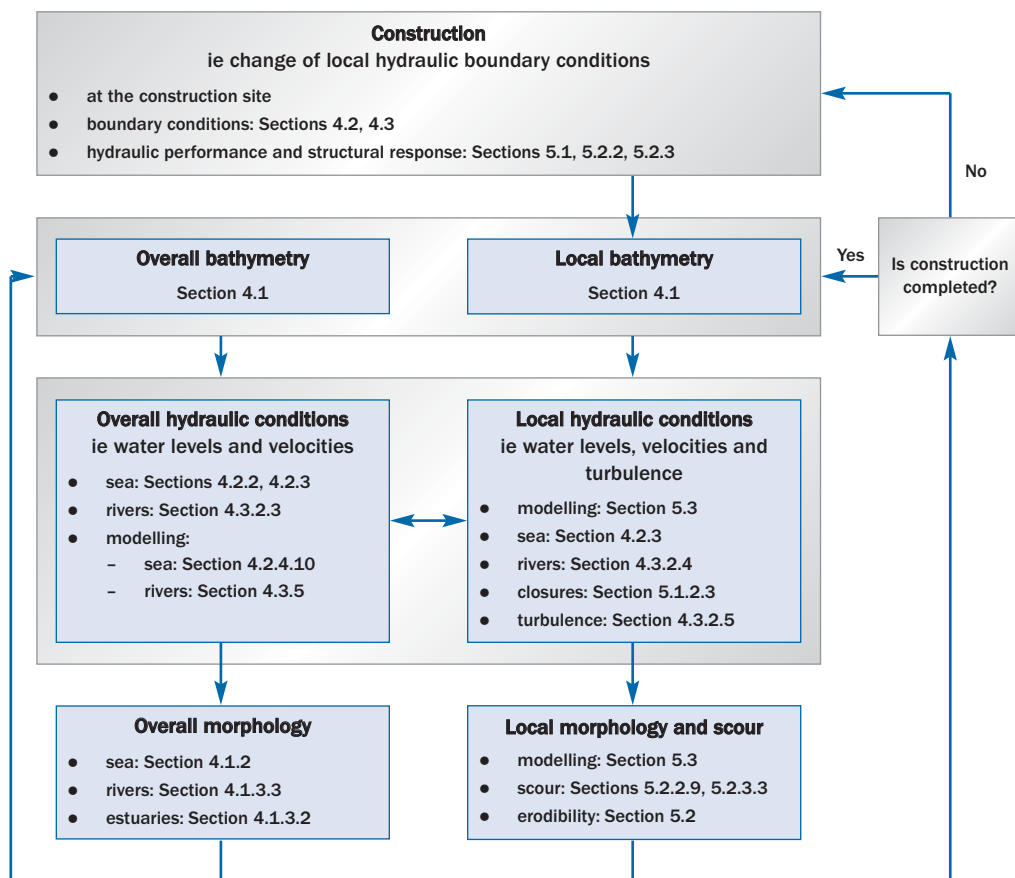


Figure 4.1 Interactions between morphology and bathymetry with reference to hydraulic conditions and construction

Sediment transport can take place as a bedload, suspended load or both. The type of sediment transport depends on the size of the bed material and the flow conditions. In general, coarse material such as gravel and coarse sand is transported as bedload, whereas fine material such as fine sand and silt is transported as suspended load. To predict the morphological behaviour of the sea bed, river bed and riverbanks, it is necessary to collect data about:

- types of sediments, ie fine or coarse, cohesive or not
- amount and type(s) of sediment transport, ie suspended or bedload transport or both
- bed-level changes
- erodibility of bed and bank material.

In general, the balance between erosion and deposition of bed material and the balance between entrainment and sedimentation of suspended sediment determine the expected morphological development. Such development can take place naturally, but it may also be due to discharge during dredging activities. A simple rule to assess the outcome of this balance and the expected depth-averaged velocities may be used. The graph presented by Hjulström (1935) (see Figure 4.2) distinguishes erosion and sedimentation based on thresholds applied to the average flow velocity. This approach gives only limited results, however, and further reference should be sought when appropriate in Sections 5.2 and 5.3.

In addition to morphological characteristics, it is necessary to determine river discharges and velocities and/or wave climate. Together with morphological data, they control bathymetry changes. Reference to the wave climate for marine structures is made in Section 4.2. Discharges and associated water levels for rivers or dams, stage-discharge curves and stage-duration curves for rivers are discussed in Section 4.3 and may need interpretation within the context of the hydrology of the catchment area of the river. Morphological, bathymetric and flow field data should be collected at an early stage of a project and should be surveyed during construction. Especially for the design of toe structures and bed protection, the joint probability of overall morphological changes and local scour may have to be evaluated (see Sections 5.2.2.9 and 5.2.3.3). In addition, a proper morphological analysis usually requires a high level of experience and expertise.

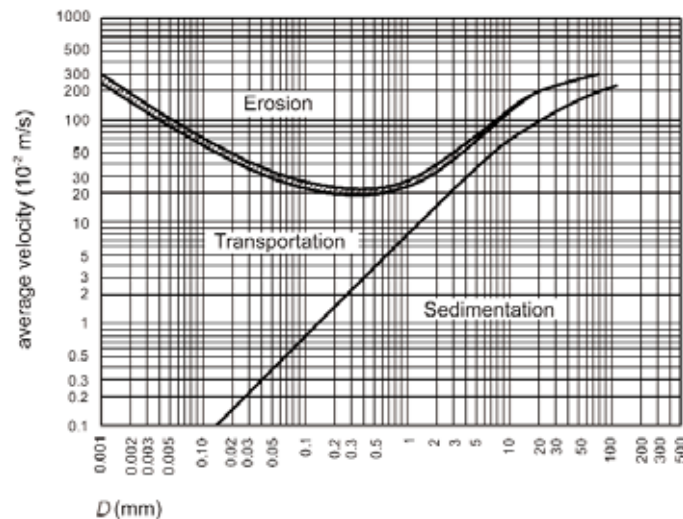


Figure 4.2 Velocity chart as a preliminary decision tool for erosion or sedimentation (Hjulström, 1935)

4.1.2 Bathymetry and morphology related to marine structures

4.1.2.1 Introduction

Knowledge of seabed bathymetry and its morphology at the structure site is fundamental to the design of coastal and shoreline structures, for example regarding wave heights limited by water depth (see Section 4.2.4.7). In many cases knowledge of morphological changes of the bed with time are as critical as the mean bed level to the design, since the lowest bed level in front of a structure is determined for use in the design. Thus, where a sea bed is either in dynamic equilibrium or is morphologically unstable, it is essential to determine the range of bed level changes that should be allowed for in the design.

The stability of the shoreline and its adjoining hinterland depends on the physical character of the shoreline, which, in turn, is determined by its geology, its geomorphology and the actions of winds, waves and tides. The assessment of the various types of physical shoreline is therefore a key issue for effective planning of rock structures.

The geomorphology has a major effect on the project planning and should be characterised with regards to the loading forces and materials. Essential information required includes:

- for **loading forces**: the marine forces factors such as wind, waves, tides, sea-level change and wave- or tide-generated currents characterised by their intensity, direction and variability with time
- for **materials**: the coastal zone geology for both the nearshore, inshore and onshore parts, including rock and softer sediments, its topography and its bathymetry, the type of mud, sand, gravel or carbonate and the distribution of mobile and non-mobile sediments.

The interaction of material and loading forces at the land-sea interface is important. This includes the type of processes, ie erosion or sediment transport or deposition, and their spatial and temporal changes. Additionally, possible structure-related local scour should be considered (see Section 5.2.2.9).

The coast morphology and bathymetry are controlled by the balance between the aggressiveness of the sea and the resistance of the land. They change over time: build-up takes place where sediment accumulates; the coastline moves landward where areas are eroded and sediment is removed offshore or alongshore. The morphology of a coast changes if the applied forces and energies change. The forces are induced by waves, tides, winds, currents and surges. Their impact on the landform depends on the type, magnitude and direction of the forces in combination with the materials strength. If the applied forces result in a change to the shape, to the composition of a landform or both, then a new relationship develops between the forces and the new landform. This relationship continues to evolve until a new dynamic equilibrium is reached. Sediment transport causes morphological changes and maintains this balance between landform and hydrodynamic forces. Typical seasonal morphological changes in a marine environment, including estuaries, are related to monsoons, typhoons or both in tropical regions and other seasonal storms in high latitudes. For example, erosion and build-up of beach alternate during winter and summer respectively in Europe.

If no data on bed levels are available at all, a first indication of the impact of variability can be obtained by comparing assumed depth velocities (current or orbital), wave characteristics (height and period) or both with threshold values for the initiation of sediment transport (Shields, 1936; Komar and Miller, 1974). Appropriate models should be used for sediment transport for currents or wave actions and known or predicted values of currents or waves may be used (see also Sections 5.2, 5.3 and 6.3). The prevailing local current, wave and sediment conditions may lead to bed variations exhibiting typical mean dimensions and time-scales. To collect representative data on bed changes, measurements should cover at least one sandwave length per section. In case of repeated measurements at one single position, a minimum sampling frequency of twice the typical frequency of the natural changes of the sea bed should be chosen.

4.1.2.2 Sandwaves

The sea bed exhibits a variety of bed patterns, like ripples, mega-ripples, sandwaves and tidal sand banks. The most changing of these bed patterns are sandwaves.

Sandwaves can be described as elongated depositional bedforms with an undulating surface. The dominant current direction defines the sandwave orientation on the sea bed. The crest of the sandwave is orientated almost perpendicular to the dominant current direction. In general the height of sandwaves varies from 1 m to 10 m and their wavelength varies from 100 m to 1000 m. Sandwaves are present in large parts of the southern North Sea, with lengths in the order of 100 m and heights about 10 m, and related sandwave return periods of 1–10 or even 100 years (Van den Brink, 1998). The movement of a sandwave along the sea bed can vary from a few metres to more than 20 m a year. Progressing mudwaves observed along the coast of Guyana also exhibit long-periodic morphological changes.

Where sandwaves may occur, the bathymetry of the site area should always be surveyed to determine existence of sandwaves and to estimate their height. Attention should be paid to sandwave movements when designing a structure in their vicinity (see Section 6.4.3.3).

4.1.2.3 Muddy shorelines: mudflats and saltmarshes

Muddy shorelines occur along the upper levels of the intertidal zone of estuaries, tidal embayments and on open, barrier coasts. In these locations, the tidal current velocities are

too low to resuspend completely the mud that settles during the time of slack high water. Consequently, the net accretion is observed to form intertidal mudflats and saltmarshes.

There is a great diversity in the morphology of mudflats that relates to the changing balance of physical, sedimentological and biological forces on the sediment. In general terms, the width of a mudflat is greater in areas of high tidal range than in areas of small tidal range. However, considerable deviations exist which indicate that there are additional control phenomena. Mudflats are exposed to cycles of erosion and deposition. It is generally considered that mudflats under erosion have a low and concave upward profile while mudflats under deposition have a high and convex upward profile. Modification of the mudflat profile causes change in the exposure to wave attack, altering the rates of erosion and deposition, possibly leading gradually to a new equilibrium.

As the upper mudflats build higher through vertical accretion of sediment, the number and duration of tidal inundations decreases. There is therefore a critical height at which the mudflat is out of the water long enough for vegetation to establish. The elevation at which vegetation can colonise a mudflat mostly depends on the availability of plant species able to withstand this environment. These plants help to reduce flow, encouraging further deposition of mud. Once a saltmarsh has become established, biological activity, sedimentation and geomorphological phenomena depend on the pattern and extent of tidal inundation at that level. Neap tides merely enter and are confined to the creeks, leaving the saltmarsh dry, whereas spring tides generally rise above the creek banks, drowning the saltmarsh for a period.

Higher intertidal mudflats and saltmarshes are generically linked. They have complex and interrelated physical and biological controls. Three broad categories of muddy shoreline morphology can be distinguished:

- a smoothly sloping surface on which there is a gradual upward and landward appearance of vegetation. Such shorelines are generally in accretion, growing seaward as well as building vertically
- a cliffed saltmarsh with an edge indicative of erosion
- a ramp of moderate slope angle, carved transversely into finger-like spurs and narrow, wave-scoured furrows. This shoreline denotes a regime of net erosion, perhaps less severe than the saltmarsh cliff coast, and it may represent a transitional stage between slope and cliff.

4.1.2.4 Beaches

A beach is an accumulation of loose sediment. Its shape changes in response to changes in wave energy. The mobility of its sediments therefore allows a beach to maintain itself in a state of dynamic equilibrium with its environment. Beaches behave differently according to their sediment size and can be subdivided into *sand*, *shingle*, *mixed* (ie poorly sorted mixture of sand and gravel) and *composite* beaches (ie a sandy lower foreshore with a shingle-dominant upper foreshore and backshore with relatively little mixing between the two). The dynamics and transports of beach materials are not covered in this manual and details can be found in the *Beach management manual* (Simm *et al*, 1996).

Although beaches are three-dimensional features, the analysis of their morphology can be conveniently broken down into the study of cross-shore profile and longshore profile.

Cross-shore profile

Even though a wide variety of troughs and ridges may be present on the beach profile, the most important morphological feature is the average slope between seaward and landward limits. The backshores of steep beaches usually display a flat-topped ridge or bar known as

the berm that forms at the limit of wave swash. The removal of the berm and the deposition of a longshore bar beneath the breaker zone marks the transition from a steep beach profile to a shallow beach profile.

When a wave breaks at the shore, sediment is pushed up the beach face by the swash and dragged back down by the backwash. Because of water percolation into the beach, the backwash tends to be weaker than the swash. Consequently, there is a net onshore movement of sediment up the beach. The rate of percolation is mainly controlled by the mean sediment size and the beach porosity or the size sorting of the beach sediment. Water percolates much more easily into a shingle beach than into a fine sandy beach, and the backwash intensity is therefore greatly reduced, setting up an onshore movement of sediment, which steepens the beach.

Small waves tend to build up beaches whereas storm waves tend to lower and flatten them. The main factor is the steepness of incident waves, which controls the shoaling, the transformation of shape profile (eg asymmetry) and the wave breaking processes in shallow water (see Section 4.2). When a steep wave breaks on to the beach, its energy is dissipated over a relatively narrow area and the swash does not move far up the beach. Thus there is less opportunity for percolation to occur and less energy is lost in moving sediment up the beach face. Consequently, the backwash is strong and significant amounts of sediment can be moved seawards to build a longshore bar. When a less steep wave (ie collapsing or surging) approaches the foreshore, significant movement of water takes place up the beach face, as the wave front either collapses or surges up the beach. In this case the swash is strong and less sediment is moved up the beach face to form a berm.

Longshore profile

The large-scale longshore shape of beaches can be divided into:

- beaches that are attached to the shoreline, ie pocket beaches
- beaches that are detached from the shoreline, such as spits, barrier islands, tombolos.

The most basic coastal configuration is an indented coast with bays and headlands. Refraction means that wave attack concentrates wave energy on the headlands and reduces wave energy in the bays, which may lead to headland erosion and bay deposition. This process continues until the coast consists of a series of smooth curved beaches, reaching the ultimate stage of wave-dominated coastal development.

For coastlines that turn abruptly landward, such as a bay or a valley opening on to a coast, a finger-like extension of the beach, also called a *spit*, may appear across the indentation. Generally spits are connected to the beach end by a narrow neck and are fed by sand eroded from further up the coast and provided by the longshore transport. Spits are usually linear features widening at their distal (outer) end, but their form depends on the physical processes such as longshore transport and supply of sediment.

An island situated immediately offshore has a significant effect on the wave conditions at the beach. Sediment is swept into the sheltered area behind the island, which can either form a salient in the beach plan shape or it can allow a neck of sediment, called a tombolo, to deposit, which then connects the island to the beach.

4.1.2.5

Coastal dunes

Coastal dunes form where there is a sufficient supply of dry sand and sufficient wind to move it. Dune systems are usually fronted by sand beaches that function in close relation with the dunes. They undergo periods of growth and erosion, both of which contribute to their dynamic evolution.

Deposition processes

Coastal dunes accumulate sand blown inland from beaches by onshore winds. The basic requirements for the formation of coastal dunes are:

- a plentiful supply of sand over a wide drying foreshore
- a backshore area of low relief
- predominant onshore winds capable of entraining sediment
- presence of vegetation as a dune-form fixer.

An ideal condition for the transport of sand from a beach to the dunes is after waves have deposited sand on the upper part of the beach and on the intertidal foreshore. At low tide the sand dries and onshore winds can carry substantial volumes of sand on to the dunes. Dunes usually begin to form at the crest of a beach where wind-blown sand accumulates around small objects or debris cast up on the strandline. After the dunes have started to form, embryonic dunes are low hills of loose sand that are colonised by pioneer plants, which both increase the resistance of the surface layer of sand to wind erosion and reduce wind speeds over the surface. These embryonic dunes may keep growing in both height and width to form a dune ridge parallel to the coastline or foredune. Embryonic dunes are highly unstable depending on the wave and wind energies they are exposed to. They may resist wave action when they reach a position on the beach that corresponds to the Mean High Water Spring Level (MHWS).

Erosion processes

Dune erosion is governed by two processes:

- surface erosion by wind action or deflation
- marine erosion of the toe and seaward face of the dunes.

Deflation is a vertical wind-driven erosion resulting in a lowering of the dune crest or blow-outs on dune sides. If the vegetation is seriously damaged, it no longer stabilises the sand; and wind action then rapidly removes the exposed loose sand, forming a blow-out.

Marine erosion of the dune may occur when the fronting beach is lowered as a result of wave action. This allows the high tide to reach the toe of the dunes. Waves can then directly attack the dune toe, causing removal of the sand and undercutting of the dune face. The front face of the dune collapses on to the beach and the sand is carried away down to the beach. As a consequence, the front face of the dune retreats, leaving a steep unvegetated surface and the beach receives an additional volume of sand. Hence, the dunes act as a temporary reservoir of sand, accumulating it during mild weather, typically during the summer, and releasing it back to the beach during storms.

4.1.2.6**Cliffs and shore platforms**

Cliffed coasts are defined as high and steep-faced coasts, consisting of consolidated or unconsolidated materials from granites to softer glacial till. In areas of low sediment supply, a shore platform commonly fronts the cliff. Shore platforms are near horizontal and similar in composition to the lower layers of the cliff.

Cliff erosion processes

Landsliding is a primary cause of cliff erosion. Cliff recession is defined as the onshore movement of the cliff and is controlled by wave attack at the cliff toe that may induce landslide. Wave action on cliffs has two effects:

- direct undercutting and erosion of the face that is related to the onshore wave energy
- removal of debris that is related to the longshore wave energy.

Shore platform erosion processes

Shore platform lowering is a three-stage process involving detachment of particles of material, transport of this material away from the foreshore and its deposition elsewhere. The global process depends on the aggressiveness of the environment and the erodability of the platform materials. Both weathering and marine processes contribute to the erosion of shore platforms. Weathering processes can directly break up cohesive material or weaken material that is more easily eroded by marine processes.

4.1.3 Bathymetry and morphology of rivers and estuaries

4.1.3.1 General points

The construction of a closure dam or river control and training structures requires morphological data covering a large area upstream and downstream of the project. Other hydraulic data such as water levels, flow velocities, sediment transport etc have to be collected.

Typical seasonal effects are storm surges (especially in estuaries), flood waves and low river discharge. They are reasonably predictable when attributed to characteristic local precipitation patterns such as monsoons. The corresponding variations in river discharge and sediment transport may cause variations in local bed levels of channels or shoals. Seasonal variations may also be of particular importance for the planning of construction. Some recommendations for the collection of morphological data are presented in Box 4.1.

Box 4.1 Recommendations for morphological data collection for rivers and estuaries

- bed geometry in the entire estuary: cross-sections every 1–5 km for general survey and cross-sections every 10–1000 m for detailed survey
- bed geometry in a river: cross-sections every 5–10 km along the entire river for general survey and cross-section every 10–1000 m for detailed survey, which should be adapted to the length of the river
- measurements should be carried out at different times of year to determine significant differences in bathymetry for various conditions
- the sediment transport in rivers should be measured at one or more locations during low and high river discharges to enable the relationship between water discharge and sediment transport to be determined. This can be used for selecting the appropriate model and equation for sediment transport prediction
- transported sediment should be sampled to determine its characteristics
- sediment transport in an estuary is difficult to measure. Because tide, waves and differences of water density cause quite rapid changes in transport, extensive measurement campaigns are needed
- along a river, bed material sampling should be done every 5–10 km. The bed should be sampled in at least three positions over each cross-section
- in an estuary, bed material should be sampled according to a survey that has a grid of between 1 km × 1 km and 5 km × 5 km, which should be adapted to the width of the estuary.

4.1.3.2 Types of estuary

An estuary is a complex system of channels, shoals and flats. The tidal flow is concentrated in the channels, whereas the shoals and flats mainly serve for water storage. The channels run more or less in the longitudinal direction of the estuary with their cross-sectional area decreasing with the distance from the sea because of the reduction of the tidal discharge. If an estuary is fed by more than one channel, secondary connection channels may exist, especially where there are phase differences among the various channels. The sediment may have different origins, incorporating either marine or riverine material. The tidal motion also produces a complex pattern of sediment transport. It results in local erosion or areas of

sedimentation, causing continuous migration of channels and shoals that are observed in almost all existing estuaries with movable beds.

Section 4.2.3 shows how the hydraulic response characteristics of estuaries can be calculated. Three types of estuaries are distinguished:

- short estuary with respect to the length of the tidal wave
- long estuary with respect to the length of the tidal wave
- tidal river.

As the flow is essentially concentrated in the channels, construction of dams on the shoals and flats hardly affects the tidal motion. The descriptors used for the river geometry may also be used for estuaries (see Section 4.1.3.3).

4.1.3.3

Types of river

General

Mobile river beds can change rapidly and may display significant variations, sometimes after only a single flood. Their geometry tends to adapt to hydraulic loadings, which in turn also change. Four main types of river bed can be distinguished (see Figure 4.3): straight, meandering, braided and interlaced or anastomosed rivers. The classification of river types is based on the shape of the channel pattern (Leopold and Wolman, 1957).

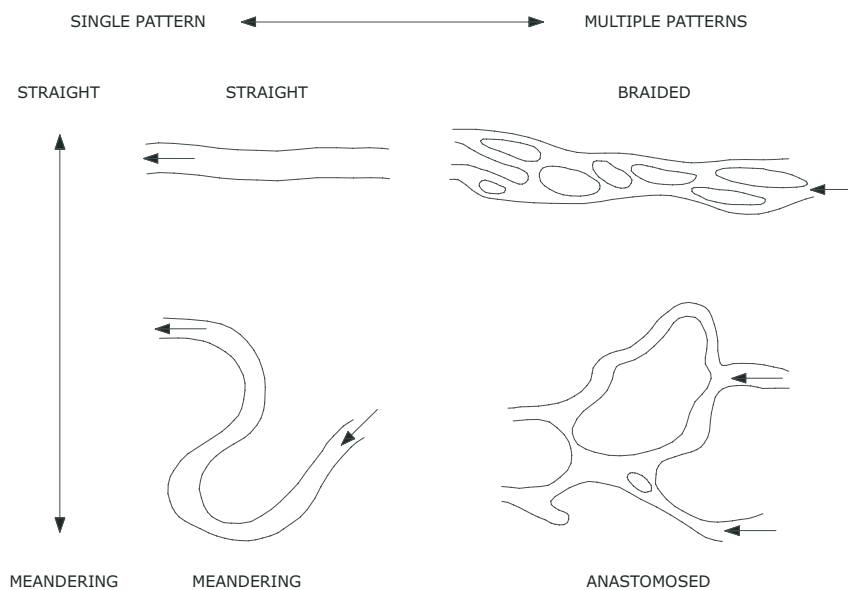


Figure 4.3 Classification of river types using criteria of sinuosity and number of patterns (after Rust, 1978)

Meandering (see Figure 4.4) and braided rivers (see Figure 4.3) can be observed in the middle and lower reaches of the river. The sediment regime is dominated by settlement and floodplains are common. In the higher reaches, erosion takes place and the river flows with steep gradients in a relatively narrow bed. The bed, as well as the banks, consist of rock. The following parameters are generally used to characterise the river shape:

λ = wavelength (m)

L = length of the thalweg (see Section 4.3.2.4 for the definition of thalweg) between two inflection points (see Figure 4.4) going in the same direction (m)

B = width of the open channel (m)

I_s = sinuosity index defined as L/λ (-).

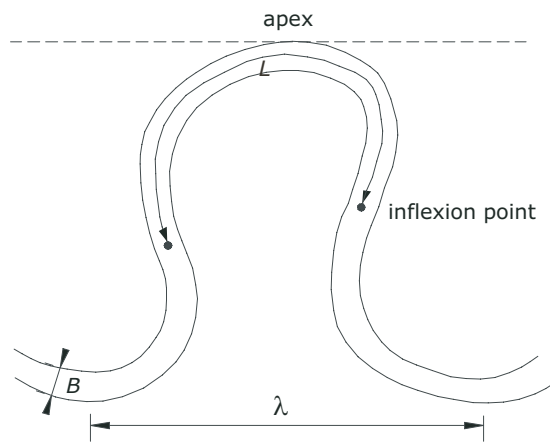


Figure 4.4 Typical shape parameters of a meandering river (after Bravard and Petit, 2000)

Two essential parameters of a river, referred to as *external parameters* or *independent parameters*, are the discharge Q (m³/s) and the bedload. Other controlling variables of the river are:

- the slope of the valley, which governs the energy of the river
- the grain size of its bed and banks as well as the vegetation of the riverbanks, both of which influence the lateral movement.

For a catchment area, these parameters are specifically governed by climate (rain, temperature), geology (topography, lithology), ground characteristics and vegetation. The use of the land for human activities is a factor that may have an impact on the river morphology.

Dependent parameters, also called *degrees of freedom*, adjust themselves to the variations of the independent parameters described above. They are shown in Figures 4.4 and 4.54 and consist of:

- channel width, B (m)
- main channel average water depth, h (m)
- bed slope, i_b (m/m)
- wavelength of the river bends, λ (m)
- sinuosity index, I_s (-)
- current velocity, U (m/s)
- maximum water depth, \hat{h} (m).

Any variation of the bedload or the discharge affects the longitudinal profile, the cross-section profile and the alignment of the river. Consequently, the design of a project in a river should maintain the fluvial continuum of the river and its equilibrium relations (see Section 4.1.3.4).

Determination of the type of the channel pattern

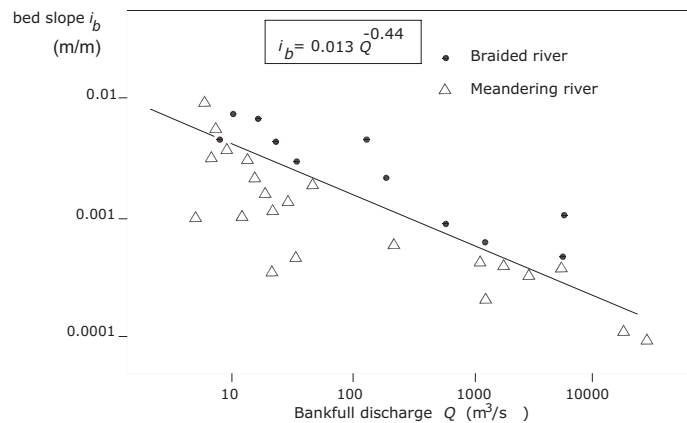
The type of a river can first be determined by examining topographic charts (scale 1:25 000) and aerial photographs. Comparison of charts from different periods will show the river's evolution over time. Sinuosity, number of channels and position of the banks should be studied over the entire longitudinal profile of a river to identify changes in the river type and to correlate them with slope or sudden bed level changes.

Brice (1964) and later Morisawa (1985) propose the use of morphology, sinuosity, type of sediment transport and the width/depth ratio to characterise the different river types. The width to depth ratio depends on the bed material. A similar geomorphological approach is also valid for floodplains. Table 4.1 summarises some characteristics of the four types of river.

Table 4.1 Classification of channel patterns (adapted from Morisawa, 1985)

Type of river	Characteristic aspects			
	Morphology	Sinuosity, I_s	Load type	Width/depth, B/h
Straight	Single channel with pool and riffles, meandering thalweg	< 1.05	Suspension mixed or bedload	< 40
Meandering	Single channel	> 1.5	Suspension mixed load	< 4
Braided	Two or more channels with bars and islands	< 1.3	Bedload	> 40
Anastomosed	Two or more channels with bars and islands	> 1.5	-	-

To distinguish between meandering and braided rivers, many definitions were suggested. Leopold and Wolman (1957) (see Figure 4.5), Ackers and Charlton (1970), Ackers (1982) proposed relationships between the bed longitudinal slope i_b and the discharge Q . This discharge corresponds either to the bankfull discharge or to the dominant formative discharge. The bankfull discharge is the discharge with the highest value of h before flows inundate the floodplain and the dominant formative discharge is the equivalent permanent flow that would create the actual river.

**Figure 4.5** Distinction between braided and meandering rivers (after Leopold and Wolman, 1957)

Alternatively, Richards (1982) distinguishes meandering from braided rivers by considering the stream power index Ω (m^3/s) defined by $\Omega = Q \cdot i_b$, with Q (m^3/s) = bankfull discharge and i_b (m/m) = channel bed slope. The threshold value Ω_{lim} is obtained by Equation 4.1. A braided river has a stream power index higher than Ω_{lim} . By contrast, a meandering river has a stream power index smaller than Ω_{lim} :

$$\Omega_{lim} = 0.011 D_{50}^{0.77} \quad (4.1)$$

where Ω_{lim} = threshold of stream power index (m^3/s), D_{50} = median sieve diameter of the bed material (m).

The unit stream power ω (W/m^2) is defined by $\omega = \rho_w g \Omega / B$ (Van den Berg, 1995). It can be used to distinguish straight rivers from braided rivers. The threshold ω_0 is given by Equation 4.2. Straight rivers have a unit stream power greater than the threshold value ω_0 , whereas braided rivers have a unit stream power smaller than ω_0 :

$$\omega_0 = 900 D_{50}^{0.42} \quad (4.2)$$

where ω_0 = threshold of unit stream power index (W/m^2), D_{50} = median sieve diameter of the bed material (m).

According to Brookes (1988), for values of the threshold ω_0 greater than $35 \text{ W}/\text{m}^2$, rivers tend to readjust their external parameters (discharge and bedload) as a result of anthropic or natural modifications.

However, all these methods are based on empirical data. River hydraulics manuals (eg Jansen, 1979; Bravard and Petit, 2000) can provide further information on, for example, particular characteristics of the river types, such as meander lengths and sinuosity.

4.1.3.4 Regime theory for rivers

The need for design guidelines for stable irrigation canals in the Indian subcontinent led to the formulation of regime theory. Subsequently, the derived relationships were also used for other rivers. However, the empirical equations are strongly related to local circumstances and are not generally applicable to all situations. The various relationships enable a prediction of the width, water depth, flow velocity, hydraulic radius, hydraulic perimeter and bed gradient from overall hydraulic parameters. Regime equations have been derived for many areas in the world, among others by Lacey (1930), Simons and Albertson (1960) and Henderson (1966).

Regime theory is the classic procedure for the design of stable channels when sediment transport occurs. Its physical basis and historic development have been described in some detail in several publications on fluvial hydraulics (eg Chang, 1988; Yalin, 1992). Many authors have studied the topic and proposed equations – see Lacey (1930), Mahmood and Shen (1971), Simons and Albertson (1960), Chitale (1966) and Mahmood (1974).

The regime equations are supported by *regime theories* and, in this respect, the following definition of a river or flow regime seems to apply. A *river regime* is the range of river discharges, corresponding water levels and their respective (yearly or seasonally) averaged values and characteristic fluctuations around these values. Regime theories may be applied even if very little information on a river is available. It is recommended that the selected regime equations be calibrated using reliable local data. Most of the regime equations relate cross-sectional and longitudinal parameters to the discharge.

Many empirical formulae provide the width of the river B according to various morphological flows, which may be defined as equivalent permanent flows that would create the actual river morphology. These flows have a return period lower or equal to two years and are called *morphologically dominant formative flow regimes*. However, whatever the flow taken into account, the wavelength of the river bends λ (see also Figure 4.4) varies schematically according to the square root of the discharge (Dury, 1955, 1976; Carlston, 1965; Ackers and Charlton, 1970; Schumm, 1963, 1968, 1977). The bankfull discharge proves to be the best approach to characterise geometry and evolution of meandering rivers.

Lacey's regime equations (see Equations 4.3 to 4.8) are applied most widely to alluvial river channels and man-made canals with a low sediment transport, ie for sediment concentration of 100–2000 mg/l and grain size of bed material of 0.1–0.5 mm.

$$P = 4.87 Q^{1/2} \quad (4.3)$$

$$A_c = 2.38 Q^{5/6} / f^{1/3} \quad (4.4)$$

$$R = 0.47 Q^{1/3} / f^{1/3} \quad (4.5)$$

$$U = 0.64 R^{1/2} f^{1/2} \quad (4.6)$$

$$i_b = 0.00030 f^{5/3} / Q^{1/6} \quad (4.7)$$

$$f = 1.59 D_{50}^{1/2} \quad (4.8)$$

where:

P	= wetted perimeter (m)	i_b	= average gradient of bed slope (-)
A_c	= cross-sectional area (m ²)	Q	= discharge (m ³ /s)
R	= hydraulic radius (m), $R = A_c/P$	f	= Lacey's silt factor (-)
U	= average flow velocity (m/s)	D_{50}	= median diameter of bed material (mm)

Suggested values for the Lacey’s silt factor, f (-), are given in Table 4.2.

Table 4.2 Lacey’s silt factor, f

Sediment	Silt	Sand	Gravel	Stones
Lacey’s silt factor, f	0.3–1.0	1.3–1.5	2.0–4.5	6.0–40

Lacey’s equations do not distinguish between bed and bank material. Simons and Albertson (1960) extended the equations to include the effect of the soil properties of the banks. Regime equations have also been developed for rivers with gravel beds. Hey and Heritage (1988) give a summary. Further details on these equations and other regime theories are given in Henderson (1966).

4.2 HYDRAULIC BOUNDARY CONDITIONS AND DATA COLLECTION – MARINE AND COASTAL WATERS

The principal relationships between the relevant hydraulic boundary conditions are shown in the diagram of Figure 4.6. The diagram also indicates relevant design parameters that should be determined.

Marine boundary conditions are caused either by meteorological forcing (eg wind, waves, storm surges) or by astronomical forcing (tides), or by seismic effects (tsunamis). Consequently, the mechanisms generating them are different, which should be considered when combinations of conditions are examined.

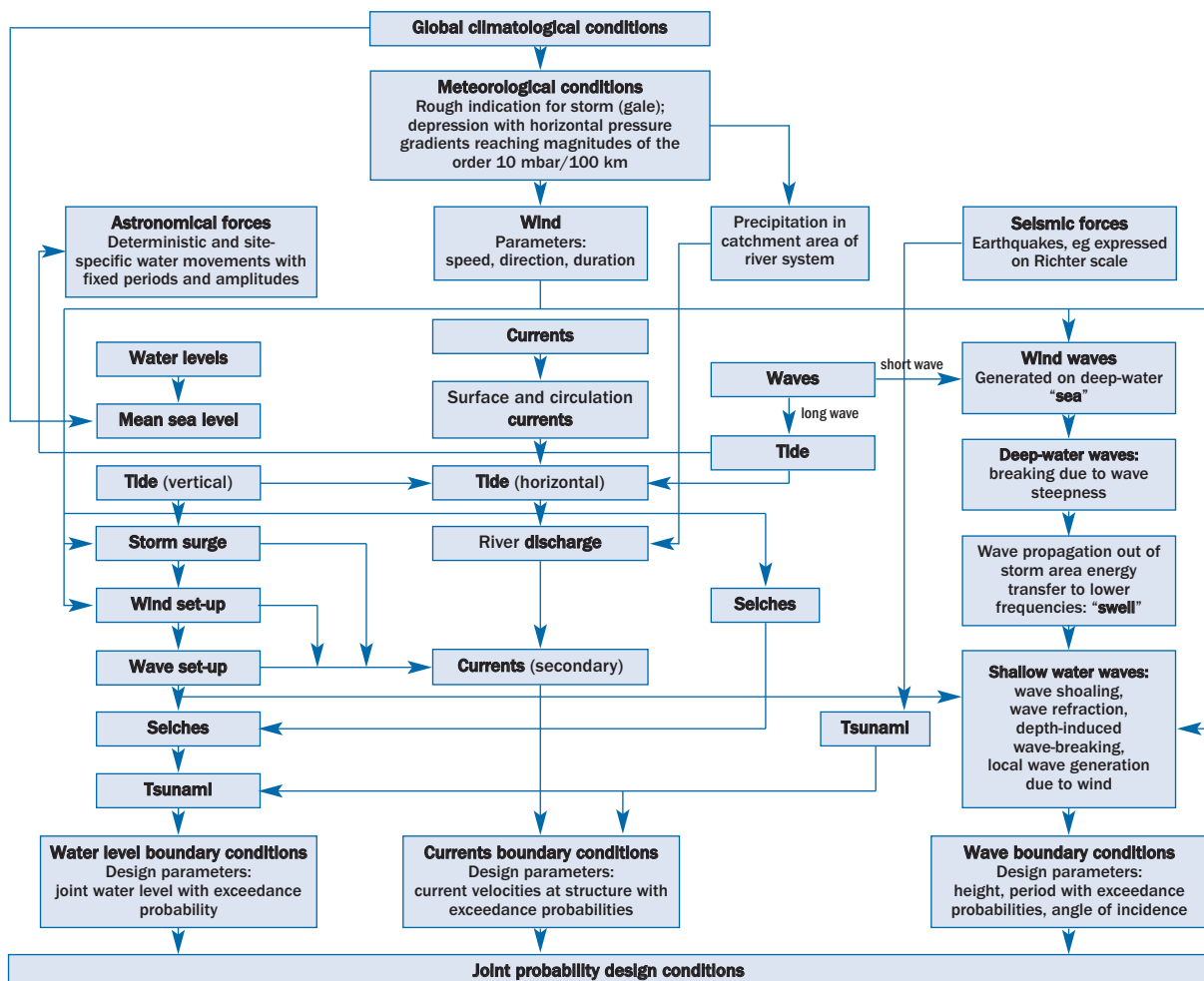


Figure 4.6 Hydraulic boundary conditions for marine and coastal waters

Combinations of two or more parameters together often determine the design loading of a structure. In these cases not only do the separate design values have to be known but also any combined design loading associated with the chosen probability of exceedance. The most elegant way, but often impractical, is to use joint probability analysis to find the probability that any combination exceeds a target design level.

Examples of combined loading include:

- water level and wave conditions, which determine the required crest level of a seawall
- current and orbital velocities, which determine the stone weight of a scour protection.

Joint probabilities of such combinations are discussed further in Section 4.2.5.

4.2.1 Wind and pressure conditions

4.2.1.1 Use of wind data

Wind is the underlying cause of most sources of coastal flood risk, but wind data are rarely used as direct input to the design of coastal structures. Wind is directly relevant when determining safe operating limits for marine construction and access to areas exposed to severe overtopping, but it is most commonly used as input to prediction models of waves (see Section 4.2.4.6) or of wind set-up and of storm surge (see Sections 4.2.2.3 and 4.2.2.4).

Where wave data are not available, or for some reason are not adequate for the intended purpose, hindcasting from wind records may be the only way to estimate the wave climate. Around most of the European coast, sequential wind records in digital format have been available from meteorological institutes since 1970. It should be noted that on-land records may easily show a 10–20 per cent reduction in wind speeds attributable to increased surface roughness compared with values measured over water. As a result, land-based wind speeds may need to be corrected (ie increased) before use in wave or storm surge models.

Other adjustments may be necessary before using wind data in numerical models, including:

- standardisation of the wind speed at 10 m above sea surface
- use of the international metric system (speeds expressed in m/s)
- selection of wind data, ie duration of 10 minutes as a minimum (peak wind velocities should not be used)
- proper consideration of stable or unstable stratification of the atmosphere at the interface with the ocean. Data obtained in unstable conditions will have to be corrected if formulae or models based on neutral air-sea interface conditions have to be employed.

Wind velocities over water are available from ships' observations or from the archives of weather models. In both cases, individual records may be unreliable but the large volume of data makes them a good source of site-specific ocean wind climate data.

Wind climate data can be conveniently depicted as a wind rose (see Figure 4.7) or summarised as a scatter table of wind speeds against directions (see Figure 4.8). Typically, wind speeds are divided into Beaufort speed ranges and 30° direction sectors.

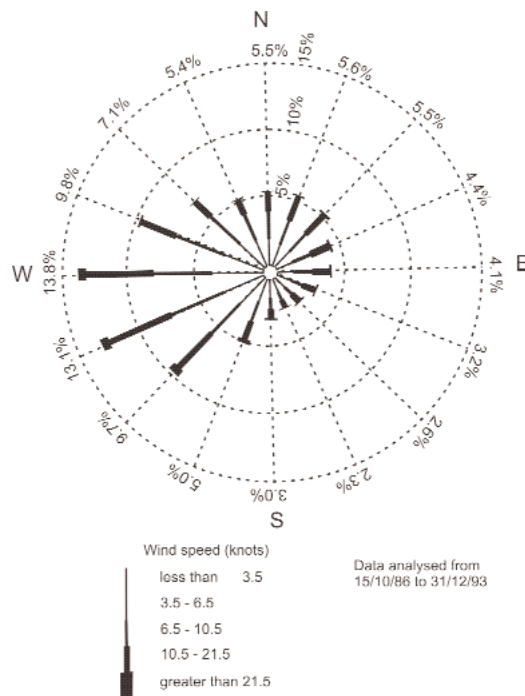


Figure 4.7 Typical wind rose

Mean wind speed		Fraction of time (%) with wind speeds from												
Knots	m/s	350°-010°	020°-040°	050°-070°	080°-100°	110°-130°	140°-160°	170°-190°	200°-220°	230°-250°	260°-280°	290°-310°	320°-340°	All directions Total
DECEMBER														
Calm														2.5
1-3	0.52-1.55													9.7
4-6	2.06-3.09	0.4	0.7	1.2	2.6	3.2	1.4	1.6	1.3	0.5	0.4	0.7	0.9	14.9
7-10	3.61-5.15	0.2	0.9	1.2	1.6	2.5	2.6	3.1	2.5	2.1	1.1	1.8	0.9	20.5
11-16	5.67-8.24	0.1	0.8	1.6	1.5	2.5	2.1	4.3	4.0	5.4	3.7	2.4	0.6	29.0
17-21	8.76-10.82	0.1	0.2	0.3	0.6	1.3	0.5	1.1	1.9	2.6	2.5	0.9	0.2	12.2
22-27	11.33-13.91	0+	0+	0.2	0.4	0.7	0.2	0.2	1.1	2.0	1.9	0.5	0.2	7.4
28-33	14.42-17.00				0.1	0.1			0.1	0.3	0.6	0.1	0+	1.3
34-40	17.51-20.60								0+	0+	0.1	0.1	0+	0.2
41-47	21.12-24.21										0+			0+
48-55	24.72-28.33													
56-63	28.84-32.45													
> 63	> 32.45													
Total		0.8	2.6	4.5	6.8	10.3	6.8	10.3	10.9	12.9	10.3	6.5	2.8	97.7
Fraction of time (%) missed														2.3
YEAR														
Calm														6.1
1-3	0.52-1.55													17.2
4-6	2.06-3.09	0.6	1.2	1.7	2.0	2.3	1.6	1.5	1.4	1.9	2.0	1.7	1.3	19.2
7-10	3.61-5.15	0.4	1.3	2.1	1.8	1.9	1.9	2.5	2.5	3.6	2.9	2.8	1.4	25.1
11-16	5.67-8.24	0.2	0.7	1.7	1.3	1.2	1.4	2.6	2.6	3.7	2.9	2.5	0.8	21.6
17-21	8.76-10.82	0+	0.1	0.4	0.4	0.4	0.3	0.7	0.8	1.1	1.1	0.6	0.1	6.0
22-27	11.33-13.91	0+	0+	0.1	0.2	0.1	0.1	0.1	0.3	0.6	0.5	0.2	0.1	2.3
28-33	14.42-17.00				0+	0+	0+	0+	0+	0.1	0.1	0+	0+	0.2
34-40	17.51-20.60						0+	0+	0+	0+	0+	0+	0+	0+
41-47	21.12-24.21									0+	0+			0+
48-55	24.72-28.33													
56-63	28.84-32.45													
> 63	> 32.45													
Total		1.2	3.3	6.0	5.7	5.9	5.3	7.4	7.6	11.0	9.5	7.8	3.7	97.7
Fraction of time (%) missed														2.3

Figure 4.8 Example of wind speed/direction scatter table

The parameters needed for the simple conversion of stationary wind condition into an equivalent wave condition are the wind speed, the wind direction, the wind duration and the stability of the air-sea interface. In practice, the wind speed and direction vary over a period of 10–20 hours long and average values should be computed. Any direct information on wind duration or persistence that may be available from the original records is lost when the data are summarised in scatter diagram or rose format.

Wind data can be prepared for use in wave prediction after three main types of treatment.

- 1 **Fit to a standard distribution of wind speeds.** A standard probability function, for example the Weibull distribution, can be fitted to the hourly wind speeds either within one direction sector or overall. It is often preferable to retain for this analysis only those values that exceed a predefined threshold for wind speed and to use the POT (peaks over threshold) method presented in Section 4.2.4.9. The fitted distribution can then be extrapolated to hourly extreme values. The hourly values can then be converted to equivalent speeds for different durations, as necessary, using the speed conversion factors listed in Table 4.3. This method is appropriate for design wind conditions but not for prediction of overall wind climate.
- 2 **Scatter diagram of wind speed and direction.** Wind information in scatter diagram or wind rose format can be broken down into percentages of data within certain classes of speed and direction (see Figure 4.8). To be conservative, a long duration can be assigned to each category of data. In effect, the wave predictions are **fetch-limited**. This approach is reasonable when estimating the directional wave climate, but neglecting the wind duration may lead to over-prediction of wave heights.
- 3 **Time series of wind speed and direction.** Sequential – eg hourly, three-hourly or six-hourly – wind speeds and directions can be used as input to wave **hindcasting** or **forecasting** models. If suitable wind data and the appropriate wave model are available this approach is the most accurate method of converting wind data into equivalent wave data. Most hindcasting models account for the actual variability of the wind records hour by hour, as well as time-averaged values. For the design of rockfill reservoir dams such numerical models are used as **forecasting**, which is often the only tool that can be used to derive design conditions for this case.

Table 4.3 Wind speed conversion factors related to duration of wind speeds

Time base (hours)	1/4	1/2	1	3	6	12	24
Factor (-)	1.05	1.03	1.00	0.96	0.93	0.87	0.80

4.2.1.2

Use of atmospheric pressure data

Although atmospheric pressure may be a key source variable for meteorological modelling, pressure data are rarely used directly in coastal engineering. Probably the only time they are used is as partial input either to modelling the coastal impacts of hurricanes or to estimation of storm surges in the absence of more direct sea level data (see Section 4.2.2.3).

In normal conditions the mean air pressure at sea level is approximately 1013 hPa (1 hPa = 0.1 kPa = 1 millibar). The central pressure in a storm, a typhoon, hurricane or cyclone is one of the key indicators of its strength and potential to cause damage. Hurricanes or typhoons very rarely affect European coasts, although severe storms can occur, characterised by low central pressures. In the storm zones of higher latitudes (above 40°) the central pressure may reach values down to 970 or 950 hPa, while in tropical storms (hurricanes, typhoons, cyclones) pressures may drop to 900 hPa. In hydrodynamic modelling of hurricane or storm effects on the sea surface, it is necessary to set up a propagating pressure field representing conditions in and around the moving storm (Holland, 1980).

Pressure and wind are the driving forces behind the development of storm surges. One component of surge comes from the inverse barometer effect in which lower than average atmospheric pressure causes a rising of the sea surface. In the open ocean or on exposed deep waters, coastal pressure statistics can provide a reasonable estimate of the likely distribution and magnitude of surge. However, at most coastal locations pressure alone gives a poor indication of surge elevation where local shallow-water effects can cause a significant amplification of surge relative to deep water (see Section 4.2.2.3).

4.2.2 Marine water levels

Water level is important because:

- most instances of flooding and/or structural damage occur during high water level
- wave overtopping and wave transmission depend on the Still Water Level (SWL)
- the force on a seawall partially protected from waves by a shallow foreshore depends on SWL
- a structure may be exposed (and possibly vulnerable) to different risks for different water levels, in turn dependent upon SWL
- the wave height may be limited by breaking before arriving at a structure
- construction and maintenance is generally affected by the overall water level regime.

Various components of water level should be considered. Apart from astronomical tides and very rare seismic (tsunami) effects there are several meteorological components of the water level to be considered, known as **residuals**. These residuals comprise storm surges, wind set-up, wave set-up and seiches.

Along the Atlantic coasts of Europe, in the English Channel and the North Sea the major phenomenon that determines the water level is the astronomical tide, which can be predicted accurately and well in advance. By contrast, meteorological effects, ie residuals, are not predictable more than, at best, a few days in advance and even then the predictions are uncertain. Seismic effects (tsunamis) are almost unpredictable or at best can be predicted a couple of hours before their arrival in areas that are generally very far from the location of the seism.

Some components of water level are partially correlated, meaning that a higher or lower value of one component tends to occur at the same time as a higher or lower value of another component. Correlations often arise between components of meteorological origin, such as storm surge, wind set-up, wave set-up and even seiches. Depending on tidal levels, these components may be affected, notably in shallow areas. For example, surges may propagate differently according to the water depth and current conditions.

Usually the two most important components of the water level at any moment are the astronomical tide and the storm surge. The former is cyclical with a period that depends on the relative significance of astronomic forces at a particular location (see Section 4.2.2.2). For example, along the Atlantic coasts of Europe the dominant period of tide is 12.42 hours (ie 12 hours and 26 minutes) on average. Storm surges occur randomly, typically as individual events with durations of approximately half a day to one day, peaking about mid-way through the period (see Section 4.2.2.3). The variation with time of the water level due to astronomical tide and storm surge is illustrated in Figure 4.9.

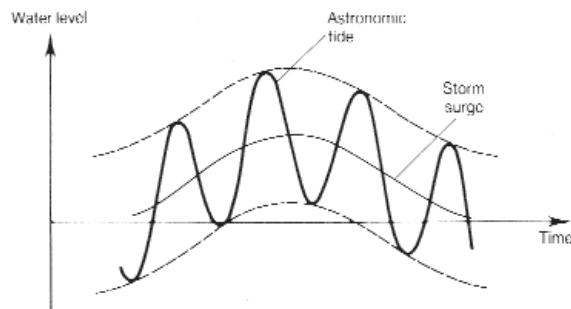


Figure 4.9 Variation in water level due to storm surge and astronomical tide

4.2.2.1 Mean sea level

For coastal waters open to the sea the **mean water level** (MWL) can in most cases be taken as a site-specific constant related to the **mean sea level** (MSL) of the oceans. In some areas, for example the eastern Mediterranean Sea, the mean sea level varies slightly, according to the time of year, in a more or less predictable manner. Observed seasonal sea level changes are between 5 and 15 cm, whereas in the rest of the Mediterranean Sea differences up to 30 cm may be observed in some locations.

Most countries have a national datum level, which is often approximately equal to the MSL: examples are Ordnance Datum in the UK, IGN69 datum level in France and NAP in the Netherlands. Chart Datum, as used by the British Admiralty in the UK and by the Service Hydrographique et Océanographique de la Marine (SHOM) in France, represents the **lowest astronomical tide** (LAT), which varies significantly from one place to another.

4.2.2.2 Tide

The basic driving forces of tidal movements are astronomical, so are entirely predictable, which enables accurate prediction of tidal levels and currents. Since tides are long waves, phenomena of resonance and shoaling effects caused by geography and bathymetry can lead to considerable amplification of tidal levels in shallow seas and estuaries. Coriolis force plays a considerable role in explaining the large tidal amplitude differences along European coasts. Locally (see Figure 4.10), at **amphidromic points**, the amplitude of the tide is zero. The tidal wave propagates around amphidromic points clockwise in the north hemisphere.

The **tidal range**, approximately equal to twice the **tidal amplitude**, is generally less than 1 metre in open oceans but increases slightly towards the continents and may increase considerably in shallow seas, for example the continental shelf. Large amplifications are found, for example, in bays along the coasts of England and Wales (spring tidal range of up to 12 m), in the Bay of Fundy, Canada (spring tidal range of up to 13 m) and around Saint-Malo in Normandy, France (spring tidal range up to 14 m), while a 3–4 m spring tidal range is common for the southern North Sea.

Tides are predominantly generated by the fundamental gravitational attractions of the Moon and Sun, which are proportional to their masses and to the inverse square of their distances from the Earth. Although the Moon is much smaller than the Sun, it has a greater influence on tides because it is much closer to the Earth. In particular, the timing of the tide is associated with the relative position of the Moon rather than with the time of day and advances at about 50 minutes a day. Another consequence of the Moon's orbit relative to the Earth is that the tide-generating forces of the Sun and Moon are continuously moving in and out of phase. Near full moon and new moon, the Sun and Moon act in the same direction to give larger tides, ie spring tides. Smaller “neap” tides are produced at around first and third quarter moons when the Sun and Moon's attraction forces oppose each other. The spring-neap cycle lasts about two weeks.



Figure 4.10 Propagation of the tidal wave in the North Sea

The orbits of the Moon around the Earth and of the Earth around the Sun are not circular. Thus tides also vary seasonally, with the largest tides of the year occurring at the spring and autumn equinoxes, when the Sun crosses the equator and night and day are everywhere of equal duration. Minor variations also occur over an 18.6-year cycle due to the variable angular disposition of the Sun and Moon. The major planets have small additional effects.

Along the Atlantic coasts of Europe, the dominant tidal components have periods of approximately half a day (semi-diurnal tides) and a full day (diurnal tides).

- **Dominant semi-diurnal tidal components** include:
 - principal lunar (M_2 , period = 12.42 hours)
 - principal solar (S_2 , period = 12.00 hours).
- **Dominant diurnal components** include:
 - principal lunar diurnal (O_1 , period = 25.82 hours)
 - luni-solar diurnal (K_1 , period = 23.93 hours).

Specific coastline geometry, for example that of channels or bays or estuaries, and bottom friction can generate phase shift of the dominant tidal components and frequencies equal to the sum or difference of basic frequencies. The contributions of these secondary frequencies may locally be significant.

The predictive character of tides can be useful when scheduling critical operations, such as manoeuvring during construction. When planning to construct, inspect or maintain a structure it is important to keep in mind that Mean High Water Spring tide (MHWS) at a given location always occur at about the same time of the day. The MHWS timing at another

place will be different and the typical **neap tide** (MHWN) timing is about six hours earlier or later than the MHWS timing. When planning work on structures it is useful to know the timing of the most extreme low waters and whether or not they occur during daylight.

For a detailed description of sea level fluctuations and tidal phenomena, see Pugh (1987).

4.2.2.3 Storm surges

Meteorological phenomena, namely atmospheric pressure and wind, may also affect the sea level in particular during storm events. This section focuses on atmospheric pressure effects while wind effects are considered in the next section. Pressure and wind effects are often combined during storms generating long waves, called **storm surges**, with a characteristic time-scale of several hours to one day and a wavelength approximately equal to the width of the centre of the depression, typically 150–800 km. These storm surges produce significant variations of the sea level, up to 2–3 m at the shore depending on the shape of the coastline and the storm intensity. In practice, the term **storm surge level** is sometimes used loosely to include the astronomical tidal component and other meteorological effects.

Local low atmospheric pressures (depressions) cause corresponding rises in water level. Similarly, high pressures cause drops in water levels. This is the so-called **inverse barometer effect**.

For open water domains, Equation 4.9 gives the relationship between the **static** rise in water level z_a (m) and the corresponding atmospheric pressure:

$$\frac{\partial \eta}{\partial x} = \frac{1}{\rho_w g d} \tau_w \quad (4.9)$$

where p_a = atmospheric pressure at sea level (hPa) and 1013 hPa is the pressure in normal conditions (see Section 4.2.1.2).

NOTE: Equation 4.9 results from simple equilibrium between the atmosphere and the ocean in static conditions. Where the atmospheric pressure is higher than the mean value of 1013 hPa, the sea level decreases, provided that it can increase at another place where the atmospheric pressure is lower than the mean value. This simple relationship does not apply for closed domains of small dimensions such as lakes. Indeed, if the atmospheric pressure is the same over the whole water domain there is no change in static water level.

Dynamic effects can cause a significant amplification of the rise in water level, however. When the depression moves quickly, the water level rise follows the depression. The height of these long waves may increase considerably as a result of shoaling in the nearshore zones. Along the coasts of the southern North Sea, storm surges with a height of 3 m have been recorded.

4.2.2.4 Wind set-up

Shear stress exerted by wind on the water surface causes a slope in the water surface (see Figure 4.11), as a result of which wind set-up and set-down occur at downwind and upwind boundaries, respectively.

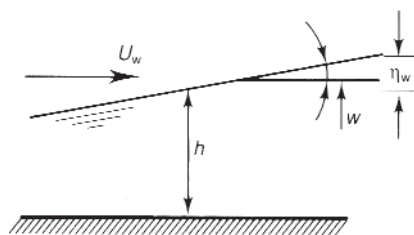


Figure 4.11 Wind set-up

For a bottom profile with straight and parallel bottom contours (1D situation), the wind-induced gradient of the still water surface, η (m), along the x axis (taken normal to the shoreline) can be computed with Equation 4.10:

$$\frac{\partial \eta}{\partial x} = \frac{1}{\rho_w g d} \tau_w \quad (4.10)$$

where $d = h + \eta$ = actual water depth, including the wind-induced set-up (m), ρ_w = mass density of the seawater (1025–1030 kg/m³) and τ_w = wind shear stress acting on the water surface in the direction normal to the coast (N/m²).

The wind shear stress, τ_w , can be evaluated with Equation 4.11 from a specific wind velocity, U_{10} , that may be computed from the wind conditions, U_w :

$$\tau_w = \rho_{air} C_D U_{10}^2 \quad (4.11)$$

where U_{10} = wind speed at an elevation of 10 m above MSL (m/s), ρ_{air} = mass density of air (1.21 kg/m³) and C_D = air/water drag coefficient with typical values of $0.8 \cdot 10^{-3}$ to $3.0 \cdot 10^{-3}$ (-), the value of which increases with wind speed (eg Abraham *et al*, 1979; Wu, 1980).

Particular solutions can be obtained by integrating Equations 4.10 and 4.11 analytically for some simple cases. For example, for a **closed water domain** (eg lake, lagoon) of length, F (m), with a **constant water depth**, h (m), and a constant wind speed, U_{10} (m/s), blowing over the water domain, the resulting maximum wind set-up, η_w (m), at the downwind coast or shoreline is given by Equation 4.12, derived by linearising Equation 4.10 by considering that $d \cong h$.

$$\eta_w = \frac{1}{2} \frac{\rho_{air}}{\rho_w} C_D \frac{U_{10}^2}{g h} F \quad (4.12)$$

In the absence of calibration data, simplified results such as those following from Equation 4.12 can only provide a guide to the likely wind set-up, because of uncertainties about the value of C_D and the choice of representative values of h and F . Other analytical and non-linear solutions can be found in Dean and Dalrymple (1991). If possible, site-specific measurements of surge, from which wind set-up can be estimated, should be made on a few windy days. This would enable site-specific calibration of the equations for use in subsequent predictions.

Operational systems used for the prediction of storm surges from meteorological forecasts are based on numerical flow models (either 2D or 3D) of the area considered. The model takes into account the stress at the sea surface due to the wind and the gradient of atmospheric pressure (see Section 4.2.2.3). Running such a numerical model with inclusion of tidal forcing is the recommended way to predict or model storm surges in real cases. This also applies to the dynamics of the meteorological forces, the effects of the bathymetry in shallow-water areas and the interactions between the tidal wave and the storm surge. The intensity of meteorological effects on the variation of MSL can be obtained by comparing the results of a simulation considering both tidal and meteorological forcings with the results of simulation considering tidal forcing only. Very often the tide and storm surge model is also run in combination with a numerical wave model. The flow model gives the water levels, for which the wave heights generated by wind are calculated.

4.2.2.5 Wave set-up

Wave set-up is localised near to the shoreline. It is mainly caused by energy dissipation caused by depth-induced breaking of the incoming waves (see Figure 4.12). For a bottom profile with straight and parallel bottom contours (1D situation), the gradient of wave set-up, η (m), along the x axis (taken normal to the shoreline) should be computed by solving Equation 4.13:

$$\frac{\partial \eta}{\partial x} = -\frac{1}{\rho_w g d} \frac{\partial S_{xx}}{\partial x} \tag{4.13}$$

where $d = h + \eta =$ actual water depth, including the wave set-up (m), and $S_{xx} =$ component of the radiation stress tensor normal to the coast (N/m).

The component S_{xx} (N/m) of the radiation stress is evaluated with Equation 4.14 according to the linear wave theory:

$$S_{xx} = \frac{1}{8} \rho_w g H^2 \left[\frac{1}{2} + \frac{2kd}{\sinh(2kd)} \right] \tag{4.14}$$

where $k =$ wave number (rad/m), $= 2\pi/L$ (rad/m) to describe the spatial periodicity, with $L =$ wavelength (m) (see Section 4.2.4.2).

For non-linear waves, Equation 4.13 has to be solved by a numerical model together with the appropriate equation (Aristaghes and Aristaghes, 1985) that governs the evolution of the wave height H along the bathymetric profile, including breaking dissipation.

NOTE: Both equations are coupled, i.e. a change of water level affects wave propagation. Consequently, the variation of wave height, in turn, modifies the set-up, and the system of equations should thereafter be solved iteratively.

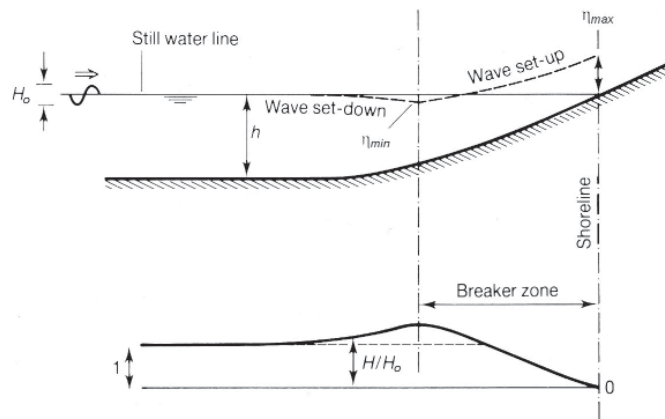


Figure 4.12 Wave set-up

Using linear wave theory for normally incident regular waves, Battjes (1974) derived a first estimate of wave set-up at the shoreline. Equation 4.15 gives the relationship between the wave set-up, η_{max} , and the wave conditions at the breaker line:

$$\eta_{max} = 0.3 \gamma_{br} H_b \tag{4.15}$$

where $\gamma_{br} =$ breaker index or maximum wave height to water depth ratio H/h (-) and $H_b =$ wave height at the breaker line for regular waves (m). The value of H_b can be found by applying a wave model to the local bathymetry using deep-water waves as a boundary condition.

For the case of a planar beach, Bowen *et al* (1968) used the shallow-water linear wave theory for the radiation stress S_{xx} and made use of the approximate relationship $H = \gamma_{br} (h + \eta)$ in the surf zone to derive Equation 4.16 for the wave set-up:

$$\eta - \eta_b = \frac{1}{K} (h_b - h) \tag{4.16}$$

where the subscript b again denotes values at the breaking point and $K = 1 + \frac{8}{3\gamma_{br}^2}$.

According to Equation 4.16, the wave set-up on a plane beach increases linearly in the surf zone.

For non-uniformly sloping profiles, Equation 4.13 should be solved numerically and coupled with a wave model. Examples of wave set-up profiles on barred beaches are given in Izumiya and Horikawa (1984).

On the basis of field measurements and numerical simulations, some relationships have been established for irregular wave conditions. For example, Hanslow and Nielsen (1992) fitted the relationships given in Equations 4.17 and 4.18 to their measurements for the shoreline set-up:

$$\eta = 0.38 H_{orms} \quad (4.17)$$

$$\eta = 0.0488 \sqrt{H_{orms} L_o} \quad (4.18)$$

where H_{orms} = incident (deep-water) root-mean-square wave height (m) (see Section 4.2.4.4) and L_o = deep-water wavelength calculated from the wave period T as $L_o = gT^2/(2\pi)$ (m).

Equation 4.18 results in a slightly better fit of measurements than Equation 4.17, although a significant scatter of experimental points is still present.

Goda (2000) proposed a chart (reprinted as Figure 4.13) where the shoreline set-up can be estimated for uniformly sloping beaches (slope = $\tan\theta$ ranging from 1/100 to 1/10) as a function of the fictitious wave steepness H'_0/L_o , where H'_0 is the **equivalent deep-water significant wave height**. This equivalent wave height is a *hypothetical* wave height obtained from the actual significant deep-water wave height H_{s0} (see definition in Section 4.2.4.4) corrected for the effects of refraction and/or diffraction from offshore to the shoreline. It is obtained as $H'_0 = K_d \cdot K_R \cdot H_{s0}$ where K_d and K_R are the diffraction and refraction coefficients respectively (see Section 4.2.4.7). Figure 4.13 shows that the shoreline set-up increases as the beach becomes steeper and as the fictitious wave steepness decreases.

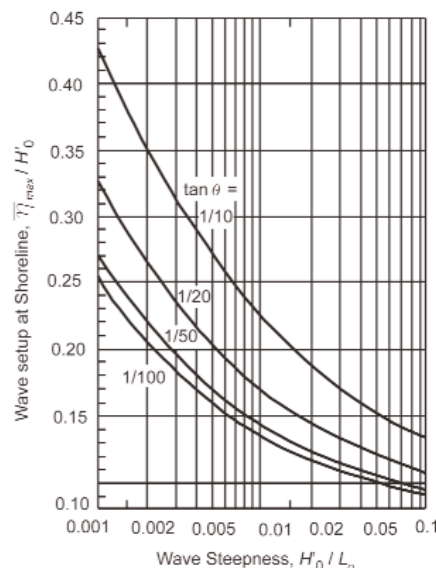


Figure 4.13

Wave set-up at the shoreline for uniformly sloping beaches (Goda, 2000)

For the design of coastal structures the important question to address is whether wave set-up should be included in the design water level or not. If the design formula to be used already includes this wave set-up in its formulation, then this effect should not be added. This is the case for formulae that were derived for shallow water. Similarly, if a structure is tested in a wave basin or a wave flume and the foreshore is modelled, ie deep-water conditions are generated by the wave-maker offshore of the surf zone; consequently the wave set-up is “automatically” modelled in the experimental tests. So the design water level should then be considered without the wave set-up. For the other cases, in particular the design formulae that do not include wave set-up, the set-up should be added to the still water level to obtain the design water level, as stated by Hamm (2001).

4.2.2.6 Seiches

Seiches are standing wave oscillations caused by some excitation mechanism and trapped by the general form and bathymetry of a water domain such as a harbour, a basin or a lake. Their periods correspond to the natural periods of oscillation for that water body. Thus when a long wave crosses the water body, it is reflected from the end and the interference with the original wave results in a standing wave pattern. If the body of water, such as a bay or estuary, is open at one end reflection may again occur at the open end and standing waves can be observed.

Possible excitation mechanisms are:

- meteorological phenomena, like squalls, impulsive winds and gusts
- tsunamis from earthquake motions
- storm surges (see Section 4.2.2.3)
- long-period wave phenomena such as surf-beat (induced variations in shoaling wave groups, see Section 4.2.2.7)
- and even current-induced vortices.

Typical time-scales are of the order of minutes (between 2 and 40 minutes); this corresponds to a frequency lower than 0.01 Hz in the energy spectrum of the sea surface. One famous location for seiches is in the Adriatic Sea where the water level at Venice can display oscillations for considerable periods. Recently de Jong (2004) investigated the origin of seiches for the port of Rotterdam. He showed that all significant seiche episodes coincided with the passage of a low-pressure area and a cold front approaching from the sea and 90 per cent of these events occur during the storm season. He developed a method for predicting the occurrence of seiches based on a criterion for the occurrence of convection cells. This criterion is expressed in terms of a minimum temperature difference between the water at the sea surface and the air at higher altitudes in the atmosphere.

Seiches are normally observed in completely enclosed water bodies such as lakes and closed seas. The simplest case corresponds to a rectangular closed basin of width, l (m), and constant water depth, h (m). As illustrated in Figure 4.14 the standing wave conditions are obtained when the ratio of the basin width, l , to half of the wavelength, L , is an integer, as written in Equation 4.19.

$$l = n L/2 \quad \text{with } n = 1, 2, 3, \dots \quad (4.19)$$

In other words, a seiche may occur when the wavelength of the incident wave is equal to certain specific wavelength $L_n = 2l/n$.

If the shallow-water approximation is used in the dispersion relationship between the wavelength L and the wave period T (see Table 4.6), the periods of seiches, T_n (s), are obtained by Equation 4.20.

$$T_n = \frac{2l}{n\sqrt{gh}} \quad \text{with } n = 1, 2, 3, \dots \quad (4.20)$$

Similarly, for a semi-enclosed basin the standing wave conditions are obtained when Equations 4.21 or 4.22 are fulfilled.

$$l = L/4 + n L/2 \quad \text{with } n = 0, 1, 2, 3, \dots \quad (4.21)$$

$$T_n = \frac{4l}{(2n+1)\sqrt{gh}} \quad \text{with } n = 0, 1, 2, 3, \dots \quad (4.22)$$

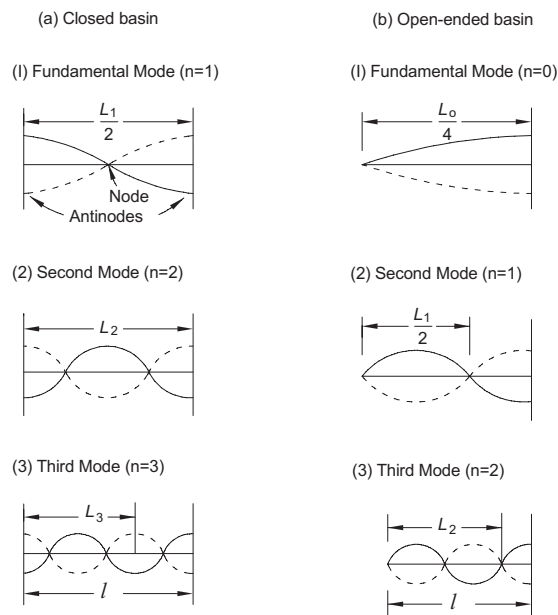


Figure 4.14 The three first modes of seiches for closed and open-ended basins with a flat bottom (adapted from Carr 1952)

Wilson (1972) and Dean and Dalrymple (1991) consider various other geometrical shapes for the bottom (for a closed basin of constant width) and also the inclusion of frictional damping.

For real cases it is very difficult to estimate the amplitude of a seiche because it depends in general on how close the forcing frequency is to the natural oscillation frequency. If they are close then large amplitudes may occur (eg the tidal amplitude in the Severn estuary, UK). If an oblong lake is suddenly exposed to a steady wind along its long axis, then the maximum rise in water level is considerably higher than the one that would be obtained by a simple balance between water slope and wind force (ie as computed from Equation 4.12). The maximum can be twice as large as the increase in level caused by wind set-up alone (see Section 4.2.2.4).

In general, analysis of local water level recordings is the only way to account properly for seiches for design purposes. Where measurements have to be carried out, the minimum sampling frequency should be at least twice the expected maximum frequency of the phenomenon of interest.

4.2.2.7

Long-period waves

Even in a stationary sea-state individual wave heights vary and it is common for groups of large waves to occur especially where some swell wave activity is present. Beneath these wave groups the mean sea level is lowered (set-down) around the breaker line. Between the groups, where the wave activity is less intense, the mean sea level is higher (less set-down). This varying level of set-down produces a long-period wave motion, with a period typically of between 30 seconds and several minutes. The oscillations give rise to **bound long waves** (ie **bound** to the wave groups in the wind-sea). These long waves typically have a modest height, of about 10–30 cm for most common situations.

The long waves propagate with the wave groups and become more important as they reach the shoreline. While the **primary waves**, ie the wind-sea and swell, are largely destroyed by breaking and frictional effects, the long waves are not and are therefore *liberated* when the primary waves break. Much of the long wave energy is reflected, leading to a partial standing wave pattern known as **surf beat**. Collectively, these bound and free long waves are also

referred to as **infra-gravity waves**. If the waves approach a beach obliquely the long waves can modify the longshore currents and also form **edge waves** that travel along the beach and are often *trapped* within the nearshore zone. Long waves also produce variations in both the set-up and the run-up in the surf zone caused by the primary waves. The long-period oscillations in these effects can cause both greater damage to, and overtopping of coastal structures.

An order of magnitude of the surf-beat amplitude in shallow water and in the surf zone can be obtained by using Equation 4.23, an empirical formula derived by Goda (2000):

$$\frac{\zeta_{rms}}{H'_0} = 0.01 \left[\frac{H'_0}{L_o} \left(1 + \frac{h}{H'_0} \right) \right]^{-1/2} \quad (4.23)$$

where ζ_{rms} = root-mean-square amplitude of the surf-beat profile (m). It is a function of the equivalent deep-water (significant) wave height H'_0 defined in Section 4.2.2.5 (m), the deep-water wavelength L_o (m) computed from the significant wave period T_s (see Section 4.2.4.4) as $L_o = g(T_s)^2/(2\pi)$, and the local water depth, h (m).

Bowers (1993) also provides formulae to estimate the amplitude of bound long waves for intermediate depths and also for surf beat significant wave height. For the case of coastal structures exposed to long waves, Kamphuis (2001) proposed the use of Equation 4.24 to estimate the zero moment wave height of the long waves, $(H_{m0})_{LW}$, at the structure as a function of the breaking significant wave height $H_{s,b}$ and the peak wave period T_p (see Section 4.2.4.5).

$$\frac{(H_{m0})_{LW}}{H_{s,b}} = 0.11 \left[\frac{H_{s,b}}{gT_p^2} \right]^{-0.24} \quad (4.24)$$

Equation 4.24 can be approximated as a rule of thumb by $(H_{m0})_{LW} = 0.4H_{s,b}$. Kamphuis (2000) also addresses the problem of reflection of these long waves on coastal structures, showing that the long wave profile (with distance offshore) may be described as the sum of an absorbed wave and a standing wave. The long wave reflection coefficient was about 22 per cent during the set of experiments.

4.2.2.8 Tsunamis

Tsunamis are seismically induced gravity waves characterised by wave periods that are in the order of minutes rather than seconds (typically 10–60 minutes). They often originate from earthquakes below the ocean, where water depths can be more than 1000 m, and may travel long distances without reaching any noticeable wave height. However, when approaching coastlines their height may increase considerably. Because of their large wavelength, these waves are subject to strong shoaling and refraction effects. Approaching from quite large water depths, they can be calculated using shallow-water theory. Wave reflection from the relatively deep slopes of continental shelves may also be an important consideration.

Some theoretical work is available (eg Wilson, 1963), as well as numerical models to describe tsunami generation, propagation and run-up over land areas (eg Shuto, 1991; Yeh *et al*, 1994; Tadepalli and Synolakis, 1996) and also some large-scale experiments (eg Liu *et al*, 1995). More information on tsunamis can be obtained from the Internet, for example at <www.pmel.noaa.gov/tsunami>.

Tsunamis are as unpredictable as earthquakes. Figure 4.15 presents observations for height and period of tsunamis from Japanese sources observed at coasts within a range of about 750 km from the epicentre of sub-ocean earthquakes.

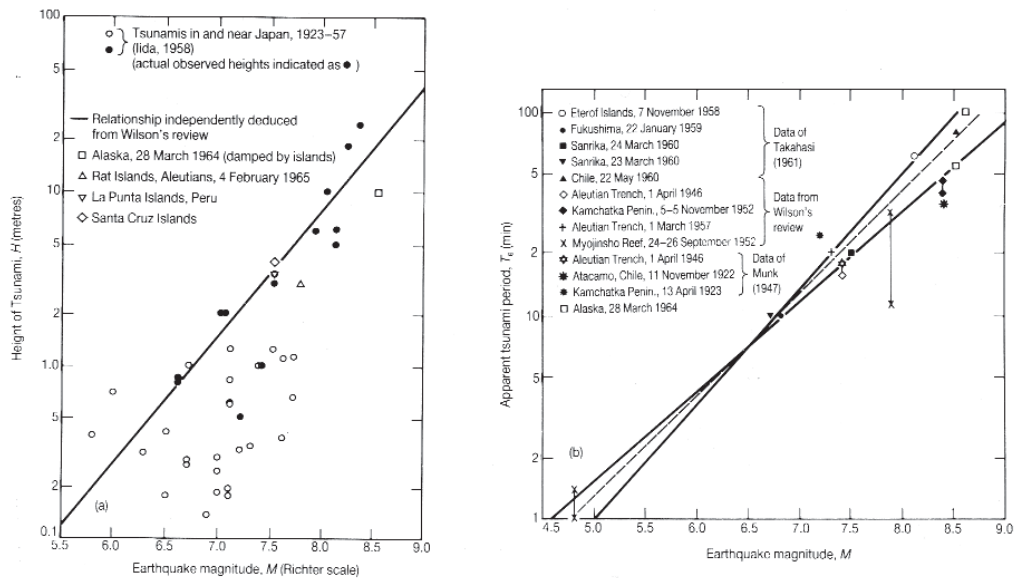


Figure 4.15 Heights (left) and periods (right) of tsunamis related to earthquake magnitude

Tsunamis are an important issue in some parts of the world, particularly along the coasts and islands of the Indian and Pacific oceans. Tsunamis occur more frequently and at greater intensity in these areas than elsewhere in the world. This risk should be carefully addressed in the design process for coastal structures. In some countries, eg Japan, tsunamis are a major concern and are dealt with during the design of any marine structure.

The rarity of tsunamis in northern Europe makes it unlikely that this component of water level would be important for that region, except where a very high standard of service is demanded of sea defences, such as those for sensitive installations. For example, the British Tsunami Initiative allowed 10 organisations to pool their knowledge on tsunami occurrence and impact. The main results are available at <www.nerc-bas.ac.uk/tsunami-risks>. The website includes information on actual occurrences of tsunamis and tentative predictions of maximum tsunami run-up for different ocean areas. Tsunamis are more common around Italy and in the eastern Mediterranean, where significant events occur at intervals of approximately 100 years. Consequently they should not be dismissed as unimportant in the design of structures in this region. For the eastern Mediterranean, the website gives 50-, 100- and 200-year values of tsunami run-up of approximately 4 m, 6 m and 8 m respectively. However, these values appear to refer to occurrence of tsunamis anywhere in the eastern Mediterranean and not necessarily to a specific location of interest.

4.2.2.9

Flood waves

Water levels in rivers are governed by the river discharge, with extreme levels being associated with flood waves (see Section 4.3.3). Flood waves may contribute to the overall water level in rivers. However, as a contribution to marine water level their impact is small compared with tide and surge and is limited to river mouths. Moving upstream from the river mouth, the tidal influence decreases and only after a certain distance upstream, in the order of 10–30 km, depending on river discharge and tidal intensity, the flood wave component may become dominant. In Section 4.3.3 the propagation of flood waves is discussed as well as the use of rating curves, as a means of relating water levels to river discharge, and stage relationships to correlate water levels at different locations along the river. Unless local tide gauge measurements are available, numerical river modelling should be undertaken during the design stage to quantify the possible effect of flood waves on the overall water level in river mouths.

4.2.2.10 **Sea level rise resulting from climate change**

Observations of sea level rise

Mean sea level rise over the last century is a well-documented phenomenon (IPCC, 2001). Long-term measurements show a rate of rise of 1–2 mm/year over the last century. In addition gradual slight changes in land level produce apparent regional variations in the rate of rise. For example, in the UK, the sea level rise in the south-east of England is higher than the average rate, while in northern Scotland it is lower than average.

Direct and indirect effects of sea level rise

In the absence of any evidence to the contrary, any increase in mean sea level would be likely to cause an equal increase in all other water levels, including extreme water levels. In many cases sea level rise may become an issue certainly if the wave heights are depth-limited. Sea level rise will then increase the wave attack on the structure.

However, future climate change may also influence weather patterns, which in turn may influence the size and frequency of storm surges, in turn influencing the total water level and risk of flooding. Some climate change projections (UKCIP, 2002) suggest that changes in storm surge could have a significant impact on extreme water level and flood risk. As well as a change in mean sea level, there is the possibility of a change in tidal range. Long-term tidal measurements show slight past trends in this respect, which may continue into the future.

What will be the sea level rise in the future?

Many institutions are involved in research on sea level rise and its implications. Since about 1980 there have been consistent predictions of an imminent increase in the rate of mean sea level rise. A certain proportion of the predicted rise is already thought to be committed regardless of any corrective action that may be taken, but there is some sensitivity to future actions in pollution control etc.

The present consensus is that in future the rate of rise will probably increase to about 5 mm/year, with some regional variations, although as yet there is no evidence that this acceleration has started.

In the Netherlands three scenarios for the future have been adopted:

- present trend 0.20 m rise per century
- increased trend 0.60 m rise per century
- extreme trend 0.85 m rise per century.

How to deal with the sea level rise?

The response to possible sea level rise depends on the activity considered, for example, whether conducting a safety assessment, considering design or reconstruction of a structure, or planning reservation of areas for future safety improvement. Each of these activities is described in more depth below.

Safety assessment. What is the effect of sea level rise on an existing structure? The answer depends on the design life of the structure and the frequency of monitoring while in service. In the Netherlands safety assessments on all flood defence structures (dikes, dunes, seawalls etc) have to be performed every five years. As the time horizon is limited to five years the **actual** sea level rise is taken into account. This actual sea level rise is not a future scenario, so for existing structures it is possible to observe the trend of the sea level and take measures when necessary.

Design of structures. If a new structure has to be designed, or an existing structure has to be repaired or upgraded, the expected sea level rise plays a role in the design process. Examples of responses to this point from the UK and the Netherlands are given below.

- **In the United Kingdom.** The Department for Environment, Food and Rural Affairs (Defra) advises coastal engineers to take account of expected sea level rise when designing or assessing sea defences. However, predictions of future changes in sea level are uncertain and are frequently updated and any such changes will be gradual. As a result, depending on the particular situation, sea level rise may sometimes be considered on a contingency basis rather than as a firm commitment. For example, rather than designing sea defences now for a 0.5 m rise in sea level over the next century which may never occur, designers may instead prepare contingency responses for review when evidence of accelerated sea level rise is more definite. MAFF (1999) recommends rates of sea level rise that should be assumed for different Environment Agency regions in England and Wales: 6 mm/year for the Anglian, Thames and Southern regions, 4 mm/year for the North-West and Northumbria regions, and 5 mm/year for the remainder.
- **In the Netherlands.** Until 2000 the Dutch government included the present trend of sea level rise into the design process. This means 0.20 m for a design lifetime of 100 years and 0.10 m for a design lifetime of 50 years. The design lifetime depends on the situation, ie whether it is relatively easy to improve the structure again or not: a dike is easy to upgrade, flood defence structures in urban areas are difficult to upgrade. In 2000 the Dutch government decided that the increased trend of 0.60 m per century was the scenario that should be taken into account during design of flood defence structures.

But what will happen to the structure after its design life? If the crest height of a structure plays an important role, as is the case for dikes and seawalls, a time will come when the height will have to be increased to match the rise in sea level. Whether it is an easy task or one that demands a completely new structure depends largely on how the structure was designed initially. What is important during the design is the robustness of the technical solution. A designer should therefore choose those options that make it reasonably easy to cope with higher design conditions (water levels, wave forces) than are expected, or that are expected after the design life of the structure.

Reservation of area for future improvement. By law the owner of a flood defence structure in the Netherlands has to reserve an area around the structure that will enable it to be improved in the long term. Use of these reserved areas by other people is highly restricted. Construction of houses or offices is prohibited, as are activities that may hamper future improvement of the flood defence structure. The boundary conditions for decision-making about reservation areas depend heavily on the expected sea level rise. They are based on the most extreme scenario – a sea level rise of 0.85 m per century – and on a time horizon of 200 years. This equates to a total sea level rise of 1.7 m. Climate change means that a 10 per cent higher (design) wind speed also has to be taken into account, which converts to an extra 0.4 m of storm surge in the North Sea (specifically for the Netherlands!) and an increase of 5 per cent in the wave conditions. With these extreme conditions an approximate design of a flood defence structure has to be produced and the space required for the reservation area will be established based on that design.

4.2.2.11

Sources of water level data

Low-cost software programs to predict astronomical tides are available from hydrographic suppliers and can be used for sites at which the tidal harmonic constituents have been established from measurements. However, this is not necessary for most situations. In practice, the user rarely needs to carry out tidal predictions because tables are composed on a routine basis and issued yearly by port or coastal authorities and by national authorities. For example, the US and British admiralties have extensive data files that provide high water (HW) and low water (LW) levels and times for major ports, usually one year ahead. These data

should be used to derive site-specific tidal constants needed for prediction at intermediate sites. Charts and tide tables also include typical tide curves to enable predictions to be made for intermediate water levels between high and low water.

In most cases, only the astronomical tide (as given in tide tables) and the overall still water level (as measured by tide gauges) is considered. Where storm surges and seiches are significant they should automatically be included in tidal measurements and for most practical purposes they need not be separated out. In most situations it should not be necessary to commission tide gauge recording or any “new” research into water levels but simply to review existing data.

Some sources of tidal and water level data are listed below:

- Admiralty tide tables and charts in the UK (for astronomical tidal ranges)
- Proudman Oceanographic Laboratory in the UK (for measured or predicted water level data, for the A class tide gauge network and for the UK on a 35 km grid)
- Service Hydrographique et Océanographique de la Marine (SHOM) in France
- open literature on extreme water levels (see Section 4.2.2.10)
- others such as consultants, universities, port authorities, local authorities, specialist literature.

Tidal level records go back over 100–150 years at a few stations around European coasts. In most cases a breakdown into separate astronomical and surge components has already been performed. This type of data should be checked for unusually high total water levels or surges.

Where water level recording is necessary, one should consider the following points:

- the gauge location should be permanent, accessible and not subject to interference by vandals or wave action
- for measurement of surges and/or sea level trends, the instrument should operate for an indefinite period
- for reliable derivation of local tidal constituents, it is recommended to have continuous tidal observations for at least a year. However, reasonable estimates can be made from as little as 14 days of data if there are constituents from a site nearby based on a longer record.

NOTE: Analysis of tidal data is not trivial: extraction of surges requires knowledge of the astronomical tide and analysis of tidal constituents requires specialist software.

4.2.2.12 Design extreme water levels

Usually the design extreme water level corresponds to the SWL, defined as the **average** sea surface elevation over an area at any instant. To determine the extreme design water level, all components of the water level must be determined as a function of the (average) probability of exceedance, alternatively expressed as average exceedance frequency or return period. Such exceedance curves, for example that shown in Figure 4.17, are based upon a long-term distribution curve, obtained by fitting water level data to a standard statistical distribution (see Box 4.10). Unfortunately, the lack of data for low frequencies (long return periods) means that extrapolation is usually necessary. The extrapolation should be checked or supported by numerical modelling of the underlying physical processes to give a better understanding of the results.

In most cases the design water level includes tidal elevations, storm surges (caused by atmospheric pressure effect and/or wind set-up) and long-period seiches, if any, but excludes localised variations caused by waves. The inclusion of wave set-up and long wave oscillations

(such as surf beat) in the design water level depends on the application and on the design formula or model to be used subsequently for the design (see discussion in Section 4.2.2.5). For example, if a model is built in a wave basin with a wave-maker located offshore in deep-water conditions, then the wave set-up and the long waves will **automatically** be produced by the bathymetry of the physical model. The design water level in the offshore part of the basin should not include the set-up and long wave components. Alternatively, if a formula for the design of a breakwater, or for the prediction of overtopping, requires the water depth at the toe of the structure then all components of water level (including wave set-up and long wave) should be included in the design water level.

There are at least three applications for which design water levels need to be (re)evaluated.

- 1 **Assessment of existing flood defence structures** (northern Europe). This corresponds to the present situation, without considering sea level rise, where high return periods often have to be estimated. For example, water defences in the Netherlands need to be assessed to a level of 1 in 10 000 years (UK and Germany are lower). Figure 4.16 gives more than 100 years of high water level measurements and the extrapolation of the measurements to 10^{-4} , giving a level of +5.0 m NAP (Dutch reference level).

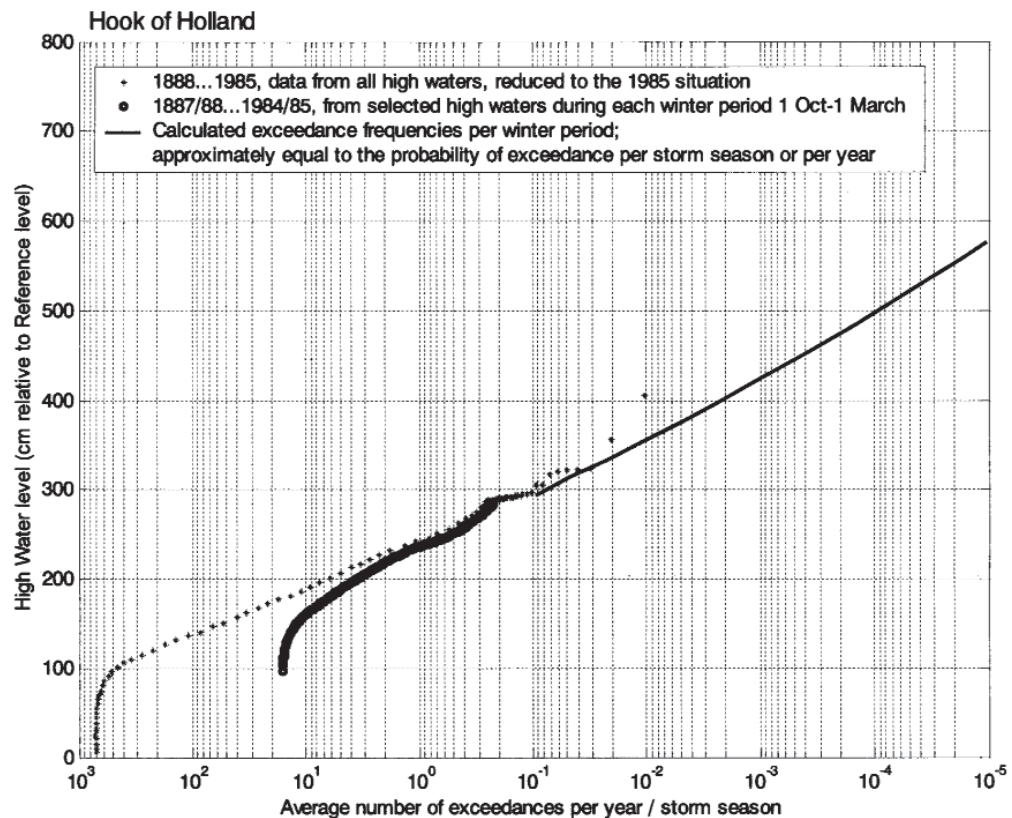


Figure 4.16 Measurements of high water levels during more than 100 years, including extrapolation to return periods of more than 10 000 years, at the Hook of Holland, the Netherlands (courtesy Rijkswaterstaat)

- 2 **Design of future flood defences** (northern Europe). Similar to the above except that the expected sea level rise should be taken into account. This can be around 0.5 m per century; the hydraulic boundary conditions will change as well (see Section 4.2.2.10).
- 3 **Design of coastal structures such as breakwaters** with return periods in the order of 50–100 years. Table 4.4 gives an example of design water levels at a specific location. Some of the contributions depend on the water depth and an estimate of sea level rise is considered on this example.

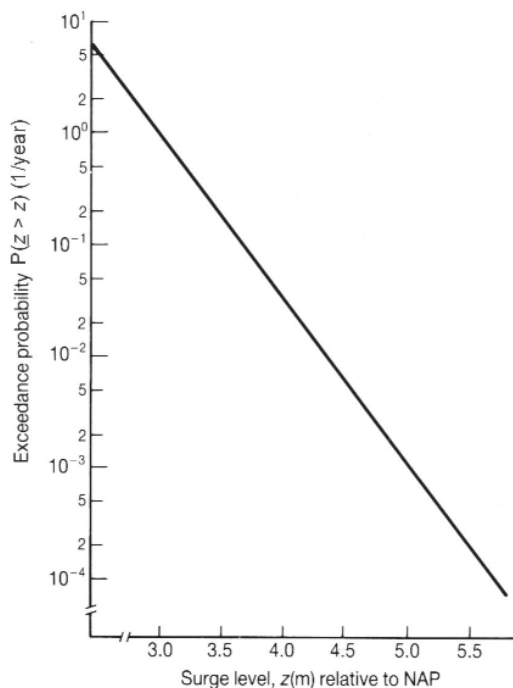
Table 4.4 Example of contributions to design water level at a specific location with a return period of 100 years

Item	Contribution to design water level (m)		
	$h = 15 \text{ m}^*$	$h = 10 \text{ m}$	$h = 5 \text{ m}$
Astronomical tide	1.3	1.3	1.3
Seasonal variation	0.10	0.10	0.10
Wind set-up/storm surge	0.20	0.25	0.30
Wave set-up	-0.03	0.03	0.10
Barometric pressure	0.20	0.20	0.20
Seiches and long waves	-	-	-
Global sea level rise	0.25	0.25	0.25
Total	2.02	2.13	2.25

Note

* h = water depth. The location has a mild sloping foreshore and is depth-limited.

Having determined the probability distribution of water levels, economic optimisation may then be used to select the appropriate extreme design level and the corresponding risk.

**Figure 4.17**

Example of fitted exceedance curve for water (storm surge) levels for a location on the Dutch coast. NAP is a local reference level

Once exceedance curves for all water level components are determined, the next step is to derive the combined (design) water level. The exceedance frequency is a function of the exceedance frequencies of the components. In the worst case, when all components are fully dependent, they occur simultaneously and the design level is simply obtained from the sum of all components corresponding to a chosen frequency. Possible reductions in the severity of the design level with respect to this worst case may arise from the degree of mutual correlation between the water level components. Analysis of the underlying physical processes may enable assessment of possible dependencies and may allow a joint probability analysis of the water level effects (see Section 4.2.5) to be carried out to produce an exceedance curve for the total water level.

Considering now the frequent problem of a design water level resulting from the combination of tide and storm surges there are two approaches that can be used.

(1) Separation of tides and storm surges

The tidal elevation is a purely deterministic motion that can be accurately predicted (see Section 4.2.2.2), therefore a first approach is to separate in the measured **high water** levels (HW), the tidal component and the storm surge component (defined as the difference between measured sea level and predicted tidal level). The deterministic characteristic of the astronomical tide means that the exceedance curve for the tidal level is known in principle with very high precision. The exceedance curve for the storm surge is obtained by fitting storm surge data to a standard statistical distribution (see Box 4.10 and Figure 4.17). Equation 4.25 derived by Simon (1994) describes the probability that the high water level, HWL (m), exceeds a given value Z^* :

$$P(Z^*) = P(\underline{HWL} \geq Z^*) = \int_{Z_{\min}}^{Z_{\max}} p(z) S(Z^* - z) dz \quad (4.25)$$

where z = tidal water level at high water, which lies between the (known) minimum and maximum values Z_{\min} and Z_{\max} respectively; $p(z) dz$ = probability that the tidal high water level lies between z and $z+dz$; $S(x)$ = probability distribution function of the storm surge component, ie $S(x) = P(\text{Storm surge} \geq x)$.

As there are on average 705.8 high waters a year, the return period of the total water level, $T_R(Z^*)$ (years) at high water is described by Equation 4.26.

$$T_R(Z^*) = \frac{1}{705.8 P(Z^*)} \quad (4.26)$$

(2) Statistics on the measured total water level

Often very limited data is available on the separate component effects leading to extreme water levels. In these cases a simple empirical approach that may be usefully adopted is the method of analysis of annual extreme water levels. The required data is often readily available from national sources, local ports and publications (eg Graff, 1981; Blackman, 1985). The method simply involves fitting the annual extreme water level data to an appropriate long-term distribution (see Box 4.10; a Gumbel distribution is recommended for water levels). The limitation is method sensitivity to outliers and the length of the records, but the overall approach is justified by the fact that correlation between astronomical tide and meteorological surge is very low in practice.

It is generally sufficient to work from the reliable published extreme water levels and to convert them to the site of interest. Any uncertainty involved in calculating extreme water levels in this way is usually small compared with uncertainties associated with prediction of extreme wave conditions and to an assessment of their correlation with extreme water levels. Examples of available extreme water level data and tables include:

- **United Kingdom.** Many long-term sets of water level data around the UK have been analysed (Graff, 1981; Coles and Tawn, 1990; POL, 1995) to predict extreme water levels at about 50 specific locations. POL (1997) goes a stage further in inferring extreme water levels at about 35 km intervals around the UK, taking account of the correlation between tides and surges at individual A Class tide gauges and the spatial correlation between nearby gauges, using a combination of statistical analysis and numerical tidal modelling.
- **France.** In France, the Service Hydrographique et Océanographique de la Marine (SHOM) has also published extreme water levels to consider for projects with return periods from 1 to 100 years along the Atlantic, Channel and North Sea coasts (Simon, 1994).

Sometimes very little data on water levels are available for the site of interest, whereas they are available for neighbouring or comparable locations. Correlation techniques, interpolation and extrapolation are useful ways to convert existing data from neighbouring locations to the

site of interest (see Box 4.2). Although such methods may save time and cost, they should be applied with care, especially around convex coastlines. Wind effects, strong currents and differences in wave set-up will invalidate use of these methods. Correlation factors between locations can be derived or verified from a limited number of simultaneous measurements, both at the site for which the main data source exists and at the sites considered. Erroneous design data may result from the use of such correlations to water level, which are beyond the range of the verification.

Box 4.2 *Simple approach to correlate extreme water levels*

To derive a first estimate of a probability distribution of extreme water levels, for a site with only basic astronomical tidal information, one approach is to correlate this site with one nearby for which both tidal data and extreme water level predictions are available. Correlation is then achieved by assuming (Graff, 1981) that the ratio given in Equation 4.27 is the same for the two sites.

$$\frac{\text{Extreme level-Mean High Water Spring (MHWS) level}}{\text{Spring tide range (MHWS- MLWS)}} \quad (4.27)$$

Where available and appropriate, a slightly more accurate estimate could be achieved by replacing spring tidal range in the above ratio with the sum of the principal semi-diurnal tidal components, $M_2 + S_2$ (see Section 4.2.2.2 for definitions).

4.2.3 Marine and estuarine currents

4.2.3.1 General

Although in a marine environment waves are usually the dominant loading (see Section 4.2.4), currents should also be considered during the design of rock structures. This particularly applies for estuaries where both marine and river dynamics are superimposed and combined (see Section 4.2.3.2). For river environments currents are often the dominant loading; river hydraulics are dealt with extensively in Section 4.3, and in particular in Section 4.3.2 for river discharges and currents. This section focuses on marine and estuarine environments.

Depending on the environment (sea, river, estuary), currents have different origins, strength, time scales and statistical characteristics. Along the coast and in estuaries most currents are related to the tide, whereas in rivers the river discharge is the dominating factor. For marine design conditions, however, wind- and wave-induced currents may also have to be considered.

Knowledge of currents may be required when considering structural design (stone stability), construction and transport (required anchoring, possible speed of vessels). Indirectly, currents may affect a structure through erosion of the sea bed.

Computation of flow conditions is based on the principle of conservation of mass and momentum. Most problems can be solved by combining the conservation laws (or simplified versions thereof) with a set of boundary conditions and experimentally determined parameters. The basic equations and their simplifications can be found in the literature (Bonnefille, 1992). For practical marine and estuarine applications two situations can be distinguished:

- a 2D horizontal area, that is the general case
- a 3D case.

Simplified equations are presented in the following sections to predict the flow conditions.

4.2.3.2 Components of marine and estuarine currents

The response of rock and coarse sediments to currents is discussed in Section 5.2.3. Principal sources and types of currents in marine and estuarine environments are (see the flow chart in Figure 4.6):

- tidal currents
- wind-induced currents
- density currents
- wave-induced currents (eg longshore currents)
- ocean circulation currents (caused by the Coriolis effect induced by rotation of the Earth)
- river discharge.

In most cases tidal currents are the most significant, and often the only ones considered in the design process. Wind-induced currents may result from local differences in wind and/or wave set-up (see Section 4.2.1 and Figures 4.11 and 4.12). Currents can be described over a given time-scale by a time-averaged magnitude, direction and variability due to spatial and turbulent effects. In addition, current velocities may vary in a vertical sense over the water depth.

Except for density- and wind-induced currents, the vertical distribution of velocities can often be described by a logarithmic function (see Section 4.3.2.4). Effects of wind, waves and turbulence on the structure of current are also addressed in Section 4.3.2.4 and are not repeated here.

Data on marine and estuarine current velocities can be obtained by direct measurement or by use of numerical models (see Section 4.2.3.4), although in the latter case measurements to provide boundary conditions (eg water levels) may still be needed. Alternatively, data on currents for preliminary design purposes can also be obtained from the sources listed below.

Charts and tables for marine currents

In many countries coast or port authorities or the admiralty can provide tables and charts of surface current velocities, observed in the vicinity of main shipping routes, ports, river mouths and estuaries. These are useful, as long as it is recognised that surface velocities may, for wind- and density-induced currents, differ significantly from the velocities closer to the bed.

Sources of data include the British and US admiralities, which hold data on surface currents in many strategic marine areas all over the world. In France, the Service Hydrographique et Océanographique de la Marine (SHOM) provides both measured tidal current velocities at numerous places and charts of tidal currents produced from an advanced numerical model. Marine and offshore activities have also often necessitated current (and other) measurements, but such data may be in the private domain and difficult to obtain.

Correlation and transformation

When current data are available from one or more nearby locations, the currents for the site of concern might be estimated from correlation, interpolation or extrapolation. However, only for tidal- or wind-induced currents a more or less reliable correlation can be assumed between neighbouring locations. The sites to be correlated should display good similarity with regard to geography (alignment of coastline, exposure to wind and waves, location relative to river mouths, bays, breakwaters) and bathymetry (depth contours). Correlation factors for one or more other locations can be derived from a limited number of simultaneous measurements both at the site and at the correlated sites.

Analytical models

Few types of current allow description with useful analytical expressions. Where such derivations are possible, solutions are found for the governing equations of momentum and continuity by making geometric simplifications and/or by neglecting terms in the equations.

Even when such solutions are available, empirical input is often needed. Examples of possibilities for analytical solution include:

- the tidal current in the entrance of a harbour basin or estuary. If the geometry allows for schematisation by a simple rectangular shape, the storage equation (based on continuity only) can be used to relate the current velocity to the (known) water levels and width and length of the basin (see Section 4.2.3.3 for examples of applications)
- longshore and density currents may allow for an analytical approach, but rarely without any empirical support (eg Bowen (1969) and Brocard and Harleman (1980)).

4.2.3.3 **Estuarine flow conditions, including basin model and density currents**

In river mouths and estuaries, river discharges determine the hydraulic conditions together with the tide. In some cases, wind waves may also have some influence on the water motion. In wide and in funnel-shaped estuaries the flow is two-dimensional, though a distinct pattern of channels and tidal flats and banks still forms the main feature of the watercourse. Density differences may also play a role. In this section attention focuses on a basin storage model and on the interaction between tide and river runoff. The hydraulic interactions with closure dams are discussed in Section 5.1.2.3.

Types of estuary and tidal inlet

From a practical point of view various types of estuary can be distinguished: short and long estuaries, tidal rivers and tidal inlets.

- **Short estuary**

The estuary length is small (less than 10–15 per cent) relative to the length of the tidal wave, which ranges between 200 km and 1000 km, depending on the water depth and the period of the tide (ie diurnal or semi-diurnal). The water surface in the estuary rises and falls as a function of the tide at sea and the characteristics of the estuary, but remains practically horizontal all the time. Analytical models of the hydrodynamics of an estuary have been published (eg Friedrichs and Aubrey, 1994; Savenije, 1998).

- **Long estuary**

The tidal wave propagates into the estuary and reflects against its inward boundary. Depending on the estuary length, the tide can be amplified considerably as a result of reflection. Freshwater inflows are usually of minor importance.

- **Tidal river**

A long and relatively narrow watercourse, where the tide penetration is mainly governed by the bed slope and the upstream river discharge. If the river mouth is funnel-shaped, reflection can also be of importance.

- **Tidal inlet**

In addition to these estuary types, tidal inlets can often also be of interest. Mehta and Joshi (1986) developed a simple hydrodynamic model of such inlets for the case of a sinusoidal tide. Their figures 2 to 5 may be used for practical applications.

The water motion in an estuary accords with physical laws (see Section 4.2.3.1) and is governed by a set of boundary conditions:

- the tide at the seaward boundary
- the geometry of the estuary

- the upstream discharge.

In the case of tidal motion the physical laws reduce to the so-called **long wave equations**, based on the assumption that vertical velocities and accelerations are negligible. Depending on the type of estuary, the long wave equations may be further simplified.

Basin storage model for closure dams in estuaries

When a closure dam is constructed in an estuary the hydraulic resistance changes during the construction phase, which affects the flow velocities and water levels in the estuary. The discharge, water level and maximum flow velocity can be estimated using a basin storage model, provided that the estuary length, L_b (m), is short relative to the length, L (m), of the tidal wave (see Equation 4.28).

$$L_b / L < 0.05 \quad (4.28)$$



Note: b is affected by horizontal closure while h_0 is affected by vertical closure.

Figure 4.18 Definition sketch of basin model

Case 1 – sill. As long as there is no appreciable constriction at the estuary mouth, ie when b/h_b is sufficiently large (see definition sketch in Figure 4.18), the discharge Q (m³/s) through the entrance attributable to the vertical tide inside the basin can be determined by using Equation 4.29:

$$Q(t) = B L_b \frac{dh}{dt} \quad (4.29)$$

where $Q(t)$ = tidal discharge (m³/s) and h = water level in the estuary or the basin (m).

In the case of a sinusoidal tide of amplitude \hat{h} , Equation 4.29 becomes Equation 4.30:

$$Q(t) = \frac{2\pi}{T} B L_b \hat{h} \sin\left(\frac{2\pi t}{T}\right) \quad (4.30)$$

where, apart from the definitions shown in Figure 4.18, \hat{h} = amplitude of tide in the estuary (m), t = time after the beginning of the tide (s), T = tidal period (s).

Cross-sectional mean velocity U (m/s) at the estuary mouth can be evaluated by Equation 4.31:

$$U = \frac{Q}{b h_0} \quad (4.31)$$

where h_0 = water depth in the gap (m) that varies with the tidal time as h and b = width of the estuary mouth (m).

Case 2 – vertical closure. When the closure dam forms an appreciable vertical constriction, the tidal discharge through the mouth starts to decrease and the mean flow velocity in the closure gap, U_0 , depends on the water levels, h and H , inside and outside the basin respectively. When the flow is into the basin, U_0 can as a first estimate be determined by using Equation 4.32:

$$U_0 = \sqrt{2g(H - h_b)} \quad (4.32)$$

where H = sea-side water level above the dam crest (m) and h_b = water level in the basin above the dam crest (m).

Further discussion of discharge and velocity through the gap is given in Section 5.1.2.3 where discharge coefficients are introduced to improve precision. A simple model to calculate the response water level of the basin, h , given the tide at the seaward side as the boundary condition, $H(t)$, is based upon Equation 4.33, which results from the combination of Equations 4.29, 4.31 and 4.32:

$$BL_b \frac{dh}{dt} = h_0 b \sqrt{2g(H - h_b)} + Q_{river} \quad (4.33)$$

where Q_{river} = river discharge into the basin (m^3/s), if relevant, h_0 = water depth on the crest of the closure dam (m) (see Section 5.1.2.3) and H , h_b and b are defined according to Figure 4.18.

Combined closure. Assuming a sinusoidal tide at sea and $Q_{river} = 0$ m/s, the maximum flow velocity in the closure gap during the tide, U_g or U_0 (m/s), can be determined with the design graph given in Figure 4.19. Note that Figure 4.19 plots $U_g/\sqrt{\hat{h}}$, which is not a non-dimensional quantity where U_g is in m/s and \hat{h} is in m. In this graph Y serves as an input parameter, the value of which should be calculated with Equation 4.34:

$$Y = 0.001 \frac{T_{M2}}{T} \frac{BL_b}{b/\sqrt{\hat{h}}} \quad (4.34)$$

where T = tidal period (s) and T_{M2} = period of semi-diurnal tide (= 44 700 s).

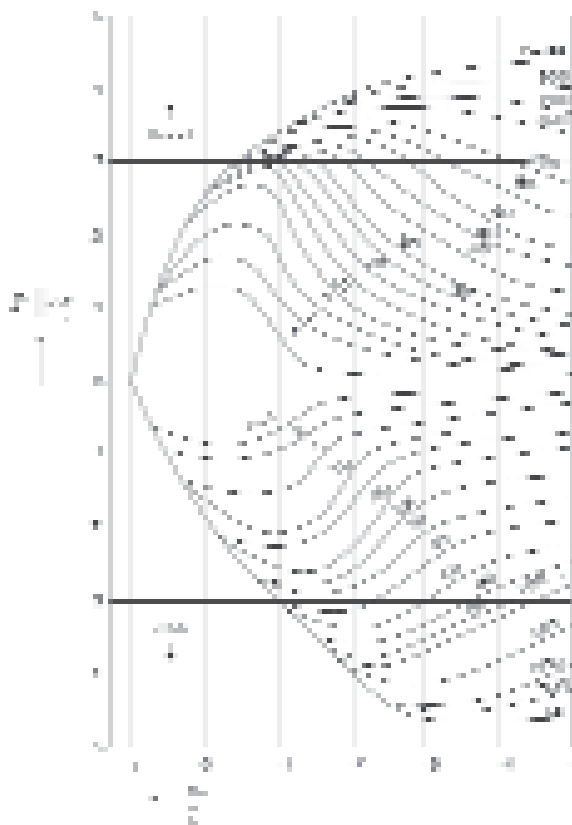


Figure 4.19

Design graph for maximum velocity; note that h_b should read h_0 , the water depth (on the sill) in the closure gap

This method is not valid for small closure gaps. If the gap is not wider than about 20 per cent of the original width, it is recommended to use more sophisticated mathematical models.

Interaction of tide and river runoff

For the discharge generated by a combination of a local horizontal tide $Q_{tide}(x)$ and river runoff Q_{river} , the resulting horizontal tide or discharge $Q(x)$, in a cross-section at a distance x inland from the entrance of the estuary, can be determined by Equation 4.35.

$$Q(x) = Q_{river} - Q_{tide}(x) \cos\left(\frac{2\pi t}{T}\right) \quad (4.35)$$

$Q_{tide}(x)$ is the local amplitude of the pure horizontal tide, the value of which varies along the estuary. The following cases can be distinguished (see Figure 4.20):

- $Q_{tide}(x) \gg Q_{river}$ entrance of the estuary
- $Q_{tide}(x) > Q_{river}$ section with bidirectional flow
- $Q_{tide}(x) < Q_{river}$ section with unidirectional flow
- $Q_{tide}(x) = 0$ river section.

Generally, the river discharge Q_{river} varies in time (see Sections 4.3.1 and 4.3.3). When Q_{river} increases, Q during ebb increases and Q during flood decreases. In addition, the respective duration of the ebb flow increases and that of the flood flow decreases. When the river discharge is smaller, the tidal penetration length is greater and the tidal amplitude at a certain location is larger.

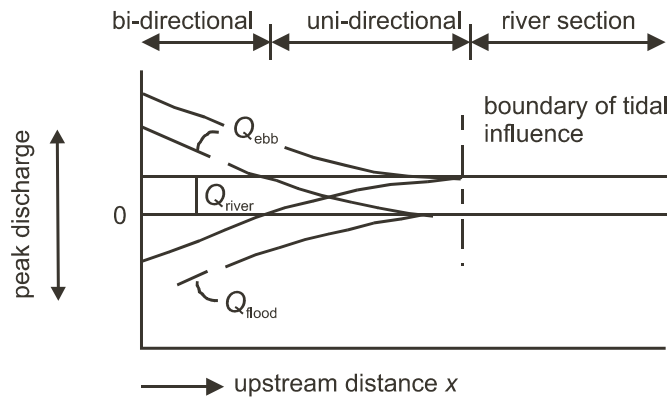


Figure 4.20 Combined tide and river discharge

Density currents

Density-induced flow components may occur because of variations in the fluid density caused by salinity (and/or temperature). The salinity of seawater is about 30 parts per thousand and varies slightly (by some 5 ppt) from place to place. For the calculation of density-induced flow velocities reference is made to the available mathematical models (see Sections 4.2.3.4 and 4.3.5.2).

Figure 4.21 shows examples of the velocity profile in an estuary with a river discharge for a highly stratified and a well-mixed estuary. The highly stratified situation is characterised by a salt wedge-type lower layer originating from the sea (with weak tidal velocities and hence weak vertical mixing) and a freshwater upper layer originating from the river discharge. In the well-mixed situation the fluid density is constant over the depth, but varies in longitudinal direction from the seawater to the freshwater value. Whether an estuary is well mixed or highly stratified can be evaluated with two stratification parameters, namely the **volume ratio number** V (see Equation 4.36), the ratio of runoff volume and tidal prism and the **estuary number** E (see Equation 4.37):

$$V = Q_{river}T / V_f \quad (4.36)$$

$$E = Fr^2 / \alpha \quad (4.37)$$

where:

Q_{river}	=	river discharge (m^3/s)
T	=	duration of tidal cycle (s)
V_f	=	volume of seawater entering the estuary at the entrance during flood (m^3)
Fr	=	Froude number at the mouth = U_{max} / \sqrt{gh} (-)
U_{max}	=	maximum velocity in the entrance during a tidal cycle (m/s)
α	=	reduction factor (-).

Criteria for stratification are presented in Table 4.5.

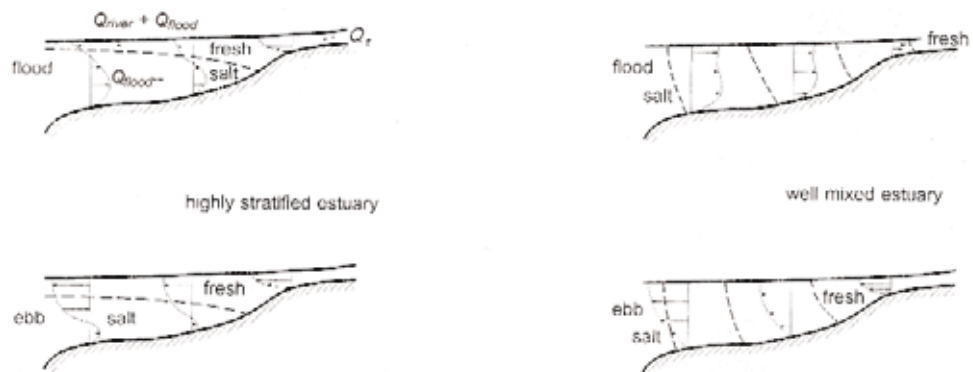


Figure 4.21 Density variations and velocity profiles in a stratified and a mixed estuary

Table 4.5 Stratification criteria for estuaries

Stratification rate	Volume ratio number V	Estuary number E
Highly stratified	$V > 1.0$	$E < 0.005$
Partially stratified	$0.1 < V < 1.0$	$0.005 < E < 0.2$
Well-mixed	$V < 0.1$	$E > 0.2$

4.2.3.4

Numerical modelling of marine and estuarine currents

Modelling of water levels and currents is discussed in details in Section 4.3.5. Nowadays numerical models are most often used to obtain current conditions in marine and estuarine environments, and physical modelling is rarely used for this purpose.

When tides are the dominant phenomenon, 2DH models are used on the basis of depth-integrated long wave equations (also called **Saint-Venant equations**). Models of this type include ADCIRC, DELFT-3D, MIKE-21 and TELEMAC-2D. An example of simulation is presented in Figure 4.22. Such models are based on structured or unstructured computational grids and use finite difference, finite volume or finite element methods to solve the mass and momentum equations of the flow. The modelling of tidal flats is usually included in such models, as well as the effect of wind stress at the free surface and atmospheric pressure gradient. These models can be coupled with wave models to compute wave set-up and wave-induced currents in the breaking zone.

For estuaries, when density and/or salinity effects are sensitive, 3D models are often employed to provide a proper description of the hydrodynamics. These models solve the Navier-Stokes equation with a free surface on a three-dimensional mesh (some examples are DELFT-3D, MIKE-3 and TELEMAC-3D).

In both cases, proper boundary conditions need to be imposed (water level and/or velocity profile or discharge) as well as forcing conditions over the domain if applicable (wind field, atmospheric pressure). The modelling of bottom roughness is often sensitive in such computations and requires some attention during the construction and the calibration of the model. To validate the model before using it for applications, it is also important to compare the numerical results to measurements for a variety of conditions.

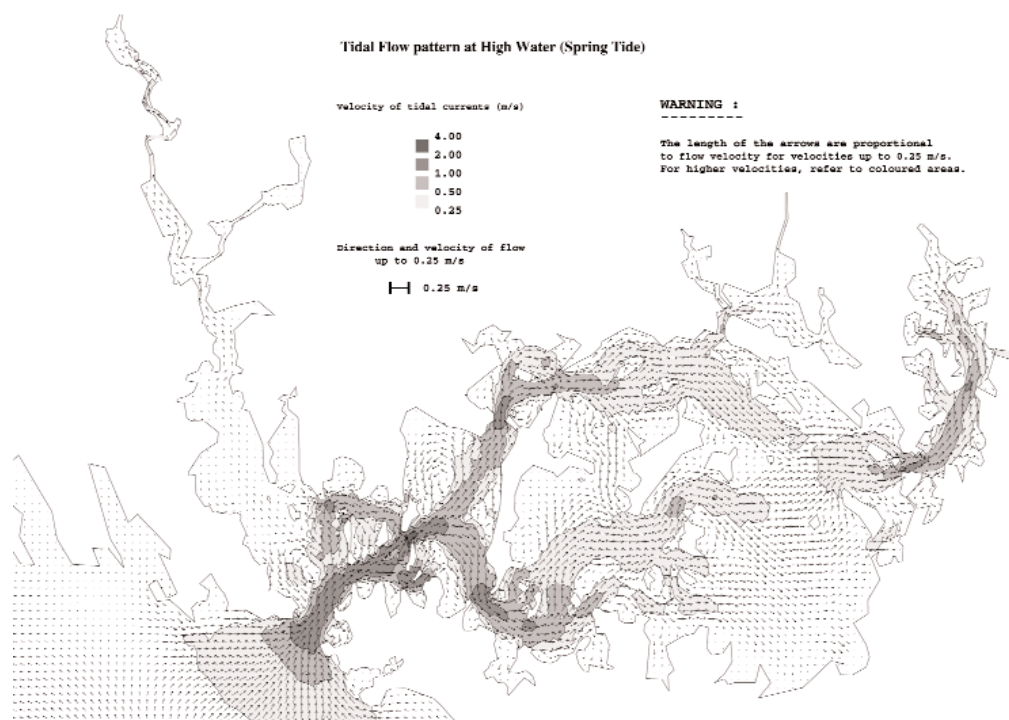


Figure 4.22 Example of tidal current field computed with a 2DH flow model (Morbihan Bay, France) (courtesy Cetmef)

4.2.4 Wind-sea and swell

The principal loadings exerted by waves upon marine structures can be subdivided into wave impact loads (short-duration pressures), drag loads (pressure plus shear) and inertia loads. In the design process these loadings should be schematised and described as functions of wave parameters. In this section, some important definitions, theoretical results and practical relationships related to waves are given to determine the design conditions for a structure exposed to wave attack.

NOTE: This section does not attempt to provide a complete text on waves. Additional information can be found in reference textbooks (eg Dean and Dalrymple (1991, 2004), Goda (2000), Tucker and Pitt (2001) etc).

4.2.4.1 General definitions related to waves, sea-states and wave climate

This section deals with gravity waves propagating at the surface of a water body (oceans, seas, lakes, rivers etc) and generated by the action of the wind at the free surface. This covers waves with typical periods ranging from 2 s to 30 s. One usually distinguishes between wind-sea and swell wave conditions:

- **wind-sea** – these waves are observed in the area where they are generated and occur as a result of wind action. Wind-seas are characterised by short periods (2 s to 10 s typically) and provide an irregular aspect of the sea surface
- **swell** – these waves were generated away from the zone where they are observed and there is no significant effect attributable to the local wind. Swell usually exhibits a more regular pattern than wind-seas, with longer periods (10 s to 30 s).

Temporal scales related to waves

Wave conditions can be analysed and considered at different temporal scales.

- *One individual wave*

A typical time-scale is in the order of one wave period, say 10 s. There are various ways of separating individual waves in a wave record (time series of sea surface elevation typically sampled at a frequency of 2 Hz over a duration of 20 min to 1 hour). Figure 4.23 schematically shows the shapes of one such isolated wave both in space (left panel) and in time (right panel). Note that the temporal and spatial profiles of the wave are symmetrical with respect to the vertical axis as the x axis was chosen in the direction of wave propagation. The **wave height**, H , is defined as the difference between the maximum and minimum elevations of the sea-surface (peak to trough wave height) over the duration of the wave. This duration is called the **period**, T , in the time domain and the **wavelength**, L , in the spatial domain. Designing a structure with respect to one individual wave (a so-called **maximum wave**) is not common practice for rubble mound breakwaters. This design approach is more frequently employed for the design of vertical breakwaters and offshore structures in deep water, such as oil or gas platforms and foundations for offshore wind turbines.

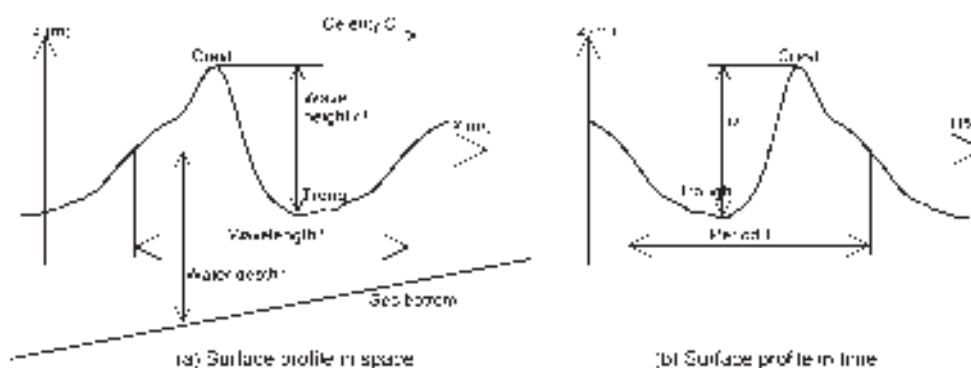


Figure 4.23 Definition sketch for individual wave parameters

- *A sea-state*

This corresponds to a period of time over which the successive individual waves, although different from each other, can be regarded as being the results of the same random process, so that they have the same average properties in a statistical sense. For this reason, the environmental conditions (such as wind speed, wind direction and water level) are assumed to be constant over the duration of a sea-state (typical time-scale in the order of 3 hours, say 300–500 waves). Characteristic wave heights and periods of a sea-state can be obtained by a statistical (or wave-by-wave) approach (see Section 4.2.4.4) or by a spectral approach (see Section 4.2.4.5). The design of marine rock structures is mainly based on such characteristic values of sea-states (eg significant wave height H_s , mean period T_m), representative of extreme conditions (see below).

- *A storm event*

A storm event can be described by several sea-states, eg the increasing phase, the maximum phase and the decreasing phase. At locations under tidal influence the typical sea-state is very often only 2–3 hours, but without tidal effects it may last 6 hours or longer depending on the evolution in time of wind conditions (typical time-scale in the order of 12 hours to one day). In the design process of marine rock structures it is important to take proper account of the actual duration of storm events (in particular due to the effect of tides) for the site of interest, when determining the sequence of sea-states (number, characteristics and duration of successive sea-state conditions) to be tested on a physical model for instance.

- *A short-term (or daily) wave climate*

This is obtained by examining the characteristics of sea-states over a period of between one and two years from a statistical approach (typical time-scale in the order of one year). It gives the distribution of wave heights, periods, directions etc and the correlation between two of these parameters (see Section 4.2.4.8). The short-term wave climate also uses a wave rose, comparable to the wind rose. In addition, seasonal effects can be examined and quantified by restricting the analysis of wave measurements to, for example, the winter season. The short-term wave climate gives insight into operability for floating equipment and crest levels for temporary haul roads. It usually provides valuable information on the incoming directions of waves, to be combined with given wave heights and periods for defining design conditions.

- *A long-term (or extreme) wave climate*

These terms describe the distribution and probability of occurrence of extreme sea-states (storm). The distribution function of extremes is different to that used for the short-term wave climate. It has to be based on a dataset of sufficient durations (typically 5–10 years) containing a sufficient number of storms, so that extreme wave heights of very low probability of occurrence can be estimated by statistical extrapolation (see Section 4.2.4.9). The extreme wave climate is used for both the functional (hydraulic response) and structural (stability) design of the structure. The typical return periods of wave events for design conditions range from 25 to 100 years or higher, depending on the design life and performance requirements of the structure (see Section 2.3).

4.2.4.2

Representation of regular/random and long-crested/short-crested waves

Waves at the sea surface always show irregular, more or less **chaotic**, patterns. The sea surface motion results from a combination of waves having different heights, periods and directions. The irregularity of wave heights and period gives rise to the terms of **irregular** or **random** waves. The irregularity in propagation directions may be observed by considering the length of wave crests on a picture of the ocean surface: when the waves have approximately the same direction their crests are clearly identifiable, long and almost parallel (so-called **long-crested waves**), whereas a spreading of wave energy over a range of directions manifests itself by rather short and non-parallel crests (so-called **short-crested waves**). Although all sea-states are irregular and short-crested in the general case, the representation of regular long-crested waves is discussed first, followed by the irregular representation.

Description and definitions for individual waves or regular waves

The simplest approach to represent a series of waves corresponds to regular and long-crested waves. In this basic representation, waves repeat indefinitely, each wave being identical to the others, with the same height H . They are monochromatic and periodic both in time (with period, T (s)), and in space (with wavelength, L (m)) and unidirectional (with propagation direction, θ (°)). Alternatively, one can use the frequency $f = 1/T$ (Hz or 1/s) or the angular frequency, $\omega = 2\pi f = 2\pi/T$ (rad/s), to describe the temporal periodicity, and the wave number, $k = 2\pi/L$ (rad/m), to describe the spatial periodicity.

The parameters describing spatial periodicity (k or L) are related to the parameters describing temporal periodicity (T , f or ω), together with the water depth, h , by the so-called *dispersion relation*, which for the case of linear (small amplitude) wave theory is given by Equation 4.38.

$$\omega^2 = gk \tanh(kh) \quad (4.38)$$

When the water depth, h , and wave period, T (or the angular frequency, ω), are known, the determination of the wave number, k (or the wavelength $L = 2\pi/k$), requires the resolution of the implicit Equation 4.38. Iterative numerical schemes may be employed to solve this

equation accurately whenever necessary, but explicit approximations, such as given in Box 4.3, can also be used.

The propagation velocity of wave crests (**phase speed**) is $c = L/T = \omega/k$ (m/s) and the propagation velocity of energy (**group velocity**) is given by $c_g = \partial\omega/\partial k$ (m/s). In linear wave theory, based on Equation 4.38, the expressions for phase and group velocity are given by Equations 4.39 and 4.40 respectively.

$$c = \frac{g}{\omega} \tanh(kh) = \sqrt{\frac{g}{k} \tanh(kh)} \quad (4.39)$$

$$c_g = nc \quad \text{with} \quad n = \frac{1}{2} \left(1 + \frac{2kh}{\sinh(2kh)} \right) \quad (4.40)$$

Note that the factor n has two asymptotic values: (1) when the relative water depth, kh (-), is small, n tends towards 1; (2) when kh is large n tends towards $1/2$; in this case the wave energy propagates at a speed that is half of that of individual waves. For these asymptotic cases, particular expressions of k , L , c and c_g may be derived analytically and are listed in Table 4.6, together with the non-dimensional criteria for using these approximations. For values in deep water (large value of kh), the subscript “0” or “o” was used conventionally (eg L_o for the deep-water wavelength). Here the latter, “o” (of offshore), is used. From Table 4.6 it should be noted, for example, that in shallow-water conditions, c and c_g do not depend any more on the wave period, T , and that all waves have the same velocity (non-dispersive waves), which, in this case, equals the velocity of energy.

Box 4.3 *Explicit approximations of the linear dispersion relation for water waves*

There are numerous approximations of the dispersion relation given by Equation 4.38. Equation 4.41 gives the rational one proposed by Hunt (1979) at order 9, which is very accurate (always less than 0.01 per cent of relative error in kh):

$$(kh)^2 = (k_o h)^2 + \frac{k_o h}{1 + \sum_{n=1}^9 a_n (k_o h)^n} \quad (4.41)$$

where $k_o = 2\pi/L_o = \omega^2/g =$ deep-water wave number (rad/m) and the values of a_n are as follows:

$$\begin{array}{lllll} a_1 = 0.66667 & a_2 = 0.35550 & a_3 = 0.16084 & a_4 = 0.06320 & a_5 = 0.02174 \\ a_6 = 0.00654 & a_7 = 0.00171 & a_8 = 0.00039 & a_9 = 0.00011. & \end{array}$$

Hunt (1979) also provides a similar formula at order 6, with a relative error in kh always less than 0.2 per cent.

Alternatively, the simpler explicit formulation by Fenton and McKee (1990) (see Equation 4.42) can be used. Although it is less accurate than the former (1.5 per cent of maximum relative error), it is easier to use on a calculator.

$$k = \frac{\omega^2}{g} \left\{ \coth \left[\left(\omega \sqrt{\frac{h}{g}} \right)^{3/2} \right] \right\}^{2/3} \quad \text{or equivalent:} \quad L = L_o \left\{ \tanh \left[(k_o h)^{3/4} \right] \right\}^{2/3} \quad (4.42)$$

Other explicit expressions have been proposed by Eckart (1952), Wu and Thornton (1986), Guo (2002).

Table 4.6 Asymptotic values of the dispersion relation and related quantities

Variable	Approximations with criteria	
	Shallow-water or long wave approximation (<i>small kh</i>)	Deep-water or short wave approximation (<i>large kh</i>)
	$h/L < 1/25$ or $T\sqrt{g/h} > 25$	$h/L > 1/2$ or $T\sqrt{g/h} < 4$
Dispersion relation	$\omega^2 = gh k^2$	$\omega^2 = gk_o$
Wave number k (rad/m)	$k = \omega/\sqrt{gh}$	$k_o = \omega^2/g$
Wavelength L (m)	$L = T\sqrt{gh}$	$L_o = gT^2/(2\pi)$
Phase speed c (m/s)	$c = \sqrt{gh}$	$c_o = gT/(2\pi)$
Group velocity c_g (m/s)	$c_g = c = \sqrt{gh}$	$c_{go} = 1/2 c_o = gT/(4\pi)$

Description and definitions for irregular waves or sea-states

For a sea-state, composed of waves having different characteristics but belonging to the same random process (ie constant environmental conditions), two approaches are used to describe the wave field.

- 1 **Long-crested random waves** are still unidirectional, but include a range of wave heights and periods. The irregular or **random** wave train is composed of successive waves having different heights and periods. Two approaches are used to describe random waves and are set out below: the statistical (or wave-by-wave) approach, which consists of determining the **statistical distributions** of wave heights, periods, directions etc (see Section 4.2.4.4), and the **spectral approach**, which is based on the determination and use of the spectrum of wave energy (see Section 4.2.4.5). In both cases, representative parameters can be calculated to characterise the sea-state (eg the significant wave height H_s and the mean wave period T_m).
- 2 **Short-crested random waves** additionally include a range of directions, defined in terms of the standard deviation of wave energy propagation direction or some other standard spreading function. A more complete description of the sea-state is given by the directional spectrum ($S(f, \theta)$), which gives the distribution of wave energy as a function of frequency and direction (see Section 4.2.4.5). Short-crested waves provide the best representation of true ocean waves, and this representation of wave conditions has now become the standard way of dealing with wave actions in the engineering practice. The direction of wave incidence and the angular spreading of wave energy have been shown to have some effects on wave-structure interaction processes, such as stability of rubble mound breakwaters, run-up and overtopping (Galland, 1995; Donnars and Benoit, 1997).

4.2.4.3**Characterisation of wave conditions and wave kinematics****Characterisation of wave conditions by non-dimensional numbers**

In order to characterise wave conditions, to investigate which processes are dominant during wave propagation and transformation, and/or to estimate wave loading on structures, several non-dimensional numbers are used. They can be computed for regular waves or random waves by using representative wave parameters. The most useful parameters are set out below.

- **The relative water depth: kh or h/L and the non-dimensional period $T\sqrt{g/h}$**

They are used to determine the manner in which seabed bathymetry affects waves. For example, the parameters were used in the previous section (see Table 4.6) to derive approximations of phase speed and group velocity in low and large relative water depths respectively.

- *The wave steepness $s = H/L$ and the relative wave height H/h*

They are measures of non-linearity of the wave (see Figure 4.23). They are used in particular to quantify the importance of non-linear effects and they appear in the formation of criteria for predicting wave breaking. A specific use of the wave steepness is made if the wave height is taken at the toe of the structure and the wavelength in deep water. In fact this is a fictitious wave steepness $s_o = H/L_o$ and is often used in design formulae for structures. The main goal in this case is not to describe the wave steepness itself, but to include the effect of the wave period on structure response through $L_o = gT^2/(2\pi)$, which is only valid offshore.

- *The Ursell number U (-)*

This is a combination of the former numbers and is presented in Equation 4.43. It is used to characterise the degree of non-linearity of the waves.

$$U = \frac{HL^2}{h^3} = \left(\frac{H}{h}\right) \left/\left(\frac{h}{L}\right)^2\right. \quad (4.43)$$

- *The surf similarity parameter ξ , also known as the Iribarren number, Ir (see Equation 4.44)*

This is used for the characterisation of many phenomena related to waves in shallow water, such as wave breaking, run-up and overtopping. It reflects the ratio of bed slope and fictitious wave steepness, s_o .

$$\xi = \frac{\tan\alpha}{\sqrt{s_o}} = \frac{\tan\alpha}{\sqrt{H/L_o}} = \frac{\tan\alpha}{\sqrt{(2\pi H)/(gT^2)}} \quad (4.44)$$

When the deep-water wave length, H_o , is used instead of H , this number is denoted ξ_o or Ir_o .

This parameter is often used for beaches, and often for design of structures too. It gives the type of wave breaking and wave load on the structure. Actually, waves can break first on the depth-limited foreshore before reaching the structure and then break once again on to the structure. On the foreshore the breaker type is generally spilling, sometimes plunging. On the structure itself it is never spilling, but plunging (gentle structure slope), surging or collapsing (see Section 4.2.4.7 for the definition of breaker types).

When using these parameters for random waves, it should be stressed and indicated (as a subscript of these parameters, for example) which characteristic wave height and period are being used in their evaluation (eg subscript “ p ” if the peak period T_p is used, and “ m ” if the mean period T_m is used).

For further discussion on the use and the notation of ξ , please also refer to Section 5.1.1.1.

Overview of methods for computing wave kinematics

Many wave theories are available to derive other wave parameters and kinematics (velocities, accelerations, pressure etc) from the above-mentioned basic parameters (eg H and T , plus possibly a flow speed). The majority of design methods are based on Stokes linear wave theory (ie small amplitude wave theory) derived for a flat bottom (ie constant water depth). A major advantage of linear theory in design procedures is that the principle of superposition can be applied to wave-related data, obtained from a composite wave field. Using linear wave theory, practical engineering approximations can be derived for regular waves propagating in deep and shallow water respectively (see Table 4.6). Expressions for orbital velocities u_x , u_y , u_z and pressure p are presented below as Equations 4.45 to 4.48 for the case of a regular wave with a height H , period T (angular frequency $\omega = 2\pi/T$) and direction θ with respect to

the x axis. Other expressions for accelerations, particle displacements, etc can be found in reference textbooks such as Dean and Dalrymple (1991).

$$u_x(x, y, z, t) = \frac{H}{2} \omega \frac{\cosh(k(h+z))}{\sinh(kh)} \cos\theta \cos(\vec{k} \cdot \vec{x} - \omega t) \tag{4.45}$$

$$u_y(x, y, z, t) = \frac{H}{2} \omega \frac{\cosh(k(h+z))}{\sinh(kh)} \sin\theta \cos(\vec{k} \cdot \vec{x} - \omega t) \tag{4.46}$$

$$u_z(x, y, z, t) = \frac{H}{2} \omega \frac{\sinh(k(h+z))}{\sinh(kh)} \sin(\vec{k} \cdot \vec{x} - \omega t) \tag{4.47}$$

$$p(x, y, z, t) = -\rho g z + \rho g \frac{H}{2} \omega \frac{\cosh(k(h+z))}{\cosh(kh)} \cos(\vec{k} \cdot \vec{x} - \omega t) \tag{4.48}$$

Linear wave theory becomes less applicable when the wave shape deviates from purely sinusoidal and when wave steepness ($s = H/L$) increases. Non-linear analytical wave theories that may be used in these situations include Stokes' higher order wave theories, cnoidal wave theory, solitary wave theory and Dean's Stream Function theory. The description of these theories is beyond the scope of this manual but can be found in Sobey *et al* (1987), Fenton (1990) and Fenton (1999), for example. An overview of the applicability of wave theories is given in Figure 4.24. Note that T_{app} stands for the period for which the applicable model of wave theory is searched (ie T_m or T_p).

Numerical stream function methods (based on a Fourier decomposition of the stream function of the flow) are superior to all analytical theories (eg Stokes or cnoidal theories), whatever the water depth. Thus the recommendation for practical applications is to use this stream function approach (see Dean, 1965; Rienecker and Fenton, 1981; Fenton, 1988). Also note that some semi-empirical wave theories have been proposed for the case of a sloping bottom, namely the cocoidal theory of Swart and Crowley (1988) and the method of Isobe and Horikawa (1982).

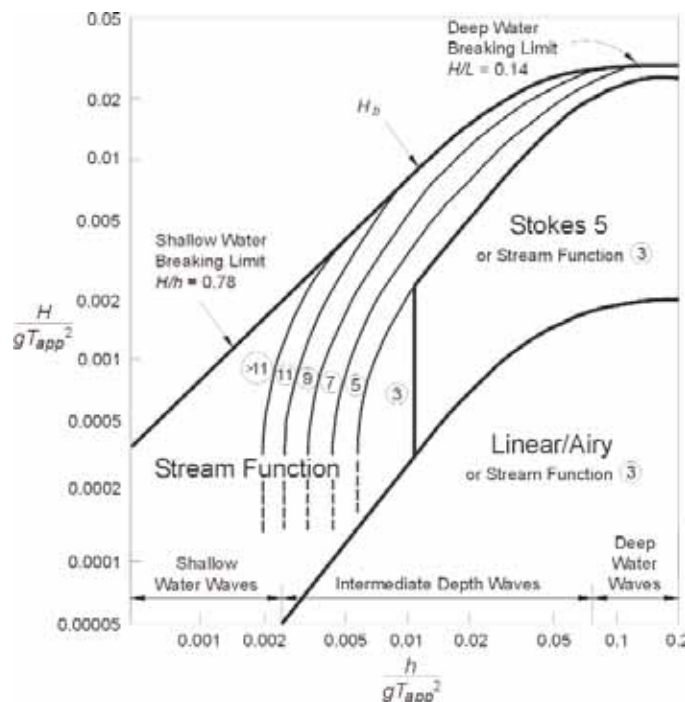


Figure 4.24
Range of applicability of wave theories (from American Petroleum Institute, 1993)

NOTE: The numbers in Figure 4.24 (3, 5... etc) stand for the order of the stream function.

Orbital velocities near the sea bed are required for design of rockfill used in offshore protection of pipelines under (combined current and) wave attack (see Section 5.2.2.5). Kirkgöz (1986) has shown that linear wave theory gives reasonable agreement with observed near-bed orbital velocities under the wave crest even at the transformation point of plunging breakers. In fact, this is true for the wave crest phase, but laboratory experiments show that

the linear theory significantly overestimates (by up to 40 per cent) the velocity under the wave trough in the breaking zone (eg Benoit *et al*, 2003).

Soulsby (1987) has provided design curves based on linear wave theory (see Figure 4.25) that enable calculation of near-bed orbital velocities for both monochromatic (regular) and random waves, where the maximum horizontal orbital bed velocity u_o was obtained from Equation 4.45 applied at the bottom (namely at $z = -h$) (see Equation 4.49).

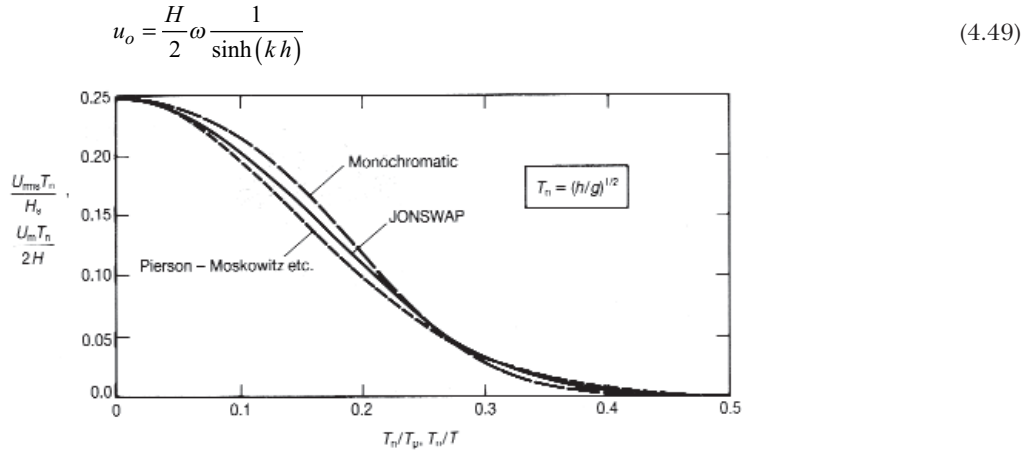


Figure 4.25 Near-bed orbital velocity for monochromatic waves and a spectrum of waves (from Soulsby, 1987)

4.2.4.4 Statistical properties and distribution of waves in a sea-state

Wave statistics play the major role in determination of design loads and risk assessment and thus in the overall design of rock structures in coastal and shoreline engineering. Some explanation of basic statistical wave properties and representative wave parameters is therefore necessary.

Wave-by-wave analysis and representative wave parameters

As indicated in Section 4.2.4.2, wind-generated waves are irregular (non-periodic) and a typical record of sea-surface elevation is depicted in Figure 4.26. This figure also illustrates the definition of the **zero-crossing** method to separate individual waves: each time the wave signal crosses the mean water level a new wave is counted. The individual wave period T_j of the wave j is the time between two successive zero-crossings and the corresponding **lowest trough to highest crest** height defines the height, H_j , of that individual wave. Two variants of the method exist: **zero up-crossing** and **zero down-crossing** (IAHR/PIANC, 1986). The latter is recommended, as the waves that are isolated by this approach have more physical meaning. The individual waves are thus composed of the trough and the following crest, as depicted on Figures 4.23 and 4.26.

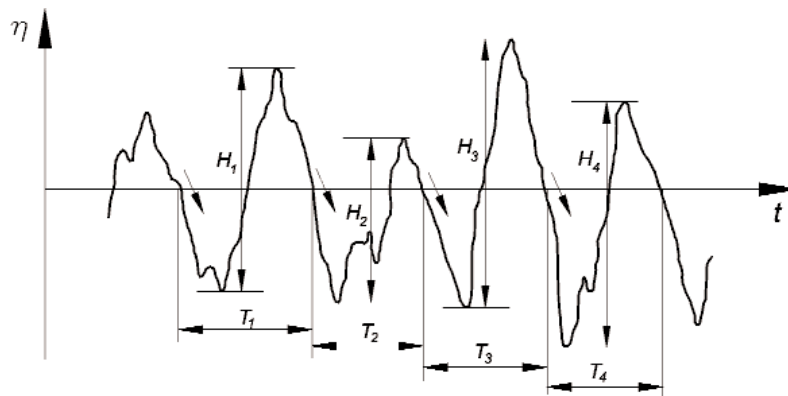


Figure 4.26 Typical record of irregular sea and principle of the zero down-crossing method

The standard recording period is 20 minutes to one hour (every three hours or every hour), but it can also be continuous. The important point is that a sea-state is a stationary process for a certain time only and so the analysis of a continuous record should be restricted to a duration over which the conditions can be assumed to be **statistically stationary**. On the other hand, to be statistically correct there should be a minimum number of waves in the record, typically at least 200 or 300 waves but preferably 500 waves.

From the records, the series of N waves (H_j, T_j) ($j = 1, \dots, N$) are sorted by decreasing wave height and a number of characteristic wave heights and periods may then be determined (IAHR/PIANC, 1986), the most often used being defined in Table 4.7.

In particular, note that two definitions are used for computing some representative wave heights of a sea-state of given duration:

- $H_{P\%}$ is the wave height that is exceeded by P per cent of the wave heights in the sea-state. In particular, $H_{2\%}$ is used in the design process of a breakwater (especially for predicting run-up and overtopping)
- $H_{1/Q}$ corresponds to the average height of the $1/Q$ largest wave heights in the sea-state. The most important wave heights of this type for design-related aspects are the significant wave height $H_{1/3} = H_s$ (average of the highest 1/3 wave heights in the sea-state), $H_{1/10}$, $H_{1/100}$ and $H_{1/250}$.

To obtain reliable estimates of larger wave heights (ie low values of P for $H_{P\%}$ and high values of Q for $H_{1/Q}$), the time-series of measured surface elevation should contain a sufficiently large number of waves. For example, the stable estimate of $H_{1/250}$ requires a very long record; for a sea-state comprising 500 waves, which is already quite a large number, $H_{1/250}$ will be determined as the average of only the two largest wave heights of that record. The same comment applies for the maximum wave height that has a large variability from one occurrence to another for given sea-state conditions. That is why the use of more stable wave heights (although larger than the mean wave height) such as $H_{1/3}$ or $H_{1/10}$ is preferred to characterise sea-state conditions.

Table 4.7 Characteristic wave heights and periods of a sea-state from a wave-by-wave analysis

Characteristic wave parameter	Definition
Mean wave height H_m	$H_m = \frac{1}{N} \sum_{j=1}^N H_j$
Root-mean-square wave height H_{rms}	$H_{rms} = \sqrt{\frac{1}{N} \sum_{j=1}^N H_j^2}$
Significant wave height $H_s = H_{1/3}$	Average of the highest 1/3 of wave heights in the record
Wave height $H_{1/10}$	Average of the highest 1/10 of wave heights in the record
Wave height $H_{1/100}$	Average of the highest 1/100 of wave heights in the record
Wave height $H_{1/250}$	Average of the highest 1/250 of wave heights in the record
Wave height $H_{2\%}$	Wave height exceeded by 2% of wave heights in the record
Maximum wave height H_{max}	Highest wave height in the record
Mean wave period T_m	$T_m = \frac{1}{N} \sum_{j=1}^N T_j$
Significant wave period $T_s = T_{1/3}$ (sometimes also referred to as $T_{H_{1/3}}$)	Average of the periods associated with the largest 1/3 of wave heights in the record (ie average of periods of the waves selected to compute $H_{1/3}$)
Period of maximum wave height T_{Hmax}	Period of the largest wave height in the record
Maximum wave period T_{max}	Largest wave period in the record

Distribution of individual wave heights in a sea-state

During each sea-state a (short-term) distribution of wave heights applies. Once the distribution function of wave heights is known, all the characteristic wave heights listed in Table 4.7 can be computed. Some basic and important results for wave distributions are summarised below: first for the deep-water case, and then for the shallow-water case. The latter is more important for the design of coastal structures, but also more difficult to model and parameterise.

- *Distribution of deep-water wave heights*

In deep water the water surface elevation usually follows a Gaussian process and thus the individual wave heights closely follow the Rayleigh distribution. Note that the Rayleigh distribution is a particular case of the Weibull distribution, with a fixed shape parameter of 2 (see Box 4.10). This distribution is fully defined by a single parameter, which may be either the mean wave height H_m or the root mean square (rms) wave height H_{rms} , or alternatively the variance of the free-surface elevation m_0 . Equation 4.50 gives the equivalent forms of the cumulative distribution function.

$$P(H) = P(\underline{H} < H) = 1 - \exp\left(-\frac{H^2}{8m_0}\right) = 1 - \exp\left(-\frac{\pi}{4}\left(\frac{H}{H_m}\right)^2\right) = 1 - \exp\left(-\left(\frac{H}{H_{rms}}\right)^2\right) \quad (4.50)$$

Equation 4.51 gives the corresponding probability density function.

$$p(H) = \frac{H}{4m_0} \exp\left(-\frac{H^2}{8m_0}\right) = \frac{\pi}{2} \frac{H}{H_m^2} \exp\left(-\frac{\pi}{4}\left(\frac{H}{H_m}\right)^2\right) = \frac{2H}{H_{rms}^2} \exp\left(-\left(\frac{H}{H_{rms}}\right)^2\right) \quad (4.51)$$

The variance m_0 can be computed from the free-surface elevation signal $\eta(t)$ (see Equation 4.52) or from the wave spectrum $E(f)$ (it corresponds to the area between spectrum and the x -axis, see Section 4.2.4.5).

$$m_0 = \eta_{rms}^2 = \frac{1}{T} \int_0^T (\eta(t) - \bar{\eta})^2 dt \quad (4.52)$$

Figure 4.27 shows (on linear-log scale) the Rayleigh distribution.

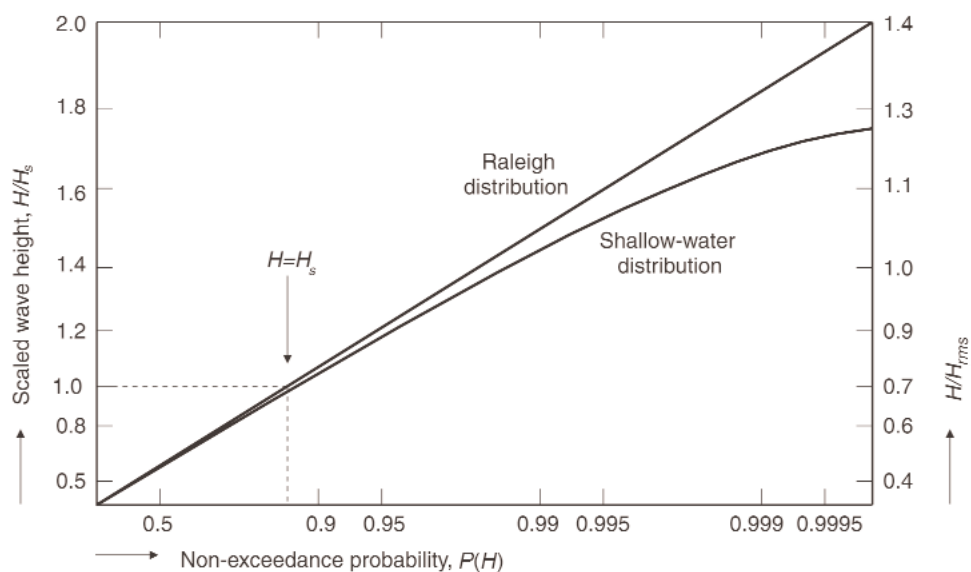


Figure 4.27 Example of a shallow-water observed distribution of wave heights compared with the Rayleigh distribution

A shortcoming of the Rayleigh distribution is that it is not bounded by an upper maximum value. Thus the maximum wave height can neither be defined nor computed in a deterministic way from this distribution. However, the representative wave heights $H_{P\%}$ and $H_{1/Q}$ can be computed analytically (see Equations 4.53 and 4.54) from the Rayleigh distribution (eg Massel, 1996; Goda, 2000).

$$\frac{H_{P\%}}{H_{rms}} = \sqrt{-\ln(P/100)} \tag{4.53}$$

$$\frac{H_{1/Q}}{H_{rms}} = Q \operatorname{erfc}(\sqrt{\ln Q}) + \sqrt{\ln Q}, \text{ with: } \operatorname{erfc}(x) = \int_x^{+\infty} \exp(-t^2) dt \tag{4.54}$$

The most important and useful results are listed in Table 4.8. An important issue is the estimation of the maximum value of the wave height for the case of sea-states of finite duration. This maximum wave height cannot be determined in a deterministic manner. One can, however, derive a probability density function for the (statistical) ratio H_{max}/H_s (eg Massel, 1996; Goda, 2000). Two important representative values, namely the mode and the mean values, can be expressed analytically (see Equations 4.55 and 4.56) and computed (see Table 4.9 for some typical results).

Table 4.8 Characteristic wave height ratios for a sea-state with a Rayleigh distribution of wave heights

Characteristic height H	Wave height ratios			
	$H/\sqrt{m_0}$	H/H_m	H/H_{rms}	H/H_s
Standard deviation of free surface $\sigma_\eta = \sqrt{m_0}$	1	0.399	0.353	0.250
Mean wave height H_m	2.507	1	0.886	0.626
Root-mean-square wave height H_{rms}	2.828	1.128	1	0.706
Significant wave height $H_s = H_{1/3}$	4.004	1.597	1.416	1
Wave height $H_{1/10}$	5.090	2.031	1.800	1.273
Wave height $H_{1/100}$	6.673	2.662	2.359	1.668
Wave height $H_{2\%}$	5.594	2.232	1.978	1.397

• **Mode of the distribution**

The most probable value of the ratio H_{max}/H_s for a record consisting of N waves is given by Equation 4.55.

$$\left[\frac{H_{max}}{H_s} \right]_{mode} \approx \sqrt{\frac{\ln N}{2}} \tag{4.55}$$

• **Mean value of the distribution**

The mean value of the ratio H_{max}/H_s for a record consisting of N waves (see Equation 4.56). The mean value is greater than the mode, because of the skewed shape of the distribution:

$$\left[\frac{H_{max}}{H_s} \right]_{mean} \approx \left(\sqrt{\frac{\ln N}{2}} + \frac{\gamma}{2\sqrt{2\ln N}} \right) \tag{4.56}$$

where $\gamma =$ Euler constant ≈ 0.5772 .



Table 4.9 Mode and mean values of the wave height distribution in a sea-state composed of N waves following a Rayleigh distribution of wave heights

Wave height distribution property	Number of waves, N , for the mode and mean values						
	100	200	500	1000	2000	5000	10 000
$(H_{max}/H_s)_{mode}$	1.52	1.63	1.76	1.86	1.95	2.06	2.15
$(H_{max}/H_s)_{mean}$	1.61	1.72	1.84	1.94	2.02	2.13	2.21

- *Distribution of shallow-water wave heights*

In shallow water, the wave height distribution is affected by non-linear effects and by wave breaking: it differs significantly from the Rayleigh distribution. The highest waves break first and, if many of the highest waves break, a lot of waves with more or less the same height are present. In Figure 4.28 an example is also shown of a shallow-water wave height distribution.

Several attempts have been made recently to propose distribution models for wave heights in the shoaling and breaking zone. They are based on the use of a Beta-Rayleigh distribution (Hughes and Borgman, 1987), a Weibull distribution (Glukhovskiy, 1966), a composite Weibull distribution (CWD) (Battjes and Groenendijk, 2000) or a modified distribution (Mendez *et al*, 2004). Among them, the CWD of Battjes and Groenendijk (2000) has been successfully tested on a large quantity of data (small-scale and large-scale experiments) and may be used for engineering applications (see Figure 4.28 and Box 4.4).

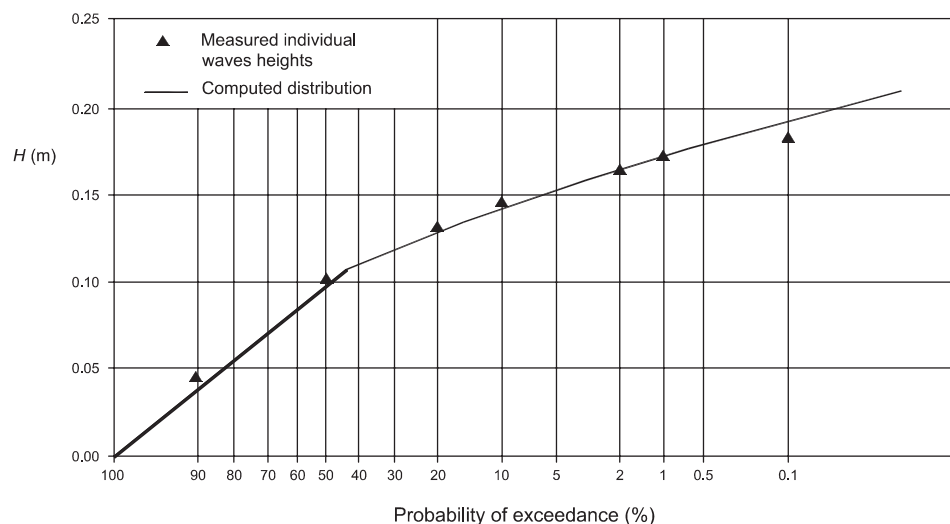


Figure 4.28 Comparison of measured (solid triangles) and calculated by the Composite Weibull Distribution (CWD) model (drawn line) wave height distributions on slope 1:100, $m_0 = 0.0011 \text{ m}^2$ and $h = 0.27 \text{ m}$ (from Battjes and Groenendijk, 2000)

Joint distribution of individual wave heights and periods

Theoretical models of the joint distribution function of wave heights and periods $f(H, T)$ for individual waves within a sea-state have been given by Longuet-Higgins (1975, 1983) and Cavanié *et al* (1976). Comparisons of these theories to experimental data can be found in, eg, Goda (1978). The scatter of the period, T , depends on the shape and width of the spectrum. Coefficients used in the above-mentioned models should be computed from the frequency spectrum (such as the spectral width parameter, v^2 , in Table 4.11).

This joint distribution is of little interest for the design of structures, however, so results are not reported here, but can be found in the references cited above. For design purposes, it is more relevant to consider the joint distribution of the significant wave height and a characteristic period (eg T_m or T_p) (see Section 4.2.4.8).

Box 4.4 The composite Weibull distribution (CWD) of wave heights in shallow water

Battjes and Groenendijk (2000) proposed use of a combination of two Weibull distributions (see Equation 4.57) to describe the cumulative distribution of wave heights in shallow water and the breaking zone:

$$P(H) = P(\underline{H} < H) = \begin{cases} 1 - \exp\left(-\left(H/H_1\right)^2\right) & \text{for } H < H_{tr} \\ 1 - \exp\left(-\left(H/H_2\right)^{3.6}\right) & \text{for } H \geq H_{tr} \end{cases} \quad (4.57)$$

where H_{tr} = transitional wave height (m), defined by Equation 4.58 and H_1, H_2 = scale parameters (m).

The use of two distributions is more suitable for describing wave breaking correctly. The largest waves break first, while there is no change for the smallest waves. This gives a non-homogeneous dataset of waves: broken waves and non-broken waves. The CWD distribution reproduces this physical effect: a Rayleigh distribution for the lowest part of the distribution (as in deep water) and a Weibull for the upper part. The transitional wave height is computed with Equation 4.58, in which the bed slope, $\tan\alpha$, and the local water depth, h , are the parameters.

$$H_{tr} = (0.35 + 5.8 \tan\alpha) h \quad (4.58)$$

The method also requires the knowledge of the root mean square (rms) wave height, but generally this wave height is not available, and the variance, m_0 , or the spectral significant wave height, H_{m0} , is known (from the application of a spectral wave propagation model for instance) (see Section 4.2.4.5). So an additional relationship (see Equation 4.59) has been proposed to start from the spectral wave height, H_{m0} .

$$H_{rms} = [0.6725 + 0.2025(H_{m0}/h)] H_{m0} \quad (4.59)$$

One has then to compute the non-dimensional transitional wave height H_{tr}/H_{rms} , which is used as input to Table 2 of Battjes and Groenendijk (2000) to find the (non-dimensional) characteristic heights: $H_{1/3}/H_{rms}$, $H_{1/10}/H_{rms}$, $H_{2\%}/H_{rms}$, $H_{1\%}/H_{rms}$ and $H_{0.1\%}/H_{rms}$. Some particular values have been extracted from this table and are included in Table 4.10, only for the ratios $H_{1/10}/H_{rms}$ and $H_{2\%}/H_{rms}$ (see Table 2 of Battjes and Groenendijk (2000) for other values of the transitional wave height and other wave heights).

Table 4.10 Values of $H_{1/10}/H_{rms}$ and $H_{2\%}/H_{rms}$ for some values of H_{tr}/H_{rms}

Characteristic height	Non-dimensional transitional wave H_{tr}/H_{rms}									
	0.05	0.50	1.00	1.20	1.35	1.50	1.75	2.00	2.50	3.00
$H_{1/10}/H_{rms}$	1.466	1.467	1.518	1.573	1.626	1.683	1.759	1.786	1.799	1.800
$H_{2\%}/H_{rms}$	1.548	1.549	1.603	1.662	1.717	1.778	1.884	1.985	1.978	1.978

The final step is the computation of the dimensional wave heights from the ratios read in the table and the value of H_{rms} . Equation 4.60 is an example: this one is for the computation of $H_{2\%}$.

$$H_{2\%} = (H_{2\%}/H_{rms})_{Table} H_{rms} \quad (4.60)$$

Figure 4.28 shows a result of the CWD distribution compared to laboratory measurements.

Wave group statistics

As already mentioned, a sea-state is composed of a series of waves that are quite different from one another: **irregular** or **random** characteristics of the sea-state, but a closer inspection often reveals that the wave heights are not randomly distributed. Very often there are short series of several (say 5–10) higher waves, and then a series of lower waves, and again a series of higher waves. This is called wave grouping. Several parameters have been proposed by various authors to measure the groupiness of waves in sea-states (eg Goda, 1970a; Kimura, 1981; Funke and Mansard, 1981; van Vledder, 1993).

Laboratory experiments have shown that wave grouping may have an effect on some aspects of wave structure interactions. It has some limited but noticeable effects on the stability of a rubble mound breakwater (damage increase with groupiness of waves), and a stronger influence on some other aspects, like run-up and overtopping, mainly due to the presence of bound long waves associated with wave groups (Galland and Manoha, 1991; Van Gent, 2001).

4.2.4.5 Spectral description of waves and wave spectra

Spectral analysis and representative wave parameters

In general an observed wave field can be broken down into a number of individual sinusoidal wave components, each with its own height H , frequency f and direction θ . The distribution of wave energy as a function of wave frequency is commonly presented by the one-dimensional wave energy density spectrum, denoted as $E_{\eta\eta}(f)$. The directional spread can be included by using a two-dimensional or directional spectrum, with f and θ as independent variables: $S_{\eta\eta}(f, \theta)$.

The estimation of the wave energy density spectrum from a record of sea-surface elevation fluctuations is obtained by Fourier transform techniques. A detailed description of these mathematical treatments can be found in, eg, Goda (2000) or Tucker and Pitt (2001). The key points of the analysis are:

- an appropriate selection of the sampling rate and of the length of the records that determine the accuracy of the analysis: 2–4 Hz is recommended, with a duration of at least 20 min, and preferably 30–60 min
- an appropriate selection of the spectral bandwidth or the degrees of freedom to be used in the spectral analysis
- an appropriate selection of the limits f_{min} and f_{max} for the computation of the spectral moments. It is recommended to choose f_{min} equal or lower than half of the peak frequency ($0.5 f_p$) or 0.033 Hz when a large band of peak frequencies is anticipated in order to separate long-period components from the short waves. f_{max} should be less than the Nyquist frequency (equal to half the sampling rate) but greater than $5f_p$ or 1–2 Hz so as to catch the high-frequency tail of the spectrum properly.

From a given spectrum $E_{\eta\eta}(f)$, several representative wave parameters (eg the spectral significant wave height, peak and mean periods) may be computed, as defined in Table 4.11 (IAHR/PIANC, 1986).

Table 4.11 Characteristic wave parameters from a spectral analysis

Characteristic wave parameter	Definition
Variance m_0	$m_0 = \int_{f_{min}}^{f_{max}} E(f) df$
Moments of order n of the spectrum m_n	$m_n = \int_{f_{min}}^{f_{max}} f^n E(f) df$
Spectral significant wave height H_{m0}	$H_{m0} = 4\sqrt{m_0}$
Mean energy wave height H_E	$H_E = \sqrt{8m_0}$
Peak frequency f_p and peak period $T_p = 1/f_p$ The peak frequency is the frequency of the maximum value (peak) of the spectrum. For a discrete spectrum, it may be the discrete frequency at which the spectrum peaks, but this choice is not very appropriate since the discrete peak frequency is not continuous. Two more convenient methods for computing f_p are given (see Young (1995) for a detailed discussion of the relevance of these various peak periods).	<p>Method 1 (so called Delft method)</p> $f_p^{Dm} = \frac{\int_{f_1}^{f_2} f E(f) df}{\int_{f_1}^{f_2} E(f) df}$ <p>where f_1 and f_2 are two frequency thresholds around the discrete peak frequency at which the spectrum values are $m\%$ of the maximum discrete peak value. Usually, $m = 80$ per cent (or sometimes 60 per cent) is used.</p> <p>Method 2 (so called Read method)</p> $f_p^{Rm} = \frac{\int_{f_{min}}^{f_{max}} f E^n(f) df}{\int_{f_{min}}^{f_{max}} E^n(f) df}$ <p>where the exponent n is usually taken as 4 or 5.</p>
Mean wave period $T_{m01} = T_{01}$	$T_{01} = 1/f_{01} = m_0/m_1$
Mean wave period $T_{m02} = T_{02}$	$T_{02} = 1/f_{02} = \sqrt{m_0 / m_2}$
Mean energy period $T_E = T_{m-1,0} = T_{-10}$	$T_E = T_{m-1,0} = T_{-10} = 1/f_{-10} = m_{-1}/m_0$
Spectral width parameter v^2	$v^2 = \frac{m_0 m_2}{m_1^2} - 1$
Spectral width parameter ε^2	$\varepsilon^2 = 1 - \frac{m_2^2}{m_0 m_4}$
Spectral width parameter κ (Van Vledder and Battjes, 1992)	$\kappa = \frac{\left \int_0^\infty E(f) \exp(i2\pi f T_{02}) df \right }{m_0}$

Note that there are various estimates of the mean wave period, among which the mean energy period T_E or $T_{m-1,0}$ (or T_{-10} in short) has recently been applied for the design of structures. It is simply the averaged period weighted by the energy spectrum (see Equation 4.61).

$$T_{m-1,0} = T_{-10} = T_E = \frac{m_{-1}}{m_0} = \frac{\int_0^{+\infty} \frac{E(f)}{f} df}{\int_0^{+\infty} E(f) df} = \frac{\int_0^{+\infty} T \cdot E(f) df}{\int_0^{+\infty} E(f) df} \tag{4.61}$$

It was observed that if bimodal waves are present, or in case of very flat spectra without peak as a result of heavy wave breaking, the mean energy period $T_{m-1,0}$ is a better parameter, as T_p is not easy to establish in those cases. This parameter gives a little more weight to the longer periods and is closer to the peak period than the mean period T_{02} , for instance.

The relationship between T_p and $T_{m-1,0}$ can be obtained by numerical evaluation of Equation 4.62 if the analytical expression of the variance spectrum $E(f)$ is known. Dingemans (1987) computed the ratio $T_{m-1,0}/T_p$ for various spectral expressions including the Pierson-Moskowitz (PM) and the JONSWAP spectra (given by Equations 4.63 and 4.67 respectively).

Some of the results obtained by Dingemans for various values of the peak enhancement factor γ in the JONSWAP spectrum are given in Table 4.12.

Table 4.12 Ratio of the peak period T_p over the mean energy period $T_{m-1,0}$ for a JONSWAP spectrum as a function of the peak-enhancement factor γ , based on Dingemans (1987)

	Peak enhancement factor, γ , in JONSWAP spectrum								
	1 (PM)	2	3	3.3	5	7	10	15	20
$T_p/T_{m-1,0}$	1.167	1.132	1.112	1.107	1.088	1.074	1.061	1.048	1.040

For single-peaked spectra with a clear peak, based on a few hundred measured spectra in wave flumes for various research projects, it was found that the ratio of T_p and $T_{m-1,0}$, as given in Equation 4.62, is a good approximation.

$$T_p = 1.1 T_{m-1,0} \quad (4.62)$$

In the absence of other information this relationship (see Equation 4.62) can be used as a rule of thumb if design formulae require the mean energy period $T_{m-1,0}$ where only the peak period, T_p is known. However, for very shallow foreshores and/or for double-peaked spectra the correct $T_{m-1,0}$ should be determined, based on physical model research or the appropriate numerical modelling.

Energy density spectra of sea-states

- *Spectra of deep-water waves*

Examples of a spectrum are given in Figure 4.29 that are frequently used to describe random wave fields. Governing parameters are also shown. A variety of semi-empirical wave spectra have been presented, each having its specific range of applicability.

Two of the most widely used are the spectrum described by Pierson and Moskowitz (1964) and the JONSWAP spectrum (Hasselmann *et al*, 1973), shown on Figure 4.29. These spectra are formulated using a power function with respect to the frequency f (or angular frequency $\omega = 2\pi f$) containing several scaling parameters and constants. They can be obtained by specifying either the wind speed, U_w , at a given elevation above the mean sea level (MSL) and the fetch length, F , or alternatively the spectral significant wave height, H_{m0} , and peak frequency, f_p .

Both these spectra were originally derived by assuming a tail proportional to f^{-5} for the high-frequency range of the spectrum. Recent theoretical work and subsequent reanalyses of data (eg Toba, 1973; Donelan *et al*, 1985; Battjes *et al*, 1987; Alves *et al*, 2003) have however concluded that a tail proportional to f^{-4} is more appropriate to describe the equilibrium spectra in the high-frequency range. The original and modified versions of these spectra are briefly presented hereafter. It is recommended to use the updated versions for wave spectra in deep water (namely the f^{-4} high-frequency tail).

The Pierson-Moskowitz (PM) spectrum: the PM spectrum represents a fully developed sea in deep water. In its original form, see Equation 4.63, it has a high-frequency tail proportional to f^{-5} and was derived as a function of a single parameter, the wind speed, $U_{19.5}$, at an elevation of 19.5 m above MSL:

$$E_{PM}^{original}(f) = \alpha \frac{g^2}{(2\pi)^4} f^{-5} \exp \left[-1.25 \left(\frac{f}{f_p} \right)^{-4} \right] \quad (4.63)$$

where $\alpha = 0.0081$, the empirically determined equilibrium range level, known as the Phillips constant (-); $f_p = \frac{g v_{19.5}^{PM}}{U_{19.5}}$ (1/s) and $v_{19.5}^{PM} = 0.14$, the non-dimensional equilibrium peak frequency.

Alternatively, this spectral form can be expressed as a function of given spectral significant wave height, H_{m0} , and peak frequency, f_p , the corresponding formulation (see Equation 4.64) sometimes also referred to as the Bretschneider (B) spectrum.

$$E_{PM}^B(f) = \frac{5}{16} H_{m0}^2 f_p^4 f^{-5} \exp \left[-\frac{5}{4} \left(\frac{f}{f_p} \right)^4 \right] \quad (4.64)$$

Similarly, Goda (2000) reformulated this expression (see Equation 4.65) as a function of the significant wave height $H_{1/3}$ and significant period $T_{1/3}$.

$$E_{PM}^{Goda}(f) = 0.257 H_{1/3}^2 T_{1/3}^{-4} f^{-5} \exp \left[-1.03 (T_{1/3} f)^{-4} \right] \quad (4.65)$$

As stated above, all recent works favour a f^{-4} power law for the high-frequency range of the spectrum and the use of the 10 m wind speed, U_{10} , as input wind velocity. Thus the recommended form of the modified Pierson-Moskowitz spectrum for fully developed seas is presented as Equation 4.66, after Donelan *et al* (1985) and Alves *et al* (2003).

$$E_{PM}^{updated}(f) = \alpha \frac{g^2}{(2\pi)^4 f_p} f^{-4} \exp \left[-\left(\frac{f}{f_p} \right)^4 \right] \quad (4.66)$$

where $\alpha = 0.00615$, the modified equilibrium range level (-); $f_p = \frac{g v_{10}^{PM}}{U_{10}}$ (1/s) and $v_{10}^{PM} = 0.123$, the non-dimensional equilibrium peak frequency (-).

The JONSWAP (JOint North Sea WAve Project) spectrum. The JONSWAP spectrum (J) (Hasselmann *et al*, 1973) represents fetch-limited sea-states, ie growing sea. Its original formulation (see Equation 4.67) includes an additional term compared to the original PM spectrum (see Equation 4.63) and also depends on the fetch length, F . It has a sharper peak than the PM spectrum. This original JONSWAP form has an f^{-5} high-frequency tail:

$$E_J^{original}(f) = \frac{\alpha g^2}{(2\pi)^4} f^{-5} \exp \left[-\frac{5}{4} \left(\frac{f}{f_p} \right)^4 \right] \gamma^\delta \quad (4.67)$$

where:

$$\alpha = 0.076 \left(\frac{gF}{U_{10}^2} \right)^{-0.22} \quad (-) \quad f_p = 3.5 \frac{g}{U_{10}} \left(\frac{gF}{U_{10}^2} \right)^{-0.33} \quad (1/s)$$

$$\delta = \exp \left[-\frac{(f/f_p - 1)^2}{2\sigma^2} \right] \quad (-) \quad \sigma = 0.07 \text{ if } f \leq f_p \text{ and } 0.09 \text{ if } f > f_p \quad (-)$$

γ = peak enhancement factor that varies between 1 (in this case giving the original PM spectrum) and 7, with an average value of 3.3 (-).

As for the PM spectrum, Goda (1988) proposed an alternative approximate expression (see Equation 4.68) for the case where the significant wave height $H_{1/3}$ and the significant period $T_{1/3}$ are specified:

$$E_J^{Goda}(f) = \beta_J H_{1/3}^2 f_p^4 f^{-5} \exp \left[-\frac{5}{4} \left(\frac{f}{f_p} \right)^4 \right] \gamma^\delta \quad (4.68)$$

where: $\beta_J = \frac{0.0624}{0.230 + 0.0336\gamma - 0.185(1.9 + \gamma)^{-1}} (1.094 - 0.01915 \ln \gamma) \quad (-)$

$$T_p = \frac{1}{f_p} = \frac{T_{1/3}}{1 - 0.132(\gamma + 0.2)^{-0.559}} \quad (s).$$

As stated above, a spectral form of the JONSWAP spectrum with a f^{-4} power law for the high-frequency range is preferable. Modified forms have among others been proposed by Donelan *et al* (1985) and Aono and Goto (1995), which are summarised in Box 4.5.

Box 4.5 Modified JONSWAP spectra compatible with a f^4 high-frequency tail

Modified JONSWAP spectrum as proposed by Donelan *et al* (1985) with input variables U_{10} and F or m_0 and T_p

Expression of frequency spectrum:

$$E(f) = \alpha (2\pi)^{-4} g^2 f_p^{-1} f^4 \exp[-(f/f_p)^4] \gamma^\delta$$

with the following relationships:

$$\alpha = 0.006 (U_{10}/c_p)^{0.55} \quad \text{for } 0.83 < U_{10}/c_p < 5$$

$$\gamma = 1.7 \quad \text{for } 0.83 < U_{10}/c_p < 1$$

$$\gamma = 1.7 + 6 \log(U_{10}/c_p) \quad \text{for } 1 < U_{10}/c_p < 5$$

$$\sigma = 0.08 + 0.32 (U_{10}/c_p)^{-3} \quad \text{for } 1 < U_{10}/c_p < 5$$

$$\delta = \exp[-(f/f_p - 1)^2 / (2\sigma^2)]$$

where c_p = phase speed corresponding to the peak frequency ($c_p = g / (2\pi f_p)$ in deep water); $U_{10}/c_p = 0.83$ corresponding to the point of full development; both f_p and c_p are a function of the wind-speed U_{10} and the fetch length F , through:

$$f_p U_{10} / g = 1.845 (g F / U_{10}^2)^{-0.23}$$

Young (1992) derived relationships to calculate the spectrum directly from the variance m_0 and the peak period T_p through:

$$\alpha = 200 g^{-1.571} (m_0)^{0.786} (T_p)^{-3.143}$$

$$\gamma = 6.489 + 6 \log[(2.649 \cdot 10^7 g^{-2.857} (m_0)^{1.429} (T_p)^{-5.714})]$$

$$\sigma = 0.08 + 6.94 \cdot 10^{-26} g^{8.571} (m_0)^{-4.287} (T_p)^{17.142}$$

Modified JONSWAP spectrum as proposed by Aono and Goto (1994) with input variables $H_{1/3}$ and $T_{1/3}$

Expression of frequency spectrum:

$$E(f) = \alpha (2\pi)^{-3} g u^* f^4 \exp[-(f/f_p)^4] \gamma^\delta$$

with the following relationships:

$$u^* = (H_{1/3})^2 / (g B^2 (T_{1/3})^3) \quad B = 0.067$$

$$f_p = 1 / (1.136 T_{1/3}) \quad f_{p^*} = f_p u^* / g$$

$$\gamma = 6 (f_{p^*})^{0.15} \quad \alpha = 0.17 \gamma^{-1/3}$$

$$\sigma_1 = 0.144 \text{ for } f < f_p \quad \sigma_2 = 0.07 (f_{p^*})^{0.16} \text{ for } f > f_p$$

$$\delta = \exp[-(f/f_p - 1)^2 / (2\sigma^2)]$$

This spectrum conforms to the 3/2 power law of Toba (1973, 1997), $H^* = B T^{3/2}$, with a slight modification of the B coefficient: 0.067 instead of the original value of 0.062 (Toba, 1973).

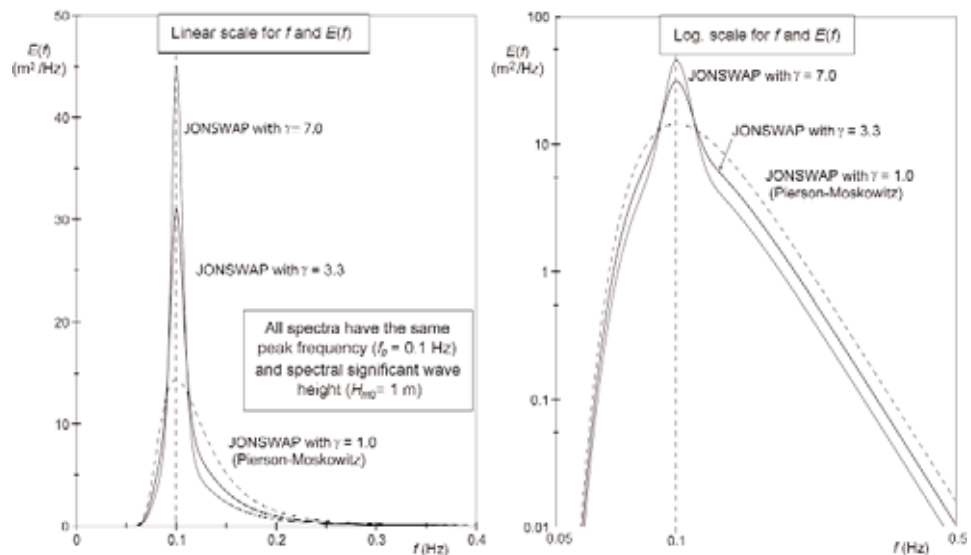


Figure 4.29 Pierson-Moskowitz and JONSWAP spectra

- *Spectra of shallow-water waves*

To cover both fetch-limited sea and shallow-water effects, the **TMA** (for **Texel-Marsen-Arsloe** experiments) spectrum were developed (Hughes, 1984; Bouws *et al*, 1985). This spectrum consists of factors originating from the Pierson-Moskowitz and from the JONSWAP spectra. Additionally, a factor $\phi(\omega_h)$ has been introduced to describe the effect of the water depth. Equation 4.69 gives the description of the **TMA** spectrum, which can be used for spectral shape in shallow-water conditions:

$$E_{TMA}(f) = E_J(f) \phi(\omega_h) \quad (4.69)$$

where: $\omega_h = 2\pi f \sqrt{h/g}$.

The additional factor $\phi(\omega_h)$ describes the influence of the water depth, h . It can be approximated within 4 per cent by Equation 4.70.

$$\phi(\omega_h) = \begin{cases} \frac{1}{2} \omega_h^2 & \text{for } \omega_h \leq 1 \\ 1 - \frac{1}{2} [2 - \omega_h]^2 & \text{for } \omega_h > 1 \end{cases} \quad (4.70)$$

The question of the equilibrium form of spectra in the surf zone was recently addressed by McKee Smith and Vincent (2003), who showed that the surf-zone spectra evolve to contain two equilibrium ranges when expressed as a function of the wave-number k . The higher-frequency range is similar to that proposed by Toba (1973, 1997) in deeper water with the form $k^{-5/2}$ and is valid for $kh > 1$. The second range, between the peak wave-number k_p and $k = 1/h$ shows a form $k^{-4/3}$, similar to the one proposed by Zakharov (1999).

Directional wave spectra

The directional wave spectrum $S(f, \theta)$ describes the dependence of wave energy or free-surface variance both on frequency, f , and direction of wave propagation, θ . Equation 4.71, which is often used in this form, describes the conventional decomposition of the directional spectrum:

$$S(f, \theta) = E(f) D(f, \theta) \quad (4.71)$$

where $E(f)$ = classical frequency spectrum, as used in the previous part of this section, and $D(f, \theta)$ = the directional spreading function (DSF).

Equation 4.72 gives the relationship between the classical frequency spectrum and the directional spectrum.

$$E(f) = \int_0^{2\pi} S(f, \theta) d\theta \quad (4.72)$$

The DSF $D(f, \theta)$ satisfying two important properties is given by Equations 4.73 and 4.74.

$$D(f, \theta) \geq 0 \quad \text{for } \theta \in [0, 2\pi] \quad (4.73)$$

$$\int_0^{2\pi} D(f, \theta) d\theta = 1 \quad (4.74)$$

The former condition or property (see Equation 4.73) expresses that the DSF is a non-negative function, whereas the latter is a direct consequence of Equation 4.71. The DSF thus models the directional spreading of the wave energy at each frequency f . The problem of directional analysis thus consists in determining the directional spectrum, $S(f, \theta)$, or equivalently the variance spectrum $E(f)$ and the DSF $D(f, \theta)$ at each frequency. To that end, at least three signals of wave properties have to be measured simultaneously. This can be

achieved by using floating directional buoys (recording either the heave, pitch and roll signals or three displacements), or an array of wave gauges etc. This is a difficult problem, however, as the continuous function $D(f, \theta)$ has to be estimated from a very limited number of measured data. A review of measuring techniques and directional analysis methods to obtain $D(f, \theta)$ is presented in Benoit *et al* (1997b).

For practical purposes analytical expressions of the DSF have been derived for uni-modal sea-states (one dominant wave direction). Examples of such DSF models are the ones from Mitsuyasu *et al* (1975) and Donelan *et al* (1985), given in Box 4.6. Additional information on directional parameters can be found in Goda (1997) and in reference textbooks (eg Massel, 1996; Goda, 2000).

Box 4.6 Two analytical models for directional spreading functions (DSF)

cos^{2s}(θ/2) model of Mitsuyasu <i>et al</i> (1975)	sech²(βθ) model of Donelan <i>et al</i> (1985)
Expression of DSF:	Expression of DSF:
$D(f, \theta) = \Delta \cos^{2s}[(\theta - \theta_m)/2]$	$D(f, \theta) = \frac{1}{2} \beta [1/\cosh[(\beta(\theta - \theta_m))]]^2$
where $\theta_m(f)$ = mean wave direction and $\Delta(s)$ = constant so that Equation 4.74 is satisfied.	where $\theta_m(f)$ is the mean wave direction.
The exponent s controls the angular spreading of wave energy (higher values of s correspond to narrower and sharper DSF). It is frequency-dependent and reads:	The parameter β controls the angular spreading of wave energy. It is frequency-dependent and reads:
$s/s_p = (f/f_p)^5$ for $f < f_p$	$\beta = 2.61 (f/f_p)^{1.3}$ for $0.56 < f/f_p < 0.95$
$s/s_p = (f/f_p)^{-2.5}$ for $f > f_p$	$\beta = 2.28 (f/f_p)^{-1.3}$ for $0.95 < f/f_p < 1.6$
$s_p = s_{max}$, value of the exponent at the peak frequency where it is maximum. This means that the angular spreading of wave energy is narrowest at the peak frequency. Mitsuyasu <i>et al</i> (1975) established that s_p varies in the range of 5 to 20 for wind-generated waves and its value is a function of the non-dimensional peak frequency as:	$\beta = 1.24$ for $1.6 < f/f_p$
$s_p = 11.5 (2\pi f_p U_{10}/g)^{-2.5}$	With these expressions the angular spreading of wave energy is minimum at a frequency about 5 per cent less than the peak frequency.
Goda (1997) proposed to simply use the following constant values:	Banner (1990) modified the last expression of β , which is frequency-independent, and found a better agreement with measured directional spectra by using:
$s_p = 10$ for wind waves	$\beta = -0.4 + 0.8393 \exp[-0.567 \ln(f/f_p)^2]$ for $1.6 < f/f_p$
$s_p = 25$ for swell with short decay distance	
$s_p = 75$ for swell with long decay distance	

Relationships between statistical and spectral parameters

- *Deep-water waves*

Assuming that the water surface elevation follows a stationary Gaussian process, and hence that the wave heights are Rayleigh-distributed, Equations 4.75 and 4.76 give the relationship between statistical and spectral parameters.

$$\text{Significant wave heights: } H_{1/3} = H_{m0} \quad (4.75)$$

$$\text{Mean wave periods: } T_m = T_{02} \quad (4.76)$$

Most sea-state parameters can be expressed in terms of the spectral moments as included in Table 4.11. See also Table 4.8 for some practical conversion factors for height parameters of Rayleigh-distributed waves.

Note that the factor “4” in the relationship $H_s = 4\sqrt{m_0}$ is a theoretical value based on the assumption that the Rayleigh distribution applies. Practically, analysis of real records display values down to 3.6 and a value of 3.8 is recommended by Goda (2000) for deep-water waves. This corresponds to $H_{1/3} = 0.95 H_{m0}$.

NOTE: Some misunderstanding may arise from the literature where the notation H_s is often used to designate either $H_{1/3}$ or H_{m0} (without precisely stating which of these wave heights is considered) and the H_{rms} notation is often used to designate H_E .

Concerning **wave periods**, it is not possible to derive universal relationships between, eg, the mean period T_m and the peak period T_p , as the ratio depends on the spectral shape. Wave data analysis and numerical simulations by Goda (1988, 2000) have revealed a range for various conversion factors:

- $T_m/T_p = 0.71$ to 0.82 for a PM spectrum
- $T_m/T_p = 0.79$ to 0.87 for a JONSWAP spectrum.

Generally, $T_{1/3}/T_p = 0.90$ to 0.96 and $T_{1/3}/T_m = 1.13$ to 1.33 were found to apply. From the analysis of simulated wave data Goda (1988, 2000) concluded that $T_{1/3}$ is a more reliable characterisation than T_m for wind-generated waves.

The mean energy period, $T_{m-1,0}$, has recently been observed to be a better and more stable characteristic period for stability design formulae (see Section 4.2.4.5). Equation 4.63 gives a practical relationship to estimate $T_{m-1,0}$ from T_p .

Dingemans (1987) computed and tabulated numerical values of the ratios of various mean periods ($T_{m-1,0}$, T_{01} , T_{02}) over the peak period T_p for PM and JONSWAP spectra, considering both f^{-4} and f^{-5} high-frequency tails, as well as different values of the peak-enhancement factor, γ (-).

- **Shallow-water waves**

It should be emphasised that Equation 4.75 applies for deep-water conditions, but that it is not suitable for shallow-water conditions. For shoaling and pre-breaking wave conditions, the ratio $H_{1/3}/H_{m0}$ becomes higher than 1, and may reach values up to 1.3 or even 1.5 (Thompson and Vincent, 1985; Hamm, 2001). In particular, Thompson and Vincent (1985) proposed Equation 4.77 for the envelope of the above ratio for pre-breaking waves:

$$\left(\frac{H_{1/3}}{H_{m0}}\right)_{max} = \exp\left(0.02289\left(\frac{h}{gT_p^2}\right)^{-0.43642}\right) \quad (4.77)$$

For shallow-water applications, the use of a shallow-water distribution model for wave heights, such as the CWD of Battjes and Groenendijk (2000) presented in Box 4.4 allows the ratio of $H_{1/3}$ over H_{m0} to be computed. But it should be kept in mind that this model invokes an empirical relationship between H_{m0} and H_{rms} , and so the results are affected by this parameterisation.

4.2.4.6 Generation of waves in the ocean and on inland waters

Mechanisms of wave generation and evolution in the ocean

The main process of interest in the course of wave generation is the action of the wind that provides energy to the wave field. The generation of waves by wind is a complex process of interactions between the atmosphere and the ocean surface. However, empirical relationships have been derived to describe the growth of wave height under the action of constant and homogeneous wind, as well as the evolution of the wave period. They are important in

engineering practice as they allow easy estimation of wave characteristics from the wind characteristics or climatology. Some of these relationships are given in this section. They can only be used when a stationary sea-state can be assumed. During storm conditions, however, this does not apply, as the wave field is developing under influence of the wind shear upon the water. A wave field under influence of wind (wind-sea) is different from a wave field that is not exposed to wind (ie swell). In general, swell can be related to distant storms and is characterised by a narrower spectrum of relatively lower frequencies (higher periods) compared to wind-sea conditions.

Few processes need to be taken into account when waves are in deep water. When designing for waves in shallow water, more influences have to be accounted for (see Section 4.2.4.7). In deep water, in addition to wave generation by wind, three other principal processes need to be considered.

- Deep-water wave **breaking** or **white-capping**. Waves in deep water may break when a certain limiting wave steepness ($s = H/L$) is exceeded (see Section 4.2.4.3). For regular waves in deep water the wave height is limited by steepness according to the breaking criterion of Miche (1944) to about 1/7 of the wavelength. In practice, only individual waves in a random sea approach this value and calculated steepnesses using significant wave height H_s and peak wave period T_p rarely exceed $s_{op} = 0.05$. For steepness computed with the mean wave period, this is $s_{om} = 0.07$. This factor is, of course, considered implicitly in the empirical wave growth formulae.
- **Energy transfer** between frequencies. Non-linear energy transfers between wind waves make the wave spectrum evolve: the peak tends to become sharper and the peak frequency decreases as the waves interact during propagation. In deep water, these interactions occur between quadruplets of waves and are resonant interactions. Combined with frequency dispersion, they lead to the formation of swell conditions (long-period and almost regular waves). Such non-linear interactions can be predicted only by the use of advanced third-generation spectral wave models, although swell can of course be measured directly.
- Wave **reflection** and **diffraction** by islands or rocks (see Section 4.2.4.7).

Empirical methods for estimating wave conditions from wind characteristics

Like individual waves under the influence of wind, the wave spectrum also displays an evolution with time and/or with distance in the wind direction. Consequently, representative parameters of the sea-states (such as H_{m0} , T_m , T_p etc) also evolve with time and/or distance. Wind-induced wave growth has traditionally been described by using empirical formulae, some of them being presented in this section.

The approach to determine sea growth by analysis and numerical modelling of the wave spectrum has been developed, but empirical methods still play an important role. Meteorological and hydraulic institutes have expended considerable effort on numerical wave forecasting. With these numerical models the instantaneous wave parameters are derived from the energy content of the wave field, which is computed as being distributed within the directional wave spectrum. The necessary input for these models is wind fields, obtained from synoptic weather charts. The models account for the above-mentioned processes, namely energy gain derived from transfer from wind energy, energy loss caused by dissipation (breaking, bottom friction), wave-wave interactions and energy transfer among individual wave components of the frequency spectrum (see Section 4.2.4.10).

Empirical wave growth formulae are based upon the relations between **characteristic** wave parameters in the **standard wind field**. This wind field is given by an average wind speed (U_w , U_{10} ; see Section 4.2.1); the fetch, F (the wind-exposed distance to the coast, measured in the upwind direction), and the duration, t , of the wind field. An additional characteristic parameter is the water depth, h , which is usually assumed constant over the area of interest.

A fully developed sea has, for a given U_w , reached its maximum (equilibrium) wave height and period. In a fetch-limited or growing sea at least one of the parameters (F , t or h) poses a limiting condition to the actual sea as long as they have not reached a certain minimum value beyond which the limiting condition vanishes. Using g/U_w^2 as scale factor for H , F and h , and g/U_w as scale factor for t and T , the empirical wave growth formulae are usually written in a non-dimensional form as $H^* = f(h^*, F^*, t^*)$ and $T^* = f(h^*, t^*)$.

● **Open ocean conditions (deep water)**

Various empirical relationships have been proposed by various authors for more than 50 years. Some of them have been plotted in non-dimensional form in Figure 4.30 for the non-dimensional significant wave height gH_s/U_{10}^2 as a function of non-dimensional fetch gF/U_{10}^2 .

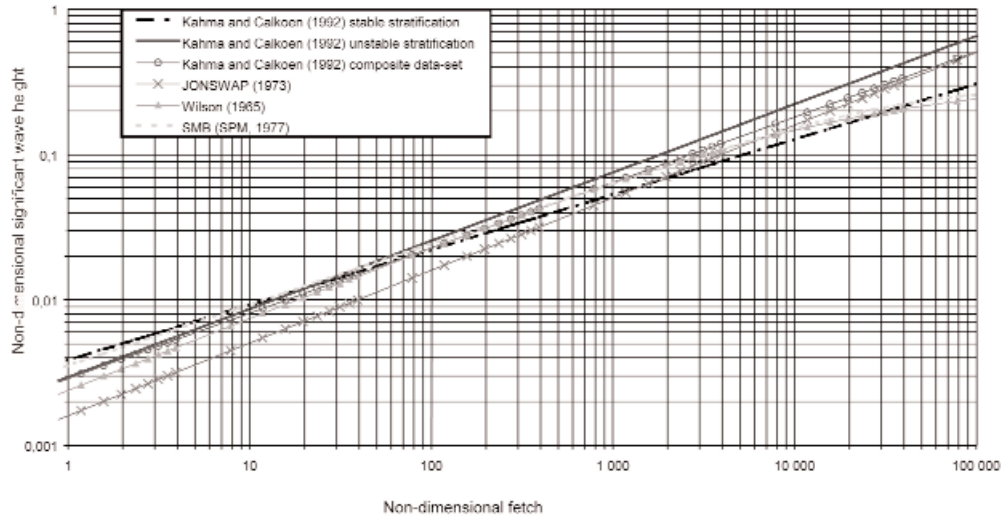


Figure 4.30 Comparison of some wave prediction formulae for deep-water conditions

It is clear from this figure that these formulae are not equivalent and produce different estimates of wave height. Based on various comparisons with experimental data, the following sets of equations are recommended.

1. Formulae from Sverdrup-Munk-Bretschneider (SMB), as presented in SPM (CERC, 1977).

These formulae were originally introduced by Sverdrup and Munk (1947) and further revised by Bretschneider (1954, 1970). They appear in the third edition of the *Shore protection manual [SPM]* (CERC, 1977). They allow estimation of the significant wave height H_s (m) (see Equation 4.78) and significant wave period T_s (s) (see Equation 4.79) generated by a constant and homogeneous wind. Information required is the velocity at 10 m above MSL, U_{10} (m/s), blowing over a fetch of length F (m), for fully developed conditions, ie if the duration of wind action is greater than t_{min} (hours), t_{min} can be calculated by Equation 4.80.

$$\frac{gH_s}{U_{10}^2} = 0.283 \tanh \left(0.0125 \left(\frac{gF}{U_{10}^2} \right)^{0.42} \right) \tag{4.78}$$

$$\frac{gT_s}{U_{10}} = 7.54 \tanh \left(0.077 \left(\frac{gF}{U_{10}^2} \right)^{0.25} \right) \tag{4.79}$$

$$\frac{g t_{min}}{U_{10}} = 0.00183 \exp \left[\left(0.0161x^2 - 0.3692x + 2.2024 \right)^{1/2} + 0.8798x \right] \tag{4.80}$$

where $x = \ln \left(\frac{gF}{U_{10}^2} \right)$

Prediction curves for significant wave height and significant wave period based on these formulae are given in *SPM* (CERC, 1977) (vol I, pp 3-36 and 3-37). Note that the fourth edition of *SPM* (CERC, 1984) contains different wave prediction formulae and curves, based on an intermediate calculation of wind stress and modified to conform to the JONSWAP formulae. The reliability for all situations of the *SPM* (CERC, 1984) formulae has recently been questioned, particularly for extreme events and/or short fetch conditions. They are now considered to be less reliable than the SMB formulae and should therefore not be used for practical applications.

2. Formulae from Wilson (1965), revisited by Goda (2003).

Wilson (1965) produced an alternative set of formulae to estimate the significant wave height $H_s = H_{1/3}$ (m) (see Equation 4.81), the significant wave period $T_s = T_{1/3}$ (s) (see Equation 4.82) and the minimum duration t_{min} (hours) (see Equation 4.83), with the same notation and convention for units as above.

$$\frac{g H_s}{U_{10}^2} = 0.3 \left[1 - \left(1 + 0.004 \left(\frac{g F}{U_{10}^2} \right)^{1/2} \right)^{-2} \right] \quad (4.81)$$

$$\frac{g T_s}{U_{10}} = 8.61 \left[1 - \left(1 + 0.008 \left(\frac{g F}{U_{10}^2} \right)^{1/3} \right)^{-5} \right] \quad (4.82)$$

$$\frac{U_{10} t_{min}}{F} = 0.01194 \left(\frac{g F}{U_{10}^2} \right)^{-0.27} \quad \text{or} \quad \frac{g t_{min}}{U_{10}} = 0.01194 \left(\frac{g F}{U_{10}^2} \right)^{0.73} \quad (4.83)$$

Prediction curves for significant wave height and significant wave period are given in Figure 4.31.

3. Formulae from Kahma and Calkoen (1992).

Kahma and Calkoen (1992) have performed a detailed analysis of wind wave growth by taking into account the stability of the air-sea interface. They showed that unstable conditions lead to an increase of wave height and period and proposed two sets of formulae: one for **stable conditions** and one for **unstable conditions**, as well as a composite formula for the entire dataset. The composite formula is in quite close agreement with the SMB and Wilson formula (see Figure 4.30). The formula for unstable conditions can be used to obtain conservative estimates of wave parameters. The three sets of formulae have the same form shown by Equations 4.84 and 4.85 with values of coefficients listed in Table 4.13.

$$\frac{g H_s}{U_{10}^2} = A \left(\frac{g F}{U_{10}^2} \right)^B \quad (4.84)$$

$$\frac{g T_s}{U_{10}} = C \left(\frac{g F}{U_{10}^2} \right)^D \quad (4.85)$$

Table 4.13 Coefficients in the wave prediction curves of Kahma and Calkoen (1992)

Coefficients in Equations 4.84 and 4.85	A	B	C	D
Stable stratification	$3.86 \cdot 10^{-3}$	0.38	0.5236	0.24
Unstable stratification	$2.94 \cdot 10^{-3}$	0.47	0.4425	0.28
Composite dataset	$2.88 \cdot 10^{-3}$	0.45	0.4587	0.27

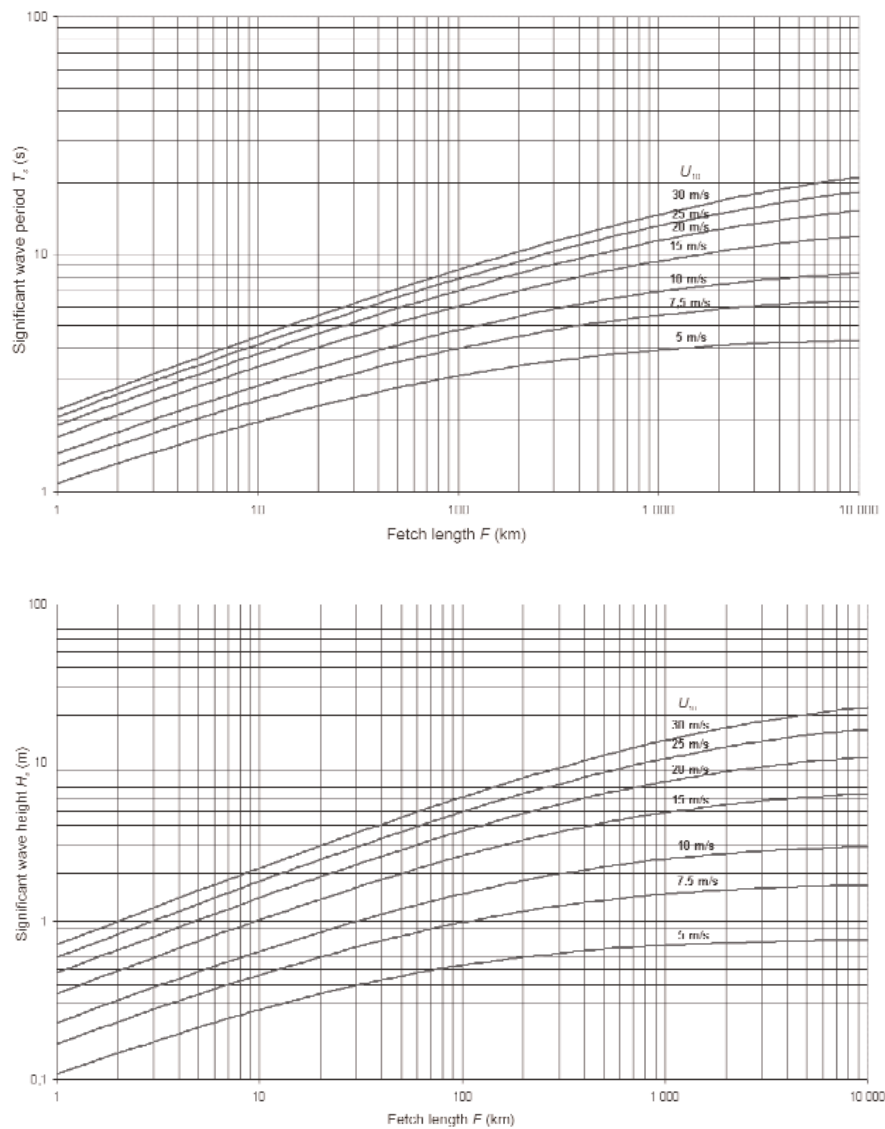


Figure 4.31 Prediction curves for significant wave period (upper panel) and significant wave height (lower panel) in deep-water conditions (from Wilson (1965), formulae revisited by Goda (2003))

Reservoirs and lakes

The prediction methods presented above cannot be directly applied to inland waters, reservoir and lakes, as the majority of all wave measurements from which these methods were derived have been carried out in open sea conditions. However, wave prediction is a particularly important consideration where reservoirs are concerned, as construction of the appropriate wave protection should be completed in advance of the filling of the reservoir and hence measurements of wave climate are excluded from the design process. Measurements obtained on UK reservoirs (Owen, 1988) showed that none of the **open ocean** methods give particularly good agreement for all conditions.

Three methods are considered here for dealing with such inland water cases: **Saville method**, the **Donelan method** and the **Young and Verhagen method**. It is suggested that these should be adopted for small and medium lakes and reservoirs. For very large fetches, open sea methods are probably the best to apply.

(a) Saville method (or SMB method with effective fetch)

This method uses the SMB wave prediction formulae and curves for open waters (see Equations 4.78 and 4.79), and adapts them to reservoirs using the concept of effective fetch (Saville *et al*, 1962). The definition of the effective fetch is illustrated in Figure 4.32. A noticeable feature is that the effective fetch is independent of wind speed. The effective fetch from Saville should not be used with any other wave prediction formulae than SMB: significant underestimates of wave height will result otherwise.

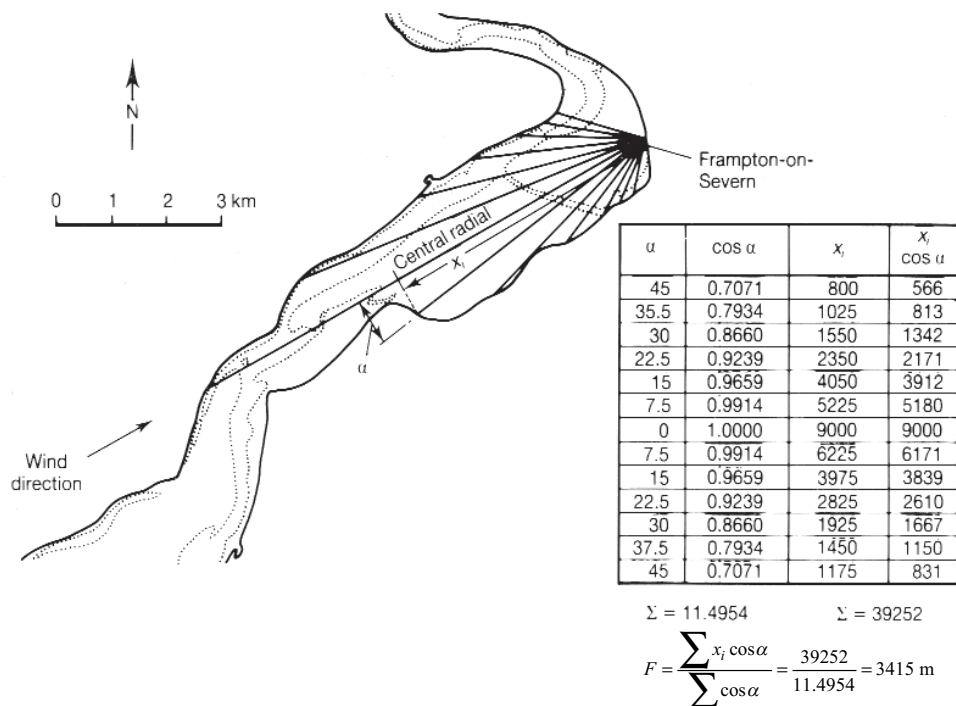


Figure 4.32 Example calculation of effective fetch length by Saville's method

(b) Donelan method

The Donelan method is presented in a series of papers (Donelan, 1980; Bishop and Donelan, 1989; Bishop *et al*, 1992; Donelan *et al*, 1992). It is based on the idea that the fetch length should be measured along the wave direction rather than the wind direction and that the wind speed used for wave prediction should therefore be the component along the wave direction. The method does not assume coincident wind direction, ϕ_w , and wave direction, θ . If the gradient of fetch about wind direction is large, one can expect that the wave direction is biased towards longer fetches. For long and narrow water bodies the wave direction is probably along the water body axis for a wide range of wind directions (rather than the wind direction). Differences up to 50° for $|\phi_w - \theta|$ have been observed on Lake Ontario.

For fetches of general shape, the predominant wave direction was assumed to produce the maximum value of wave period (for a given wind speed). For a point with known fetch distribution F_θ (F_θ is the fetch along the direction θ), the relation between the wave direction, θ , and the wind direction, ϕ_w , can be obtained by maximising the product $\cos(\phi_w - \theta) F_\theta^{0.426}$.

For any irregular shoreline, and a given wind direction, the value of θ satisfying this condition can only be determined by trial and error (Bishop and Donelan, 1989; Massel, 1996). As θ is independent of wind speed only one set of calculations is needed for a particular water body. Once θ has been determined, the significant wave height, peak period and minimum wind duration are derived from Equations 4.86–4.88 (modified from the JONSWAP formulae).

$$\frac{g H_s}{(U_{10} \cos(\theta - \phi_w))^2} = 0.00366 \left(\frac{g F_\theta}{(U_{10} \cos(\theta - \phi_w))^2} \right)^{0.38} \quad (4.86)$$

$$\frac{g T_p}{U_{10} \cos(\theta - \phi_w)} = 0.542 \left(\frac{g F_\theta}{(U_{10} \cos(\theta - \phi_w))^2} \right)^{0.23} \quad (4.87)$$

$$\frac{g l_{min}}{U_{10} \cos(\theta - \phi_w)} = 30.1 \left(\frac{g F_\theta}{(U_{10} \cos(\theta - \phi_w))^2} \right)^{0.77} \quad (4.88)$$

The value of the directional fetch, F_θ , is limited by the criterion expressed by Equation 4.89 to avoid over-development of wave energy.

$$\frac{g l_{min}}{U_{10} \cos(\theta - \phi_w)} = 30.1 \left(\frac{g F_\theta}{(U_{10} \cos(\theta - \phi_w))^2} \right)^{0.77} \quad (4.89)$$

At this value of non-dimensional directional fetch, F_θ , fully development of waves is reached, resulting in Equations 4.90 and 4.91.

$$\frac{g H_s}{(U_{10} \cos(\theta - \phi_w))^2} = 0.285 \quad (4.90)$$

$$\frac{g T_p}{U_{10} \cos(\theta - \phi_w)} = 7.56 \quad (4.91)$$

(c) Young and Verhagen method

Young and Verhagen (1996) analysed a large set of wave measurements performed on Lake George (Australia). From this comprehensive dataset they were able to propose wave prediction formulae including both the effect of fetch F and water depth h (see Equations 4.92 and 4.93). The formulae are based on the form of the formulae of SPM (1984) for wave generation in finite water depth:

$$\frac{g H_s}{U_{10}^2} = 0.241 \left(\tanh A_1 \tanh \left(\frac{B_1}{\tanh A_1} \right) \right)^{0.87} \quad (4.92)$$

where: $A_1 = 0.493 \left(\frac{gh}{U_{10}^2} \right)^{0.75}$ and $B_1 = 0.00313 \left(\frac{gF}{U_{10}^2} \right)^{0.57}$.

$$\frac{g T_p}{U_{10}^2} = 7.519 \left(\tanh A_2 \tanh \left(\frac{B_2}{\tanh A_2} \right) \right)^{0.37} \quad (4.93)$$

where: $A_2 = 0.331 \left(\frac{gh}{U_{10}^2} \right)^{1.01}$ and $B_2 = 0.0005215 \left(\frac{gF}{U_{10}^2} \right)^{0.73}$.

This latter method offers the advantage of taking account of the actual water depth, which is important for reservoirs. Indeed, the mean water level in a reservoir may change significantly over a year leading to significant variations of fetch length and water depth. Both these parameters are present in the above formulae.

Later Young (1997) observed that these formulae fail to correctly model the wave height for short fetches, which was attributed to the fact that the formulae revert to JONSWAP formulae (Hasselmann *et al.*, 1973) for such cases. For a better treatment of this case, he proposed an equation that has to be integrated numerically to obtain a wave growth curve.

Hurricane waves

Hurricane wave conditions can be predicted by the parametric wave model of Young (1988). The model captures the physics of tropical cyclone waves via the JONSWAP formulation of wave spectrum. The model is forced by the surface wind beneath the moving storm and prescribes maximum wave height and period, which is the severe swell wave generated by the storm. The US Army Corps of Engineers has adopted this formulation and a monogram in the *Coastal engineering manual [CEM]* (USACE, 2003).

Comments on the applicability of wave prediction formulae

The simple prediction formulae listed above may be used on real cases provided that the water depth does not vary significantly over the area and that the wind field is homogenous (both in speed and direction). The following should be noted on their general applicability:

- 1 The above formulae may not be suitable for the particular situation where fetches are very limited (shorter than 1 km), but where the wind is extremely strong (in the order of 100 km/h or more). This is the situation encountered in the estimation of the wave height in a harbour basin or a reservoir in violent storm conditions. This corresponds to non-dimensional fetches gF/U_{10}^2 close to 1 or less. In such situations the wave heights grow to 1 m within a few hundred metres of fetch. Most of the wave prediction formulae are not calibrated in this situation. Van der Meer *et al* (2003) addressed this item and compared a number of formulae, with the final conclusion that the Wilson (1955) formulae are suitable in this situation (Equations 4.81 and 4.83).
- 2 Only simple methods are given here for the derivation of wave conditions. Nowadays in many situations numerical wave models are used. Most of these models are third-generation spectral wave models (such as WAM, SWAN, TOMAWAC, WAVEWATCH models for example). Of course numerical modelling requires more human and computational effort to obtain wave predictions, but it is much more reliable than the simple methods described above. Such numerical models should be employed when the bathymetric configuration is irregular and/or when the wind condition is not homogeneous over the water domain or changing with time. Such wave models are briefly described in Section 4.2.4.10.

4.2.4.7 Transformation of waves in the nearshore and coastal zones

For coastal structures, the effects of water-depth reduction and coastal forms on the incoming waves should be accounted for. These factors transform the incoming waves by refraction, shoaling, diffraction and eventually wave breaking. Wave breaking results in significant dissipation of energy and is often the major factor limiting the design wave height and consequently the loading on the structure. All these phenomena are a function of water depth, so a proper description of bathymetry is required (see Section 4.1). This section presents graphs and formulae for the designer to make a first assessment of the influence of these phenomena. However, to complete a full, spatial description of wave parameters, appropriate numerical models of wave propagation should be used (see Section 4.2.4.10).

Refraction

Refraction is the change in the wave propagation velocity, and consequently also in the direction of wave propagation, when waves propagate in varying water depth. In decreasing water depth the direction of wave incidence, β ($^\circ$), relative to the structure inclines towards the direction normal to the depth contours. This usually implies that the wave crests tend to become more parallel to the coastline when approaching more shallow water (see Figure 4.33). The corresponding change in wave height (relative to the deep-water wave height, H_0), caused by redistribution of energy along the wave crests, is usually expressed in the refraction coefficient K_R .

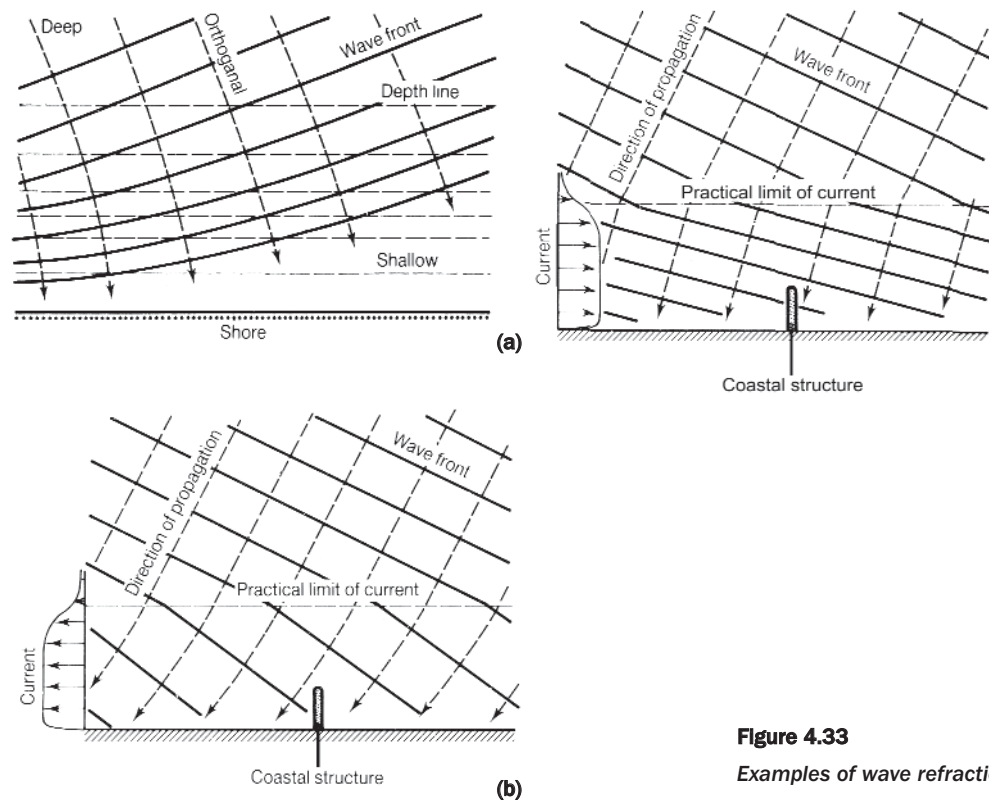


Figure 4.33
Examples of wave refraction

Applying linear wave theory to a regular wave with wave number k and direction β_0 in deep water the local wave direction β at a water depth h is found from Equation 4.94.

$$\beta = \arcsin(\sin \beta_0 \tanh(kh)) \quad (4.94)$$

The corresponding refraction coefficient, K_R , is computed from Equation 4.95.

$$K_R = (\cos \beta_0 / \cos \beta)^{1/2} \quad (4.95)$$

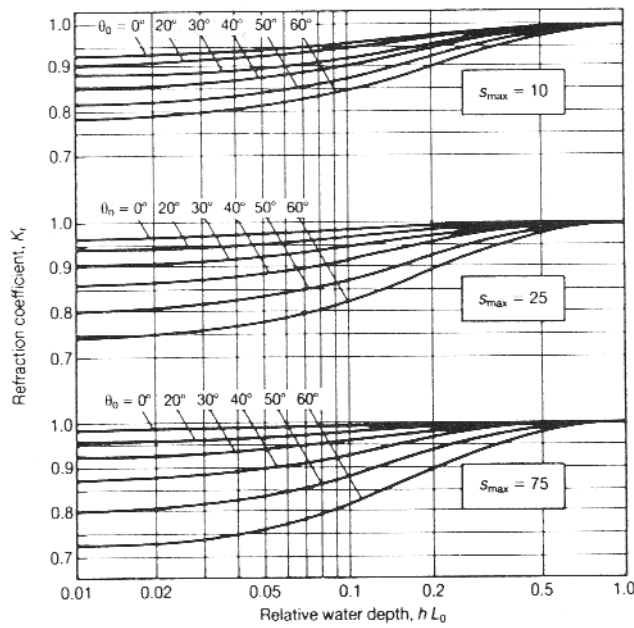
For irregular seas, a representative effective value should be obtained by applying an averaging procedure to a range of relevant frequencies f , or corresponding wave numbers k , and offshore directions β_0 . Thereby weight factors should be determined to account for the relative contributions $(\Delta E)_{ij}$ from intervals $(\Delta f, \Delta \beta)$ to the total energy content m_0 of the directional spectrum $S(f, \beta)$.

Neglecting shoaling effects, this leads to Equations 4.96 and 4.97.

$$(\Delta E)_{ij} = \frac{1}{m_0} \int_{\Delta f} \int_{\Delta \beta} S(f, \beta) df d\beta \quad (4.96)$$

$$K_R = \sqrt{\sum_i \sum_j (\Delta E)_{ij} (K_R)_{ij}^2} \quad (4.97)$$

For practical reasons, intervals Δf and $\Delta \beta$ of varying widths are usually chosen, centred on a number of representative values for f and β respectively (eg requiring equal energy contributions for each interval). Applying an extended form of this procedure, Goda (2000) has given diagrams (see Figure 4.34) for K_R in a directional wave field on a coast with straight, parallel depth contours.



Note: s_{max} is a parameter used to describe directional spreading. Goda (1985) suggests the following values:

- i) Wind waves: $s_{max} = 10$
- ii) Swell with short decay distance: $s_{max} = 25$
(with relatively large wave steepness)
- iii) Swell with long decay distance: $s_{max} = 75$
(with relatively small wave steepness)

Figure 4.34

Refraction coefficient, K_R , for an irregular directional wave field on a coast with straight, parallel depth contours (Goda, 2000)

Shoaling

Shoaling is a change in wave height when waves propagate in varying water depths. The shoaling effect is normally expressed in terms of the shoaling coefficient, K_S , which is defined as the local wave height H relative to H_0 . Using linear wave theory K_S can, for a given wave period T , be written as a function of water depth h (see Equation 4.98).

$$K_S = \left[\tanh(kh) \left(1 + \frac{2kh}{\sinh(2kh)} \right) \right]^{-1/2} \tag{4.98}$$

Under the usual limitations related to the linear wave theory, the above equation gives appropriate estimates for engineering purposes. It can also be applied to irregular sea-states by making use of H_{m0} and T_p . In this latter case (distribution of energy over frequency), and as a result of non-linear (finite amplitude) effects, deviations of approximately 10 per cent from Equation 4.98 were reported by Goda (2000). When individual waves are considered, however, the deviation is stronger in the nearshore zone, and in this case the analytical approach of Shuto (1974) may be used.

Of course, the above expression of K_S has a limitation: it can never grow to very high values, because of wave breaking. This effect is discussed below. If the structure is located in the surf zone, the shoaling has no effect, because waves break first before they reach the structure. Shoaling is only important if the structure is situated in this shoaling area. In this case deep-water wave conditions may **increase** by shoaling before they reach the structure. This is particularly true for low-steepness waves on steep slopes where this increase of wave height can be very significant and may lead to strong (plunging or surging) breakers.

Dissipation caused by bottom friction

Except for the case of long swell propagating over long distances on continental shelves or in the nearshore zone, energy dissipation caused by bottom friction is usually of less importance compared with the other processes considered in this section (Hamm *et al*, 1993).

Interactions of waves with ambient currents

Where waves interfere with a (tidal) current the wave propagation and the wave parameters are affected. Therefore to obtain appropriate design conditions, the problem of joint probabilities arises (see Section 4.2.5). The effect of an ambient current with velocity U and direction θ_U is a resulting (modified) angular wave frequency of ω_a (rad/s) given by Equation 4.99:

$$\omega_a = \omega_r + k U \cos(\theta - \theta_U) \quad (4.99)$$

where $k = 2\pi/L =$ wave number, $\omega_a = 2\pi/T_a =$ absolute angular frequency (ie measured in a fixed frame of reference), $\omega_r = 2\pi/T_r =$ relative angular frequency (ie measured in a frame moving at the current velocity U).

The relative angular frequency, ω_r (rad/s), is to be determined by solving the **classical** dispersion relation given by Equation 4.38.

The interaction of waves with currents also causes refraction. This is due to the change of wave propagation velocity when waves are running into a current. In Figure 4.33 the effect of current refraction is shown for waves opposing and following a local current with a certain inclination. Examples of this phenomenon may be found in tidal and longshore currents and near the mouth of rivers where ebb currents increase the wave heights quite significantly.

Another design aspect of the combination of currents with waves is the influence on design flow velocities near the sea bed, eg for bed or scour protection. A method of assessing and designing for this combined flow loading is addressed in Sections 5.2.1.9, 5.2.2.5 and 5.2.3.2.

Diffraction

Obstacles and structures such as piles, breakwaters, headlands and islands interfere with propagating waves. The resulting wave field around the structure generally shows a marked change relative to the undisturbed wave field. The resulting wave field is a superposition of three elements.

- 1 Incoming waves (partly attenuated by the structure).
- 2 Waves reflected by the structure.
- 3 Wave energy radiated from limiting points of the exposed part of the structure.

The resulting change of wave height, expressed as the local wave height relative to the original undisturbed wave, is expressed by the diffraction coefficient K_d (-). The amplitude of the components (2 and 3 from above list) is largely determined by the reflection characteristics of the structure.

A diffraction analysis is often performed by using numerical models, as alternatives are available only for very simple geometries, eg alignment and cross-section of seawalls, breakwaters, groynes. The principle of the numerical methods is the solution of the stationary Laplace equation for the wave velocity potential for the case of constant water depth (Sommerfeld, 1896). Common boundary conditions applied are impermeable structures with a vertical wall. More sophisticated models are based on the **mild slope equation** (Berkhoff, 1972) that represents the combined effects of refraction, shoaling, diffraction and reflection on structures. Like the Laplace equation, this equation is based on the linear wave theory, ie small-amplitude waves. It was originally developed for regular waves but can readily be extended to the case of random short-crested waves by using a linear superposition of computations in regular conditions. Depth-induced breaking and bottom friction dissipation can also be included.

This principle can be used to create normalised diagrams of the spatial distribution of diffracted wave conditions. These should, however, be based on random rather than regular waves, as the classic regular wave diagrams can lead to underestimation of wave heights. Using a similar procedure to that described for refraction, effective diffraction coefficients K_d can be calculated for a directional random wave field. Results from Goda (2000) are shown in Figures 4.35 to 4.37, for normally incident waves on breakwaters, where x and y are the rectangular co-ordinates of the point considered from the breakwater tip, with the x -direction being along the breakwater axis. Each figure comprises four diagrams covering both locally generated wind waves ($s_{max} = 10$) and almost unidirectional swell waves ($s_{max} = 75$) in areas both near to and distant from the breakwater(s) (see Box 4.6 for the definition of spreading factor s_{max}). Figure 4.35 shows the results for a semi-infinite breakwater and Figures 4.36 and 4.37 show results for a gap in an infinite breakwater. In the gap case, the leading parameter is the relative gap width B/L ($L =$ local wavelength at gap of width B). Two cases are shown: $B/L = 1$ and $B/L = 4$. For B/L greater than about 5, both breakwater parts interfere with the waves independently and superposition of results obtained with the principle of Figure 4.35 gives a better approximation for K_d .

For oblique angles of incidence ($\beta \neq 0^\circ$, relative to normal), the diagrams can still be used when the breakwater is rotated, maintaining the original co-ordinates, but with B reduced to an imaginary width equal to $B \cos \beta$.

In conclusion, it should be appreciated that the given diagrams can only be used for a rough estimate of K_d when the conditions do not differ too much from the cases given. It should also be stressed that directional wave diffraction diagrams based on regular wave conditions should not be used as the diagrams tend to underestimate K_d and hence also wave heights. It is preferable to use a numerical wave propagation model solving the mild slope equation (Berkhoff, 1972) with random wave conditions imposed at the seaward boundaries.

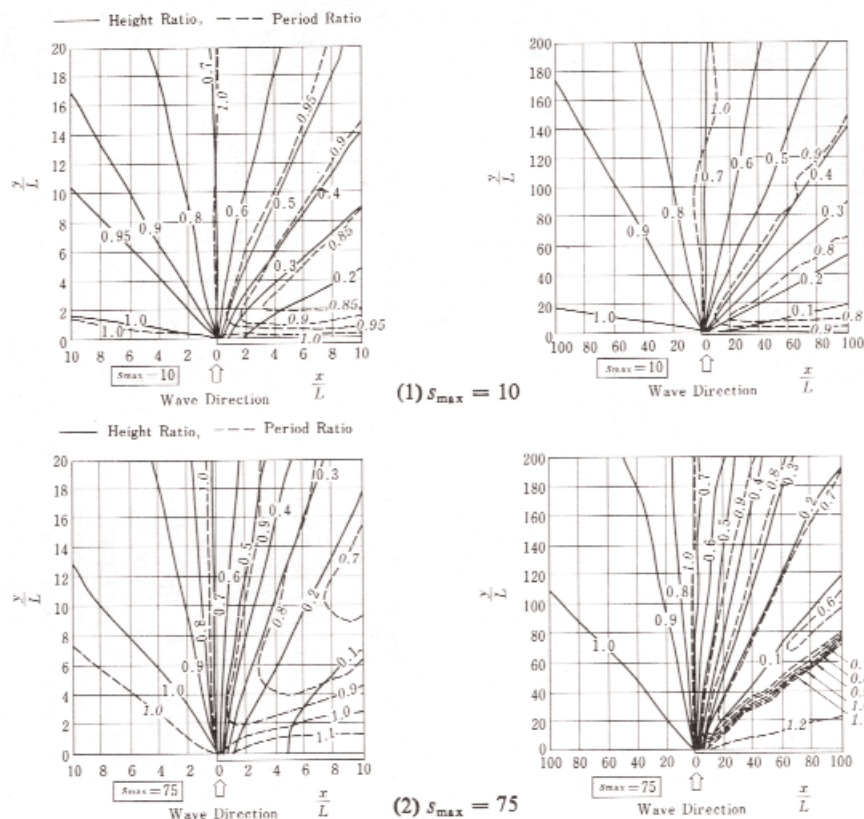


Figure 4.35 Diffraction diagrams for a semi-infinite breakwater for random waves of normal incidence (Goda, 2000)

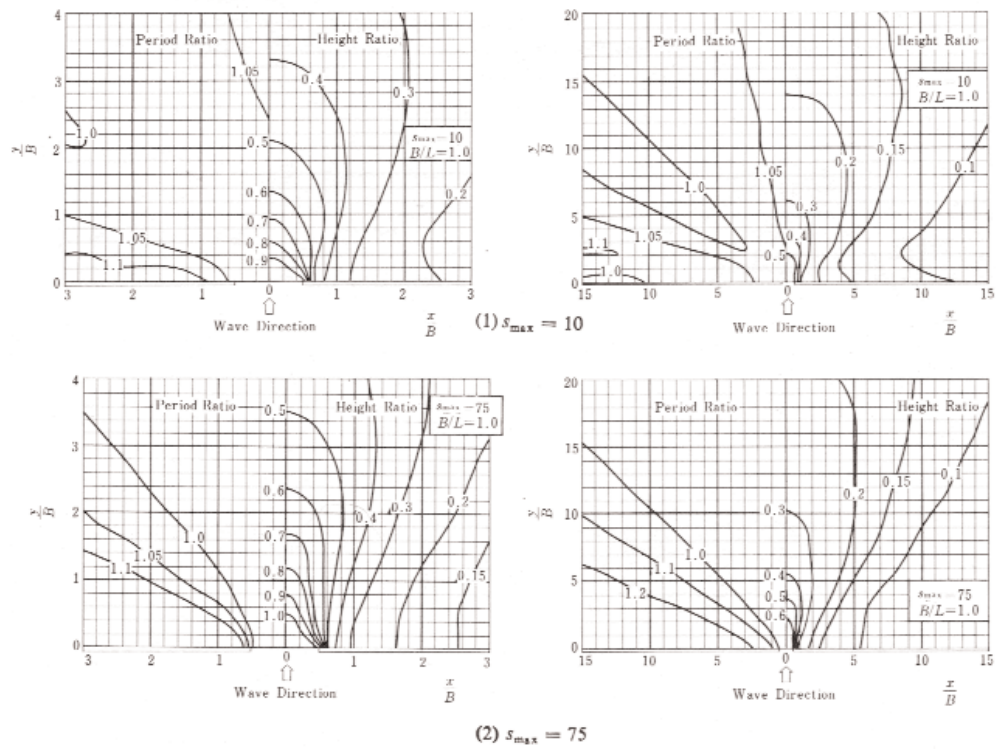


Figure 4.36 Diffraction diagrams for a breakwater opening with $B/L = 1.0$ for random waves of normal incidence (Goda, 2000)

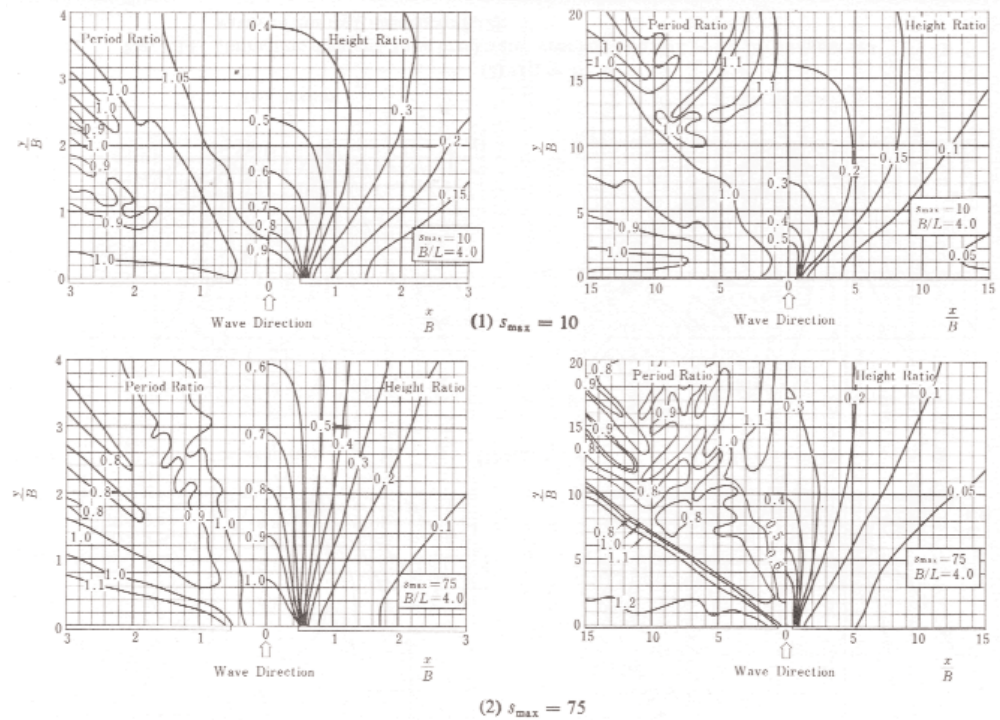


Figure 4.37 Diffraction diagrams for a breakwater opening with $B/L = 4.0$ for random waves of normal incidence (Goda, 2000)

Dissipation caused by breaking

General considerations about wave breaking

Wave breaking occurs mainly when either the steepness ($s = H/L$) or the relative wave height (H/h) becomes too large. Both the depth and the steepness therefore limit the maximum wave height. In shallow water, depth-induced breaking is usually the dominant factor, while the limit of steepness should be considered mainly for the generation of waves (offshore of the structure). A brief review of breaking criteria is given in Box 4.7.

In shallow water, different types of wave breaking may be distinguished depending on the value of the bottom slope and on the characteristics of the incident waves (height and period in particular). Breaking caused by depth limitation ranges from spilling (the most gradual type of breaking), through plunging and collapsing (the most spectacular) to surging (see Figure 4.38). The type of breaking waves is an important factor when considering the wave-induced loadings (see Chapter 5) and is a function of the surf-similarity parameter, ξ (see Section 4.2.4.3).

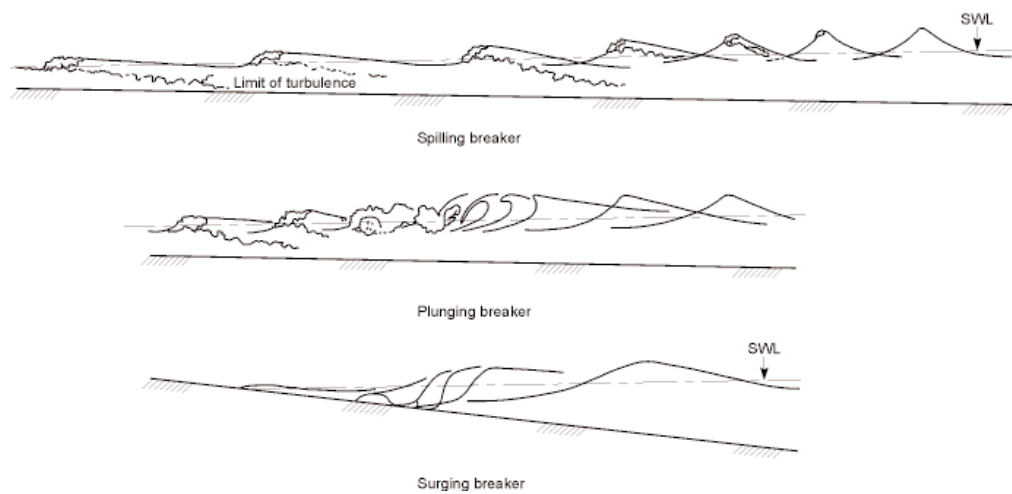


Figure 4.38 Three types of wave breaking in shallow water (from Dean and Dalrymple, 1991, after Svendsen et al, 1979)

Box 4.7 Brief overview of breaking criteria

1 Breaking caused by limiting steepness. Breaking due to exceedance of the steepness criterion is the main limiting factor in deep and medium water. The steepness criterion is given by Equation 4.100 (Miche, 1944).

$$H/L \leq [H/L]_{max} = 0.14 \tanh(2\pi H/L) \tag{4.100}$$

2 Breaking caused by water depth. The breaking criterion due to water depth is normally given by a useful non-dimensional parameter called the breaker index γ_{br} , defined as the maximum wave height to depth ratio H/h (see Equation 4.101) where the subscript b stands for **the value at the breaking point**.

$$H/L \leq \gamma_{br} = [H/h]_{max} = H_b/h_b \tag{4.101}$$

For stable and progressive waves **over a flat bottom** γ_{br} has a theoretical maximum value of 0.78 (McCowan, 1894). Note, however, that γ_{br} is not constant, but ranges roughly between 0.5 and 1.5 depending on the bottom slope and the wave period of the incident waves. Numerous criteria to predict the value of γ_{br} have been proposed. A comprehensive review and comparison of most of them can be found in Rattanapitikon and Shibayama (2000). For regular waves normally incident on a uniform slope, m (ie $m = \tan(\alpha)$), two criteria (see Equations 4.102 and 4.103) may be recommended for practical use:

$$\text{Goda (1970b)} \quad \gamma_{br} = \frac{H_b}{h_b} = 0.17 \frac{L_o}{h_b} \left\{ 1 - \exp \left[-1.5\pi \frac{h_b}{L_o} \left(1 + 15m^{4/3} \right) \right] \right\} \tag{4.102}$$

$$\text{Weggel (1972)} \quad \gamma_{br} = \frac{H_b}{h_b} = \frac{b(m)}{1 + a(m) \frac{h_b}{L_o}} = b(m) - a(m) \frac{H_b}{L_o} \tag{4.103}$$

where $a(m) = 6.96 [1 - \exp(-19m)]$ and $b(m) = 1.56 [1 + \exp(-19.5m)]^{-1}$

Other criteria and a comparison of them on a large set of data can be found in Rattanapitikon and Shibayama (2000) and in Rattanapitikon *et al* (2003), who also proposed a new criterion giving the best fit to the experimental points of the validation database (see Equation 4.104):

$$\frac{H_b}{L_b} = \left[-1.40m^2 + 0.57m + 0.23 \right] \left(\frac{H_o}{L_o} \right)^{0.35} \tag{4.104}$$

where L_b = wavelength computed at the breaking point (depth h_b) by the linear wave theory.

For irregular waves (represented by the significant wave height H_s) typical values are found to be $\gamma_{br} = 0.5$ to 0.6. The actual limiting wave height ratio γ_{br} depends mainly on such parameters as ξ and may reach values as large as 1.5 for **individual waves**. Figure 4.39 gives a good impression of the relationship between γ_{br} and ξ_o (see Section 4.2.4.3) and the related scatter of the data.

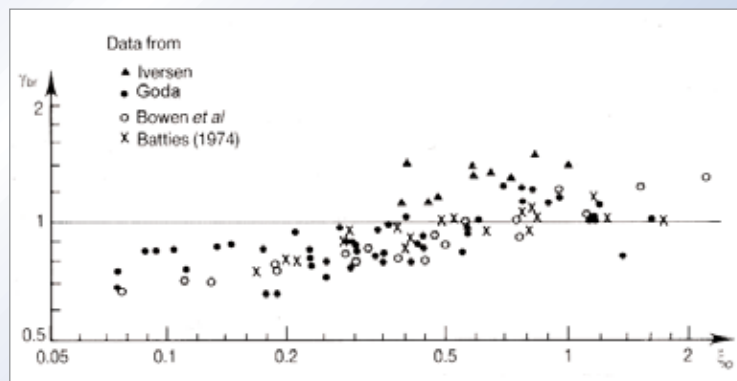


Figure 4.39
Breaker index, γ_{br} as a function of deep-water surf similarity parameter, ξ_o

Depth-limited significant wave height for constant bottom slopes

Wave breaking becomes increasingly important in shallow water, and wave models accounting for breaking should be used. The main effect of wave breaking is a lower significant wave height. But there are other changes due to wave breaking which might have an effect on structures. These changes occur both in the time as well as in the frequency domain. The wave height distribution changes as well as the shape of the spectrum. This section describes the decay in significant wave height due to breaking, while the changes of wave height distribution and spectral shape are addressed in Sections 4.2.4.4 and 4.2.4.5 respectively.

Wave breaking on an irregular foreshore is difficult to describe by simple manual methods. In this case, only sophisticated numerical models (see Section 4.2.4.10) or physical models may give a reliable answer. On the other hand, a rule of thumb for a mild sloping beach (gentler than 1:50) gives that the significant wave height is around 0.5–0.6 of the local water depth. A more reliable and still manual option is described in Box 4.8 for uniform foreshore slopes and based on the graphs of Figure 4.40. Five graphs are given for different wave steepnesses in deep water, $s_{op} = 0.01, 0.02, 0.03, 0.04$ and 0.05 (see Box 4.8 for explanations).

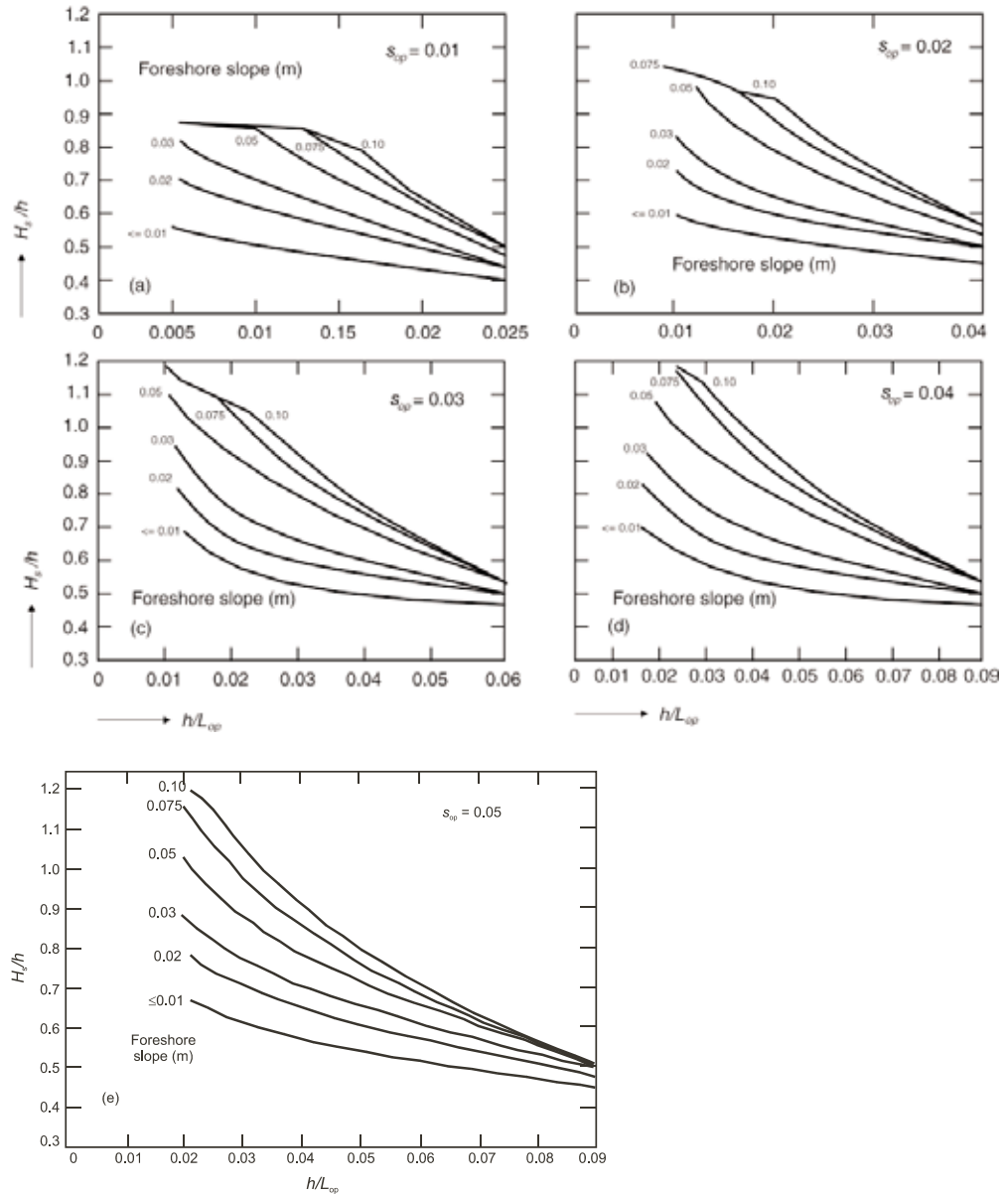


Figure 4.40 Shallow-water significant wave heights on uniform sloping foreshore

Additionally, the effect (through refraction) of wave incidence β_o can be found from Figure 4.41 for $\beta_o = 30^\circ$ and 50° to compare with normal incidence ($\beta_o = 0^\circ$). This can be done for combinations of $s_{op} = 0.01$ or 0.05 and $m = 1:13$ or $1:50$. Refraction is discussed at the beginning of Section 4.2.4.7.

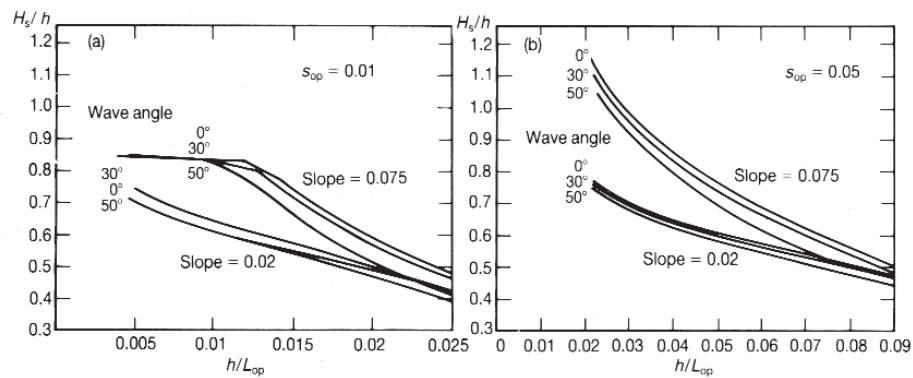


Figure 4.41 Effect of angle of wave incidence on shallow-water significant wave heights on uniform sloping foreshore

Box 4.8 Simplified method to estimate H_{m0} on shallow foreshores under the influence of breaking

Results obtained from a simple 1D energy decay numerical model (van der Meer, 1990) in which the influence of wave breaking is included, are presented in Figure 4.40. Tests have shown that wave height predictions using the design graphs from this model are accurate for slopes ranging from 1:10 to 1:100. For slopes flatter than 1:100, the predictions for the 1:100 slopes should be used.

The method for using these graphs is as follows.

- 1 Determine the deep-water wave steepness, $s_{op} = H_{so}/L_{op}$ (where $L_{op} = gT_p^2/(2\pi)$). This value determines which graphs should be used. Suppose here for convenience that $s_{op} = 0.043$, then the graphs of Figure 4.40 for $s_{op} = 0.04$ and 0.05 have to be used, interpolating between the results from each.
- 2 Determine the local relative water depth, h/L_{op} . The range of the curves in the graphs covers a decrease in wave height by 10 per cent to about 70 per cent. Limited breaking occurs at the right-hand side of the graphs and severe breaking on the left-hand side. If h/L_{op} is larger than the maximum value in the graph this means that there is no or only limited wave breaking and one can then assume no wave breaking (deep-water wave height = shallow-water wave height).
- 3 Determine the slope of the foreshore ($m = \tan \alpha$). Curves are given for range $m = 0.075$ to 0.01 (1:13 to 1:100). For gentler slopes the 1:100 slope should be used.
- 4 Enter the two selected graphs with calculated h/L_{op} and read the breaker index H_{m0}/h from the curve of the calculated foreshore slope.
- 5 Interpolate linearly between the two values of H_{m0}/h to find H_{m0}/h for the correct wave steepness.

Example. Suppose $H_{so} = 6$ m, $T_p = 9.4$ s, foreshore slope is 1:40 ($m = 0.025$). Calculate the maximum significant wave height H_{m0} at a water depth of $h = 7$ m.

- 1 The wave conditions on deep water give $s_{op} = 0.043$. Graphs with $s_{op} = 0.04$ and 0.05 have to be used.
- 2 The local relative water depth $h/L_{op} = 0.051$.
- 3 The slope of the foreshore ($m = 0.025$) is in between the curves for $m = 0.02$ and 0.033 .
- 4 From the graphs, $H_{m0}/h = 0.64$ is found for $s_{op} = 0.04$ and 0.68 is found for $s_{op} = 0.05$.
- 5 Interpolation for $s_{op} = 0.043$ gives $H_{m0}/h = 0.65$ and finally a depth-limited spectral significant wave height of $H_{m0} = 3.9$ m.

Alternative graphs and formulae to determine the effect of both shoaling and wave breaking are presented by Goda (2000) for uniform foreshore slopes, which have been adopted widely. These formulae are summarised in Box 4.9.

Depth-limited significant wave height for irregular bottom profiles

For detailed wave prediction on composite profiles a numerical simulation is preferable. This holds for all cases in which the required accuracy of the predicted wave heights does not allow for any of the profile schematisations given in this manual. If the edge slope begins further than two (local) wavelengths from the structure, the effect of this slope is much reduced and the uniform foreshore slope curves may provide an adequate prediction.

Distribution of wave heights in shallow water and in the breaking zone

The above methods give the spectral significant wave height, H_{m0} , in shallow water. In some cases, the significant wave height $H_s = H_{1/3}$ or the wave heights $H_{1/10}$ or $H_{2\%}$ are required for design formulae. Section 4.2.4.4 gives the outline of the method proposed by Battjes and Groenendijk (2000) to calculate these wave heights from H_{m0} (see Box 4.4).

Wave spectra in shallow water and in the breaking zone

Many wave spectra have a single peak and are well described by a significant wave height H_{m0} and a peak period T_p . In shallow water, however, the spectral shape changes. The peak becomes less pronounced and more energy becomes present at higher and lower frequencies. If severe breaking occurs, the spectrum may become so flat that the peak period is difficult to identify from the spectrum.

In such cases, and also when bimodal or double-peaked spectra are present, the use of the mean energy period $T_{m-1,0}$ instead of the peak period is recommended (see Section 4.2.4.5 and Equation 4.61). This mean energy period has proven to be a reliable period in research on wave overtopping and also stability. It is used extensively in Chapter 5.

Box 4.9 *Formulae for wave height estimation within the surf zone*

Goda (2000) developed formulae to estimate the significant wave height (see Equation 4.105) and the maximum wave height (see Equation 4.106) in the surf zone.

$$H_{1/3} = \begin{cases} K_S H'_0 & \text{for } h/L_o > 0.2 \\ \min\left\{\left(\beta_0 H'_0 + \beta_1 h\right), \left(\beta_{max} H'_0\right), \left(K_S H'_0\right)\right\} & \text{for } h/L_o < 0.2 \end{cases} \quad (4.105)$$

$$H_{max} = H_{1/250} = \begin{cases} 1.8 K_S H'_0 & \text{for } h/L_o > 0.2 \\ \min\left\{\left(\beta_0^* H'_0 + \beta_1^* h\right), \left(\beta_{max}^* H'_0\right), \left(1.8 K_S H'_0\right)\right\} & \text{for } h/L_o < 0.2 \end{cases} \quad (4.106)$$

The coefficients β_0 , $\beta_1(\cdot)$, ... are given in Table 4.14. H'_0 is the equivalent deep-water significant wave height, defined in Section 4.2.2.5.

Table 4.14 Coefficients for $H_{1/3}$ and H_{max}

Coefficients for $H_{1/3}$	Coefficients for H_{max}
$\beta_0 = 0.028 (H'_0 / L_o)^{-0.38} \exp(20m^{1.5})$	$\beta_0^* = 0.052 (H'_0 / L_o)^{-0.38} \exp(20 \cdot m^{1.5})$
$\beta_1 = 0.52 \exp(4.2m)$	$\beta_1^* = 0.63 \exp(3.8m)$
$\beta_{max} = \max\{0.92, 0.32 (H'_0 / L_o)^{-0.29} \exp(2.4m)\}$	$\beta_{max}^* = \max\{1.65, 0.53 (H'_0 / L_o)^{-0.29} \exp(2.4m)\}$

The above shoaling coefficient K_S is obtained using linear wave theory (see Equation 4.98). m is the beach gradient.

Goda (2000) advises that this numerical formula may overestimate wave heights by several per cent. In particular, for waves of steepness greater than 0.04, the formulae overestimate significant wave heights by at least 10 per cent around the water depth at which the value of $H_{1/3} = \beta_0 H'_0 + \beta_1 h$ becomes equal to the value of $H_{1/3} = \beta_{max} H'_0$. A similar difference also appears for the case of H_{max} . Waves of large steepness may have a discontinuity in the estimated height of H_{max} at the boundary $h/L_o = 0.2$. Caution should be taken when applying Goda's formulae with regard to such differences and discontinuities.

4.2.4.8 Short-term or daily wave climate

In the above sections, attention was paid to individual waves within a sea-state (Sections 4.2.4.2 and 4.2.4.3) and then to characteristic waves of a sea-state (Sections 4.2.4.4 to 4.2.4.7). In order to describe the total hydraulic boundary conditions a **distribution** of wave conditions have to be defined, both height and period, both in deep and in shallow water. The climatology of sea-states has to be analysed (based on some representative parameters such as the significant wave height, the mean or peak period, the mean wave direction etc) on the basis of a set of data covering several months to several years (typically one year) and covering a range of storm conditions.

Results of the daily or short-term wave climate are often useful for the design of a structure (which is in fact dictated by the long-term wave climate; see Sections 4.2.4.9). Furthermore, they are very important for the definition of operating conditions for the structure, the operability of floating equipment, the knowledge of typical wave conditions during the construction or maintenance phases.

Based on a series of sea-state parameters (given every three or six hours typically), it is possible to build several useful tables and graphs describing the short-term or daily wave climate.

- **Histograms of significant wave height, mean (or peak or significant) period, mean wave direction** etc. For each parameter a set of classes of values is defined and, from the measured series of sea-states parameters, the number of events per class (and so the empirical probability of occurrence) is estimated from the data. The analysis may be restricted to a particular period of the year (to analyse the seasonal effects), to a range of incoming wave directions (to separate different wave regimes) etc.
- **Wave roses**, in the same manner as wind roses, as presented in Section 4.2.1.1. This type of representation allows a combined view of the most frequent incoming wave directions and associated wave heights. Again, different wave regimes can thus be separated (eg swell and wind-sea conditions) (see Figure 4.42 built from the scatter diagram of Figure 4.43).
- A **scatter diagram** of wave height and period which gives the fraction of waves found within each of a number of predefined classes of H_s and T_m . The scatter diagram is created by counting the total number of individual sea-states falling within classes ΔH_s and ΔT_m . Division by the total number of sea-states gives an estimate of the 2D (H_s, T_m) joint-distribution function (see Figure 4.43).

1

2

3

4

5

6

7

8

9

10

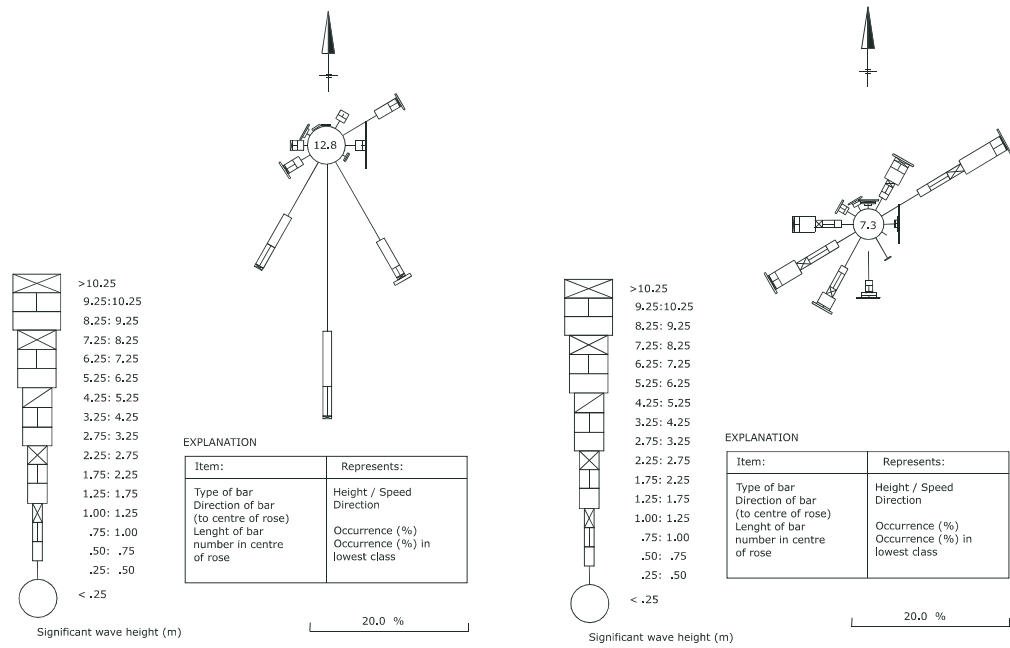


Figure 4.42 Wave roses built from the data of Figure 4.43

NOTE: In Figure 4.42, the wave conditions have been split into swell conditions (left panel) and wind-sea conditions (right panel).

An example of scatter diagram of wave conditions (both wind-sea and swell are considered) is given on Figure 4.43. It should be stressed that the focus is on the correlation between representative parameters of the sea-state, and not between parameters of individual waves. This latter correlation is briefly described in Section 4.2.4.4, but is of lesser interest for the design of structures. The joint distribution of (H_s, T_m) or (H_s, T_s) is far more useful, as it allows definition of combined conditions for the design procedure.

Significant wave height (m)	Significant wave period (s)														Total
	< 3.5	3.5–4.5	4.5–5.5	5.5–6.5	6.5–7.5	7.5–8.5	8.5–9.5	9.5–10.5	10.5–11.5	11.5–12.5	12.5–13.5	13.5–15.5	15.5–17.5	> 17.5	
< 0.25	0.32	3.57	5.96	1.45	1.06	0.64	0.28	0.32	0.30	0.19	0.12	0.57	-	-	14.78
0.25–0.50	-	7.41	21.81	5.54	3.32	1.58	0.95	0.32	0.12	0.09	0.14	0.08	-	-	41.36
0.50–0.75	-	2.97	12.77	4.78	2.53	1.25	0.57	0.30	0.19	0.03	-	-	-	-	25.37
0.75–1.00	-	0.73	6.35	3.28	1.15	0.58	0.41	0.23	0.07	-	0.03	-	-	-	12.82
1.00–1.25	-	0.03	1.07	2.08	0.81	0.28	0.05	0.14	0.04	0.03	-	-	-	-	4.51
1.25–1.75	-	-	0.07	0.38	0.47	0.08	0.03	-	-	0.01	-	0.01	-	-	1.06
1.75–2.25	-	-	-	-	0.03	0.07	-	-	-	-	-	-	-	-	0.09
2.25–2.75	-	-	-	-	-	-	-	-	-	-	-	-	-	-	-
2.75 <	-	-	-	-	-	-	-	-	-	-	-	-	-	-	-

Figure 4.43 Scatter diagram (% of time) in given wave height and period classes for a specific area in an average year and for all incoming directions (note these data are plotted on Figure 4.42)

The main interest is usually focused on the distribution of wave heights, and in particular on the determination of wave heights that are exceeded (for example) 10 per cent, 1 per cent or 0.1 per cent of time on average over one year (or alternatively for the winter season or the

summer season). This information can be extracted from the empirical distribution of significant wave heights. To that end, the empirical distribution of wave height may be presented in the form of Figure 4.44, for example.

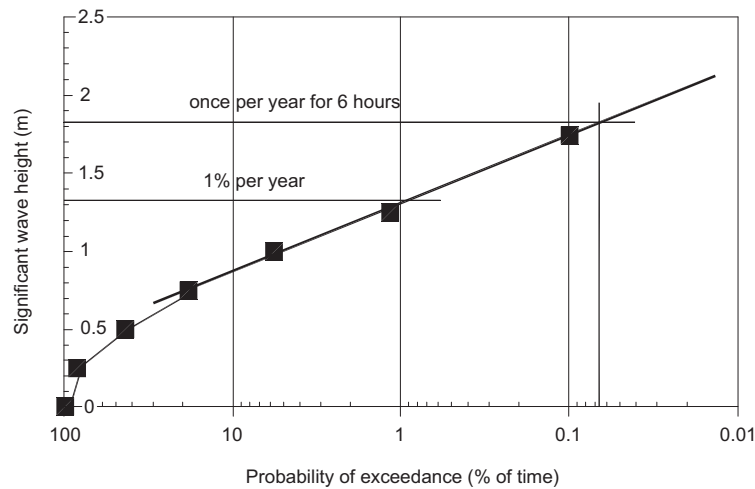


Figure 4.44 Daily wave climate based on data of Figure 4.43

NOTE: The 1%-per-year wave height is 1.33 m, which occurs on about three or four days a year. Considering a sea-state duration of 6 hours, the wave height that is exceeded once per year is given at $100\% \times 6 \text{ h sea-state} / (365 \text{ days} \times 24 \text{ h}) = 0.068\%$. This gives a significant wave height of 1.82 m.

4.2.4.9

Long-term wave climate – analysis of extreme waves

Introduction

For the design of a structure exposed to wave attack, the definition of design conditions requires knowledge (or estimation of) the distribution of probability of large and extreme events. The purpose of the determination of the long-term climate is to associate a wave height to a given return period (typically 30 to 100 years), and if possible with a confidence level.

Extremes analysis procedures are usually applied only to **significant wave heights**. Extrapolation of the validity of a distribution beyond the range covered by the measurements should be done with care. However, this is generally the only way of predicting low-frequency (long return period) events. The procedure adopted is to fit to a theoretical extreme-value distribution and then to extrapolate the fitted distribution to extreme values.

Note that at least five complete years of wave height data are required for extreme wave analysis, but for reliable extreme predictions 20–50 years are necessary.

Distribution of significant wave height in deep-water conditions

There is no theoretical argument in favour of the use of any particular probability density function in all situations. Some examples of widely used probability models are given in Box 4.10. In the majority of cases (Mathiesen *et al.*, 1994) the three-parameter Weibull distribution provides a fit to H_s data that is as good as any other candidate distribution, which is illustrated in more detail in Box 4.11.

Box 4.10 Extreme value probability distributions

The following extreme value probability distributions (see Equations 4.107 to 4.110) are commonly used to fit the long-term distributions of wave height, water levels etc.

$$\text{Gumbel} \quad P(X) = P(\underline{X} \leq X) = \exp[-\exp(-aX + b)] \quad (4.107)$$

$$\text{Weibull} \quad P(X) = P(\underline{X} \leq X) = 1 - \exp\left[-\left(\frac{X-a}{b}\right)^c\right] \quad (4.108)$$

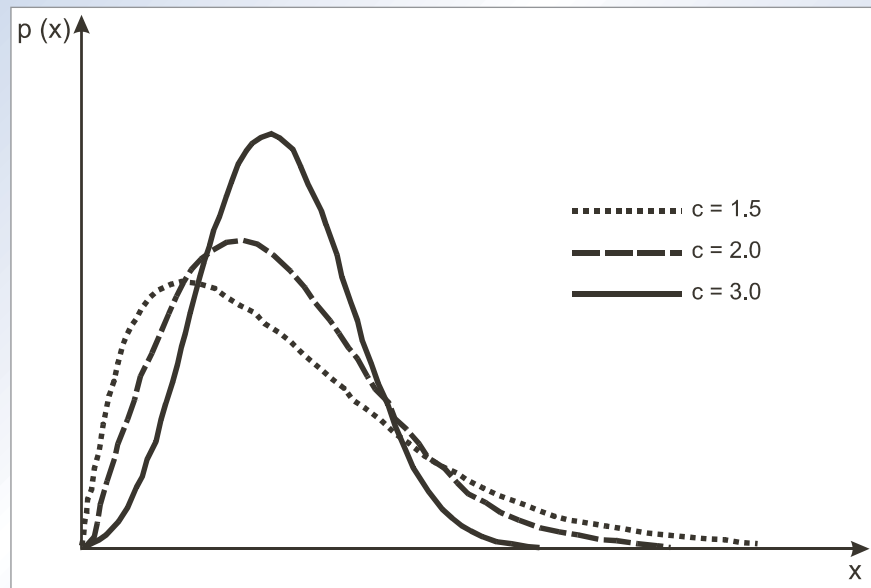
$$\text{Log-normal} \quad p(X) = \frac{1}{aX\sqrt{\pi}} \exp\left[-\left(\frac{\ln(X)-b}{a}\right)^2\right] \quad (4.109)$$

$$\text{Exponential} \quad P(X) = P(\underline{X} \leq X) = 1 - \exp\left[-\frac{X-a}{b}\right] \quad (4.110)$$

where $P(X)$ is the cumulative probability function, ie the probability that \underline{X} will not exceed X , ie $P(\underline{X} \leq X)$, and $p(x)$ is the probability density function of x and $p(x) = dP/dx$.

Note that the three-parameter Weibull distribution reduces to the shifted Rayleigh distribution if $c = 2$ and $a \neq 0$ and to the classical shifted Rayleigh distribution if $c = 2$ and $a = 0$ (see Figure 4.45).

With $c = 1$, the three-parameter Weibull corresponds to the exponential distribution, very often used for extreme wave climate analysis. The more universal nature of the Weibull distribution means that this is often the preferred model.



Note: The curve with $c = 2$ corresponds to the Rayleigh distribution presented in Section 4.2.4.4.

Figure 4.45 The two-parameter Weibull distribution (third parameter $a = 0$)

Box 4.11 Three-parameter Weibull distribution

The three-parameter Weibull distribution is defined by Equation 4.111.

$$P(\underline{H} \leq H_s) = 1 - \exp\left(-\left(\frac{H_s - a}{b}\right)^c\right) \quad (4.111)$$

where H_s = significant wave height and a , b , c = parameters of the distribution to be found.

Rearranging and taking logs twice results in Equation 4.112.

$$\log(-\log(1 - P(H_s))) = c(\log(H_s - a) - \log b) \quad (4.112)$$

Consequently, x , defined by Equation 4.113, and y , defined by Equation 4.114, can be plotted on linear scale.

$$x = \log(H_s - a) \quad (4.113)$$

$$y = \log(-\log(1 - P(H_s))) \quad (4.114)$$

Alternatively, and more conveniently, appropriate graph paper is available with a logarithmic scaling following Equation 4.112. The parameters of the distribution are calculated after plotting the various exceedence levels on this Weibull scaled graph paper (see Equation 4.112) and drawing the best-fit straight line through the points (see Figure 4.46). As a check, this procedure can be reproduced by a computer program and the results compared.

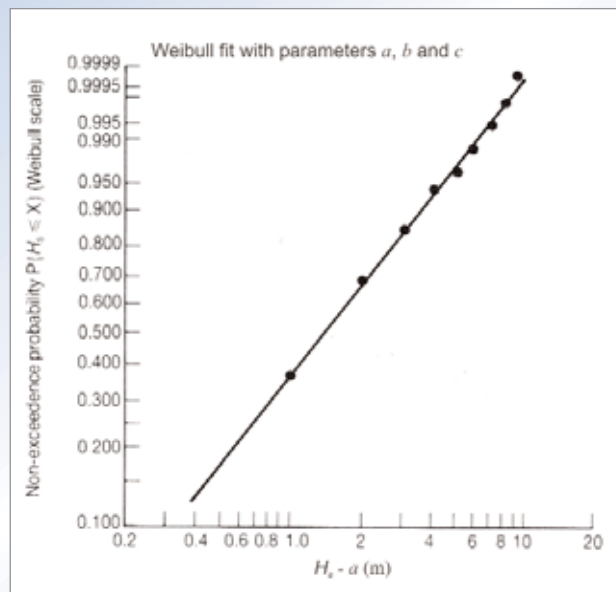


Figure 4.46
Weibull fit to long-term
wave height distribution

The following two points are more important than the choice of a particular candidate model to fit available samples of events:

- **is the distribution steep or not?** A steep distribution means that very extreme conditions may be much higher than the considered design conditions. This is not the case for flat distributions
- **what is the confidence interval of any estimation?** This is particularly sensitive for long return periods, ie low occurrence probability.

Analysis procedure

The recommended procedure for analysing the data comprises the following steps:

- 1 Select the data for analysis.
- 2 Fit candidate distribution(s) to the data.
- 3 Compute return values from the fitted distribution(s).
- 4 Consider confidence in the predictions.

Selection, checking and preparation of data together form probably the most important stage in the analysis procedure. For extraction of storm wave height data, the peaks-over-threshold (POT) method is recommended. In this method, only the storm peak wave heights above some chosen threshold (eg $H_s = 3$ m) are used in the extremes analysis. It is recommended that the wave height threshold is selected to achieve that the average number of selected data values per year (typically 5–10) above the threshold is equal to or less than the average number of storms per year (typically 10–20). For areas where there is a strong seasonal variation of storms, an appropriate threshold can be obtained by the requirement that one storm per year from the calmer season is to be included in the dataset.

Three methods are commonly used to determine the optimum parameter values for the distribution to be fitted, namely the maximum likelihood method, the method of moments and the least squares method. The method of moments works by equating statistical moments (mean, standard deviation, skewness etc) of the model distribution to the moments of the observed distribution. The number of statistical moments used is equal to the number of parameters of the model distribution. Several model distributions are described in Appendix 5 of Tucker and Pitt (2001) and in Goda (2000) for example, together with the relationships between the moments and the parameters of the distributions.

The return value $x(T_R)$ is the threshold value equalled or exceeded on average once during a time interval, T_R (the return period (years)). Knowing T_R , cumulative distribution $P(x(T_R))$ can be determined using Equation 4.115:

$$P(x(T_R)) = 1 - \frac{T_c}{T_R} \quad (4.115)$$

where T_c = average time between storms (year).

$P(x(T_R))$ can be also found from Equation 4.111 in Box 4.11, which in turn allows $x(T_R)$ to be determined from a fitted distribution such as described in Box 4.11.

An alternative way of considering an event with a given return period is to consider that (for $T_R \geq 5$ years) the probability of its occurrence in any one year is approximately equal to $1/T_R$. For example, a 10 000-year return period event is equivalent to one with a probability of occurrence of 10^{-4} in any one year (see Section 2.3.3.2 and Table 2.4 for further discussion).

Over an envisaged lifetime of N years for a structure (not necessarily the same as the design return period) the probability of encountering the wave condition with return period T_R , at least once, is given by Equation 4.116.

$$P(\underline{H} \geq H(T_R)) = 1 - \left(1 - \frac{1}{T_R}\right)^N \quad (4.116)$$

Figure 4.47 presents curves for this **encounter probability** with values between 1 per cent and 80 per cent shown as a function of T_R and N .

Uncertainties in the computed extreme values depend mainly on:

- inaccuracy or unsuitability among the source data
- inherent statistical variability, ie sampling variability
- uncertainty due to possible incorrect choice of extreme value distribution
- uncertainty in the computation of significant wave height due to a record of limited length.

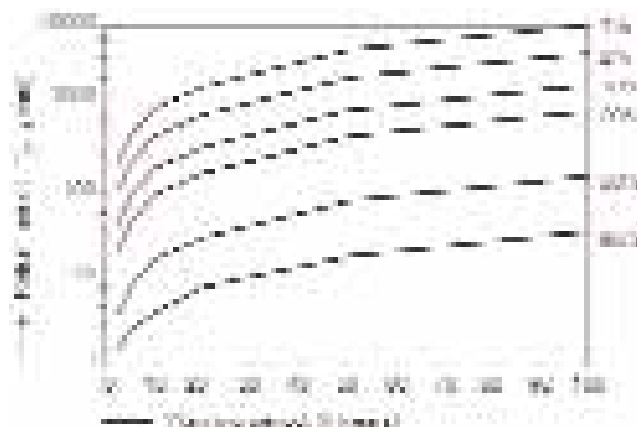


Figure 4.47 Encounter probability

NOTE: This figure is an extended visualisation of the data in Table 2.4.

Confidence interval formulae take account only of statistical variability, and not of uncertainties in the source data or the choice of fitted distribution. They should therefore be used with some caution, and a confidence estimate based on experience and sensitivity testing may be more reliable.

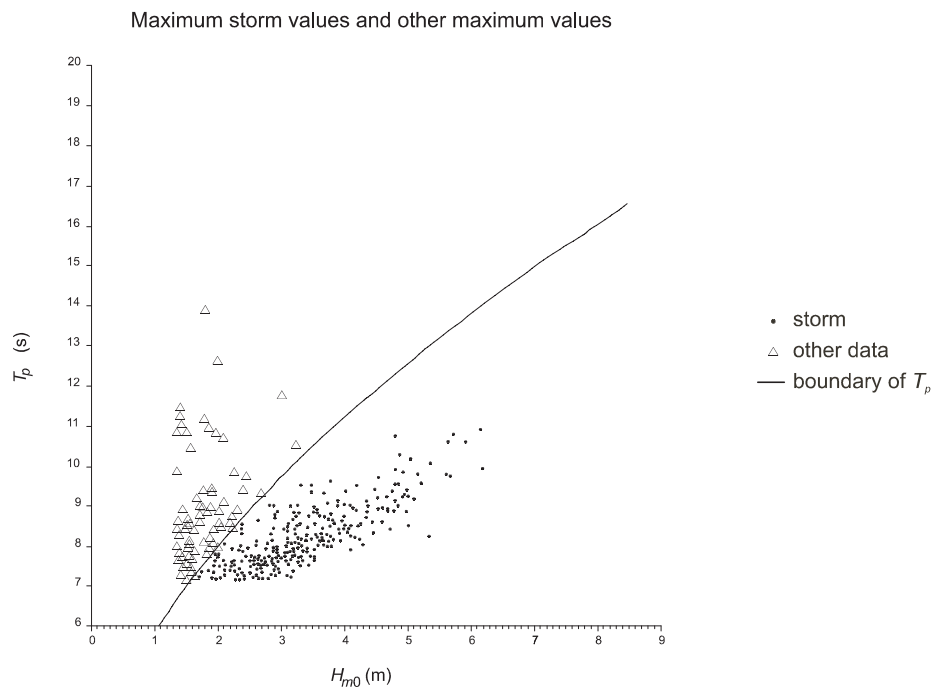
The most obvious and sometimes most effective goodness-of-fit test consists of plotting the source data against the fitted distribution, on scales (for example, log scales) designed to give visual emphasis to the highest values. Mathiesen *et al* (1994) discuss a number of statistical goodness-of-fit tests applicable to particular distributions.

Estimation of wave period

In the design of rock structures it is usually necessary to know the mean wave period, T_m , as well as the significant wave height, H_s , derived from extremes analysis. Any treatment of wave period is usually based on the assumption that wave height and wave period are strongly correlated, as already analysed for the short-term or daily wave climate (see Section 4.2.4.8), perhaps being related by a constant wave steepness. Any treatment of wave direction is usually based on a **conditional analysis** where the condition is that the wave records analysed have directions within a particular angular sector. In other words, wave data within different direction sectors are considered as being members of different populations, which can be analysed separately.

A common approach is to look at the joint distribution of (H_s, T_m) among the highest few percent of wave conditions in the source data. The average wave steepness ($2\pi H_s / (g T_m^2)$) for these data can be computed and then applied to the predicted extreme wave heights. Wave steepness in deep water is typically in the range 0.045–0.065. It tends to have a lower value in shallow water, where wave height may have reduced but wave period is little changed from deep water. If there is any doubt about the exact wave steepness to use, note that the use of a lower wave steepness (hence higher wave period) tends to be conservative for most design purposes. An example of such treatment is presented on Figure 4.48 for wave data collected in the North Sea.

The ratio between peak period, T_p , and mean period, T_m , varies slightly depending upon the type of weather conditions, and upon the shape and size of the wave generation area, but in the absence of site-specific effects, T_p tends to be about 25 per cent greater than T_m (see Section 4.2.4.5).

**Note**

Triangles are combined sea and swell, dots are only storm waves. It is possible to make lines with constant wave steepness in the graph, for example $s_{op} = 0.03$ and 0.04 , which gives an indication of the relationship between wave height and period for extremes (storms).

Figure 4.48 Measured peak wave period T_p and wave heights H_{m0} on the North Sea

Estimation of the maximum individual wave height

The highest individual wave height, H_{max} , over a period of three hours is typically about 1.8 times H_s in deep water (see Table 4.9 in Section 4.2.4.4), reducing gradually to about 1.6 in shallow water just before breaking.

Special considerations for shallow-water conditions

The model probability distributions applicable in deep water may be less suitable for use in shallower water and/or close to the coast for two main reasons.

- 1 Differences between populations of waves, eg storm waves and swell waves, hurricane and non-hurricane, or easterly waves and westerly waves, may become more marked closer to the coast. In addition, wave transformation and possible impact on structures may depend upon wave direction. It is often necessary to divide extreme wave predictions into more than one direction sector, and sometimes into as narrow as 30° sectors, and to analyse each relevant sector separately.
- 2 The highest wave conditions may be limited in height by the shallow-water depth, affecting both the distribution fitting and the validity of any extrapolation beyond the sample range, and introducing a dependence upon the assumed sea level. If possible, extremes should not be predicted in this situation, but if it is unavoidable, then the predicted extremes should be checked to see if they could possibly exist in the depth of water available.

The usual procedure is to transfer the deep-water extreme wave climate just offshore of the location of the structure, very often in shallow water, to obtain the conditions to be used for design of the structure.

- 1 Establish the deep-water extreme wave climate and find the significant wave heights associated with various return periods (eg one year, five years, 10 years, 20 years, 50 years, 100 years), and determine associated peak periods.
- 2 Transfer these wave conditions to the design water depth for the structure, by using either a numerical propagation model or the schematic procedure outlined in Section 4.2.4.7 for estimating H_{m0} at the design water depth. It is essential that the method used to transfer the offshore conditions properly accounts for refraction, shoaling and breaking (and bottom friction dissipation and diffraction as well, if significant).
- 3 From the transferred dataset, compute the local significant wave heights $H_s = H_{1/3}$ and the 2 per cent wave height $H_{2\%}$ by using the method of Battjes and Groenendijk (2000) outlined in Section 4.2.4.4.
- 4 Plot the variations of the local wave heights (including also the deep-water wave height) as a function of the return period. This type of figure shows how extreme waves break and that the wave condition at the structure is limited due to the water depth. In this case, a larger return period gives larger deep-water wave heights, but marginally larger shallow-water wave heights, which is very important information for the design.

In addition to the results presented in Section 4.2.4.4 on distribution of wave heights in shallow water, practical relationships are given by Stive (1985). The relationships are based upon prototype and laboratory data and give $H_{1\%}$ (see Equation 4.117) and $H_{0.1\%}$ (see Equation 4.118) as a function of H_s and local depth h .

$$H_{1\%} = 1.517H_s / (1 + H_s/h)^{1/3} \quad (4.117)$$

$$H_{0.1\%} = 1.859H_s / (1 + H_s/h)^{1/2} \quad (4.118)$$

In Equations 4.117 and 4.118, the coefficients 1.517 and 1.859 represent conversion coefficients for the significant wave height that follows the Rayleigh distribution while the remaining parts of the equations reflect the depth limitation.

4.2.4.10 Numerical and physical modelling of wave conditions

Numerical wave modelling

Applications of numerical wave modelling

Numerical modelling of waves can be undertaken for several purposes among which two are discussed in this section.

- 1 **Obtaining data on the wave climate offshore of the structure to be designed.** These data can be used in combination with wave measurements or as an independent source of data to obtain information on the short-term or daily offshore wave climate (see Section 4.2.2.8). From this data, extreme wave analysis (see Section 4.2.2.8) can also be performed if sufficient duration of sea-state simulations is available
- 2 **Modelling wave transformation from offshore into the nearshore zone** where the structure has to be built. In this step the offshore wave climate is transferred to the vicinity of the structure and consideration needs to be given to shallow-water processes such as refraction, shoaling, breaking and diffraction (see Section 4.2.2.7).

A third use of numerical modelling consists of wave propagation from a location just offshore of the structure to the structure (and possibly on and in the structure), which is discussed in Section 5.3.3.1.

Types of numerical wave model

It is important to distinguish between two main classes of wave models: **phase-averaged** and **phase-resolving** wave models, which are briefly described below (a more detailed description is given in Box 4.12).

- 1 **Phase-averaged models** are also referred as spectral wave models. They assume that the length scale of variation of wave properties is quite large compared to the wavelength. In this case, it is possible to work with variables resulting from an average over a wave period, eg wave energy, or wave energy (directional) spectrum. The dominant physical processes that are included are: wind input, dissipation by white-capping and bottom friction, refraction and shoaling. These models can also deal with depth-induced breaking. When they work with the full frequency directional spectrum (the so-called third-generation wave models), non-linear transfers of energy between quadruplets of waves (in deep water) and/or between triplets of waves (in shallow water) can also be considered. Such models cannot properly consider short-scale processes, such as diffraction or reflection.
- 2 **Phase-resolving models** classically solve conservation equations for mass and momentum with a discretisation of 10–50 points per wavelength and wave period. They are designed to precisely determine the evolution of each individual wave of a wave train. Thus, they are particularly recommended when the waves evolve rapidly (ie over distances in the order of or less than the wavelength). Diffraction and reflection are usually well handled by these models, in addition to refraction and shoaling, bottom friction and depth-induced breaking.

Considering the two objectives of wave modelling mentioned at the beginning of this section, the applications of these types of models are as follows.

- 1 To obtain data on offshore wave climate only phase-averaged models (either second generation or preferably third generation) can be used. These models are then driven by wind fields provided on a grid covering the area of interest including sufficient fetch length to correctly model all meteorological conditions and incoming wave directions. The wind information can be obtained from meteorological reanalysis or satellite measurements and are usually provided with a time step of 3–6 hours (see Section 4.2.1.1). Such numerical wave climate databases are available for various parts of the world.
- 2 To transfer offshore wave data to the toe of the structure both types of models can be used, depending on the size of the computational domain and the dominant processes to be modelled. If diffraction and reflection effects are significant, phase-resolving models should be used. In other cases, phase-averaged models (such as HISWA, SWAN, TOMAWAC etc) can be used at a regional or local scale, which is the most frequent situation. These models are driven by wave conditions imposed at the offshore boundary of the model (ie with a wind field provided over the whole domain). An example of model application is provided in Figure 4.49.

Box 4.12 Overview of phase-averaged and phase-resolving models**1 Phase-averaged (or spectral) wave models**

If diffraction and reflection effects can be neglected, a third generation spectral wave model may be used such as WAM (WAMDI Group, 1988), SWAN (Booij *et al*, 1999; Ris *et al*, 1999), WAVEWATCH (Tolman, 1991; Tolman and Chalikov, 1996) or TOMAWAC (Benoit *et al*, 1997a). These models include breaking dissipation and non-linear interactions and they provide full directional wave spectra, as well as synthetic parameters such as the significant spectral wave height, H_{m0} , and various mean spectral periods ($T_{m-1,0}$, T_{01} and T_{02}) computed from the moments of the spectrum (see Section 4.2.4.5).

Alternatively, somewhat simpler spectral models suitable for steady-state computations and based on some simplification of the physics, such as the HISWA model (Holthuijsen *et al*, 1989), may be used, as well as for 2D applications. In this case, the directional spreading of wave energy is computed, but the spectral spreading is only represented by the first two moments of the spectrum. In some circumstances 1D models can also be used, such as ENDEC (Stive and Dingemans, 1984; Van der Meer, 1990), REPLA (Hamm, 1995), or the 1D version of SWAN (Booij *et al*, 1999), which models the transformation of a random wave field from the transformations of its constituent components (by using linear or non-linear flat-bottom theories). These models produce the local wave characteristics for any arbitrarily specified beach profile, taking into account the energy dissipation caused by breaking.

For all spectral models, there is no condition on the number of grid points per wavelength. The step lengths Δx and Δy are dictated by requirements of numerical stability and related to the grid of the input data, so that the final mesh should correctly represent the coastal morphology. Where there are bathymetric variations (bed level changes: trenches, scour holes, shoals), the step length Δx should be selected to fit at least several times in the characteristic length of the bathymetrical variation (in the x -direction of wave propagation). For coastal applications, models based on a curvilinear grid (eg SWAN) or an unstructured finite element type grid (eg TOMAWAC) are preferred, as they offer the possibility to refine the mesh in areas of interest and/or rapid variations of bottom elevations.

2 Phase resolving (or deterministic) wave models

If non-linear effects need to be more precisely taken into account and/or if reflection and diffraction effects are significant, non-linear phase-resolving models based on extended Boussinesq-type equations should be used. This type of model has received a lot of attention in recent decades and a lot of improvements have been achieved (see eg Dingemans, 1997 for a review), so that industrial versions of these models can now be used for practical studies. Some models are FUNWAVE (eg Wei *et al*, 1995), TRITON (Borsboom *et al*, 2001) etc. However, these models require significantly larger computer resources compared with phase-averaged models. The step lengths Δx and Δy have to be in the order of $L/50$ to $L/20$ and the time step is often dictated by stability considerations and usually also lies in the range $T/50$ to $T/20$. Until recently these models were mainly 1D models, but 2D versions based on curvilinear (boundary-fitted) grids (eg Shi *et al*, 2001) or finite-element grids (eg Sørensen and Sørensen, 2001) have been proposed. With the progress made by these models and the continuous improvements in computer performance, it is likely that 2D applications of such models over areas of several kilometres of size are nowadays achievable.

3 Modelling of wave breaking and its effects

When the modelling of energy dissipation due to depth-induced breaking in shallow water is important, it is highly recommended to compute simultaneously the variations of mean sea level (MSL) that result from wave breaking, ie set-down and set-up (see Section 4.2.2.5). For some phase-resolving models, these variations of mean sea level can be computed within the wave module itself by the same equations. More often, the set-up is computed after the wave conditions have been propagated, and then it is necessary to iterate the wave computations, as a variation of MSL affects the wave propagation. Usually two or three iterations are sufficient to reach an equilibrium state both for the wave conditions and the MSL.

1

2

3

4

5

6

7

8

9

10

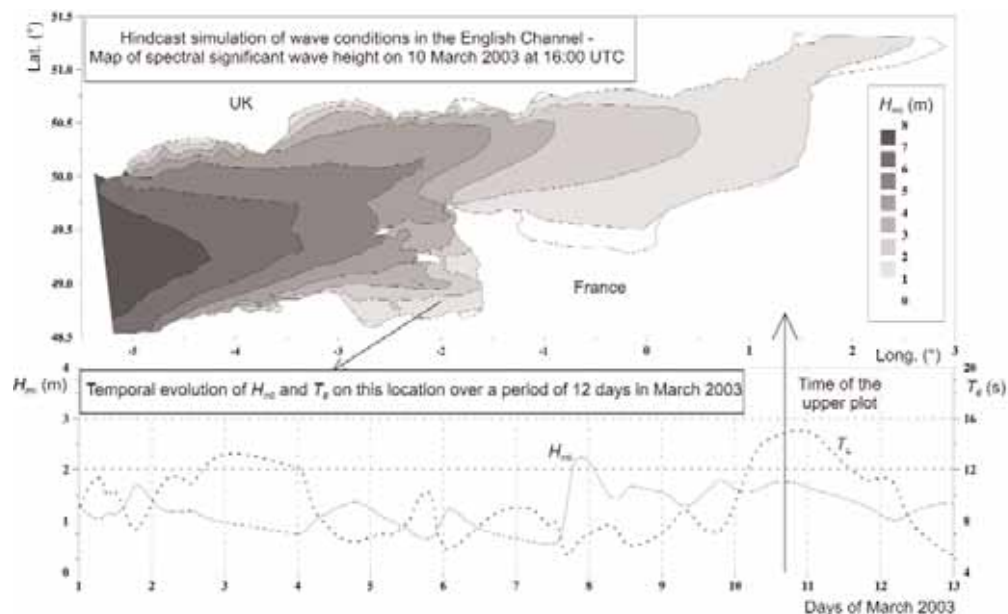


Figure 4.49 Numerical modelling of wave conditions

Characteristics of wave models

When selecting the most suitable wave model for a particular problem one is usually faced with the following options:

- 1 **Frequency spreading of wave energy.** Some models are monochromatic or regular wave models (one single frequency), but nowadays most models are irregular wave models that are able to deal with a continuous spreading of wave energy over a range of frequencies. Usually this latter type of approach is preferred, as it provides a better representation of the irregular nature of actual sea-states.
- 2 **Directional spreading of wave energy.** Similarly, the models may deal with only one incoming wave direction (unidirectional or long-crested waves) or with multi-directional waves (ie the wave energy is spread over a range of directions, which may depend upon the frequency).
- 3 **Physical processes to consider.** Depending on the specific case, this includes energy sources (wind input) and/or sinks (eg bottom dissipation, breaking), refraction, shoaling, diffraction, reflection etc.
- 4 **Linear or non-linear modelling.** The models may be linear for modelling propagation or non-linear, including non-linear effects resulting from wave-bottom and wave-wave interactions. Usually, for shallow-water conditions, non-linear effects are quite important and should be considered. For this reason, non-linear models should be preferred. But since these models are quite difficult and expensive to use, simpler models based on linear theory for wave propagation, but including non-linear effects in source/sink terms (depth-induced breaking typically), are still widely used.

It should also be noted that correct water level data has to be known or supplied to ensure correct results from any wave model. Procedures discussed in Section 4.2.5 should be followed to avoid any component being overlooked and to achieve the correct water level for the envisaged design conditions. This water level should then be used in the wave model.

Physical wave modelling

Physical wave models can only be used for the second objective of numerical wave modelling (see above), ie transferring wave data from offshore to the vicinity of the structure. For this

purpose they can be used as a predictive scale model for the prototype or as verification of results from a numerical model.

As the present state of the art in numerical wave modelling is often considered sufficient for standard design purposes, physical modelling is mainly required when a complicated bathymetry in front of a structure causes significant variations in the near-structure sea-state and/or when specific interactions with the structure (eg run-up, overtopping, toe scour, stone movements) have to be clarified. Wave diffraction may be another reason to use a physical model. It is mainly its capability to deal with complex interactions that leads to selection of physical models. However, for many of the more standard design problems numerical models may be the more economical option. Thus expected accuracy should be balanced against cost of both numerical and physical modelling. Scale factors and scaling effects should also be considered in this balancing of options and in the final design of the physical model, if chosen. An impression of a physical wave model is shown in Figure 4.50.

The use of physical models for the design of structures is discussed with more details in Section 5.3.2.



Figure 4.50 *Physical modelling of wave conditions*

4.2.5 Joint probability of waves and water levels

Derivation of climates, ie the long-term distributions of winds, waves, water levels etc, is considered in earlier sections of this chapter (see in particular Section 4.2.2.12 for water levels and Section 4.2.4.9 for waves). The joint occurrence of, say, wave heights and periods or wave heights and directions, is automatically included in the resulting predictions (see Section 4.2.4.8). This section concentrates on the determination of design conditions resulting from the joint occurrence of extreme water levels and extreme wave conditions.

4.2.5.1 Introduction

Overtopping, coastal flooding events and damage to coastal structures are usually associated with the simultaneous occurrence of both large waves and high water levels. It is therefore important to consider both parameters in the design and assessment of coastal structures. The relative importance of large waves and high water levels in a particular situation depends on the particular coastal or structure response being considered. For example, groyne stability is largely dictated by wave height, while overtopping of dikes is more sensitive to water level and wave period.

The volume of data available on marine water levels means that extreme water levels can usually be calculated quite reliably (see Section 4.2.2.12). The intermittent nature of wave recording and the variability of wave conditions in coastal waters makes prediction of extreme wave conditions usually slightly more difficult and uncertain (see Section 4.2.4.9). However, an aspect of equal importance, which is sometimes not explicitly addressed in design, is the dependence between high waves and high water levels, ie the likelihood of both occurring simultaneously.

There are two main reasons why the occurrences of large waves and of high water levels may be correlated.

- 1 The more general reason relates to **meteorological conditions**. Certain weather conditions tend to produce both large waves and high storm surges (see Sections 4.2.2.3 and 4.2.2.4). The correlation between water level and waves remains modest in areas where the astronomical component of the tides is much larger than the storm-surge component; conversely, it is more significant for areas with lower tidal influence.
- 2 The more localised reason relates to the **behaviour of waves in the nearshore zone**. Shallow-water wave transformations, particularly in very shallow water, depend upon water depth (see Section 4.2.4.7). If the wave prediction point is very close inshore or protected by sandbanks, then wave conditions may be depth-limited, in which case there would be a strong correlation between large waves and high water levels.

Joint probability extremes can be calculated and presented either offshore or inshore. Offshore results are applicable over a larger area, but may need to be transformed to inshore conditions before further use. Inshore results are more site-specific, but may be applicable only in one small area. Wave predictions and joint probabilities are often calculated as a function of direction. This is important, since general exposure to waves, correlation between large waves and high water levels, and inshore transformation, may all depend upon storm direction.

The concept of a return period, when dealing with joint probabilities, is less straightforward than when dealing with a single variable. A joint probability extreme can be defined in terms of the probability that a specific wave height is exceeded simultaneously with a specific water level. For any particular return period, there will be a range of combinations of wave heights and water levels, each of which is expected to be equalled or exceeded once, on average, in each return period. For example, one could consider a very severe wave condition with a modest water level, or a very severe water level with a modest wave condition: both will occur and both may have the same combined return period. This definition is helpful in interpreting and assessing correlation as well as in expressing results in terms of two primary variables. Only one combination is a **worst case** in terms of run-up, overtopping or damage, but it may be necessary to test several combinations in order to find that worst case. Other definitions of return period may be more useful and appropriate where it is possible to work directly in terms of the probability of the coastal structure response variable. These are based either on integration of the joint probability densities or on direct extrapolation of the response variable itself.

A joint probability assessment requires, at least, a good knowledge of the distribution and extremes of wave conditions (alone) and of water levels (alone). A skilled person, armed with this knowledge, could make an intuitive assessment of the correlation between high waves and high water levels and then an estimate of the joint probability extremes. However, a full and objective joint probability assessment requires better-quality data and techniques, the knowledge of a specialist, and dedicated methods and software. At least a few years of simultaneous water level and (usually hindcast) wave data are required to make a detailed assessment of correlation and of its possible dependence upon storm direction and severity.

Hawkes and Hague (1994) describe several theoretical and practical approaches to joint probability analysis. They also include a comparison of the results derived from different

methods and limited validation against field data on the occurrence of damage at sea defences. HR Wallingford and Lancaster University (1998) describe development of a robust method for extrapolation of joint probability **densities**, and validation against both synthetic and field data. Hawkes *et al* (2002) present a method for joint probability analysis, using the Monte Carlo simulation approach, based on distributions fitted to water level, wave height and wave steepness, and to the dependence between them. Defra/Environment Agency (2004) summarises this and other related work in the form of a best practice guide for use of joint probability methods in flood and coastal defence work.

4.2.5.2 **The independent and dependent cases**

The joint exceedance probability of two variables (X and Y) is given by the likelihood $P(\underline{X} \geq x$ and $\underline{Y} \geq y)$ (in the range $[0;1]$) of variable \underline{X} being not less than a given value x , at the same time as variable \underline{Y} being not less than a given value y . \underline{X} and \underline{Y} may refer to still water level (SWL) and significant wave height H_s at each successive high water.

Two simple cases of joint probability are: **complete dependence** and **complete independence**. Two variables, SWL and H_s , are completely dependent if a given water level always occurs at the same time as a given wave height, H_s , when the return periods of each of the two variables would be equal (see Equation 4.119).

$$P(SWL \geq x \text{ and } H_s \geq y) = P(SWL \geq x) = P(H_s \geq y) \quad (4.119)$$

However, if they are completely independent, there is no correlation between them and the joint probability is simply the product of the two marginal probabilities (see Equation 4.120).

$$P(SWL \geq x \text{ and } H_s \geq y) = P(SWL \geq x) \cdot P(H_s \geq y) \quad (4.120)$$

In the case of waves and water levels, the assumption of complete dependence would lead to a very conservative design since the 100-year event would have to comprise a 100-year wave height condition coupled with a 100-year water level. Conversely, the assumption of independence would lead to under-design in some cases, since any increase in the probability of high wave heights at times of very high water levels would have been ignored. The correlation between waves and water levels usually lies between the two extreme situations of complete dependence and complete independence. The partially dependent situation is, to an extent, best determined from analysis of actual data.

Often, only conditions at high water are of interest, and at most locations peak surge levels persist for less than half a day (see Sections 4.2.2.3 and 4.2.2.4). Therefore, conditions at each successive high water (approximately 706 per year, see Section 4.2.2.2) can conveniently be taken as independent and assumed to persist over the duration of high water, accompanied by wave conditions that (subject to depth limitations) persist over the tidal cycle. Therefore, for arithmetic purposes in combining probabilities, a one-year return period event, for example, has a probability of occurrence of 1/706. As the independent and dependent cases are simple to calculate, and as they represent the most optimistic and most pessimistic scenarios respectively, it may be worth deriving them early in any project. They may help in judging the value of any more detailed joint probability analysis.

4.2.5.3 **Desk study methods of analysis**

A possible method to estimate correlation is intuitive and based on general experience and the shape and size of the sea area around the prediction point. A better method, if constraints on time, budget and data permit, is to examine several years of simultaneous wave and water level data in order to assess correlation and to derive joint probability extremes. This allows the correlation analysis to be performed in a similarly objective scientific manner, which would be applied to the individual wave and water level predictions.

The correlation is determined by scatter diagram analysis of pairs of values of wave height and water level at each high water over a period of several years. Lines joining areas of the scatter diagram with an equal density of observations can then be thought of as probability density contours. Any skewness in the contours would be indicative of dependence between the two variables.

As examples, Figures 4.51 and 4.52 are scatter diagrams of surge against significant wave height, for high waters during periods of over ten years at two locations along the coasts of UK. Figure 4.51 demonstrates negative correlation between high waves and high surges. In this situation the largest wave heights would tend to coincide with **negative** surges. Conversely, Figure 4.52 demonstrates **positive** correlation between high waves and high surges. In this situation the largest wave heights would tend to coincide with positive surges. Defra/Environment Agency (2003) maps dependence around the UK between several variable-pairs relevant to flood risk.

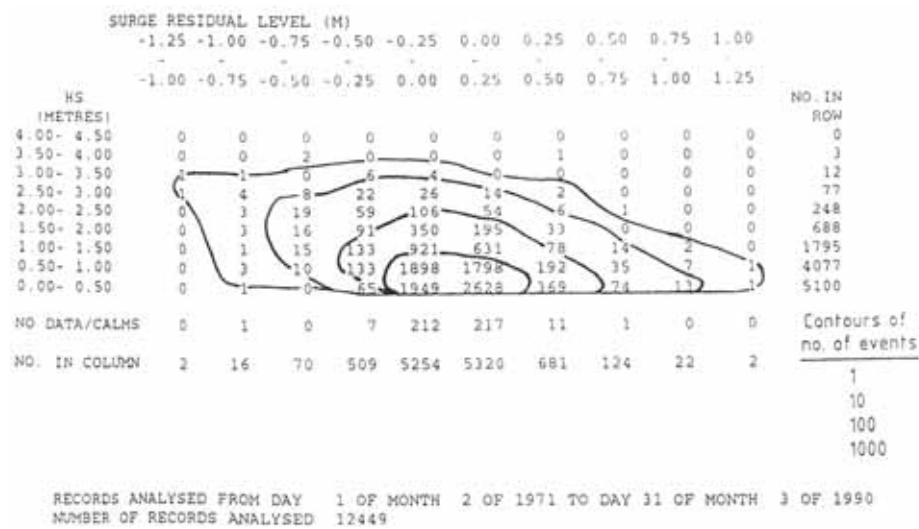


Figure 4.51 Example of probability contours demonstrating negative correlation between surge and significant wave height (off Hythe, Kent, UK)

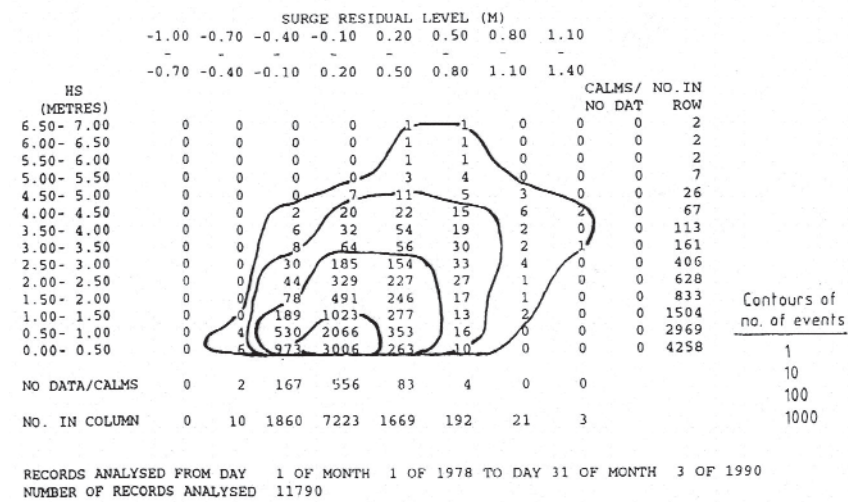


Figure 4.52 Example of probability contours demonstrating positive correlation between surge and significant wave height (Christchurch Bay, Dorset, UK)

The assessment may conclude that there is a modest correlation and that, for example, high waves and high water levels with a 100-year joint return period are 10–100 times **more** likely to occur together than the assumption of **independence** (see Section 4.2.5.2) would suggest. It may conclude that there is a strong correlation and that, for example, high waves and high water levels with a 100-year joint return period are only 10–100 times **less** likely to occur than the assumption of **dependence** (see Section 4.2.5.2) would suggest. The probability ratio between the independent and dependent cases is 706×100 (corresponding to 706 high-water-per-years over a duration of 100 years).

As an example, combinations of wave heights and water levels (each specified in terms of its marginal return period) with a joint probability return period of 100 years are given in Table 4.15. It is intended that **all** combinations of waves and water levels with a given degree of correlation be tested for **each** design consideration in turn, in order to find the worst case for each one. The table compares the combinations that would be appropriate for different assumed degrees of correlation between wave heights and water levels. A **correlation factor** is introduced here, which is the ratio of the actual joint probability to the value that would be associated with independent variables.

Table 4.15 Combinations of conditions with a 100-year joint probability return period for different assumed correlation factors

High water level return period (years)	Wave condition return period (years) for a correlation factor given below			
	2	20	100	500
0.02	14	100	-	-
0.05	6	57	-	-
0.1	2.8	28	100	-
0.2	1.4	14	71	-
0.5	0.6	6	28	100
1	0.28	2.8	14	71
2	0.14	1.4	7	35
5	0.06	0.6	2.8	14
10	0.03	0.28	1.4	7
20	-	0.14	0.7	4
50	-	0.06	0.28	1.4

Note

It is assumed that there are 70 600 high tides in 100 years. The extremes are expressed in terms of their marginal return periods. The four alternative example levels of dependency are **none**, **modestly correlated**, **well-correlated** and **strongly correlated**.

The suggested minimum correlation factor is 2, since any lower value would be rather risky without more detailed calculations. This would be appropriate where waves and water levels were expected to be independent. Correlation factor 20 represents a modest level of dependency, appropriate if some correlation is expected even if there is no particular evidence for it. Correlation factor 100 represents well-correlated conditions such as one might expect where strong winds moving along a narrowing sea area would produce both high surges and high waves. The strong correlation factor 500 represents a dependence level that is quite unusual along European coasts. It might be appropriate in an area where a strong correlation between storm surges and wave heights would be expected, and where the astronomical tide is low.

It is quite common to calculate joint probability extremes in fairly deep water offshore and then to assume that they are applicable over quite a wide area. Before use at the coast, it may be necessary to transform these conditions inshore and then to assess the ability of the sea defences to withstand each combination of waves and water levels at the inshore point.

4.2.5.4 Other methods of analysis

The return period approach to wave heights and water levels

The return period of a particular combination of wave height and water level can be estimated, from first principles, directly from scatter diagram data. The number of occurrences of data exceeding a given wave height threshold at the same time as exceeding a given water level threshold can simply be counted and compared with the total length of the dataset. For example, a combination of wave height (y) and water level (x) exceeded (ie $SWL \geq x$ and $H_s \geq y$) 100 times in 10 years would have a return period of 0.1 year, and another one exceeded 10 times in 10 years would have a return period of one year. There will be several combinations of wave heights and water levels corresponding to any given return period.

Probability contours of rarer events could then be sketched in, retaining the shape of the known contours. The spacing between the extrapolated contours should be approximately equal for each factor of 10 (or any other convenient factor) increase in rarity of event represented. So, for example, the 1-, 10- and 100-year return period contours should be drawn so as to have roughly the same shape and spacing. The positions of the contours as they meet the x - and y -axes are fixed by the values of the marginal extremes, ie the extreme water levels (for all waves) and the extreme wave heights (for all water levels).

As an example, Figure 4.53 is a scatter diagram of water level against significant wave height, for high waters during a period of about 10 years. Probability contours for return periods of 0.1 and 1 year are drawn in directly from the data. Marginal extremes are determined so as to fix the positions of the higher return period contours on the x - and y -axes. Contours for higher return periods are then drawn in using the manual extrapolation procedure described above. Having determined the positions of the contours, several combinations of wave heights and water levels with a given joint return period can be extracted for subsequent use in design, assessment or further modelling.

Alternatively, extremes can be determined more objectively by extrapolating wave heights for increasingly rare water levels, and water levels for rare wave heights. This involves setting a series of thresholds ($x_i, i = 1 \dots n$) for (say) water level, and performing extremes analysis only on the wave height data **above** the threshold, for each threshold in turn. The resulting extremes distribution (for threshold x_i) $P(H_s \geq y)$ also forms part of the joint extremes distribution as $P(H_s \geq y \text{ and } SWL \geq x_i)$. By combining these extrapolations, contours can be drawn joining combinations of wave height and water level with equal joint return periods.

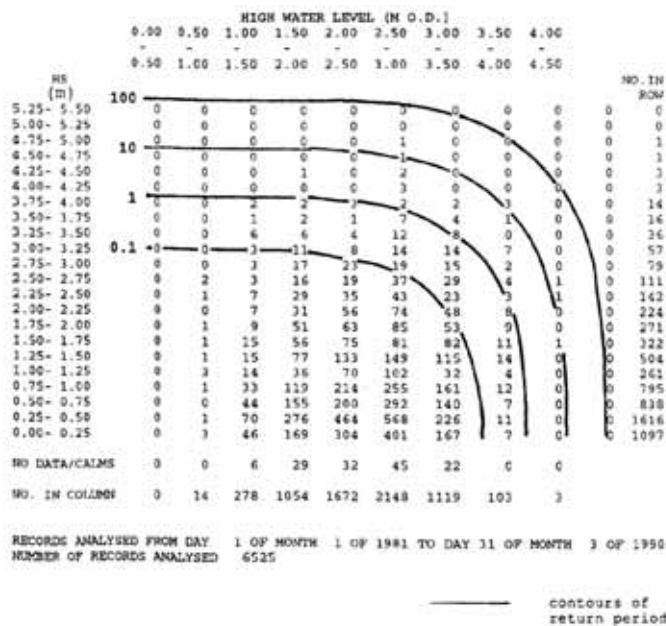


Figure 4.53 Example of manually drawn extreme joint probability contours of water level and significant wave height (off Shoreham, West Sussex, UK)

For a given joint exceedance return period, all the combinations of offshore wave conditions and water levels could be converted into, for example, rates of overtopping at a particular location (if overtopping is the critical consideration). This would indicate which combination of offshore conditions is critical in terms of overtopping, and this combination could then be highlighted for further use by the coastal engineer during the design. This type of result presentation is convenient, but it should be used with caution, since the conditions highlighted above would have very specific application. At nearby sites, or for alternative variables (run-up or force), it is likely that some other combination of offshore waves and water levels would be critical in design. It should be noted that not all combinations of wave height and water level which may be calculated for a given joint exceedance return period will result in the same degree of response or failure. In addition, this type of approach offers only an approximation to the return period of any response function.

The continuous simulation approach

The design variable(s) of interest at the chosen inshore site(s) could be continuously hindcast for whatever period of wave and water level data is available. For example, if 20 years of simultaneous wave and water level data were available, it could be used to hindcast (ie to produce a value for every hour) rates of overtopping directly at an inshore site of interest. This method incorporates wave period as an independent variable in the analysis, in addition to wave height and water level. The rates of overtopping could then be examined and used to infer a probability distribution and extreme values for use in design.

This continuous simulation approach is a useful way of carrying out and presenting the results from a joint probability assessment. Instead of a rather unwieldy table containing several combinations of offshore conditions, it produces a single overtopping extreme as required by the designer. This approach should be adopted with some caution. The behaviour of the structure may change dramatically under extreme values of one or more of the input variables, for example from gentle erosion to overtopping or retreat. In this situation of a discontinuous coastal response function, the direct hindcasting approach may give a misleading design prediction. Also, results presented in this way may not be applicable at similar sites nearby and would not provide equivalent values of **any** other variable (wave height, water level, run-up etc). If results were required later for some other variable, or some other point, or perhaps even to test a modified structure design, it would probably be necessary to repeat the entire hindcasting exercise, since no general results would be available.

The extrapolated joint density approach

This approach models and extends the joint probability contours without particular reference to the return period of events. This is more appropriate for risk analysis for existing situations, where the emphasis is on calculation of the probability of a particular response, as opposed to design where particular input parameter values may be needed.

Figures 4.51 and 4.52 are examples of joint probability density contours drawn manually within the body of the data. Probability distributions (for example the Weibull or Normal distributions; see Box 4.10 in Section 4.2.4.9) can be fitted to each of the individual variables, with another equation to define the degree of correlation between them. If this is possible, then the positions of the extrapolated contours can be determined objectively from the extreme values of the fitted distributions and correlation equation.

HR Wallingford and Lancaster University (1998) describe a method of transforming real wave and water level data into idealised bi-variate normal distributions whose dependence characteristics are already well known. A Monte Carlo simulation method is applied to the transformed distributions, the results being transformed back to equivalent results for the original distributions. Extreme values can then be extracted from the long-term simulation without the need for further extremes analysis. In principle, this method is not limited to two variables (usually wave height and water level), and wave period is routinely included as an additional variable dependent on wave height. The coastal responses of interest (eg structural failure, overtopping etc) are then determined by integration over the joint probability contours. This approach is more mathematically rigorous than the return period approach, but requires more input data and specialist software and expertise.

4.2.5.5 Design with joint waves and water levels

Joint probability analysis results can be expressed as a range of combinations of wave conditions and water levels, each with the same return period. Each one is expected to be exceeded once, on average, in each return period. In designing or assessing a structure, its resistance to every combination of wave height and water level for the return period being used should be verified. In other words, for each coastal response variable of interest, each combination of extreme water level and wave condition should be tested, to determine the worst case for each response variable.

Alternatively, the results of a joint probability analysis may be presented in the form of a climate scatter diagram (eg Figures 4.51, 4.52 and 4.53) with or without extrapolated joint probability density contours. This form of presentation is more appropriate for building up a probability distribution of a coastal response variable, found by integrating the response function over the joint ranges of each of the primary input variables. This might be helpful where damage to a structure builds up over a period of time, as opposed to damage occurring during a single rare event.

If the wave heights and water levels are derived for a location other than the point where they are to be applied, some adjustment of values may be necessary. The most obvious case is the need to modify wave conditions calculated offshore to allow for shallow-water transformations prior to their arrival at coastal defences. If wave periods are required these can be assigned to particular significant wave heights based on a typical wave steepness ($2\pi H_s/gT_m^2$) for storm waves. If wave direction is important, perhaps in wave transformation or in coastal response, then separate calculations may be required for each direction sector of interest.

The degree of correlation between large waves and high water levels varies between locations and wave direction sectors, and even between offshore and nearshore. It may therefore be inappropriate to assume that the most severe sea-states offshore give rise to conditions as severe as those at the coast. At open coasts, where the largest waves offshore also give rise to

the largest waves inshore, the correlation with high water levels is similar for both situations. However, where waves are strongly depth-limited before arriving at the sea defences, then wave period (and therefore possibly a different type of sea condition) may be much more important nearshore than offshore. In addition, for locations protected by headlands from the largest offshore waves, the nearshore situation may differ from that offshore.

Joint probability analysis is normally based (even if indirectly) on measurements taken during recent years, assuming that they are representative of longer-term conditions. If the wave conditions or water levels are known to be subject to any long-term variations (such as a rise in mean sea level; see Section 4.2.2.10) or if the period of measurement is known to be unrepresentative, then allowance should be made for this.

4.3 HYDRAULIC BOUNDARY CONDITIONS AND DATA COLLECTION – INLAND WATERS

4.3.1 Hydraulic parameters

4.3.1.1 River geometry

Channel geometry is required for any hydraulic study. Its elements are properties of the channel that can be defined entirely by the geometry of the section and the depth of flow, as shown in Figure 4.54.

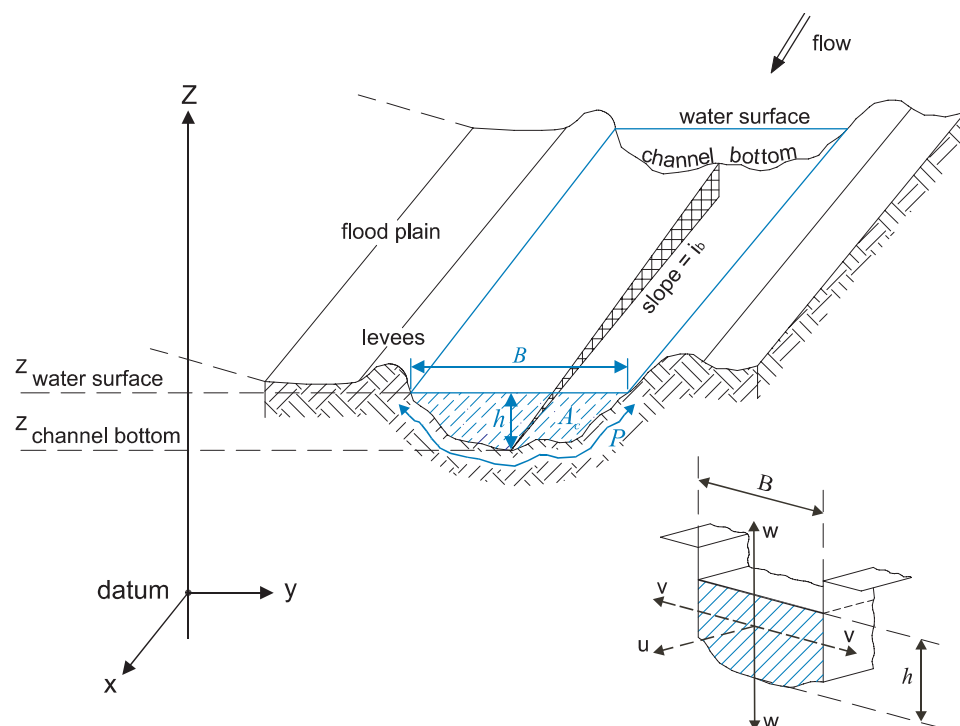


Figure 4.54 River geometry (courtesy CETMEF)

The term **channel cross-section** used in this manual refers to the cross-section of a channel taken in the normal direction to the flow. The cross-section should be measured in the vertical plane, as is usual in surveying practice, rather than perpendicular to the river gradient, ie with an angle to the vertical. A **vertical channel section**, however, is the vertical longitudinal section passing through the lowest or bottom point of the channel section. In flood conditions, the **channel** may consist of a main channel section carrying normal discharges and one or more side channel sections (including natural, defended and artificial floodplains) that accommodate the excess flows. Artificial channels are usually designed with sections of regular geometric shapes. Cross-sections of the floodplain areas may be obtained directly from an accurate

topographic map, if available. Otherwise, cross-sections should be obtained by field (eg traditional ranging or GPS) or aerial surveys (eg by stereoscopic photogrammetry or LiDAR).

The **water depth**, h (m), is the vertical distance between the channel bed and the water surface. It can be calculated as the perpendicular water depth, h_p (m), divided by $\cos i_b$, where i_b is the channel slope. For channels with a moderate slope (say $\tan i_b < 0.1$, ie inclination less than 10 per cent), this term is often interchangeable with the water depth perpendicular to the bed level, h_p (Graf and Altinakar, 1993).

The **stage** is the elevation or vertical distance of the free surface above a datum. If the lowest point of the channel section is chosen as the datum, the stage is identical to the depth of flow.

The **top width** B (m) is the width of channel section at the free surface.

The **water area** A_c (m²) is the cross-sectional area of the flow normal to the direction of flow.

The **wetted perimeter** P (m) is the length of the line of intersection of the channel wetted surface with a cross-sectional plane normal to the direction of flow. It can also be defined as the length of the cross-section along which there is friction between the fluid and the boundary. It should be used to calculate the **hydraulic radius**, R (m), which is the ratio of the water area to its wetted perimeter, ie $R = A_c/P$. For relatively wide rivers, where B is greater than $20 \times h$, R may be approximated by the water depth, h .

Levees or **dikes** are earthen embankments that prevent floodwaters from inundating the floodplain.

4.3.1.2 Hydraulic data

Water levels and discharges are principal boundary conditions for the design of rock structures. This is because other hydraulic boundary conditions used in the design of rock structures are closely related to the actual water level.

Variations in water level and discharges are caused by meteorological influences. Water levels also depend on the local bathymetry (see Section 4.3.2.3).

Water level data

Water levels are generally the most accurate type of hydraulic data, although measurements can be affected by the recording technique device used and sometimes by meteorological factors such as gravity waves induced by wind or freezing of the float chamber.

Flow data

The **discharge** Q (m³/s) of a river is the volume of water that passes through the cross-section of the river per unit of time.

For a uniform steady discharge (not changing in time or space), Equation 4.121 can be written:

$$Q = U_1 A_{c1} = U_2 A_{c2} = \dots = U_i A_{ci} \quad (4.121)$$

where Q = volumetric flow rate (m³/s), U = average flow velocity (m/s), A_c = cross-sectional flow area (m²) and the subscripts on U and A_c designate different river section locations.

This definition is not valid where the discharge changes along the river. The discharge remains constant unless water runs into or out of the river from, for example, tributaries, sources, storm drains, drainage canals, collections, infiltration or side-channel spillways.

Where such conditions occur the flow is called **spatially varied**. When the discharge at a section changes in time, the flow is called **unsteady**.

The flow in a river is not directly measured but derived. There are several methods of gauging used to obtain discharges (Herschy, 1999; Ackers *et al*, 1978) including:

- 1 Estimation of the velocity distribution in the cross-section from:
 - point gauges with propeller or electromagnetic velocity meters
 - line averages from ultrasonic transmission
 - acoustic-Doppler current meter profile.
- 2 Artificial controls such as weirs or flumes constructed to standard designs.
- 3 Electromagnetic gauging at an instrumented site.
- 4 Sampling to estimate the dilution of a tracer injected into water.
- 5 Direct volumetric measurements.

These methods provide the initial required knowledge of instantaneous discharges. Further steps are necessary to constitute a time-series of discharges, either by recording or by reading **water levels** at the site from a continuously recording autographic gauge or graduated scale relative to a known vertical datum (a **staff gauge**). To interpret the data from a water level recorder installed at a gauging station the relationship between water levels and discharges, called a **rating curve**, should be known. An example is shown in Figure 4.55. Periodic flow measurements, using velocity meters for example, are initially used to define a rating curve and then to define shifts (seasonal, systematic and random) from the rating curve. The **shifted** rating curve is then used routinely to derive the discharges from a particular river stage where the discrete flow measurements are the only solid data. At the gauging station, discharges are determined from the depths of flow, which are read once or twice per day on a staff gauge or continuously recorded by an autographic gauge.

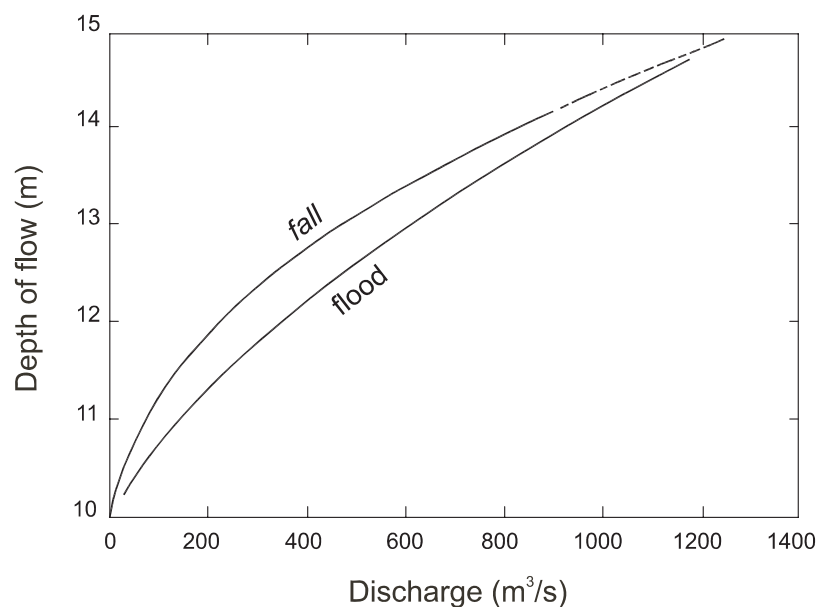


Figure 4.55 Example of a stage-discharge or rating curve in flood and in fall on the Sobat (tributary of the White Nile) (Shahin, 1985, modified in Bravard and Petit, 2000)

Rating curves can be used to determine flows only if the relationship between the depth of flow and the discharge is unique, ie if one and only one discharge corresponds to a specific depth of flow. This tends to occur at gauging stations where the morphology of the river bed does not vary significantly or where the slope of the water surface is constant, in the rise and fall of a flood. It is also the case for stations controlled within a fixed section, eg by weirs. In certain rivers, the values of gaugings obtained in the rise and fall of a flood differ for the same water level from those on a rating curve established in steady flow conditions. A loop appears around the steady flow rating curve. This effect is called **hysteresis**, with the discharge for a given water level being higher on the rise of the flood than on the fall (see Figure 4.55). The maximum discharge does not necessarily correspond to the maximum depth of flow. This deviation from the steady-flow rating curve often varies from one flood to another, but for large rivers subject to a significant annual flood, there is often one typical curve for the rise of the flood and another for the fall.

Discharge data include measured and/or synthesised flows along with frequency, velocity, duration, and depth information. Measured data at gauges are the preferred source for this category, but there are rarely enough measured data available.

River energy

The hydraulic head, H (m), defined as an energy level at a specific point in a channel that is subjected to a steady and uniform flow, can be calculated by Equation 4.122:

$$H = z + \frac{h_p}{\cos i_b} + \frac{\alpha U^2}{2g} \tag{4.122}$$

where:

- i_b = angle of the bed ($^\circ$)
- z = level of the riverbed compared with the reference level (m)
- g = gravity acceleration (m/s^2)
- h_p = water depth perpendicular to the river bottom (m)
- U = mean flow velocity (m/s)
- α = Coriolis (energy) coefficient (-)

The Coriolis coefficient α takes into account the fact that the velocity distribution in the section is not homogeneous. It is often assumed to be equal to 1.0 (Carlier, 1972), but it can reach values close to 1.35 in natural river channels (Sellin, 1969) and values in excess of 2 are possible for compound sections of a channel with floodplain (Henderson, 1966).

Figure 4.56 shows the variation in energy between two cross-sections A and B separated by a distance of length L (m) in a gradually varied flow.

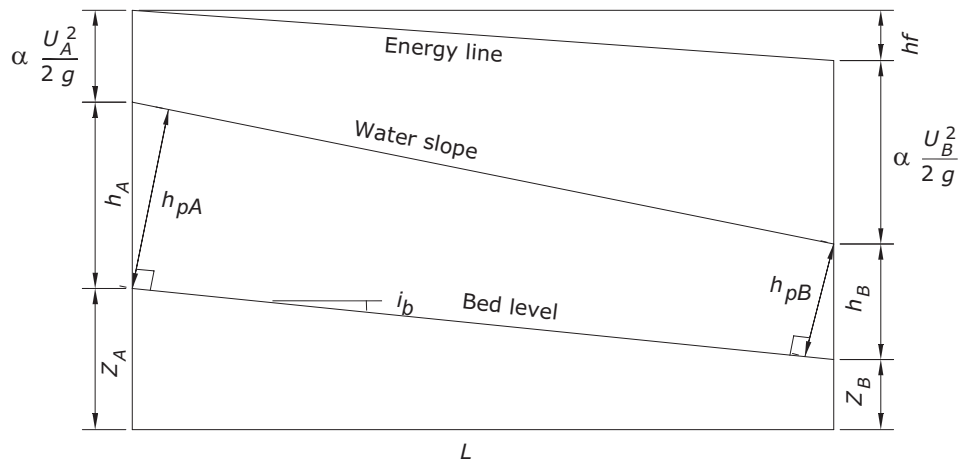


Figure 4.56 Energy in two cross-sections A and B separated by a distance of length L in a gradually varied flow (Bravard and Petit, 2000)

As illustrated in Figure 4.56, the energies at points A and B can be connected as expressed by Equation 4.123 because of the conservation of energy:

$$z_A + h_A + \alpha U_A^2 / (2g) = z_B + h_B + \alpha U_B^2 / (2g) + h_f \quad (4.123)$$

where h_f = loss of energy or **head loss** (m).

In reality, energy cannot be lost from the system and the energy loss accounts for transfers of kinetic and potential energy in the primary flow into other forms of energy not accounted for in Equation 4.123.

The ratio h_f/L stands for the slope of the energy line. It reflects the losses to the primary balance of potential and mainstream kinetic energy caused by:

- internal viscous friction of the flow, which transfers turbulent energy into heat
- accelerations and decelerations of the current, which change the turbulent energy
- frictional drag on the banks and the bottom of the bed
- transport of sediments.

The relationship between the slope of the energy line, h_f/L (-), and the slope of the water level, $[z_A - z_B + (h_A - h_B)]/L$, reflects the loss of energy and conversion between the potential energy and the kinetic energy.

4.3.2 River discharges and currents

4.3.2.1 General

Computation of flow conditions is based on the principle of conservation of mass and momentum. Most problems can be solved by combining the conservation laws (or simplified versions thereof) with a set of boundary conditions and experimentally determined parameters. The basic equations and their simplifications can be found in literature (Chow, 1959; USACE, 1993; Henderson 1966; Graf and Altinakar, 1993). For practical applications two situations can be distinguished:

- a 2D, approximately horizontal area, eg a river confluence or complex configuration
- an approximately prismatic flow channel, eg a river.

The ability to predict the stage, discharge and eventually velocity of any point on a river as a function of time is important for studies related to floodplain information, flood control channel design, navigation, water quality assessment, environmental impact or enhancement analysis, for example; and also for design of bed and bank protection works.

Hydraulic characteristics refer to the following properties of the flow: discharge, velocity, water surface elevation (depth), boundary shear stress, rate of energy dissipation, and sediment transport rate.

Hydraulic conditions in rivers, ie water level and flow velocity, are mostly influenced by river discharges associated with bed slope. Other influences include:

- floodplains and embankments
- structures in the river such as spur-dikes, barrages
- the roughness of the river bed and floodplains
- confluences, bifurcations, weirs and spillways.

A study and design scheme referring to parts of this section, Section 4.3.2 and to sections of other chapters, is shown in Figure 4.57.

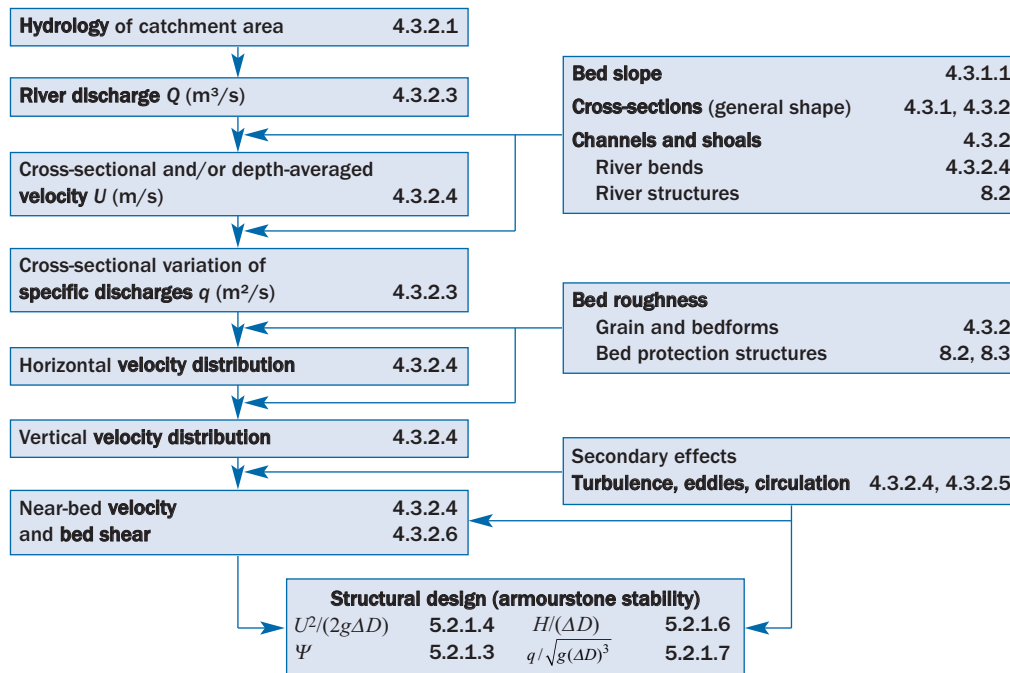


Figure 4.57 Relevant sections of the manual for the design of rock structures exposed to currents

River discharges may vary considerably with time. This is determined by climatological and hydrological factors (see Section 4.3.2.2).

4.3.2.2 Hydrology and design discharges

A typical hydraulic analysis requires simulated data from hydrological models as well as information on historical events, usually floods. Where data on river discharges are lacking, or where existing data should be interpreted, the hydrology of the catchment area should be studied. An understanding of the corresponding climatological characteristics can also be helpful. Although hydrological methods are beyond the scope of this manual some principal concepts are mentioned in this section (see Box 4.13).

A structure is usually designed to perform a function at a specific discharge. It should be designed to work safely for a wide range of possible flows. Flood control structures are usually designed for the discharge corresponding to a specific flood frequency, or design event, while navigation studies use a discharge for a specific low flow duration or frequency.

Box 4.13 Operational hydrology tools and data availability

Precipitation over a river catchment results in some discharge (or runoff) to the river. The relative lag time between precipitation and discharge depends on the hydrological properties of the area. The principal hydrological parameters are topography (slopes, terraces), soil properties (permeability, layer thicknesses) and vegetation. Various methods exist to relate the discharge of the catchment area into the river to the intensity of the precipitation. A sample of the methods used is described below and more information can be found in MEDD and METATLM (2005).

- **Specific summary methods**, like the Myer formula, provide a **maximum discharge** starting from only data of the surface of a catchment area. These methods can be used if no hydrometric data is available. They give an instantaneous maximum discharge. The Myer formula gives the 10-year return period discharge with the Crupedix method and the Sogreah method, both of which use statistical relationships between the peak discharge, the daily 10-year return period rainfall and other parameters of the catchment area.
- **Volumetric methods** take into account the runoff volume in a more or less simplified way. Rational, Socose and SCS methods use a model of loss then a transfer law, with statistically fixed parameters.
- **Statistical estimation methods** may be used to estimate design flows from an analysis of annual maximum (AM) discharges or peaks over threshold (POT), potentially for different durations. It is essential to undertake a preliminary validation of the data and check for continuity of the time-series. Various extreme-value distribution laws are used for the frequency assessment, among which are:
 - the Gumbel distribution (or General Extreme Value type I), which is applied to AM values
 - the exponential law (coupled to a Poisson distribution for the occurrence of annual floods during each year) in the renewal method, which applies to POT data series.

These methods make it possible to estimate the discharge for a given annual probability or return period.

- **Hydrometeorological methods** use additional information, in particular on precipitation, to estimate discharge beyond the limiting return period, defined as two times the number of years of observations. The principal method is that of **Gradex**, based on the assumption that for a certain return period the slope of the discharge distribution is supposed to be equal to the slope of precipitation distribution. In other words, beyond a certain threshold the retention remains constant and any additional precipitation runs off. The gradex thus makes it possible to extrapolate the distribution of discharges beyond the usual limiting return period.

The **Agrégée method**, or **progressive gradex**, provides a smooth transition between the two statistical and gradex frequency curves and limits the over-estimation of rare discharges associated with the gradex method.

The **QdF** (discharge-duration-frequency) method defines flood modes based on three categories of catchment area, a standardisation of the shapes of QdF curves and a selection criterion among the three models of reference based on the precipitation regime. The QdF method provides a consistent approach to flood flow estimation in a river reach with a common return period along the reach for the peak discharge as well as for the mean discharge for several durations. Without hydrometric data on the studied catchment area, regional methods allow estimation of a peak discharge for **comparison with measured catchment areas**.

- **Historical methods** make it possible to estimate the peak discharge of a historical flood using different types of historic information, for example depths and flow conditions. In fact, these approaches mainly consist of adding historical events to extend the record length of a time-series to improve extrapolations towards low annual probabilities (ie large return periods).

The many **Integrated software packages** that are commercially available typically integrate a hydrological module, a runoff generation and routing module and a hydraulic channel in network module. The input of the model is provided by an observed or synthetic rainfall while the output is given as discharges (or hydrographs) obtained on each sub-catchment area and at the nodes of the network.

1

2

3

4

5

6

7

8

9

10

With the methods mentioned in Box 4.13, a preliminary analysis of the available data (hydrographs, see Section 4.3.3.2) should be made to determine the design discharge of the project. Information on the application of those methods can be found in MEDD and METATLM (2005).

Bankfull discharge

For design of hydraulic rock structures, the bankfull discharge is the most significant discharge that should be used in the analysis of the river regime. The bankfull discharge is generally close to the dominant discharge for the beginning of bedload and evacuation of sediments (Leopold *et al.*, 1964; Dury, 1969). The bankfull discharge frequency is a function of the size of its catchment area, when a relatively homogeneous regional context is considered (Gregory and Walling, 1985; Petts, 1977). The return period of the bankfull discharge was initially regarded as oscillating between one year and two years (Leopold *et al.*, 1964; Tricart, 1977). Recurrence depends on catchment basin lithology, permeability and surface area. It can be higher than two years for permeable catchment areas and lower than one year for impermeable ones. The reader should refer to Bravard and Petit (2000) for further information.

Andrews (1980) gives a possible relationship (see Equation 4.124) between the values of the bankfull discharge, Q (m³/s), and the size of the catchment area:

$$Q = aA^b \quad (4.124)$$

where A = catchment area (m²) and a, b = coefficients (-).

Table 4.16 summarises the values of the coefficients a and b in Equation 4.124 found in the literature. There is a wide variability in the estimation of bankfull discharge inferred from these coefficients and so their use should be limited to the initial pre-feasibility stages of an investigation only.

a	b	Source	Remarks
0.277	0.828	Nixon, 1959	
1.705	0.774	Hey, 1982; Richards, 1982	
0.209	0.791	Andrews, 1980	
1.161	0.666	United Kingdom	Based on relations established for several regions of the UK <ul style="list-style-type: none"> • Derbyshire (Petts, 1977) • Cheshire (Hooke, 1987) • Pennine Chain (Carling, 1988)
0.087	1.044	Petit <i>et al.</i> , 1994	

Table 4.16 Values of the coefficients a and b (Bravard and Petit, 2000)

4.3.2.3

River discharge and velocity

Where the river discharge, Q (m³/s), is known, it is possible to determine the cross-sectional averaged velocity U (m/s) directly from Q and from the cross-sectional area of the stream, A_c (m²), using Equation 4.125.

$$U = Q / A_c \quad (4.125)$$

When the average depth, h (m), is small compared with the top width, B (m), say for an *aspect ratio*, B/h of 20 or more, the cross-sectional averaged velocity, U (m/s), can be approximated by Equation 4.126.

$$U = Q / (Bh) \quad (4.126)$$

When no instantaneous discharge is available, a **stage-discharge (or rating) curve** (see Section 4.3.1.2) can provide the discharge, Q (m^3/s), corresponding to an actual water level, h (m). Measurement of an actual water level is much easier than measurement of Q . It can then be used with the stage-discharge relationship to find Q , provided the actual river bed is known (see Section 4.1.3).

Where neither information on the discharge Q nor a rating curve is available, the depth-averaged velocity U in a river cross-section can be obtained for steady uniform flow by Manning-Strickler or Chézy formulae (see Equations 4.127 and 4.130 respectively).

Manning-Strickler formulation

The cross-sectional averaged flow velocity, U (m/s), can be calculated using the Manning-Strickler formula as given by Equation 4.127:

$$U = \frac{R^{2/3} i^{1/2}}{n} \quad (4.127)$$

where R = hydraulic radius (m), the ratio of the water area and the wetted perimeter (see Section 4.3.3.1), i = slope of the energy line, or water surface slope (-), n = Manning's roughness coefficient ($\text{s}/\text{m}^{1/3}$).

Manning's roughness coefficient, n , takes into account that the roughness of the banks and the bottom results in head losses by friction. Consequently, head losses become more significant as roughness increases. Roughness depends mainly on the nature of the materials on the river bed and the vegetation.

Using the Cowan (1956) procedure, Manning's roughness coefficient, n ($\text{s}/\text{m}^{1/3}$), can be computed using Equation 4.128:

$$n = (n_0 + n_1 + n_2 + n_3 + n_4) m_5 \quad (4.128)$$

where:

- n_0 = factor that depends on the constitutive material of the channel ($\text{s}/\text{m}^{1/3}$); it can either be determined with Strickler's formula: $n_0 = 0.048 D_{50}^{1/6}$, where D_{50} = median particle diameter of the bed sediment (m); or with $n_0 = 0.038 D_{90}^{1/6}$ (Simons and Senturk, 1977), with D_{90} = grain size not exceeded by 90 per cent (by mass) of the bed sediment. The relationship between n_0 and D_{90} is approximately constant for a range of relative depths given by $7 < h/D_{90} < 150$
- n_1 = factor that depends on the degree of surface irregularity
- n_2 = factor that depends on the variations of the cross-section form ($\text{s}/\text{m}^{1/3}$)
- n_3 = depends on the effects of obstruction (bridge etc) ($\text{s}/\text{m}^{1/3}$)
- n_4 = factor that depends on the vegetation that modifies the flow conditions ($\text{s}/\text{m}^{1/3}$)
- m_5 = coefficient that indicates the sinuosity degree of the channel (-).

Table 4.17 gives the values of the coefficients used in Equation 4.128 for different channel conditions.

Table 4.17 Values of Manning's coefficient proposed by the US Soil Conservation Service (Chow, 1959)

Channel conditions		Components of n	
Material involved	Earth	n_0	0.020
	Rock cut		0.025
	Fine gravel		0.024
	Coarse gravel		0.028
Degree of irregularity	Smooth	n_1	0.000
	Minor		0.005
	Moderate		0.010
	Severe		0.020
Variations of channel cross-section	Gradual	n_2	0.000
	Alternating occasionally		0.005
	Alternating frequently		0.010–0.015
Relative effect of obstructions	Negligible	n_3	0.000
	Minor		0.010–0.015
	Appreciable		0.020–0.030
	Severe		0.040–0.060
Vegetation	Low	n_4	0.005–0.010
	Medium		0.010–0.025
	High		0.025–0.050
	Very high		0.050–0.100
Degree of meandering	Minor	m_5	1.000
	Appreciable		1.150
	Severe		1.300

James (1994) proposed a linearised expression for m_5 (see Equation 4.129) that depends continuously upon the sinuosity I_s (see Section 4.1.3.3 for the definition of I_s).

$$m_5 = \begin{cases} 1.0 & \text{for } I_s = 1.0 \\ 0.57 + 0.43I_s & \text{for } 1.0 < I_s \leq 1.7 \\ 1.3 & \text{for } I_s > 1.7 \end{cases} \quad (4.129)$$

The Manning- Strickler formula (Equation 4.127) can be applied for the average value of n when discharges corresponding to observed water surface profiles are known. If data show that n varies with stage, n should be determined from a curve of n versus stage or from the observed profile that most closely approaches the stage of the desired profile. If no record can be provided by the competent authority (eg navigation authorities, Environment Agency), values of n computed for similar stream conditions or values (such as in Table 4.17) obtained from experimental data should be used as guidance to select appropriate values of n . Tables and photographs as provided by Chow (1959) may be used for selection of values of n . When discharge measurements are made to determine values of n , it is desirable also to obtain water surface slopes. Such data can be used to derive more reliable values of n than can be determined from high-water marks alone.

Considering the Strickler coefficient, K (m/s), as the inverse of the Manning coefficient ($K = 1/n$) and expressing Equation 4.127 as a function of K , other tables can be determined to characterise the riverbed roughness and to calculate hydrodynamic flow characteristics (Q or U) of a river (see, for example, Degoutte, 2001).

Chézy formulation

The cross-sectional averaged flow velocity U (m/s) can also be calculated from the well-known Chézy formula given by Equation 4.130:

$$U = C\sqrt{Ri} \quad (4.130)$$

where R = hydraulic radius (m), i = slope of the energy line (or water surface slope) (-) and C = bed friction Chézy coefficient ($\text{m}^{1/2}/\text{s}$).

The Chézy coefficient, C , is a measure of the riverbed and riverbank roughness and it has been defined by Bazin, as expressed by Equation 4.131:

$$C = \frac{87}{1 + \frac{\gamma}{\sqrt{R}}} \quad (4.131)$$

where γ = parameter representative of the bed roughness ($\text{m}^{1/2}$), the value of which varies from 0.06 for a smooth bed to 1.75 for a grassed ground bed and cobbles.

It can also be determined by Equation 4.132 with the roughness length scale of Nikuradse, k_s (m):

$$C = 18 \log(12h/k_s) \quad (4.132)$$

where h = water depth (m) and k_s = hydraulic roughness (m), discussed below in Box 4.14.

It should be noted that for small water depths, Equation 4.132 cannot be used. For such cases, Christensen (1972) provides a practical alternative approach. By changing Prandtl's mixing length (Prandtl, 1925), Christensen (1972) determined an associated alternative formula for C given by Equation 4.133.

$$C = 18 \log(1 + 12h/k_s) \quad (4.133)$$

For $h/k_s > 2$, this formula is close to the common form given in Equation 4.132.

Box 4.14 Grain and bedform roughness – Chézy coefficient

This box deals with methods based on bedform characteristics, particularly those developed by Van Rijn (1989). The hydraulic roughness consists of two parts:

- grain roughness, k_{sg} (m)
- bedform roughness, $k_{s\Delta}$ (m).

The *grain roughness*, k_{sg} , can be approximated by Equation 4.134 (Van Rijn, 1982).

$$k_{sg} = 3D_{90} \quad (4.134)$$

For engineering purposes, the scatter of k_{sg} in the case of *graded sediment* can be described by $k_{sg}/D_{90} = 1$ to 3. Somewhat arbitrarily assuming that $D_{90}/D_{50} = 2$, which implies $k_{sg}/D_{50} = 4$ (actual estimates for D_{90}/D_{50} are given in Section 3.4.3).

For **uniform sediment** the range of grain roughness is given by $k_{sg}/D_{50} = 1$ to 2. Despite scatter, on average the best results seem to be obtained using $k_s = D_{90} \cong 2 D_{50}$ for fine sediments and $k_s = 2 D_{90} \cong 4 D_{50}$ for coarse material, assuming no bedform roughness.

The *bedform roughness*, $k_{s\Delta}$, should be calculated using the roughness predictors given in Van Rijn, 1989. The empirical relation (see Equation 4.135) is based on the dimensions of the dune bedforms that are present in the river bed.

$$k_{s\Delta} = 1.1D_b \left(1 - \exp(-25D_b / L_b)\right) \quad (4.135)$$

where D_b = average bedform height (m) and L_b = average bedform length (m).

Values for D_b and L_b depend on the flow regime and should be determined from echo-soundings of the river bed. The overall hydraulic roughness is given by Equation 4.136.

$$k_s = k_{sg} + k_{s\Delta} \quad (4.136)$$

In general, the contribution of k_{sg} to the hydraulic roughness is small compared with the contribution of $k_{s\Delta}$. Substituting k_s according to the above formulae in the equation for the Chézy coefficient should generally result in values in the range of: $C = 25$ to $60 \text{ m}^{1/2}/\text{s}$.

NOTE: For a silty bed (eg in estuaries), C may be up to $80\text{--}90 \text{ m}^{1/2}/\text{s}$.

Other methods of determining hydraulic roughness exist; see for example EDF *et al* (1992).

Determination of k_s and the resulting values of C are discussed below, where it appears again that practically C is a function of water depth, h , and sediment grain size, D . By using Equations 4.130 and 4.132 the depth-averaged velocity, U , can be found for given (average) water depth, h , water surface gradient, i , and hydraulic roughness, k_s . Statistical variations of these parameters may also be considered.

Clearly there is a close relationship between the Manning-Strickler formulation and Chézy formula through an appropriate description of C in terms of R and n in Equation 4.130. Historically, more complicated cross-sections have been analysed using the Manning-Strickler method and this is discussed below under the title of composite cross-sections.

Composite cross-sections

A cross-section may need to be analysed as a composite section either if the geometry of the section is irregular such as a channel set within a floodplain or if the character of the hydraulic roughness varies significantly across the section. The starting point for the analysis is the definition of discharge, Q , in terms of the velocity across the section given in Equation 4.121. Two approaches are possible: *traditional hand calculation* procedures and **computer-based** methods.

- The **traditional approach** for calculation by hand is to divide the section into several components, usually with plane boundaries, and to assume that the shear stresses in the planes between adjacent parts are zero. By making one or more assumptions, the effective mean value of the hydraulic resistance can be calculated as described below.
- In more modern **computational procedures** the transverse velocity distribution is estimated from the shape (and possibly planform) of the section and the distribution of hydraulic roughness. Integration of this velocity distribution across the section then provides the total discharge. The computational procedures can also provide the velocities close to the boundary of the section for use in sizing bank protection materials.

Traditional calculation methods

For a composite cross-section the values of the hydraulic roughness for the various zones usually differ. Early publications on the approach used the Manning-Strickler method for irregular river cross-sections. In such cases, which are very common, the effects of banks and channels on the current distribution have to be considered. An irregular cross-section should be schematised using one of the following approaches.

- 1 A general method is to divide the cross-section into vertical slices parallel to the river axis, each with a more or less constant water depth, as shown in Figure 4.58a.

For the determination of the equivalent roughness, the water area is divided into N parts with the wetted perimeters P_1, P_2, \dots, P_N (m) and the Manning coefficients of roughness n_1, n_2, \dots, n_N (s/m^{1/3}) are known.

By assuming that each part of the area has the same mean velocity, the equivalent coefficient of roughness may be obtained by Equation 4.137 (Einstein, 1934; Yassin, 1954; Horton, 1933).

$$n = \left(P_1 n_1^{3/2} + P_2 n_2^{3/2} + \dots + P_N n_N^{3/2} \right)^{2/3} / P^{2/3} \quad (4.137)$$

By assuming that the total force resisting the flow is equal to the sum of the forces resisting the flow developed in the subdivided areas (Pavlovski, 1931; Mülhofer, 1933; Einstein and Banks, 1950), the equivalent roughness coefficient is given by Equation 4.138.

$$n = \left(P_1 n_1^2 + P_2 n_2^2 + \dots + P_N n_N^2 \right)^{1/2} / P^{1/2} \quad (4.138)$$

Lotter (1933) assumed that the total discharge of the flow is equal to the sum of discharges of the subdivided areas (see Figure 4.58a). Thus the equivalent roughness coefficient can be computed from Equation 4.139.

$$i = U_1^2 / (R_1 C_1^2) = U_2^2 / (R_2 C_2^2) = U^2 / (R C^2) \quad (4.139)$$

- 2 Where a main channel and a floodplain can be clearly distinguished, the cross-section should be divided into two separate parts (see Figure 4.58b). Then, using the Chézy formulation, the conditions of equal water surface gradient i and continuity yield to Equations 4.140 and 4.141.

$$i = U_1^2 / (R_1 C_1^2) = U_2^2 / (R_2 C_2^2) = U^2 / (R C^2) \quad (4.140)$$

$$U A_c = U_1 A_{c1} + U_2 A_{c2} \quad (4.141)$$

This results in Equations 4.142 and 4.143.

$$U A_c = U A_{c1} \left(\sqrt{\frac{R_1}{R}} \frac{C_1}{C} \right) + U A_{c2} \left(\sqrt{\frac{R_2}{R}} \frac{C_2}{C} \right) \quad (4.142)$$

$$\sqrt{R} = (A_1 \sqrt{R_1} C_1 + A_2 \sqrt{R_2} C_2) / (A C) \quad (4.143)$$

The overall C -value can be computed from Equation 4.144.

$$C = (b_1 C_1 + b_2 C_2) / b \quad (4.144)$$

where $b = b_1 + b_2$ (see Figure 4.58b).

- 3 If the area of the cross-sections (A_{c1} and A_{c2}) cannot be estimated accurately, as in Figure 4.58c, then the application of the hypothesis of Einstein is recommended. Einstein assumed $U_1 = U_2 = U$, resulting in Equation 4.145.

$$1/(R_1 C_1^2) = 1/(R_2 C_2^2) = 1/(R C^2) \quad (4.145)$$

Equation 4.145 results in the relationships given by Equations 4.146 and 4.147.

$$R_1 C_1^2 = R_2 C_2^2 = R C^2 = Q^2 / (A_c^2 i) \tag{4.146}$$

$$R_2 / R_1 = C_1^2 / C_2^2 \tag{4.147}$$

Especially for this schematisation in Figure 4.58c, Strickler provides a practical alternative (see Equation 4.148) to the Chézy friction coefficient, C ($m^{1/2}/s$), given by Equation 4.132.

$$C = 25(R/k_s)^{1/6} \tag{4.148}$$

Equation 4.148 gives a reasonable approximation for the original value of C in the range of $C = 40$ to 70 $m^{1/2}/s$ and transfers Equation 4.147 into Equation 4.149.

$$R_2 / R_1 = (k_{s2} / k_{s1})^{1/4} \tag{4.149}$$

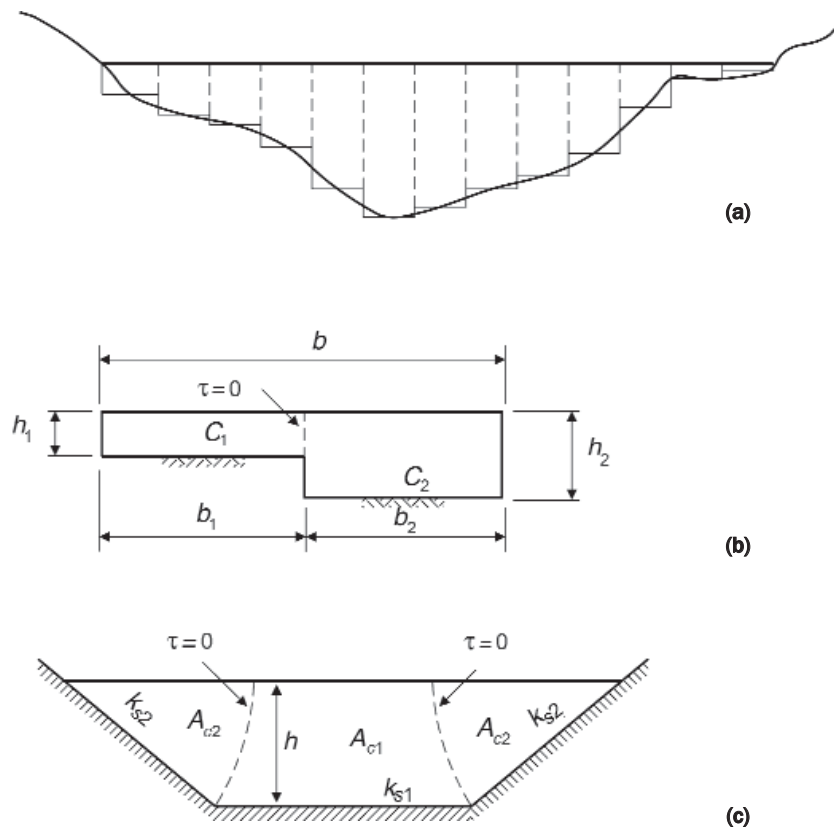


Figure 4.58 Schematisations of composite cross-section

Many other hand traditional calculation methods exist, some separating the left floodplain and the right floodplain from the main channel (eg James and Wark, 1992)

Computational methods

All one-dimensional mathematical models of open channel hydraulics include computational methods for assessing the discharge capacity (conveyance) of cross-sections. They have increased in sophistication over the decades of increasing model development and use. Many models use the traditional calculation methods described above or some variant to represent the conveyance of the sections.

However, some models attempt to be more physics-based for the representation of conveyance. More recently, methods have been developed and are based upon differential equation models of the cross-stream variation of velocity. Refer to Vreugdenhil and Wijnbenga (1982) or James and Wark (1992) for further information.

McGahey and Samuels (2003) provide a brief summary of approaches and describe the method adopted in the UK Environment Agency's Conveyance Estimation System (CES). The CES method is designed for both straight and meandering channels with associated floodplains. The resulting model can reproduce both the variation of discharge with water level and the transverse velocity distribution within the same model structure.

When interpreting results for the design of bank protection it is important to take account of the particular method and representation of velocity that underlies the calculation model, which should be available in the documentation of the software. It should also be noted that the value of resistance coefficient for the same circumstances may vary between models depending on the details of the calculation method. Section 4.3.5 below discusses modelling in more detail.

4.3.2.4 Structure of currents

The flow in a river is generally not uniform but varies in both the vertical and the horizontal direction. Consequently, to evaluate shear stresses on the river bed, for example, it may be necessary to know more than only the depth-averaged velocity U (m/s) and the vertical and/or horizontal velocity distributions have to be determined. This section discusses non-uniform velocities and other design considerations, which require a more detailed picture of the current profile, as follows.

- 1 Bed roughness (see Section 4.3.2.3).
- 2 Vertical velocity profile (see Section 4.3.2.4).
- 3 Transversal or horizontal velocity distributions (see Section 4.3.2.4).
- 4 Composite cross-sections (banks and channels, see Section 4.3.2.3).

The bed shear stress is introduced in Section 4.3.2.6 and discussed in Section 5.2.1 as an important parameter for items 2 and 3 above, for the flow pattern as well as for the structural response discussed in Section 5.2.3.

A current velocity may represent a loading parameter in the design of rock structures. In rivers, the dominating factor is the river discharge associated with the water level and the current velocity.

Velocity distribution

Owing to the presence of a free surface and friction along the channel wall, the velocities are not uniformly distributed in the channel section (see Figures 4.59 to 4.61). The maximum velocity is approximately 10–30 per cent higher than the cross-section averaged velocity ($= Q/A_c$).

Vertical profile distribution

If the hydraulic conditions are known, the velocity distribution both vertically and horizontally can be computed. For a hydraulically rough boundary (defined as $u_* k_s/\nu > 70$), the vertical flow distribution $u(z)$ is commonly used and determined with Equation 4.150:

$$u = \frac{u_*}{\kappa} \ln(z/z_0) \quad (4.150)$$

where u_* = shear stress velocity (m/s) (see Section 5.2.1.2), z_0 = reference level near the bed (m) defined below, κ = von Karman's constant ($\kappa = 0.4$).

The reference level near the bed, z_0 (m), is defined by $u(z = z_0) = 0$. For $u_* k_s / \nu > 70$, where k_s is the hydraulic roughness (m) and ν is the coefficient of kinematic viscosity (m^2/s), z_0 is defined by Equation 4.151.

$$z_0 = 0.033 k_s \tag{4.151}$$

Equation 4.150 implies that velocities are maximum at the water surface and so $u_{max} = u(h)$. The velocity $u(z)$ just equals U at $z = 0.37 h$. In Figure 4.59, the velocity profile is shown in a non-dimensional form.

For many engineering applications the velocity distribution can also be approximated by a power function in z/h , as given by Equation 4.152.

$$u = u_{max} (z/h)^p \tag{4.152}$$

where u_{max} = maximum velocity at the surface ($z = h$) (m/s).

The exponent p depends on the bed roughness and the Reynolds number (see Box 5.7 and Ackers, 1958); values between 0.16 and 0.10 have been found and $p = 0.14$ is commonly applied.

The flow velocity at a given height above the bed is smaller when the hydraulic roughness is larger. An example of the vertical flow velocity distribution is shown in Figure 4.59.

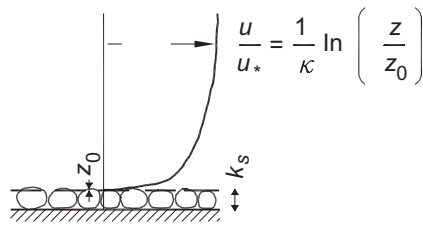


Figure 4.59 Vertical velocity profile

Horizontal profile distribution

The horizontal velocity distribution results from the presence of banks on both sides of a channel. In Figure 4.60, velocity distributions in the transverse direction are shown. The flow velocity near a bank in a straight channel may be up to 25 per cent smaller than the velocity in the axis of the channel, which obviously influences the shear stress acting on the banks (see Section 4.3.2.6).

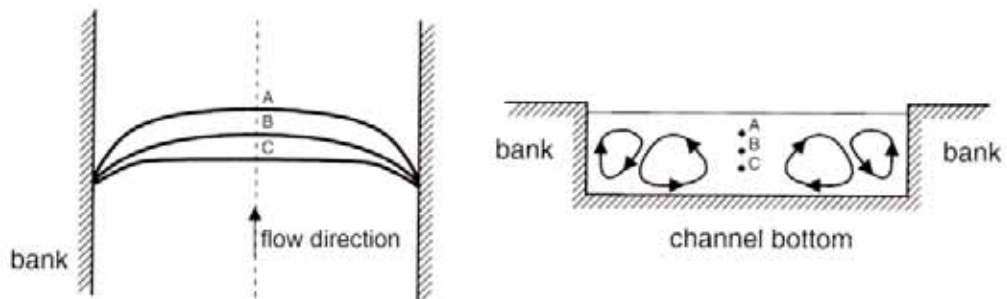


Figure 4.60 Horizontal velocity profile

Cross-sectional distribution

The measured maximum velocity in ordinary channels usually occurs at a distance of 5–25 per cent of the depth below the free surface; the closer to the banks, the deeper is the

maximum. Figure 4.61 illustrates the general pattern of velocity distribution over various vertical and horizontal sections of a rectangular channel section and the curves of equal velocity in the cross-section. The general patterns for velocity distribution in (a) a trapezoidal channel and (b) a natural irregular channel are also shown in Figure 4.61.

In addition to the shape of the section the velocity distribution in a channel section depends on the roughness of the channel and the existence of bends. In a broad, rapid and shallow stream or in a very smooth channel, the maximum velocity may often be found at the free surface. The roughness of the channel causes the curvature of the vertical velocity distribution curve to increase. In a bend the velocity increases greatly at the convex side owing to the centrifugal action of the flow.

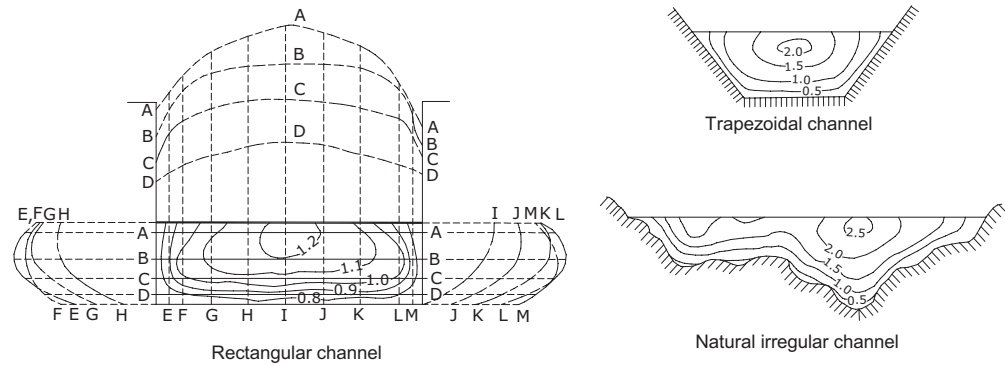


Figure 4.61 Velocity distribution in a rectangular channel, a trapezoidal and a natural irregular channel (Chow, 1959)

Effect of wind

Wind can generate currents in inland waters that are generally limited and thus negligible for the design of rock structures. However, fetch can be significant and wind-generated waves should be taken into account for inland structures. Wind blowing in a sustained way over a large expanse of water such as a reservoir has the potential to generate currents that are strong enough to warrant appropriate assessment. Hedges (1990) suggested that under steady state conditions the current velocity can be taken as about 2–3 per cent of the wind speed. However, for the purpose of protection design it is generally accepted that these currents can be neglected. Further information is given in Section 4.2.

The influence of wind waves on the vertical distribution of velocity is shown in Figure 4.62.

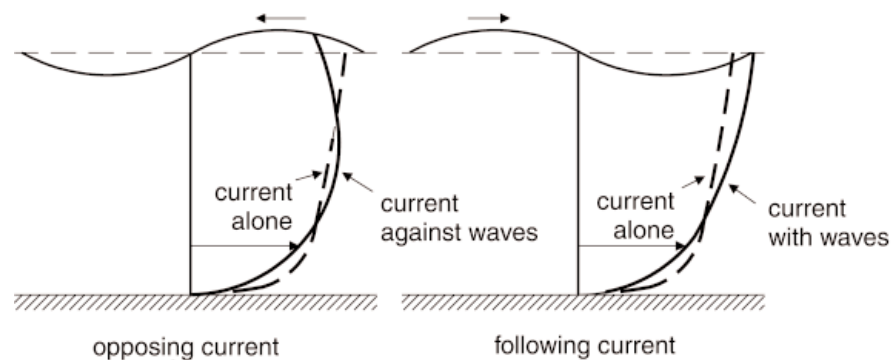


Figure 4.62 Effect by waves on the velocity profile

Local and secondary currents

Where there are changes in the geometry of the river or modifications in the bed roughness or where structures are present, the current distribution is three-dimensional and appropriate models should be used, discussed in more detail below.

The velocity component in the transverse channel section is usually small and insignificant compared with the longitudinal velocity components. However, in natural rivers with irregular cross-section shape and in channel bends, the flow velocity distribution differs from that in a straight channel. In curved channels, local currents can result in a **spiral motion**, which is an important phenomenon to consider in design. In Figure 4.63, an example of a small stream (running from left to right) over a layer channel is shown. Secondary transverse currents are inferred from measured transverse velocity components in the cross-over flow region. The relative depth of the stream to the channel is 0.09, the sinuosity, $I_s = 1.37$ (see Section 4.1.3.3), and the inner channel bedform is natural. The variability of the local flow is illustrated by the variation of flow for the different sections.

Interactions with structures contribute significantly to the local currents. Common examples are eddies between spur-dikes along rivers. For design purposes, the most important characteristics of such currents are maximum velocities, associated turbulence and the spatial extent of these currents. Figure 4.63b shows local currents near river training structures.

Since the types of flow discussed here are highly dependent on local conditions and are of a complex nature, no general practical guidance can be given. Physical modelling is recommended along with 2D or 3D modelling, which may be able to provide some insight into the expected flow pattern.

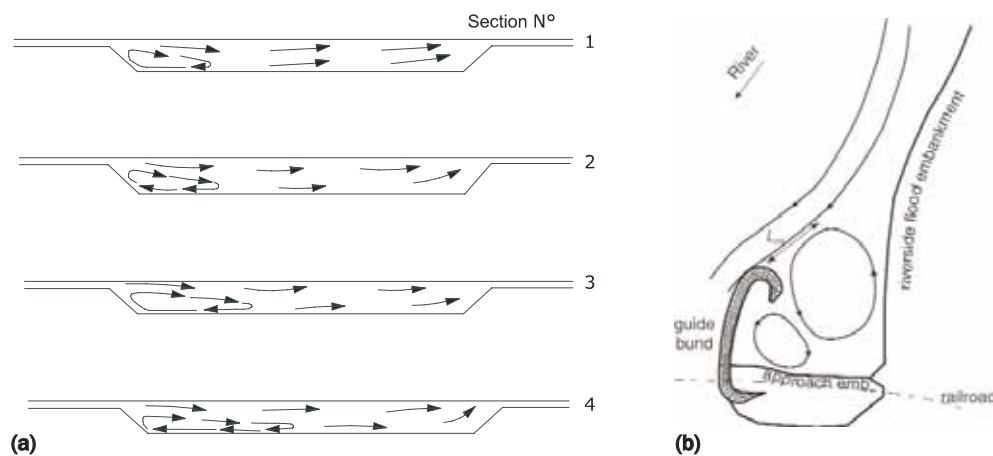


Figure 4.63 Example of local or secondary current (a) in cross-over flow region (b) caused by a structure

Flows affected by changes in river shape

At the outer bends of meandering rivers the flow velocity is higher than the velocity in the river axis. The main features of a meandering channels are the:

- **thalweg**, ie the line connecting the deepest points in a series of cross-sections (see Figure 4.64). The maximum velocity occurs approximately in the thalweg and its position varies with the flow discharge, sometimes coming close to the inner bend. The location of the thalweg should be investigated before carrying out river works
- **zones of sediment deposition** in the form of point bars, inside the bends
- **inflexion point**, or the point where the thalweg crosses the centreline of the channel.

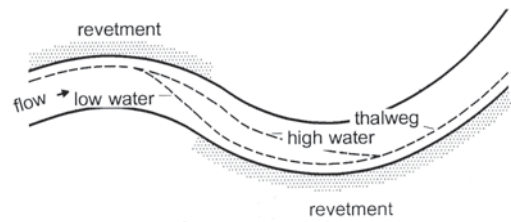


Figure 4.64 Definition of the thalweg

The effect on the flow velocity patterns is greater for sharper bends. Usually, account is taken of the effect of bends on the flow characteristics and on the stability of the banks by means of the ratio of the centreline radius of the bend r and the water surface width B . When $r/B \geq 26$, channels are generally considered as straight for the design of erosion protection on banks and beds. Empirical coefficients, such as the velocity distribution coefficient that combine several flow parameters have been introduced in stability equations to account for the effect of bends (see Section 5.2.3.1).

In bends, the curvature of the flow results in a transverse water surface slope i_r (-), a secondary circulation develops and combines with the main flow into a **spiral flow** (see Figure 4.65). The radial gradient i_r can be determined with Equation 4.153:

$$i_r = \partial h / \partial r = \alpha U^2 / (gr) \quad (4.153)$$

where r = (centre) radius of the curved river section (m); U = depth averaged velocity (m/s) and α = coefficient defined below (-).

The coefficient α accounts for the vertical flow velocity distribution, from $u = 0$ at the bed to $u = u(h)$ at the water surface, and is about equal to $\alpha = 1.05$. The transverse water surface slope is largest near the inner bend because the radius of the inner bend is generally smaller than the radius of the outer bend.

The result of the curved flow is a higher water level in the outer bend compared with the water level in the inner bend. The flow velocity is increased near the inner part of the bend because of the larger gradient of the longitudinal water surface and the smaller water depth. Therefore, the flow velocity is largest near the inner part of the bend.

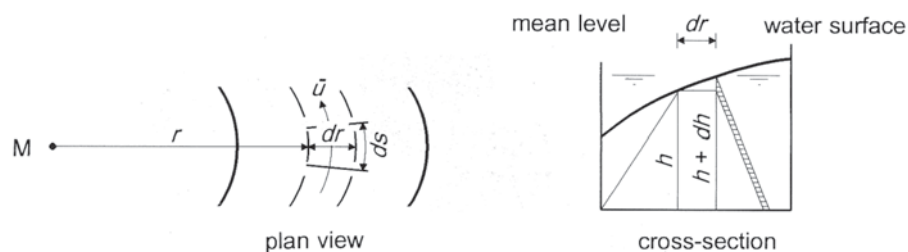


Figure 4.65 Flow in a river bend

Flows affected by structures

Structures in the flow such as bridge piers, abutments, caissons, cofferdams, weirs, gated structures or training works, generate marked changes in:

- the shape of the vertical velocity profile
- the local magnitude of the flow velocity
- the water level
- the level of turbulence of the flow.

The rise in water levels is illustrated in Figure 4.66 for a schematic case of a prismatic main river channel and floodplains, with various lengths of bridge approaches in the floodplains.

NOTE: Engineering works in the main river channel, eg to control water depth required for navigation, may also result in higher water stages.

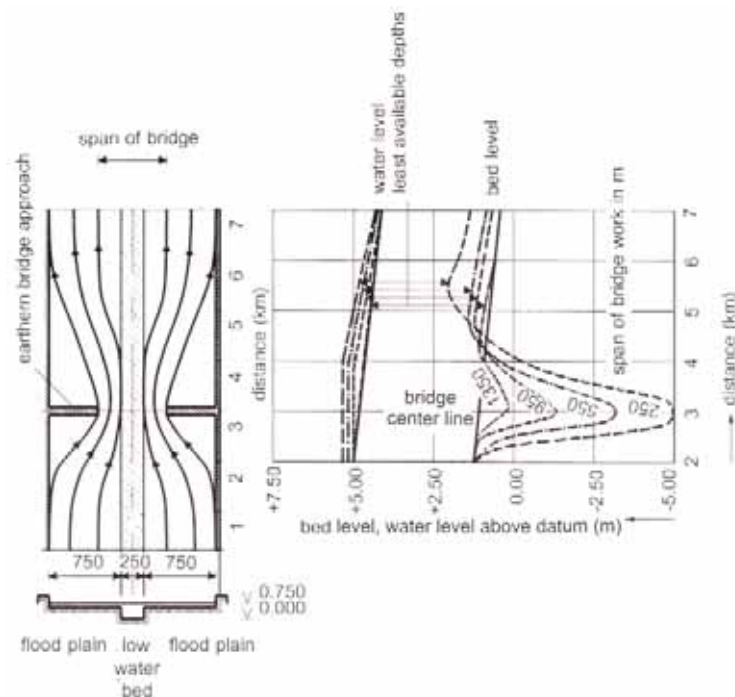


Figure 4.66 Backwater effects of a local horizontal river constriction

The influence of a horizontal channel constriction (ie a change of width, B) on the water depth h and water surface gradient i is shown in Figure 4.67. It shows a schematic case based on Equations 4.154 to 4.157, using the Chézy method for $B \gg h$. The initial situation and the post-constriction situation are denoted with index 0 and index 1 respectively.

Equations for water discharge:

$$\text{continuity: } Q_0 = Q_1 \quad (4.154)$$

$$\text{motion: } Q = BC\sqrt{h^3i} \quad (4.155)$$

Equations for sediment transport:

$$\text{continuity: } S_0 = S_1 \quad (4.156)$$

$$\text{motion: } S = BaU^b \quad (4.157)$$

where S = sediment transport (m^3/s).

For any particular river, the parameters a and b should be determined by using available transport data.

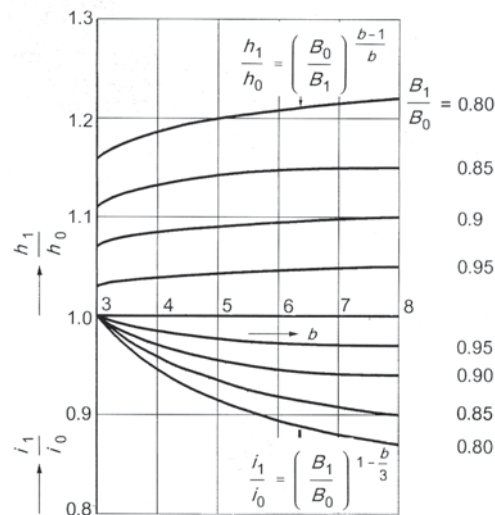


Figure 4.67

Consequences of a horizontal river constriction for the equilibrium river depth

Erosion of beds and banks is known as **scour** and can result from the interaction between structures and currents. It is important to protect the foundations of bridge piers, using aprons for example, to prevent development of local scour holes. References such as May *et al* (2002) and Hoffmans and Verheij (1997) should be consulted to establish the risk of scour development. Specific guidance on how to estimate and control scour at bridge piers is given, for example, in Melville and Coleman (2000) and in Transport Association of Canada (2001).

4.3.2.5

Turbulence

Turbulence may have a considerable local impact on the stability and movement of sediment or stone. When added to the local time-averaged velocity, u (m/s), the random turbulent velocity component, u' (m/s), causes an increase in the effective instantaneous velocity: $u + u'$. To assess the stability of sediment and stone, it is important to note that most stability formulae implicitly assume a **normal** turbulence. Consequently, where the turbulence exceeds the **normal** level a velocity correction should be applied.

The turbulence level can be quantified by various means, but the **turbulence intensity**, r (-), is most commonly used. It is defined as a ratio of the variation of flow velocity around the mean in relation to the mean flow velocity (or sometimes the shear velocity) and can be determined by Equation 4.158. For further details see for example (Escameia, 1998):

(4.158)

$$r = u'_{rms}/u \quad \text{where } u'_{rms} = \text{root mean square of the random turbulent velocity components, } u' \text{ (m/s),}$$

u = local time-averaged velocity (m/s).

Normal turbulence intensities can be characterised by $r \cong 0.1$ (10 per cent), which is found in uniform flow in laboratory flumes and rivers with a low flow regime and flat or rippled bed (so excluding beds with relatively high sand dunes). Above a rough bed, such as a bed protection consisting of armourstone, values of $r \cong 0.15$ (15 per cent) apply.

Turbulence levels in excess of these normal levels of (say) 10–15 per cent are typically the result of hydraulic interaction between the flow and structures including:

- flow separation, ie sudden widening of flow cross-section
- vortex shedding, eg bridge piers, large stones
- changes in the bed and/or slope roughness.

As well as having an effect on water levels, on flow surface disturbance and on sediment transport, turbulence (or turbulence levels above those expected in straight river or channel sections) also modifies the forces imposed by the flow on the river or channel boundary. Turbulence is therefore an important, but often neglected, parameter to consider in the interaction between fluvial currents and rock revetments and bed protection. Highly turbulent flows can be found in a number of situations, as illustrated in Figure 4.68. Local turbulence levels depend strongly on the specific dimensions, geometry and roughness of the turbulence-generating structure, so no general guidelines can be given. If there is an expected source of turbulence, separate turbulence modelling (see Section 4.3.4) may have to be conducted to quantify the likely impact on stability. Section 5.2.1 provides advice on ways to accommodate it in design.

NOTE: Excessively high levels of turbulence can persist at considerable distances from a structure or hydraulic jump and should be considered in stability design.

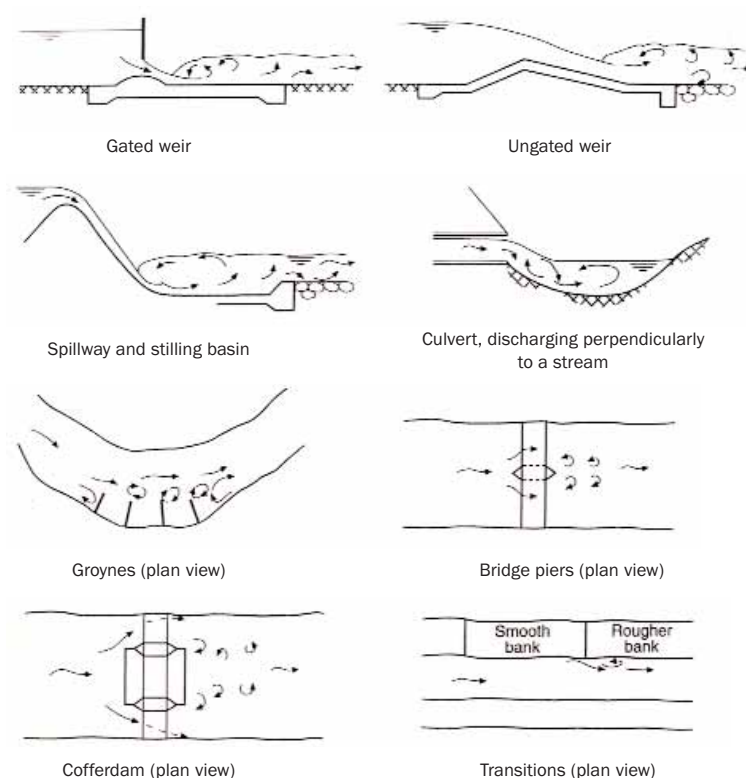


Figure 4.68 Examples of situations with high turbulence (from Escarameia, 1998)

4.3.2.6

Bed shear stress

Some detailed design problems can only be solved when good, site-specific information on velocity distributions and/or other flow characteristics is known. A key parameter in such considerations is the **bed shear stress**, which is also a parameter used to determine sediment transport and to assess stability of stone. This is a typical parameter of hydraulic interactions and structural responses. Approaches to approximate the overall shear stress, τ , at the bed are discussed below.

The simplest approach is to assume that the interaction between the current and the river walls (bed or banks, protected or not) is only controlled by the bed shear stress, τ (N/m^2), and the mean gradient of the water surface, i (-). In this approximation, τ can be expressed as a function of the major hydraulic characteristics (see Equation 4.159):

$$\tau = \rho_w g R i \quad (4.159)$$

where ρ_w = water density (kg/m³), i = mean water surface gradient (-) and R = hydraulic radius (m).

A practical parameter, derived directly from the shear stress, τ (N/m²), is the shear velocity, u_* (m/s), commonly defined as given in Equation 4.160.

$$u_* = \sqrt{\tau/\rho_w} \quad (4.160)$$

From Equation 4.159, the shear velocity, u_* (m/s), can be expressed as a function of the hydraulic radius, R (m), and water surface slope, i (-) (see Equation 4.161).

$$u_* = \sqrt{g R i} \quad (4.161)$$

Combining Equations 4.130 and 4.159, the relationship between the shear stress, τ (N/m²), and the current velocity, U (m/s), is established by Equation 4.162:

$$\tau = \rho_w g (U/C)^2 \quad (4.162)$$

where C = Chézy coefficient (m^{1/2}/s).

Because the Chézy coefficient, C , is basically a function of h/k_s or h/D (see Section 4.3.2.3), Equation 4.162 describes the dependency of the shear stress, τ , on the water depth, h , and the current velocity, U . In Section 4.3.2.3, the importance of a proper estimate of the hydraulic roughness, k_s , is emphasised.

The vertical current distribution is presented in Section 4.3.2.4. The general and conventionally used method to describe the vertical distribution of the current velocities is based upon the logarithmic distribution (see Section 4.3.2.4). This distribution results from the interaction of the current with the bed shear stress. An example of the vertical flow velocity distribution is shown in Figure 4.59 of Section 4.3.2.4.

A transverse velocity distribution is the result of the interaction with riverbanks and/or sub-channels (see Section 4.3.2.4). Such a non-uniform velocity distribution in the transverse direction may even occur in the case of a long straight channel. In Figure 4.69, the transverse (or horizontal) shear stress is shown for a straight prismatic channel. Measurements have indicated that the flow velocity near a bank may be approximately 40 per cent of the cross-sectional averaged velocity, which may be observed at the bank toe. Usually, the cross-sectional averaged flow velocity is applied. Because of the lower flow velocity over the banks the shear stress on the banks is also less than the bed shear stress. Measurements have shown that the bank shear stress may be reduced to approximately 75 per cent of the bed shear stress (see Figure 4.69).

1

2

3

4

5

6

7

8

9

10

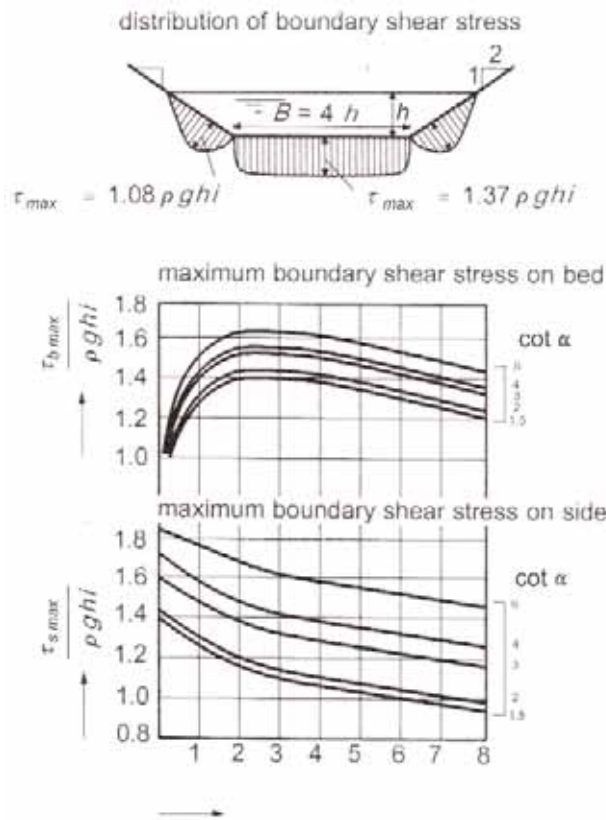


Figure 4.69

Shear stress, transverse distribution (after 1995 edition)

Bed shear stresses, although they have been evaluated, represent an average over a lapsed period of time. For more accurate analysis it is recommended to observe fluctuations in time. Compared with the average bed shear stress, the instantaneous bed shear stresses were found to be nearly 10 times greater. This result is comparable with those of Kalinkse (1943), who concluded that instantaneous current velocities can reach three times the average velocity if time is taken into account.

4.3.2.7 River confluences and bifurcations

A real river system generally contains confluences and bifurcations that complicate the movement of water and sediment and thus its determination. For example, the rainfall in the catchment areas of the confluence of two rivers may either be in phase or out of phase, which can be observed by a double-peaked hydrograph; or the bed material of these rivers may have completely different characteristics (see Figure 4.70). The risk of erosion can be very high in the vicinity of the confluence of two rivers.

At a **confluence** the difference between the regimes $Q_1(t)$ and $Q_2(t)$ is the dominating factor. Strong backwater effects can occur in the upstream rivers, which may cause a loss of equilibrium at the confluence, resulting in an excessive supply of sediment to the main river. Therefore, discharge and sediment measurement stations should be selected away from the confluence.



Figure 4.70 Schematisation of a river system

At a **bifurcation** the local geometry determines the local flow pattern and, therefore, the division of the sediment discharge S_0 into S_1 and S_2 . Consequently, sediment measurements should be carried out away from the bifurcation. However there are no objections to measuring discharge relatively close to a bifurcation. In the long term, a bifurcating system is generally not stable. After some time one of the branches may become blocked completely.

4.3.3 Flood waves

4.3.3.1 General

Water levels in rivers are governed by the river discharge and extreme levels are associated with flood waves. In Section 4.3.3.2, the propagation of flood waves is discussed as well as the use of rating curves, as a means to relate water levels to river discharge, and stage relationships to correlate water levels at different locations along the river. The sea level at the mouth of a river, ie the river base, can be the boundary condition for computations upstream in the river.

Several types of flood can be distinguished:

- **flash floods:** of small catchment areas with immediate response to rain
- **fast floods:** with short concentration times, for example, from a few hours because of strong rains (Cevennes storms); or in catchment areas with sharp slopes
- **plain floods:** with slow kinematics, caused by overflow from the main channel
- **groundwater floods:** which are combined with overflow from rivers and are very slow not only to spread in the floodplain but also to subside.

4.3.3.2 Hydrographs (duration/exceedance and rating curves) and stage relationships

Data collected on, for example, discharges or water levels, can be presented in a graphical way. The following diagrams/relationships may be determined at a given site.

- **hydrographs:** water level or discharge as a function of time (see Figure 4.71)
- **mass curves:** cumulative discharge as a function of time (see Figure 4.72)
- **duration curves:** number of days a certain discharge or water level is (not) exceeded (see Figure 4.73)
- **discharge exceedance curves:** number of days a certain discharge or water level is equalled or exceeded (see Figure 4.74)
- **stage relation curve:** stage at various stations as a function of one specific stage (see Figure 4.55)
- **rating curve:** relationship between discharge and water level at one station (see Figure 4.75).

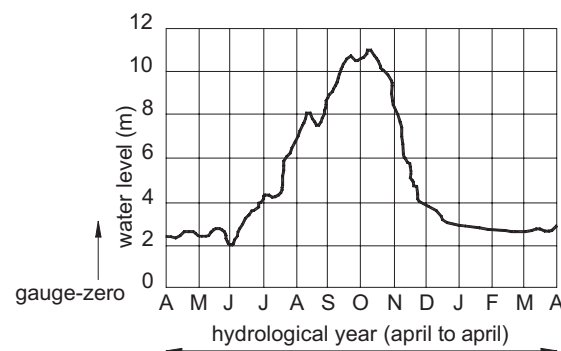


Figure 4.71 Example of a hydrograph

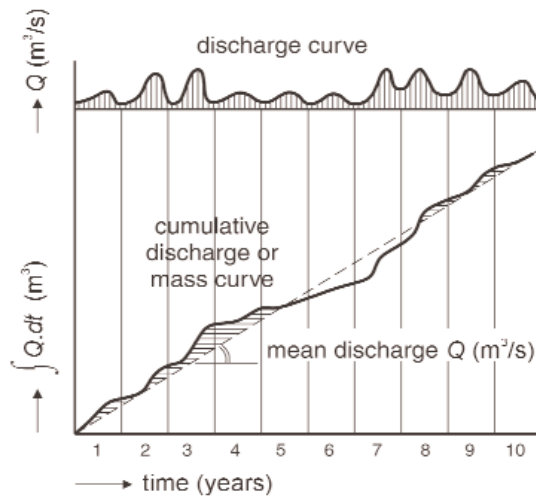


Figure 4.72

Example of a mass curve

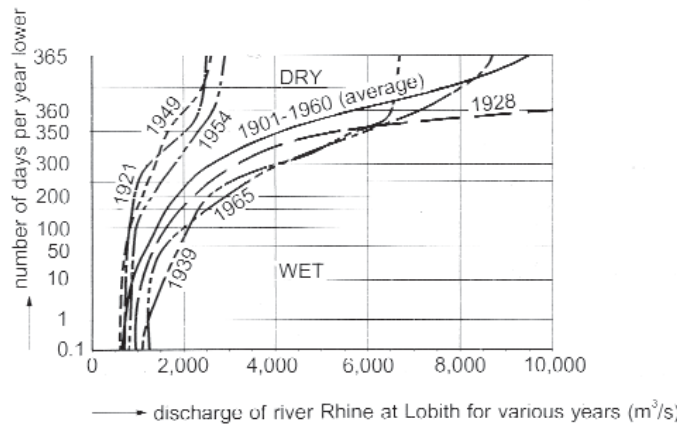


Figure 4.73

Examples of discharge duration curves

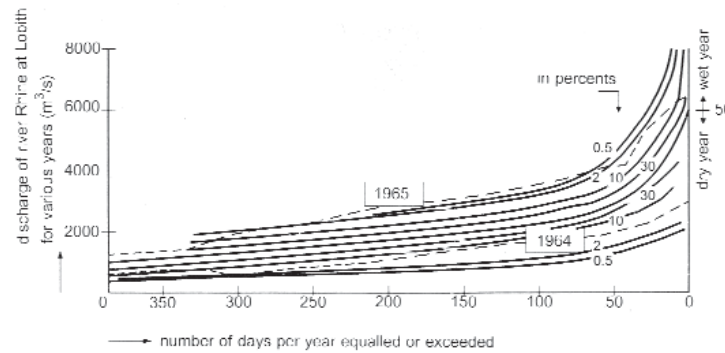


Figure 4.74

Example of discharge exceedance curves

From these relationships, predictive equations may be derived. As an example, the relationship for the rating curve is given by Equation 4.163, but the reader is advised to contact competent authorities to determine whether rating curves already exist for the river and to check if new river training works make existing data irrelevant:

$$Q = aB(h + z_0)^p \tag{4.163}$$

where:

- a = calibration coefficient
- p = power number (-)
- B = river width at gauging station, usually = $f(h)$ (m)
- h = water depth above reference level at gauging station (m)
- z_0 = "reference" level used as a fitting coefficient (m).

For a wide channel, the power number, p , theoretically equals 1.5 assuming the Chézy Equation and $p = 1.67$ assuming the Manning-Strickler Equation (see Section 4.3.2.3). In

addition, p depends on several other factors including the value of z_0 chosen, the shape of the cross-section, the presence of floodplains, seasonal effects of growth and die-back of vegetation, the transport of sediments and downstream controls. In practice, the power is usually found to be in the range of $1.0 < p < 2.5$.

Graphically, z_0 is determined by trial and error, requiring that the stage-discharge curve, when plotted on a double-log scale, shows a straight line. As z_0 is obtained in this way, p is subsequently determined using a least squares method. In Figure 4.75 an example is shown of a stage relationship for $h + z_0$ for $z_0 = 0$ to 2, with a straight line obtained with $z_0 = 1.5$. Note that p does not necessarily take the value $p = 1$.

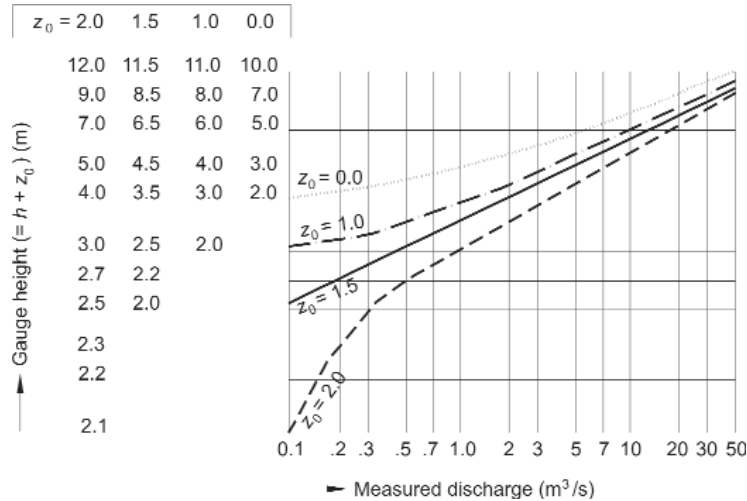


Figure 4.75 Example of fitting of data into a rating curve

This discharge is divided over the main channel and the floodplains if present. The rating curve changes significantly as soon as the floodplains are flooded, as shown in Figure 4.76.

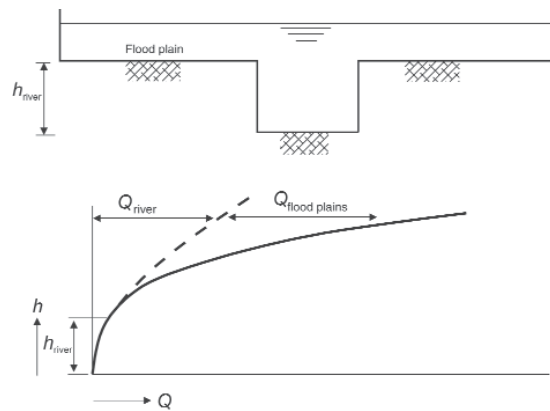


Figure 4.76 Example of the influence of floodplains on the rating curve

4.3.3.3 Flood waves and translation waves

The primary assumptions of a steady flow analysis are that:

- peak stage nearly coincides with peak flow
- peak flow can accurately be estimated at all points in the riverine network
- peak stages occur simultaneously over a short reach of channel.

In fact, for moderate bed slopes ($< 1‰$), or for highly transient flows (such as those from a dam breakage), peak stage does not coincide with peak flow, which always precedes peak stage. This phenomenon, the **hysteresis effect**, results from changes in the energy slope.

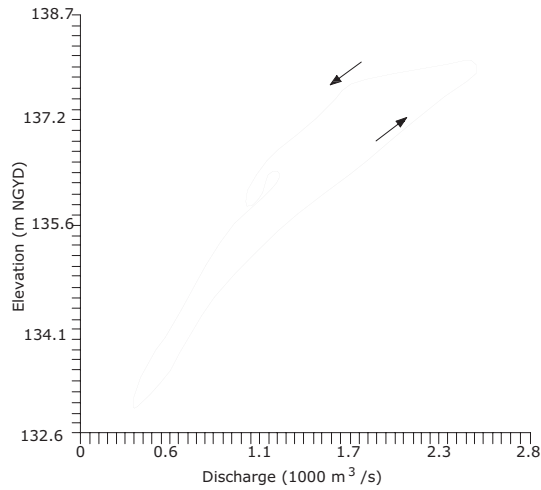
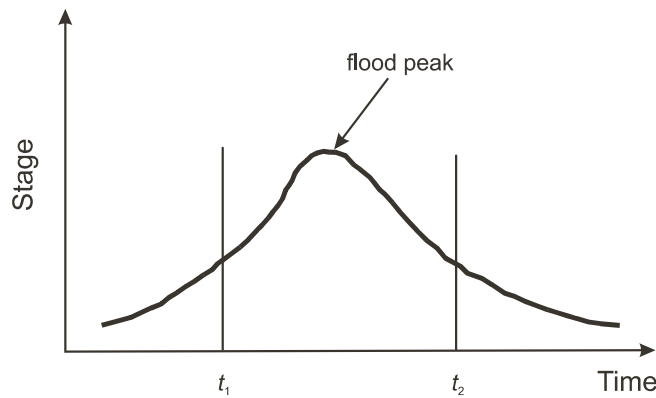
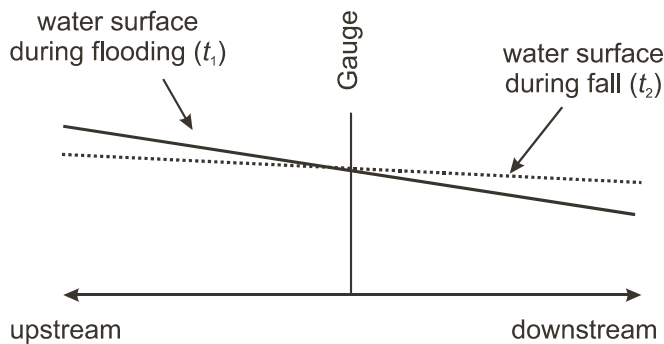


Figure 4.77
 Looping rating curve for the Illinois River at Kingston Mines, 15 Nov 1982–31 Jan 1983 (USACE, 1993)



(a)



(b)

Figure 4.78
 Explanation for looped rating curve effect (USACE, 1993): (a) variation of stage at the gauge with time (b) water surface in the vicinity of the gauge

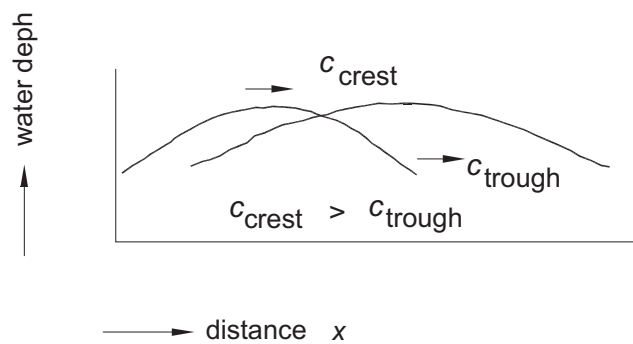


Figure 4.79
 Flood wave propagation

The effect of a flood wave on discharges and water levels can be shown by a rating curve (see Figure 4.77). The change in slope can be caused by backwater from a stream junction or by the dynamics of the flood wave. The hysteresis can be explained with the help of Figure 4.78. Figure 4.78a shows the effect of the flood wave at a gauge, ie an increase of water level before

the flood peak, at t_1 , and a decrease of water level after the peak, at t_2 . Figure 4.78b shows the effect of the flood and fall on the water surface slope in the vicinity of the gauge. The slope of the water surface is greater on the flood than on the fall, so the flow is accelerating on the rise and decelerating on the fall.

A rating curve therefore gives accurate estimates only when the hysteresis effect is absent. However, this effect is inherent to flood waves, especially in the higher reaches and only disappears where bed resistance fully dominates. Usually, this is the case in the lower reaches of the river, where the flood wave is flattened (Jansen, 1979).

NOTE: To assume the crest stage occurs simultaneously at two cross-sections is not recommended. Effectively, it is imprecise, since all flow is unsteady and flood waves advance downstream. As the stream gradient decreases and/or the rate of change of flow increases, the hysteresis effect becomes more pronounced (see Figure 4.79, where c is the propagation velocity of the flood wave (m/s)). Reflecting the wave-like character of flood behaviour, hydrographs at successive stations are displaced in time and peaks occur later at each successive downstream station. In other words, downstream hydrographs lag upstream hydrographs. Also, hydrograph peaks tend to display subsidence, which is a decrease in peak value with distance downstream if there is no significant tributary inflow.

The passage of a **flood wave** is characterised by a gradual rise and fall of the water surface with a time-scale of a few days to a few weeks and a wavelength of at least 100 km. For very slow floods, the approach of Seddon (1900) shows that the propagation velocity of the flood wave c (m/s) can be expressed as Equation 4.164:

$$c = 5/3U \quad (4.164)$$

where U = average flow velocity in the river (m/s).

In practice, however, a lower value of the constant is found for natural rivers, with Wilson (1990) quoting the work of Corbett *et al* (1945) (see Equation 4.165).

$$c = 1.3U \quad (4.165)$$

The coefficient of 5/3 (in Equation 4.164) as derived from assuming the Manning-Strickler equation, is valid for a wide rectangular channel, and the lower value of 1.3 incorporates the effects of typical cross-section shapes.

The propagation velocity has the same order as the flow velocity, U , because of the dominating effect of bed friction (in contrast to the translation wave, discussed below). During the propagation of the wave, the crest height decreases and simultaneously the wavelength increases, resulting in a flatter wave (see Figure 4.79). The wave crest propagates faster than the surrounding trough regions of the wave, because the propagation velocity increases with increasing water depth. Tang *et al* (2001) show how the flood wave celerity may be estimated at a reach scale from typical cross-section geometry: the wave celerity depends strongly on river discharge in a non-linear fashion, especially around the bankfull capacity of the river channel.

Another surface-wave phenomenon is the **translation wave**. Usually, this type of wave is generated by a sudden increase or decrease of the local discharge or of the water surface. An example is the sudden opening of a weir. For following or opposing currents, U (m/s), the propagation velocity, c (m/s), of a small (relative to water depth) translation wave can be estimated by Equation 4.166:

$$c = U \pm \sqrt{U^2 + \frac{gA_c}{b}} \quad (4.166)$$

where A_c = channel cross-sectional area (m^2), b = channel width (m).

When a translation wave approaches a smaller or a wider cross-section the wave is partially reflected and partially transmitted. In Figure 4.80 the situation with a wider cross-section is shown. The reflected and transmitted waves can easily be calculated if the discharge, the width and the propagation velocity are known.



Figure 4.80 Reflection and transmission of translation waves

4.3.4 Ship-induced waves and water movements

The banks and beds of inland waterways, such as rivers and navigation canals, should be designed to allow for ship-induced water movements. In marine and coastal waters, loads generated by ships underway or manoeuvring may affect structures. Examples of affected structures in inland, marine and coastal areas are: armour layers covering sills in which pipelines or motorway tunnels crossing the navigation channel are buried, bed protection downstream of navigation locks, breakwaters, groynes and bed protections for quay walls.

The relevant parameters for calculating the ship-induced water movements are defined in Figures 4.81 and 4.82 and are as follows:

- **primary ship wave**, consisting of (a) transversal front wave, (b) water level depression alongside the ship, and (c) transversal stern wave
- **return current** within the primary wave
- **secondary ship waves**
- **propeller jet**.

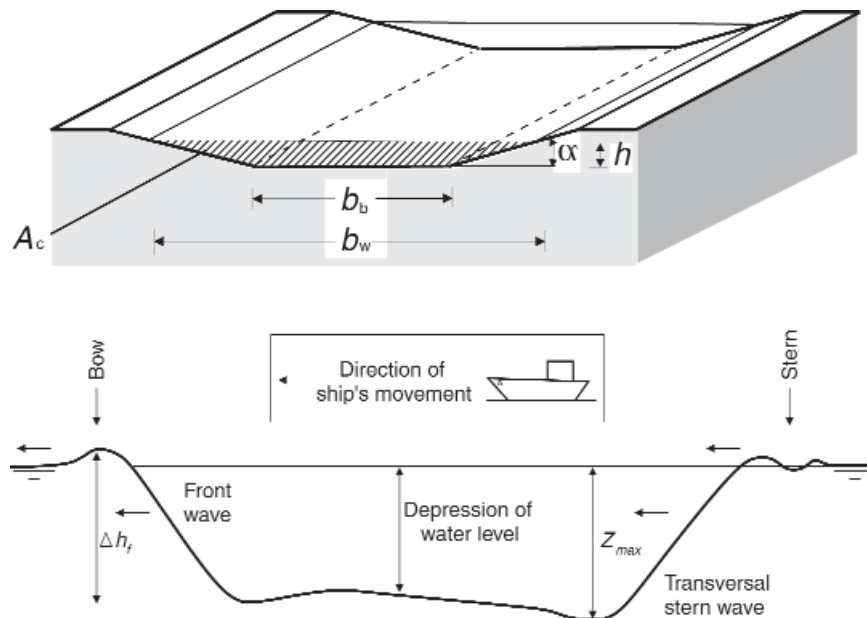


Figure 4.81 Definition sketch of ship-induced water movements

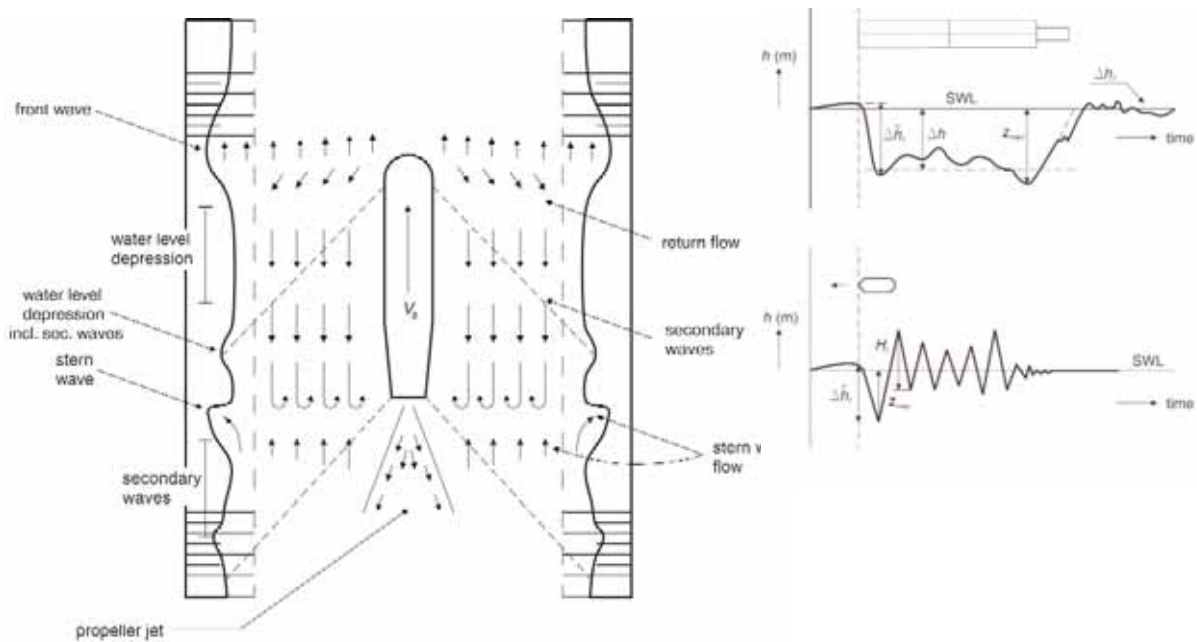


Figure 4.82 Characteristics of ship-induced water movements related to bank stability. Note: dotted lines represent the interference peaks of secondary waves of which the propagation direction is 35° with respect to the vessel's propagation direction (see Section 4.3.4.2)

Ship types, sailing behaviour (ie ship speed and position in the waterway) and dimensions and the geometry of the waterway determine the induced water movements. In most cases, push-tow units or loaded conventional motor vessels are responsible for the severest primary wave (transversal stern wave z_{max} (m) and return current U_r (m/s)) and fast-moving vessels, such as loose tugs, service vessels and recreational ships for the severest secondary waves H_i (m).

Relevant parameters for calculating ship-induced water movements are:

- ship length L_s (m) and ship beam B_s (m)
- ship sailing speed V_s (m/s)
- loaded ship draught T_s (m) (or the average empty draught)
- ship position, relative to the fairway axis y (m) or bank y_s (m)
- cross-sectional area of the waterway A_c (m²)
- water depth of fairway h (m)
- width of fairway at the bed b_b (m) and at the waterline width b_w (m).

A first estimate on the order of magnitude of the different water movement components can be obtained by applying the formulae presented in this section. Figure 4.83 presents a flow chart for calculating ship induced waves and water movements. Equations related to this flow chart are presented in Section 4.3.4.1 and 4.3.4.2. Propeller jet velocities are discussed in Section 4.3.4.3.

It should be noted that only a general overview of basic relationships is presented in this section. For a more comprehensive discussion on ship-induced water movements in navigation canals, reference is made to PIANC (1987) and Przedwojski *et al* (1995). The computer program DIPRO (DIDimensioning PROtections), developed in the Netherlands (the 2002 version is available from Rijkswaterstaat), enables designers to determine bank protection requirements.

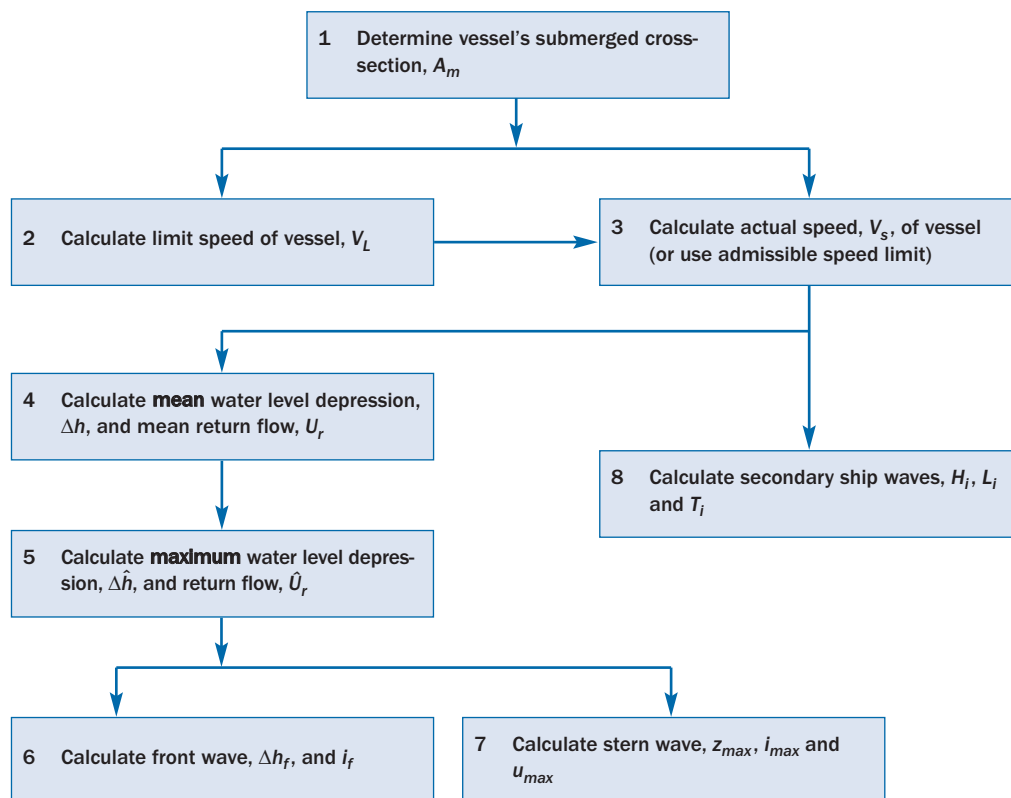


Figure 4.83 Calculation scheme for ship-induced water movements

4.3.4.1

Return current, water level depression, front and stern waves

The height of water level depression Δh , front wave Δh_f and transversal stern wave z_{max} varies at the bank with an average between 0.3 m and 0.5 m although occasionally heights of 1.0 m may occur. The duration of the water level depression varies between 20 s and 60 s depending on the type of ship and the ship speed. The period of the front and transversal stern waves is about 2–5 s. Return currents U_r up to 1.5 m/s are possible.

Formulae related to the flow chart given in Figure 4.83 are outlined below. An example is given in Box 8.5 in Section 8.3.5.2.

1 Vessel's submerged cross-section, A_m

The vessel's submerged cross-section, A_m (m²), is evaluated by Equation 4.167.

$$A_m = C_m B_s T_s \quad (4.167)$$

where C_m = midship coefficient related to the cross-section of the ship (-); B_s = beam width of the ship (m); T_s = draught of the ship (m). Appropriate values of C_m are:

- $C_m = 0.9$ to 1.0 for push units and inland vessels
- $C_m = 0.9$ to 0.7 for service vessels, tow boats and for marine vessels.

2 Limit speed of vessel, V_L

The limit speed of the vessel, V_L (m/s), is calculated by Equation 4.168.

$$V_L = F_L \sqrt{g A_c / b_w} \quad (4.168)$$

where $F_L = \left[\frac{2}{3} \left(1 - \frac{A_m}{A_c} + 0.5 F_L^2 \right) \right]^{3/2}$; A_c = cross-sectional area of the waterway (m²); b_w = width of the waterway at the waterline (m). Other relevant speed limits are given by Equations 4.169 and 4.170.

$$V_L = (gL_s / 2\pi)^{1/2} \quad (4.169)$$

$$V_L = (gh)^{1/2} \quad (4.170)$$

The minimum value should be applied in further calculations.

3 Actual speed, V_s

The actual speed of the vessel, V_s (m/s), is evaluated as a factor of the limit speed V_L (see Equation 4.171):

$$V_s = f_v V_L \quad (4.171)$$

where $f_v = 0.9$ for unloaded ships and $f_v = 0.75$ for loaded ships.

For loaded push-tow units and conventional motor freighters the actual speed can also be determined from Equation 4.172.

$$V_s = 2.4 \sqrt{\frac{A_c}{b_w}} \exp\left(-2.9 \frac{A_m}{A_c}\right) \quad (4.172)$$

Note: Equation 4.172 is derived by implicitly assuming that ships sail with a speed of 0.9 times V_L ($f_v = 0.9$).

4 Mean water level depression, Δh and mean return flow, U_r

The mean water level depression, Δh (m), is calculated by Equation 4.173.

$$\Delta h = \frac{V_s^2}{2g} \left[\alpha_s \left(A_c / A_c^* \right)^2 - 1 \right] \quad (4.173)$$

where:

α_s = factor to express the effect of the sailing speed V_s relative to its maximum (-),

$$\alpha_s = 1.4 - 0.4 V_s / V_L$$

A_c^* = cross-sectional area of the fairway next to the ship (m²),

$$A_c^* = b_b (h - \Delta h) + \cot \alpha (h - \Delta h)^2 - A_m$$

A_c = cross-sectional area of the fairway in the undisturbed situation (m²), $A_c = b_b h + h^2 \cot \alpha$

α = slope angle of the bank (-).

The mean return flow velocity, U_r (m/s), is calculated by Equation 4.174.

$$U_r = V_s \left(A_c / A_c^* - 1 \right) \quad (4.174)$$

5 Maximum water level depression, $\hat{\Delta h}$ and return flow, \hat{U}_r

The maximum water level depression, $\hat{\Delta h}$ (m/s) can be calculated by Equation 4.175:

$$\hat{\Delta h} / \Delta h = \begin{cases} 1 + 2A_w^* & \text{for } b_w / L_s < 1.5 \\ 1 + 4A_w^* & \text{for } b_w / L_s \geq 1.5 \end{cases} \quad (4.175)$$

where $A_w^* = y h / A_c$ (-).

For ratios of A_c / A_m smaller than about 5 (ie comparable with $b_w / B_s < 10$) the flow field induced by sailing ships might be considered as one-dimensional. For these situations Equation 4.176 is applicable.

$$\hat{U}_r / U_r = \begin{cases} 1 + A_w^* & \text{for } b_w / L_s < 1.5 \\ 1 + 3A_w^* & \text{for } b_w / L_s \geq 1.5 \end{cases} \quad (4.176)$$

For larger ratios, ie $A_c / A_m > 5$ or $b_w / B_s > 10$, the flow field is two-dimensional. Then, the gradient in the return current and the water level depression between the ship and the bank should be taken into account. In the computer program DIPRO these formulae are incorporated.

At some places horizontal berms are present in embankments. Depending on the water depth, the water motion may become super-critical. More information on situations in which the Froude number related to ship speed and water depth above the berm plays a role can be found in Van der Wal (1989).

6 Front wave height, Δh_f and steepness, i_f

The characteristics of the front wave can be calculated by Equations 4.177 and 4.178.

$$\Delta h_f = 0.1\Delta h + \Delta \hat{h} \quad (4.177)$$

$$i_f = 0.03\Delta h_f \quad (4.178)$$

7 Stern wave height, z_{max} , steepness, i_{max} and velocity, u_{max}

The characteristics of the stern wave can be calculated by Equations 4.179 to 4.181:

$$z_{max} = 1.5\Delta \hat{h} \quad (4.179)$$

$$i_{max} = (z_{max}/z_0)^2, \text{ with: } i_{max} < 0.15 \quad (4.180)$$

where $z_0 = 0.16 y_s - c_2$, $y_s = 0.5 b_w - B_s - y$, $c_2 = 0.2$ to 2.6 .

$$u_{max} = V_s (1 - \Delta D_{50}/z_{max}) \quad (4.181)$$

where D_{50} = roughness of the bed (m) and Δ = relative buoyant density of the material (-).

Return currents in a groyne field

The ship-induced return currents in a groyne field along a navigation canal or river can be estimated by Equation 4.182 (see also Figure 4.84):

$$\frac{U_{local}}{U + U_r} = \alpha \left(\frac{h}{h_{ref}} \right)^{-1.4} \quad (4.182)$$

where:

U_{local}	=	maximum flow velocity at a location in a groyne field (m/s)
U	=	average flow velocity in the river (m/s)
U_r	=	average return current in front of the groyne heads exclusive of the natural flow velocity (m/s)
h	=	average water depth in the river (m)
h_{ref}	=	average water depth in the river at a discharge at which the groynes submerge (m) ($h_{ref} \sim 7$ m in the River Waal)
α	=	coefficient depending on the location in the groyne field (-), $\alpha = 0.20$ to 0.60 .

NOTE: Equation 4.182 is an empirical equation for the River Waal in the Netherlands that predicts the maximum flow velocity just downstream of the groyne when the stern of a push-tow unit passes (see Figure 4.85). Designers should be aware that applying this equation for other rivers might not be valid.

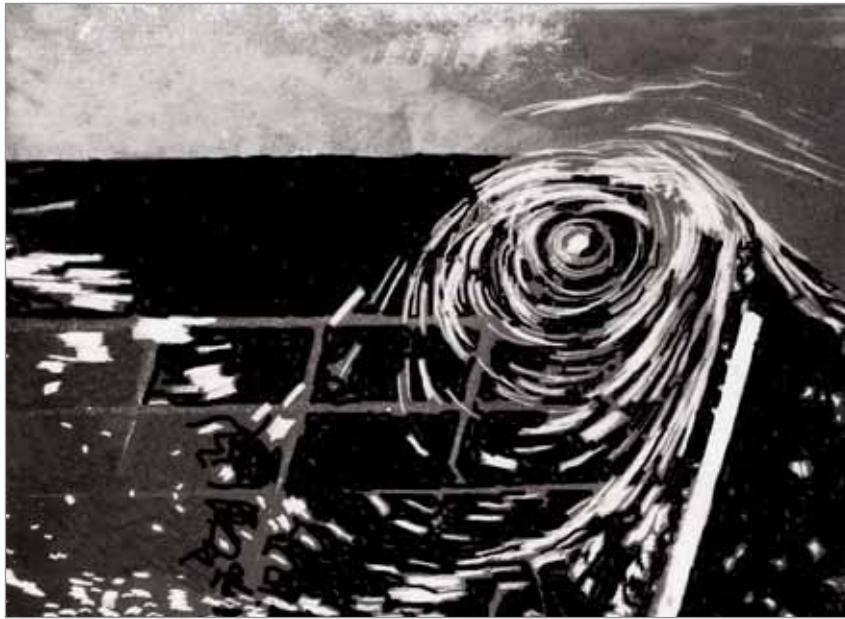


Figure 4.84 Eddy downstream of a groyne directly after the stern of a push-tow unit passed by to the right

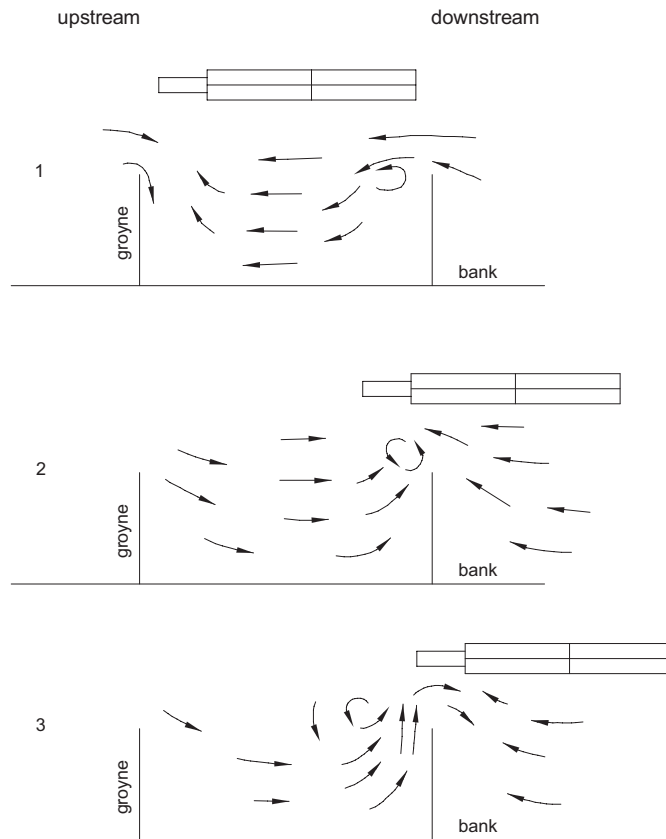


Figure 4.85 Flow field in a groyne field induced by a passing four-barge unit

Return current underneath ships

Tunnels and pipelines crossing navigation canals or rivers cannot always be buried deep below the canal or river bed and may require a cover layer to protect the structure against the induced water motions below the ship keel. Also bed protections in harbour approaches to locks are influenced by water motions caused by ships sailing over them. Equation 4.183 can be used to predict flow velocities underneath ships. However, it should be noted that this formula can only be applied for first estimate purposes:

1
2
3
4
5
6
7
8
9
10

$$U_{r, \text{belowkeel}} = c \cdot U_{r, \text{average}} \quad (4.183)$$

where $c = 1.5$ to 2.0 .

In the Netherlands, research is being conducted to develop more accurate prediction formulae.

4.3.4.2 Secondary ship waves

Ships create transversal and longitudinal waves of which the interference peaks are called secondary waves. The interference peaks can be observed on lines making an angle of 19° with the vessel axis, their direction of propagation makes an angle of 35° with the axis of the ship (or 55° with the normal to the bank).

Fast-moving ships, for example container vessels, loose tugs or freighters that are not fully loaded, generate the most severe secondary waves H_i . Ship wave heights vary between 0.25 m and 0.5 m, with maximum values of H_i of about 1.0 m. The wave period T_i is 2–4 s. Fast ferries also generate ship waves, but their characteristics differ from those of other types of ship because fast ferries sail above the critical speed limit. The height of the waves (often called **wash**) generated by a fast ferry can be up to 1.0 m, particularly if it is accelerating or decelerating close to the critical speed. A typical wave period for fast ferry waves is 9 s.

The typical effect of secondary ship waves has some proven similarity with the effect of wind waves on rock structures (Section 5.2.2.2), so basic equations for wind waves can be applied. Formulae for predicting run-up for ship-induced waves are presented in Section 5.1.1.2.

The flow chart step (from Figure 4.83) to calculate secondary ship waves is outlined below. For previous calculation steps see Section 4.3.4.1.

8 Secondary ship waves, H_i , L_i and T_i

Characteristics of the largest secondary waves can be approximated (for $V_s/\sqrt{gh} < 0.8$) with Equations 4.184 to 4.186:

$$H_i = 1.2\alpha_i h (y_s/h)^{-1/3} V_s^4 / (gh)^2 \quad (4.184)$$

$$L_i = 4.2 V_s^2 / g \quad (4.185)$$

$$T_i = 5.1 V_s / g \quad (4.186)$$

where

- α_i = coefficient depending on the type of ship with the following recommended values:
- α_i = 1 for tugs and recreational craft and loaded conventional ships
- α_i = 0.35 for unloaded conventional ships
- α_i = 1 for unloaded push units.

4.3.4.3 Propeller jet velocities

Near-bed velocities in the propeller jets of the main propulsion system behind a ship might reach 6 m/s or even higher. Flow velocities in bow and stern thrusters can reach up to about 3 m/s. These flow velocities occur if the ship is manoeuvring, ie they are usually found in or next to locks, near quay walls, or in swinging basins (see Figure 4.86). The water velocities in the propeller jets of a sailing ship can be ignored for most situations.

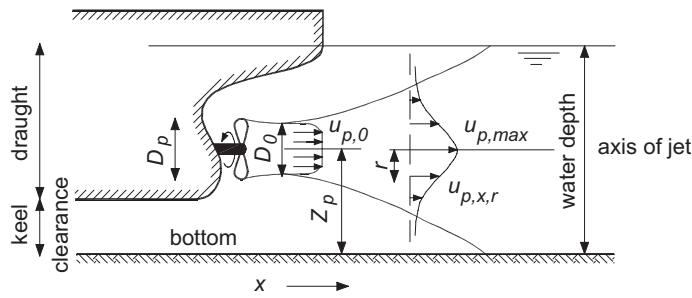


Figure 4.86 Water movements due to a main propeller

Equations 4.187 to 4.190 can be used to estimate the time-averaged current velocities in propeller jets caused by main propellers (see Figure 4.86, for ship speed $V_s = 0$ or otherwise relative to the ship when underway) or caused by bow or stern thrusters.

Velocity behind propeller (see Equation 4.187):

$$u_{p,0} = 1.15 \left(P / \rho_w D_0^2 \right)^{1/3} \quad (4.187)$$

Velocity along jet axis (see Equation 4.188):

$$u_{p,axis}(x) = a u_{p,0} (D_0/x)^m \quad (4.188)$$

Velocity distribution (see Equation 4.189):

$$u_p(x,r) = u_{p,axis}(x) \cdot \exp \left[-br^2/x^2 \right] \quad (4.189)$$

Maximum bed velocity along horizontal bed (see Equation 4.190):

$$u_{p,max bed} = c u_{p,0} (D_0/z_p)^n \quad (4.190)$$

where P = applied power (W), D_0 = effective diameter of propeller, $D_0 = 0.7$ (for free propellers without nozzle) to 1 (for propellers and thrusters in a nozzle) times the real diameter D_p (m), z_p = distance between the propeller axis and the bed (m).

A wide range of values for the empirical coefficients a , b , c , m and n in Equations 4.187 to 4.190 is available because different researchers have taken into account different influences such as the influence of a quay wall and the influence of a rudder. In addition to the approach presented below, reference is made to Fuehrer *et al* (1987), Römish (1993) and EAU (1996, 2004) where alternative values are presented. For more information, reference is also made to a special publication of the PIANC Working Group 48 (PIANC, in preparation).

In the Netherlands these coefficients are generally used for design, neglecting the influence of rudders and confinements with the following values: $m = n = 1$, $a = 2.8$ and $b = 15.4$, which results in $c = 0.3$ (Blaauw and Van der Kaa, 1978). In this approach the influence of lateral confinement by a quay wall in some cases is taken into account by increasing the velocity according to Equation 4.190 by 10–40 per cent. Blokland and Smedes (1996) measured a 40 per cent higher bottom velocity in the case of a jet that displays an angle of 16° with the quay wall.

In the case of a propeller jet perpendicular or oblique against a sloping embankment, the velocities above the embankment can be estimated using Equation 4.189. In fact, the velocities in the jet are influenced by the presence of the embankment. In PIANC (1997) this influence is neglected for practical purposes. Hamill *et al* (1996) found that the velocities above the embankment are delayed.

In the case of a propeller jet perpendicular to a quay wall (eg caused by bow or stern thrusters, see Figure 4.87) the current velocity above the bottom in front of the quay wall can be estimated using Equation 4.188 for the velocity along the axis of the propeller jet. Blokland and Smedes (1996) propose to use Equation 4.188 with $m = 1$, $a = 2.8$ and $x = \max(x_{pq} + z_p; 2.8 z_p)$, where x_{pq} = distance between propeller (or the end of the propeller duct) and quay wall. If the propeller or thruster is not close to the quay wall, $u_{p,bed}$ calculated by Equation 4.190 ($n = 1$) can be larger than $u_{p,axis}$ calculated by Equation 4.188 (see Figure 4.87).

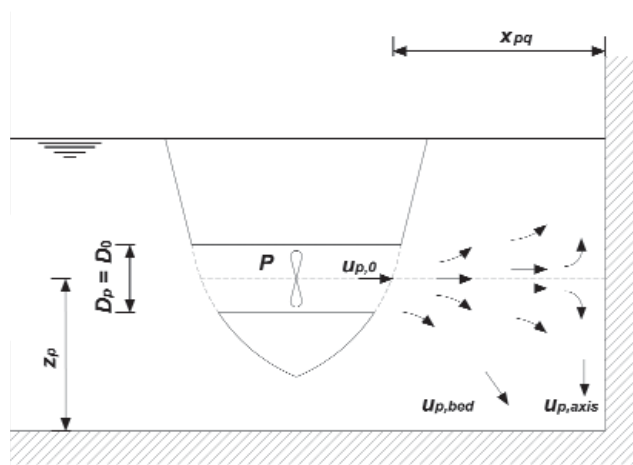


Figure 4.87 Flow field generated by a bow- or stern-thruster perpendicular to a quay wall

The calculated propeller jet velocities can be used with Equation 5.226 in Section 5.2.3.1 for the design of armourstone bed and slope protection against propeller jet attack. This equation includes a turbulence factor, k_t^2 (see also Section 4.3.2.5) to take into account turbulence levels, as the propeller jet velocities given by Equations 4.187 to 4.190 are time-averaged velocities and stability is determined by turbulent peak velocities.

Different values of the turbulence factor for propeller jets can be found in literature. It is important that the value for the turbulence factor is selected in combination with the value for the coefficient c in Equation 4.190 (and thus a , b and m). PIANC (1987) presents for the turbulence coefficient a value that can be converted into: $k_t^2 = 5.2$. Design experience has shown that this value for the turbulence coefficient together with $c = 0.3$ can be used for cases when vessels are often not fully loaded and the berthing position is not always the same. If the maximum impact of the propeller jet occurs frequently and always at the same place (ro-ro and ferry) a value of $k_t^2 = 6$ is recommended together with $c = 0.3$.

Very often the propeller diameter is not known. WL|Delft Hydraulics found an empirical relationship given by Equation 4.191 between propeller diameter D_p and installed engine power P (W) (see also PIANC currently in preparation for publication).

$$D_p = 0.0133P^{0.365} \quad (4.191)$$

This formula is valid for main propellers as well as bow and stern thrusters.

Finally, some modern twin-hulled ships, such as ferries, have high-powered water jets located at the water level. These jets generate much higher flow velocities, up to 25 m/s at the outflow orifice. Being at the water level, these jets hardly affect the bed material but may affect slopes or quay walls behind ships. Bed stability is at greater risk when the ship is sailing backwards. In this situation the jet is directed not just to the bow of the ship but also to the bed under an angle of about 30° with the horizontal. This may result in flow velocities near the bed of about 10 m/s. Protection against these high-powered water jets requires particular care during the design.

4.3.5 Modelling of water levels and currents

4.3.5.1 Modelling

Numerical models are essential tools to solve a set of mathematical equations for the variable(s) of interest. These equations are a schematic description of the underlying physical processes. In this section a short outline only is given on the possibilities of modelling the principal environmental conditions. See also Section 5.3, which focuses on hydraulic modelling and discusses modelling of hydraulic interactions rather than boundary conditions. In general, models are grouped with regards their dimensions, for example 1D, 2D or 3D. Further specifications are given by adding H, V or T (for horizontal, vertical and time, see Section 5.3).

Numerical (or mathematical) models can be made for simplified phenomena only because:

- the understanding of the processes involved is still limited and must be expressed by mathematical equations
- the computational costs should be acceptable.

The use of a **physical model** is also limited for the following reasons:

- the costs of model investigations limits the scale of investigation
- a sufficiently small model should be used with a time-scale that allows for testing within the time available for the total study
- the reduction in scale introduces scale effects.

Obviously, a mathematical model is not subject to scale effects, but it can only reproduce the phenomena included in the mathematical equations.

4.3.5.2 Numerical modelling of water levels and currents

1D flow models usually perform well for average currents in well-defined current systems with pronounced flow concentrations. However, in some cases 2D or 3D flow models are required. Selecting the right schematisation and computation is important to obtain realistic results.

The principal types of models for calculating depths of flow and velocities in rivers are:


- 2D current models, averaging flow over the depth at a particular point
- 1D current models, averaging flow over the entire cross-section
- hybrid models, coupling a 1D channel model with a storage reservoir model in the floodplain and calculating water exchanges between the main channel and the floodplain or within the floodplain itself.

Perhaps the most important factor to remember is to ensure that the implied boundary conditions (discharges, water levels) are correct. In particular, spatial variations (gradients) are critical when models are used to solve questions related to morphology. In general, boundary conditions involving water levels and/or discharges should be imposed sufficiently far from the structure to allow possible numerical disturbances to damp out before reaching the studied area. If this leads to an excessively large model, efficient use can be made of **nested models**. The principle of nested models is that boundary conditions for a small area model with a fine grid are provided by a larger, surrounding model, usually a 1D model. The first, coarse model does not necessarily contain the envisaged structure itself, which is only contained in the fine model.

In particular, where stone stability or sediment transport are concerned, the detailed model may be a physical model instead of a 2D or 3D mathematical model.

The following diagram (see Table 4.18) illustrates the approach adopted by engineers to simulate various processes and the types of models used.

Table 4.18 *Field of application of numerical models of simulation (CETE Méditerranée, 2003)*

Catchment area of concern	Subject of study	Appropriate model
Watershed  Ocean or sea	Water concentration in watershed outlets	Hydrological models
	Flows in steep valleys	1D models Torrential 1D models
	Main channel flooding	1D model
	Flooding storage area	Hybrid models, coupling a 1D channel model with a storage reservoir model in the floodplain
	Flows in floodplains where there are confluences, tributaries, hydraulic structures	2D or 3D models
	Flows in estuaries	1D model
	Phenomena of tides, wind and waves	Hybrid models 2D models

The area of concern and associated boundary conditions depends on the objective for the modelling. For example, an analysis of extreme loadings (water levels, waves) of a closure dam involves a large area, whereas for the final stage of construction, only local flow, stone stability and scour in the direct vicinity are important.

The expected flow velocities and in particular sediment transport (ie bed versus suspended load) mean that the objectives of the study may require more than one model, which then imposes the difficulties of providing a proper transition between the results and data transfer.

When flow and morphological models are used together the different time-scales of changes of flow and sea/river bed should be acknowledged. Principally, both extreme loadings, obtained from long-term statistics, and short-term loadings, for planning of construction, should be modelled.

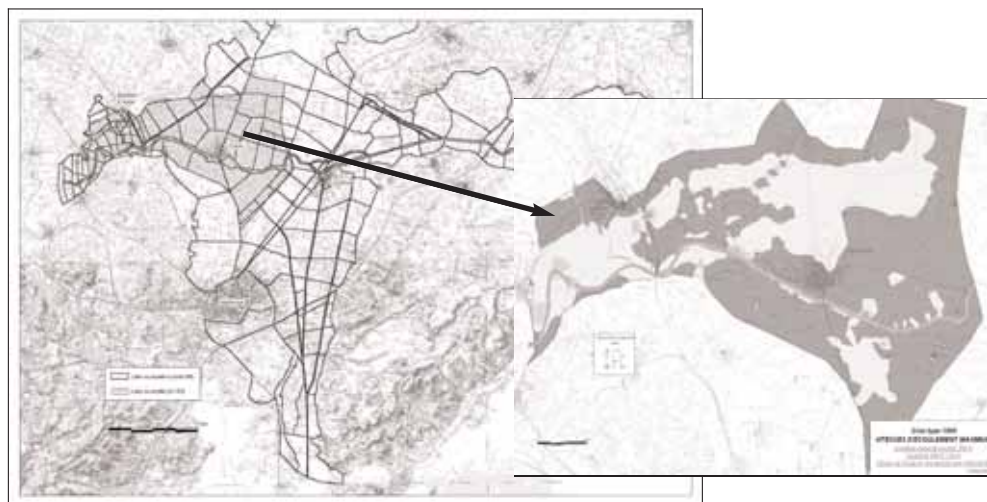


Figure 4.88 *Example of nested models: lower plains of the Aude river, France (CETE Méditerranée, 2003)*

An example is given in Figure 4.88, showing nested models applied for a study of the lower plains of the Aude (France).

It is difficult to represent the full dynamics of floodwaves with 1D models, since the flow direction remains related to the main channel direction. For generalised floods in the floodplain, the flow axis is directed by the floodplain slope and, as a consequence, is more braided. Hence for **small** floods (or intermediate flood between bankfull discharge and a whole-valley, generalised flood) 1D models are not really appropriate and should be used with caution where the river valley is not well confined.

Increasingly engineers are using 2D models to simulate flood waves. However these models require calibration of many coefficients, such as the roughness or the viscosity of the flow. 2DH current models require input of geometry and bathymetry as well as bed friction, especially in the floodplain, but also data on the nature and delimitation of the vegetation, culture or occupation of the floodplain. They also take into account very complex geometry and topography.

Where there are lateral levees, the topography induces overflows that fill the floodplain with flows disconnected from the main channel. It can even happen that the flows never join the main channel. To deal with these specific cases, 2D models can be too sophisticated. For this reason, hybrid models coupling 1D channel models and storage reservoir models in the floodplain have been developed. This kind of model represents the floodplain as a succession of storage reservoirs that are connected with each other or with the main channel of a river by hydraulic laws (relationships linking discharge and hydraulic head for a spillway or a levee for example). This reservoir representation should be used only in zones where velocities are negligible. Where the velocity field is complex and/or cannot be neglected, 2D models should be used.

An example of a 1D model is shown in Figure 4.89 and an example of a 2D model is shown in Figure 4.90.

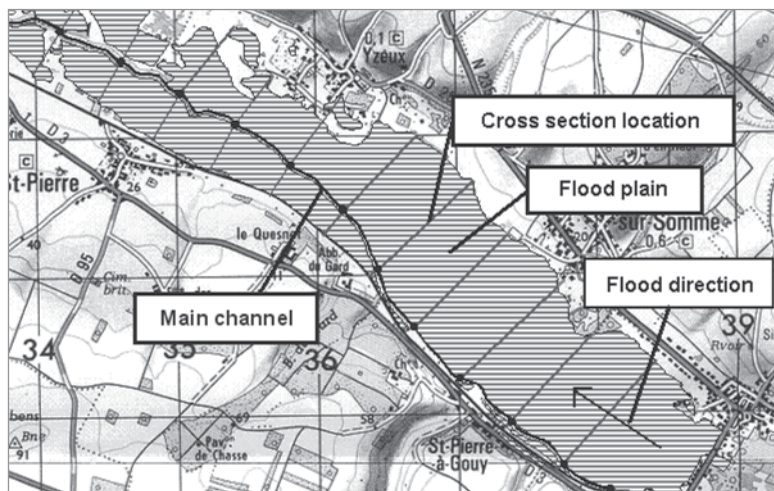


Figure 4.89 Example of application of a 1D river model: River Somme, France

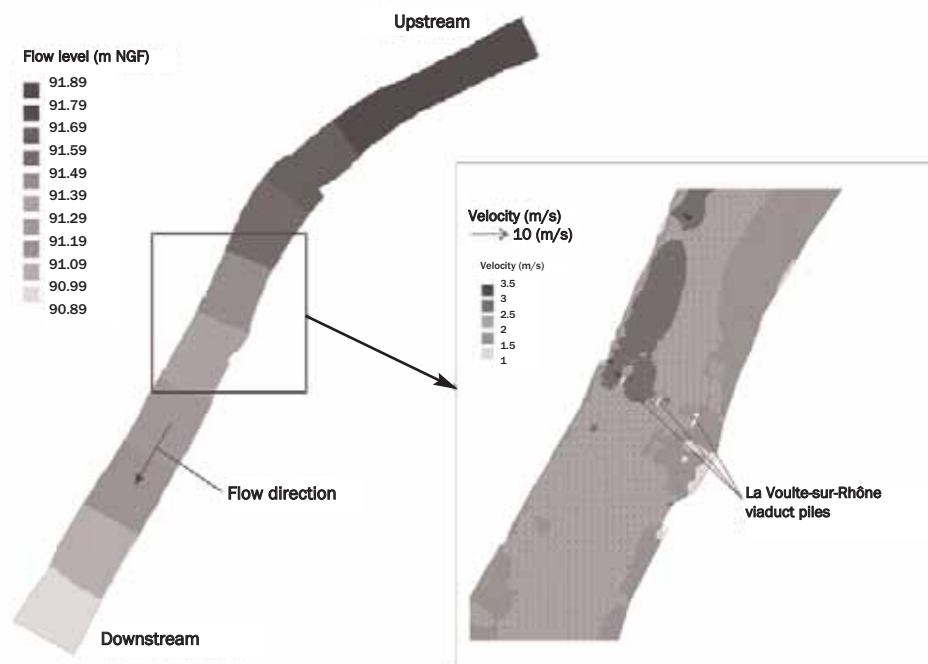


Figure 4.90 Example application of a 2DH flow model: La Vouite-sur-Rhône, France – depths of flow on the left, velocity distribution on the right

4.3.5.3

Physical modelling of water levels and currents

Physical modelling is an important option for complicated, usually 3D, current patterns. Despite their complexity, the boundary conditions for these patterns can be well reproduced in the laboratory. Typical cases are structures exposed to combined current and wave action, complex bathymetry, unconventional structure geometry etc.

Physical modelling can be particularly useful in a number of situations, such as where:

- interference of currents and waves is concerned (although numerical models are being developed to cover this situation; Yoo *et al.*, 1989)
- verification of, or comparison with, a numerical model is required
- a physical model can be built and operated at competitive cost in relation to other options.

Distorted models

In general, flow models have a fixed bed. In small-scale models the flow field and water levels are studied for present and future situations (see Figure 4.91). Mobile bed small-scale models are applied for studying the morphology of present and future situations. Note that overall (ie global) models and detailed models should be distinguished. Considering the costs and the required space, an overall model is usually distorted, ie the horizontal and vertical scales are different. This means that phenomena strongly related to the vertical distribution of the velocity cannot be investigated in such models (eg suspended sediment transport). Detailed models should be undistorted; to limit their size they usually cover only a limited area around the structure, for example of the estuary around the location of the closure gap. The models are usually run as steady-state models, reproducing the occurrence of maximum ebb and maximum flood current. Tidal models are however possible in principle. When modelling hydraulic structures, such as closure dams, weirs or barrages, an undistorted model is required since the water movement is 3D in nature at the structures. The models should be at a sufficiently large scale to avoid viscosity effects.

In general, the scale factor n_x of a parameter is defined as the ratio $n_x = X_p/X_m$, where X_p is the X -values in reality and X_m is the X -values in the model. Thus scale factors n_L , n_h , n_C and n_{Fr} can be defined for length, depth, roughness and Froude number respectively. A correct small-scale model with a fixed bed to model the free water surface flow should satisfy the following scale requirements:

- a sufficient degree of turbulence should be present in the model (Reynolds number, $Re \gg 2300$)
- the ratio between kinetic and potential energy in the model should be equal to the real one, which results in a similar Froude number in the scale model and in reality, $n_{Fr} = 1$
- the flow field in the scale model and in reality must be similar. This results in a bed roughness condition for the scale model, $n_{C2} = n_L/n_h = 1$ in the case of undistorted models.

If the morphology also needs to be studied in the model, then a mobile bed model is needed that complies with the following requirements:

- bed material particles in the small-scale model should follow the same track as in reality. This leads to an undistorted scale model (horizontal scale equals vertical scale), $n_L = n_h$
- the same degree of non-linearity of the sediment transport should be present in the model as in reality. This results in a scale condition for the flow velocity in a mobile bed model. The scale condition for a model with a mobile bed overrules the Froude condition, ie in that case $n_{Fr} \neq 1$ (but does not differ considerably from 1).

Imposing more than one scale condition at the same time, for example a Froude and a Reynolds condition, forces a compromise. It means that it is unavoidable to deviate, to a certain degree, from one or more of the scale requirements. In principle this leads to scale effects, which can deceive the designer unless there are proper insights into the magnitude and direction of these scale effects. To maximise the reliability of the scale model, assessment of scale effects can further be supported by a proper mathematical description of the flow problem considered or by a scale series, followed by comparison of results. Sensitivity analysis to scale effects can then be obtained by applying different scale factors.



Figure 4.91 Example of a physical model of a river with mobile bed

When physical modelling is problematic, problems often relate to scale effects arising when the principal forces within the process are not properly scaled. Most flow and wave models are organised to scale the dominant gravity forces properly, represented by the Froude number, $U_c / \sqrt{g/L_c}$, where U_c and L_c are characteristic velocities and dimensions respectively. Where there are conflicts with other forces (eg friction forces represented by the Reynolds number, $U_c L_c / \nu$, where ν = kinematic viscosity), adjustments are made accordingly, eg by providing additional corrective friction elements in the case of Reynolds number problems.

4.3.5.4 **Hybrid modelling of water levels and currents**

The above paragraphs describe the principal solution methods and some of their advantages and disadvantages. Common practice has been to use several modelling methods jointly, with each method being applied to the relevant portion of the study. For example, field data are usually used to define the most important processes and to verify a model that predicts hydrodynamic or sedimentation conditions in the river. Combining physical modelling with numerical modelling is referred to as **hybrid modelling**. Combining them in a closely coupled fashion that permits feedback among the models is referred to as an **integrated hybrid solution**. By devising means to integrate several methods, the modeller can include effects of many phenomena that otherwise would be neglected or poorly modelled, thus improving the reliability and detail of the results.

4.4 **GEOTECHNICAL INVESTIGATIONS AND DATA COLLECTION**

This section gives an outline of the objectives, the organisation and the technical requirements of geotechnical data collection. It does not describe in detail the various test methods, but focuses on the requirement for geotechnical investigations to provide information required at the different stages of the design (see Section 2.2). Further references are given in Section 4.4.4, which describes standard methods for geotechnical investigations and testing techniques. Eurocodes and standards from several countries are also listed there.

Depending on their use, hydraulic structures have to withstand different combinations of actions, eg those induced by gravity, waves, currents, differences in water levels, seismicity, ship collisions and ice forces. The structure should be designed to resist these actions in both serviceability limit state (SLS) and ultimate limit state (ULS) conditions (see Section 5.4). Investigations are needed to establish the geotechnical conditions at the site before conception, dimensioning and justification of the structure, these different standard steps being defined in the Eurocodes. The flow chart in Figure 4.92 shows the various steps of the geotechnical investigation and their links to other sections of this manual.

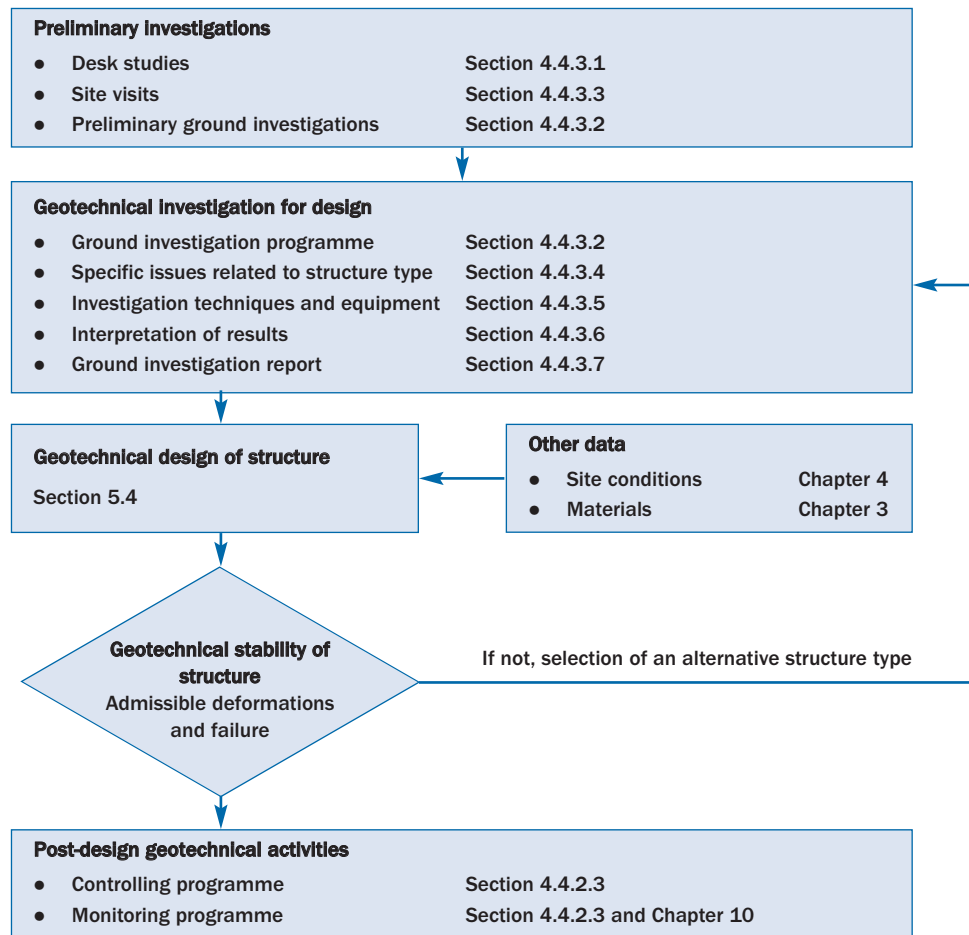


Figure 4.92 Flow chart of geotechnical investigations in the design process

4.4.1 Objectives of geotechnical investigations

Geotechnical investigations should provide the information and data at the various stages of the project that are needed to:

- identify and evaluate the project hazards
- facilitate the design, dimensioning and justification of the structure – the latter can be carried out by calculations, physical modelling or *in situ* load tests (see Section 5.4)
- check the adequacy of the project assumptions with the actual ground conditions.

Geotechnical investigations aim to establish a consistent geotechnical model of the site including the geometry of soil and rock formations, their physical and mechanical properties, and the groundwater conditions. They can also provide additional information about the site, such as geology, geomorphology, seismicity, hydrology and hydrogeology.

4.4.2 Procedures for geotechnical investigations

Geotechnical investigations should normally be performed in phases depending on the questions raised during project planning, design and construction. The following successive phases are discussed separately in this section:

- preliminary investigations
- detailed design investigations
- controlling and monitoring

The premise applies that the results from one phase are available for the next one. In cases

where preliminary and design investigations are performed at the same time, the corresponding provisions should be adapted. Additional investigations may be needed within each of the above phases, if (a) unexpected soil features are encountered, (b) the position of the structure is revised, (c) a new foundation type is introduced, requiring specific soil parameters.

Further reducing the uncertainties about the ground, soils and rocks will help improve the economy of the design or maintenance.

4.4.2.1 Preliminary geotechnical investigations

The preliminary investigations should provide the information needed to:

- assess the general suitability of the site including its overall stability
- assess the suitability of the site in comparison with alternative sites, as relevant
- indicate the most appropriate position for the structure
- evaluate the possible effects of the proposed works on the surroundings, eg neighbouring buildings, structures and sites
- identify borrow areas
- consider the possible foundation methods and ground improvement techniques
- plan the design and control investigations, including identifying the extent of ground that may have a significant influence on the structure's behaviour.

For this purpose, information and estimates of data are needed on:

- the types of soils or rocks and their stratification or structure
- the groundwater table or pore pressure profile
- the strength and deformation properties of soils and rocks
- the potential occurrence of contaminated ground or groundwater that might be hazardous to health or the durability of the structure.

The programme of geotechnical investigations generally consists of:

- a site visit
- desk studies
- ground investigations, such as geophysical measurements, a limited number of drillings, excavations, field tests and laboratory tests.

4.4.2.2 Geotechnical investigations for design

Design investigations should be carried out to:

- provide the information required for an adequate design of the temporary and permanent works
- provide the information required to plan the method of construction
- identify any difficulties that may arise during construction
- and finally select the optimum design, construction and maintenance alternative.

The geometry, structure and properties of all ground relevant to or affected by the proposed structure should be identified in a reliable way before the start of the final design. The following features should be considered:

- ground profile
- natural or man-made cavities
- degradation of the ground (soil) or construction materials (fill materials)

- hydrogeological effects
- faults, joints and other discontinuities
- creeping soil and rock masses
- expansible and collapsible soils and rocks
- presence of waste or man-made materials
- history of the site and its surroundings.

The programme should provide adequate information and characteristic values of data and consist, if relevant, of additional:

- site visits
- desk studies
- ground investigations, such as field testing, soil and rock sampling and laboratory testing, groundwater measurements, additional geophysical investigations and large-scale tests as further described in Section 4.4.3.4.

4.4.2.3 **Controlling and monitoring**

During construction works, and after the completion of the project, investigations and measurements should be performed, and are known as controlling and monitoring respectively. They should check that:

- the design assumptions are in accordance with the actual ground conditions
- the quantities and properties of delivered construction materials correspond to those planned in the design
- the construction works are executed according to the project specifications
- the structure and its surroundings behave as expected.

For this purpose, the following should be determined:

- quantities of delivered and placed materials
- deformations of the ground affected by the structure
- pore-water pressures
- displacements of the structure, such as vertical or horizontal movements, rotations.

Particular attention should be paid to critical parts of the structure or its surroundings.

The programme should incorporate additional checks and tests, such as:

- verification of ground profile when excavating
- inspection of the bottom floor of the excavation
- measurements of groundwater levels or pore-water pressures and their fluctuations
- measurements of the behaviour of neighbouring structures, services or civil engineering works
- measurements of the behaviour of the structure during construction.

If relevant (see Section 10.2), the monitoring should be continued after completion of the construction works.

4.4.3 Key elements of geotechnical investigations

4.4.3.1 Desk studies

Desk studies are based on existing information, which has to be identified, gathered and analysed. Usual sources of information are:

- local maps provided by public organisations
- topographic and bathymetric maps, including old maps describing the previous use of the site
- geological, seismic, hydrological, geotechnical maps and associated booklets
- aerial and satellite photographs and geophysical investigations, including existing interpretations
- previous investigations at the site and its surrounding area, including all published data
- experience from previous projects in the area, including historical geotechnical failures
- local climatic conditions.

Desk studies should be performed before designing the ground investigation programme and may need additional developments during the period of geotechnical investigations.

4.4.3.2 Ground Investigations

General features of ground investigations

Ground investigations are used to determine the anticipated type, dimensions, location (offshore, nearshore or onshore) and construction methods of the structure. Special attention should be paid to sites that have been previously used, where disturbance of the natural ground conditions may have taken place such as for structure upgrading or repair.

Ground investigations should consist of both field investigations and laboratory testing, including, as relevant:

- geophysical investigations such as echosounding, side-scan sonar imaging, sub-bottom profiling, seismic refraction profiling, ground penetrating radar, resistivity measurements and down-hole logging
- field testing, such as the cone penetration test (CPT), cone penetration test with pore pressure measurement (CPTU), standard penetration test (SPT), dynamic probing, pressuremeter test (PMT), flat dilatometer test (DMT), plate load test, field vane test (FVT) and permeability test
- soil and rock sampling by means of drilling, coring and excavation for description and laboratory tests of the soils or rocks
- groundwater measurements to determine the groundwater tables or the pore pressure profiles and their fluctuations
- *in situ* loading tests, for example to determine the bearing capacity or the behaviour directly on prototype elements.

Ground investigation programme

The ground investigation programme is based on the:

- conclusions of desk studies
- observations made during site visits
- type(s) of structure and the parameters needed for design

- stage of the project
- skills, facilities and opportunities available for investigations and the corresponding costs.

The ground investigation programme should contain:

- a plan with all field investigations
- the type, number and depth of each investigation
- the type, number and depth of samples to be taken
- the type, number and depth of laboratory tests
- the type, number and depth of the groundwater measurements
- the standards to apply
- the types of equipment to be used, if relevant.

The ground investigation programme should be reviewed as the results become available. In particular, the location, type, density and depth of investigations should be modified as required to account for the complexity, variability and unexpected features of the ground at the site. If necessary, additional testing may be specified.

The choice of the types of tests and sampling procedures depends on the expected type of ground at the site under study. Different procedures are used in soils and in rocks, in soft soils and in firmer soils and also with land-based and waterborne investigations. In addition, local experience may influence the choice of the test results used for design (see Box 4.15 and Box 4.16). Indications on the suitability of field and laboratory tests and sampling procedures are given in Table 4.19. The reader could refer to Part 2 of Eurocode 7 for further information. Where underground cavities may occur, appropriate geophysical methods may be used (Fauchard and Potherat, 2004). Details about investigation methodology for longitudinal river dikes and bank protections are given in Lino *et al* (2000). Fauchard and Mériaux (2004) provide details and comparison about investigations for these structures.

French standard NF P 94-500 describes different typical geotechnical investigations or studies and specifies their content.

1

2

3

4

5

6

7

8

9

10

Table 4.19 In situ test methods and their perceived applicability (after Robertson and Campanella, 1983)

Soil parameter	Geophysical methods					Field tests					Borings			
	S	ER	EM	N		CPT	CPTU	SPT	FVT	PMT	DMT	Dist	Undist	Monit
Soil profile	C/B	C/B	C/B	-		A	A	A	B	B	A	A	A	-
Classification	-	-	-	-		B	B	B	B	B	B	A	A	-
Water content	-	-	-	-		-	-	-	-	-	-	A	A	-
Pore water pressure	-	-	-	-		-	A	-	-	B/C	-	-	-	A
Permeability	-	-	-	-		-	B	-	-	B	-	C	A	B/C
Dry/wet density	-	-	-	A		C	C	C	-	-	-	C	A	-
Density index	-	-	-	-		B	B	B	-	C	C	-	A	-
Angle of internal friction	-	-	-	-		B/C	B/C	B/C	C	C	C	-	A	-
Undrained shear strength	-	-	-	-		B	B	C	A	B	B	-	A	-
Compressibility	-	-	-	-		B/C	B/C	-	-	C	C	-	A	-
Rate of consolidation	-	-	-	-		-	A	-	-	C	-	-	A	C
Creep settlement	-	-	-	-		-	-	-	-	-	-	-	A	-
Elasticity modulus	A	-	-	-		B	B	B/C	A/B	B	B	-	A	-
In situ stress	-	-	-	-		C	C	-	C	B	B	-	A	-
Stress history	-	-	-	-		C	C	C	B	B	B	-	A	-
Stress/strain curve	-	-	-	-		-	C	-	B	B	C	-	A	-
Liquefaction susceptibility	-	-	-	-		A/B	A/B	A/B	-	-	-	-	A	-
Ground conditions														
Hard rock	A	-	A	A		-	-	-	-	A	-	A	A	C
Soft rock, till etc	A	-	A	A		C	C	C	-	A	C	A	A	A
Gravel	A	B	A	A		B/C	B/C	B	-	B	-	A	C	A
Sand	A	A	A	A		A	A	A	-	B	A	A	A	A
Silt	A	A	A	A		A	A	A/B	B	B	A	A	A	A
Clay	A	A	A	A		A	A	C	A	A	A	A	A	A
Peat-organics	C	A	A	A		A	A	C	B	B	A	A	A	A

Abbreviation of geophysical methods
 S Seismic
 ER Electrical resistivity
 EM Electro-magnetic
 N Nuclear

Abbreviation of field test

CPT Cone penetration test
 CPTU Cone penetration test with pore pressure measurement
 SPT Standard penetration test
 FVT Field vane test
 PMT Pressuremeter test
 DMT Flat dilatometer test

Abbreviation of boring types

Dist Disturbed sampling
 Undist Undisturbed sampling
 Monit Monitoring wells

Ranking of applicability

A High
 B Moderate
 C Limited
 - If no ranking is given, the method is not suitable.

Density and depth of ground investigations

The extent of the zone of influence of common structures is known for homogeneous conditions and rules are given in the technical literature. Some of them are presented below. For unusual structure types or geometries, the extent of the zone of influence should be assessed before the ground investigation programme is defined. For hydraulic problems, the zone of influence may be much larger than for stability or settlement analysis. This should be accounted for in the ground investigation programme and in the design.

Most of the structures covered in the manual are linear and therefore their zone of influence is band-shaped and is subjected to settlement, differential settlement, lateral and head slope instability and bearing capacity problems. Consequently, investigations should be located both along the axis and on the sides of that band.

Strategies of ground investigations are based on two sets of rules:

- rules based on the influence of a given structure in homogeneous water and ground conditions
- rules aimed at checking the homogeneity *versus* variability of the investigated site.

The density and depth of ground investigations thus depend on expected geotechnical structure and natural variability of the ground. For example, deltaic deposits are expected to display greater variability than homogeneous layers of lacustrine or marine clays.

A larger number of investigations at smaller spacing is required around discontinuities found in the ground.

Typical spacings for ground investigations are given in Table 4.20. They depend on the stage of geotechnical investigations (preliminary or design investigations), on the expected geotechnical conditions, on the information required for design and on the cost and duration of each type of test. Geophysical surveys, static and dynamic cone penetration tests, standard penetration tests and destructive borings are usually chosen to obtain a general view of the ground types and thicknesses. The values of the geotechnical parameters used for design are then obtained from more expensive and time-consuming intact sampling and laboratory tests and from correlations with field test results.

Indicative depths of investigation (below the lowest point of the foundation or excavation base excavation) are given in Table 4.21 and may be used as guidance.

1

2

3

4

5

6

7

8

9

10

Table 4.20 Tentative rules for the location and density of ground investigations

Type of test or technique	Site with homogeneous ground conditions	Site with heterogeneous ground conditions
Preliminary site investigations		
Geophysical surveys	Along project axis	Along axis and on both sides
Rapid tests (CPT, CPTU, DPT, SPT, destructive boring)	At 100 m intervals on the axis (minimum 2)	At 30 m intervals alternatively on the axis and on the sides
Intact sampling and laboratory tests	At 300 m intervals on the axis (minimum 1)	At 300 m intervals on the axis (minimum 1)
Other tests (PMT, FVT etc)	None	None
Groundwater measurements	Depending on the site	Depending on the site
Detailed site investigations		
Geophysical surveys	None	None except for specific needs
Rapid tests (CPT, CPTU, DPT, SPT, destructive boring)	At 50 m intervals on the axis and on both sides	At 20 m intervals on the axis and on both sides
Intact sampling and laboratory tests	At 100 m intervals on the axis	At 50 m intervals on the axis
Other tests (PMT, FVT etc)	Depending on the type of structure	Depending on the type of structure
Groundwater measurements	Depending on the site	Depending on the site

Notes

- 1 The number of locations for ground investigations may be reduced in difficult marine environments.
- 2 CPT: cone penetration test; CPTU: cone penetration test with pore pressure measurement; DPT: dynamic cone penetration test (see Eurocode 7-part 2); SPT: standard penetration test; PMT: pressuremeter test; FVT: field vane test.

Table 4.21 Suggested values of the investigation depth below the structure under study

Expected ground conditions	Investigation depth	Comments
Homogeneous rock strata	2 m	<ul style="list-style-type: none"> • In rocks where cavities may be expected, the investigation depth should be increased.
Indistinct rock formations	5 m	<ul style="list-style-type: none"> • Where cavities may be expected and if soluble rocks are present, the investigation depth should be increased. Some boreholes should be taken down to a minimum depth equal to the width of the structure footprint.
Homogeneous soil deposits	max (5 m; 1.5 <i>b</i>)	<ul style="list-style-type: none"> • At least one borehole should be taken down to the rock substratum when possible. • For soft soils, the investigation depth should be increased to reach the bottom of the weak deposit or to the depth below which the soil has no more significant influence on foundation behaviour. • If the rock substratum is reached, it should be investigated as suggested above.
Indistinct soil deposits	max (5 m; 1.5 <i>b</i>)	<ul style="list-style-type: none"> • At least one borehole should be taken down to the rock substratum when possible. • For soft soils, the investigation depth should be increased to reach the bottom of the deepest weak deposit or to the depth below which the soil has no more significant influence on foundation behaviour. • If the rock substratum is reached, it should be investigated as suggested above. • Greater investigation depths should always be selected where unfavourable geological conditions, such as weak or compressible strata below strata of higher bearing capacity, are presumed.

Note

b is the width of the structure footprint (m).

Box 4.15 Example of ground investigation programme for a breakwater

The Port 2000 project aims at providing the city of Le Havre with new port facilities and notably includes construction of a breakwater in the estuary of River Seine.

Different geophysical methods were used prior to field penetration tests. Figure 4.93 shows the layout and types of geophysical measures, field tests and borings performed. The results of ground investigation were used for breakwater design and construction, for dredging of the channel and for design and construction of the quay wall.

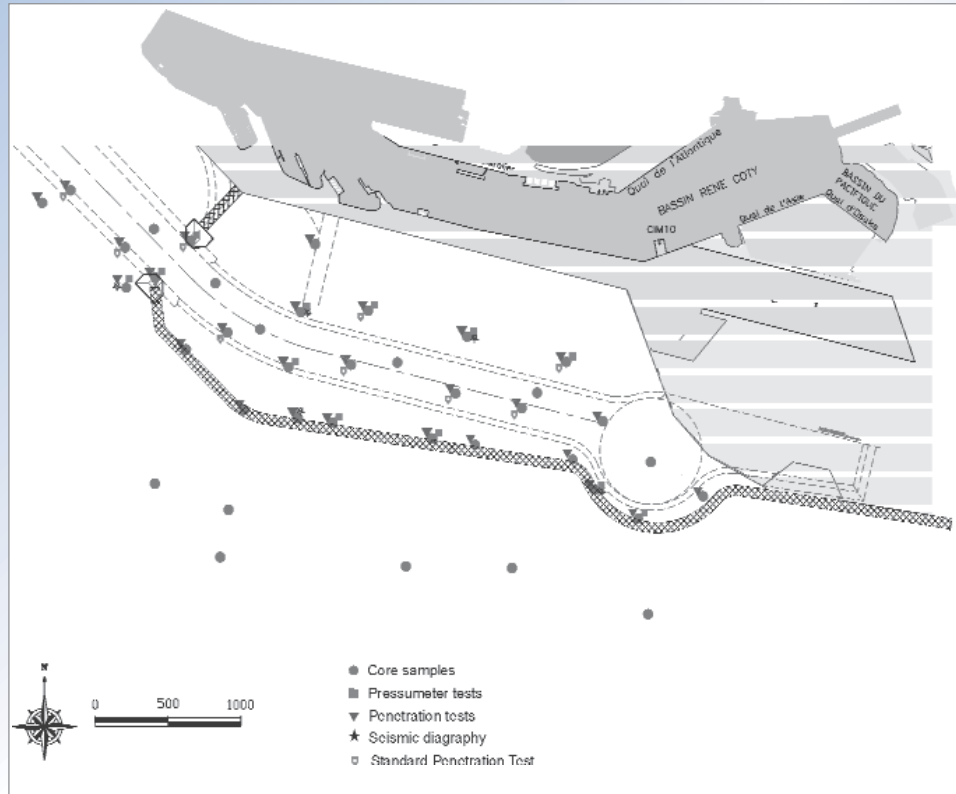


Figure 4.93 Layout of geophysical and field tests and borings, Le Havre, France

Box 4.16 Example of ground investigation for an inland waterway project

For this project, the riverbanks had to be modified (new cross-section and protection by armourstone) to create parking areas, playgrounds and to allow navigation of small boats. Figure 4.94 shows the layout of the *in situ* tests performed.

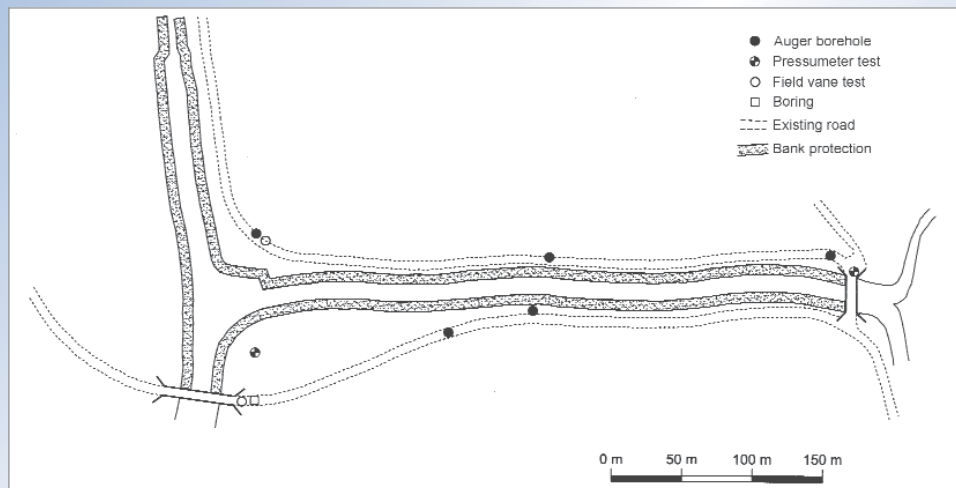


Figure 4.94 Layout of the field tests: inland waterway project in the west of France

4.4.3.3 Site visit

No geotechnical investigations should be planned or performed without a site visit.

A site visit will provide a general impression of the site including its history, topography, geology and hydrogeology, the local climatic conditions, the state of existing infrastructure, the natural hazards affecting the area, accessibility, potential borrow areas etc. Visits in different kinds of weather will provide useful information on the range of conditions at the site. Photographs should be taken during the visit and included in the site visit report, which should form part of the geotechnical investigation report. Lino *et al* (2000) also provide information about visual inspection of river dikes that can be easily extended to riverbanks.

4.4.3.4 Specific issues related to structure types

Table 4.22 gives additional information on the specific requirements of investigations related to structure types and site conditions.

Table 4.22 Investigation requirements for structures covered in this manual

Type of structure	Investigation requirements for structure design	Constraints and requirements related to site conditions
Marine structures		
Breakwaters	<ul style="list-style-type: none"> • Crown structures and rock revetments need particular attention with regard to settlement • Stability of slopes and soil under the structure need to be checked • Attention should be paid to behaviour of structures and soil materials under cyclic loads • Erosion of soil near the structure can cause damage or failure (eg slope failure, sliding of armour layer, foundation instability) • Particular attention should be paid to erosion near roundheads 	<ul style="list-style-type: none"> • Presence of materials sensitive to erosion in foundation layers • Investigation equipment is waterborne: investigation period is highly dependent on tide, wave and maritime traffic conditions • Investigation needs to be undertaken beneath and on both sides of the projected structure
Seawalls and shoreline protection	<ul style="list-style-type: none"> • Rock revetments need particular attention with regard to settlement • Stability of slopes and soil under the structure needs to be checked • When used as retaining wall characteristics of retained soils and foundation soil need to be determined • Erosion of beach/soils on the exposed part of the structure can cause damage or failure in structures (eg collapse of rock revetment toe) 	<ul style="list-style-type: none"> • Presence of materials sensitive to erosion in front of the structure • Access to site location may be limited by tides and weather • Foreshore condition (eg soft material) may require that investigation is undertaken from floating plant. • Access to site may be limited due to environmental considerations (eg nesting birds) • Access to site may be limited by navigation (eg existing moorings)
Groynes	<ul style="list-style-type: none"> • Rock groynes require consideration of settlement along their longitudinal axis • Erosion along the structure especially near the extremity of structures 	<ul style="list-style-type: none"> • Same as seawalls and shoreline protection

Table 4.22 Investigation requirements for structures covered in this manual (contd)

Type of structure	Investigation requirements for structure design	Constraints and requirements related to site conditions
Closure works		
Closure dams	<i>During closure operation:</i> <ul style="list-style-type: none"> Scouring processes in closure gap 	<ul style="list-style-type: none"> Material composition of the top layers down to the expected depth of the scour hole Investigate the presence of cohesive layers Investigation should not only cover the closure gap, but also the end of the bed protection
	<i>Final situation after closure:</i> <ul style="list-style-type: none"> Settlement of the subsoil Piping processes under structure 	<ul style="list-style-type: none"> Presence of soft layers, compressibility of the material Presence of granular material, permeability of this material Presence of impermeable horizontal layers at greater depth
Reservoir dams	<ul style="list-style-type: none"> Settlement of the subsoil Piping processes under structure 	<ul style="list-style-type: none"> Same as closure dams, final situation after closure
Inland waterways structures		
Groynes	<ul style="list-style-type: none"> Scour holes along the structure and especially near the structure head 	<ul style="list-style-type: none"> Presence of layers sensitive to erosion in the river bed Investigations need to be undertaken perpendicular to the axis of river, waterborne investigation equipment needed Investigation period highly dependent on river level and discharge, boat traffic conditions, environmental considerations
Longitudinal dikes	<ul style="list-style-type: none"> Scour holes and riverbed erosion Settlement of the subsoil and piping processes under the structure Slope failure in case of rapid or accidental drawing-off 	<ul style="list-style-type: none"> Presence of layers sensitive to erosion in the river bed Investigations should be undertaken beneath and on both sides of the dike, waterborne investigation equipment needed for rivers and existing channels. Same as groynes for waterborne investigation period For investigation period on ground, environmental conditions and access conditions (eg presence of road) should be considered For piping processes, same as reservoir dams
Bank protections	<ul style="list-style-type: none"> Scour holes or erosion of the river bed can cause sliding of the revetment or damage to the lower parts of bank protection Slope failure in the case of rapid or accidental drawdown 	<ul style="list-style-type: none"> Presence of layers sensitive to erosion in the river bed Investigations should be undertaken in the river bed and beneath the banks, waterborne investigation equipment needed for investigations in river bed. Same as groynes and longitudinal dikes for investigation period

4.4.3.5 *Investigation techniques and equipment*

Most of the techniques used for geotechnical investigations of hydraulic structures are common to all types of geotechnical studies and are described in handbooks, recommendations and standards. The reader should refer to this literature to obtain technical information on these investigation techniques and the corresponding equipment. Some reference publications in this field are listed in Section 4.4.4.

Over-water investigations require special equipment such as a survey vessel, an anchored barge, a drilling rig or a jack-up platform. The choice largely depends on the water depth, tidal variation, waves, currents and the local availability of equipment and experience. The choice has, in turn, a large influence on the optimal combination of geotechnical investigation techniques. The operational costs of such equipment often form the major part of the total investigation costs. More information about over-water investigations can be found in ISSMGE-TC1 (2005).

4.4.3.6 *Interpretation of results*

Interpretation of ground investigation results requires a thorough knowledge of the equipment used to collect the information, the way soil samples are handled, and experience with such equipment and handling techniques. Geological expertise is often indispensable for estimating the layering and understanding the background of relevant soil properties.

4.4.3.7 *Ground investigation report*

This document contains the information used for the geotechnical design of the structure (see Section 5.4). It consists of a presentation of all available geotechnical information including geological features with relevant data and a geotechnical evaluation of the information, stating the assumptions made in the interpretation of test results.

The presentation of geotechnical information should include a factual account of all field and laboratory work, and documentation on the methods used to carry out the field investigations and laboratory testing.

The presentation of geotechnical information should also include the following elements:

- names of consultants and subcontractors
- purpose and scope of the geotechnical investigation
- history of the site, geology of the site including faulting, interpretation of aerial photographs, local experience of the area, seismicity of the area
- procedure used for sampling, transportation and storage of samples; type of field equipment used
- tabulation of quantities of field and laboratory work
- compilation of boring logs including photographs of the cores, description of the subsurface based on field descriptions
- dates of the ground investigation operations
- field reconnaissance on the general area, noting particularly behaviour of neighbouring structures, exposures in quarries and borrow areas, areas of instability and difficulties during excavation.

4.4.4 *References and standards*

The section below presents a selection of handbooks and papers, recommendations and standards for further reading.

Handbooks and papers

Dunnicliff, J (1994). *Geotechnical instrumentation for monitoring field performance*. John Wiley & Sons Inc, New York, 608 pp

Hawkins, A B *et al* (eds) (1985). *Site investigations practice*. Proc 20th Reg Mtg Eng Group Geol Soc

Power, P T and Paysly, J M (1986). "The collection, interpretation and presentation of geotechnical data for marine pipeline projects". *Oceanology*. Graham and Tratman, London, pp 301–4

Van den Berg, H J (1987). "In-situ testing of soils". In: F G Bell (ed), *Ground engineering reference book*, Ch 25. Butterworth, London

Van den Berg, H J (1987). "Laboratory testing of soils". In: F G Bell (ed), *Ground engineering reference book*, Ch 20. Butterworth, London

Recommendations

US Corps of Engineers. Engineer Manuals (EM):

EM 1110-1-1804 *Geotechnical investigation*, Jan 2001

EM 1110-1-1802 *Geophysical exploration for engineering and environmental investigations*, Aug 1995

EM 1110-2-1906 *Laboratory soils testing*, Aug 1986

EM 1110-2-1907 *Soil sampling*, 1972

ISSMGE-TC1 (2005). "Geotechnical investigations for offshore and nearshore developments" <www.issmge.org> - Technical committees - TC1

Eurocodes

Eurocode 7 Geotechnical design (EN 1997-1 and EN 1997-2). Idem, Part 2: Design assisted by laboratory and field tests. CDoc.N368, Dec 2002.

European standards

EN ISO 22475 *Drilling and sampling methods and groundwater measurements* (in preparation)

EN ISO 22476-1 *Cone penetration tests* (in preparation)

EN ISO 22476-2 *Dynamic probing* (in preparation)

EN ISO 22476-3 *Standard penetration test* (in preparation)

EN ISO 22476-4 *Menard pressuremeter test* (in preparation)

EN ISO 22476-5 *Flexible dilatometer test* (in preparation)

EN ISO 22476-6 *Self-boring pressuremeter test* (in preparation)

EN ISO 22476-7 *Borehole jack test* (in preparation)

EN ISO 22476-8 *Full displacement pressuremeter test* (in preparation)

EN ISO 22476-9 *Field vane test* (in preparation)

EN ISO 22476-10 *Weight sounding test* (in preparation)

EN ISO 22476-11 *Flat dilatometer test* (in preparation)

EN ISO 22476-12 *Lefranc water test*

EN ISO 22476-13 *Lugeon water test*

EN ISO 22476-14 *Pumping test*

CEN TS 17892-1 *Water content*

CEN TS17892-2 *Density of fine grained soil*

CEN TS17892-3 *Density of solid particles*

CEN TS17892-4 *Particle size distribution*

CEN TS17892-5 *Incremental loading oedometer test*

CEN TS17892-6 *Fall cone test*

CEN TS 17892-7 *Unconfined compression test*

CEN TS 17892-8 *Unconsolidated undrained triaxial test*

CEN TS 17892-9 *Consolidated triaxial compression tests*

CEN TS 17892-10 *Direct shear tests*

CEN TS 17892-11 *Permeability tests*

CEN TS 17892-12 *Determination of the Atterberg's limit*

US standards

ASTM (2002). "Soil and rock" (1). *Annual Book of ASTM*, vol 04.08, D420-D5779

British standards

BS 5930:1990 *Code of practice for site investigation*

BS 1377:1990 *Methods of tests for soil for civil engineering purposes*

Dutch standards

NEN 3680, 5106, 5107, 5108, 5119 and 5120. *Normen voor terreinproeven*

NEN 5117 and 5118. *Normen voor laboratoriumproeven*

French standards

NF P 94-500 *Geotechnical missions – classifications and specifications*. Provides elements about different types of geotechnical investigations missions and specifications on the content of these missions

NF P 94-040 and NF P 94-041 *Determination of particle size and blue value of 0/50 mm soils*

NF P 94-049 and NF P 94-050 *Determination of the water content on a mass basis*

NF P 94-051 and NF P 94-052 *Determination of Atterberg's limits*

NF P 94-053, NF P 94-054, NF P 94-059 and NF P 94-064 *Determination of soils density*

NF P 94-055 and NF P 94-056 *Granulometric analysis*

NF P 94-068 *Determination of methylene blue absorption of a rocky soil*

NF P 94-070 and NF P 94-074 *Shear strength test with triaxial test apparatus*

NF P 94-071 *Direct shear test with shear box apparatus*

NF P 94-072 *Laboratory vane test*

NF P 94-077 *Uniaxial compression test*

NF P 94-061 and NF P 94-062 *In situ determination of soil density*

NF P 94-110 *Menard pressuremeter test*

NF P 94-112 *Field vane test*

NF P 94-113 *Cone penetration test*

NF P 94-114 and NF P 94-115 *Dynamic penetration test*

NF P 94-116 *Standard penetration test*

NF P 94-119 *Piezicone test CPTU*

NF P 94-130 *Pumping test*

NF P 94-131 *Lugeon water test*

NF P 94-132 *Lefranc water test*

NF P 94-157 *Piezometric measurements*

1

2

3

4

5

6

7

8

9

10

4.5 ICE CONDITIONS

4.5.1 Introduction

To solve the various problems of interaction of ice with engineering structures, knowledge of ice conditions is required. The present section together with Section 5.2.4 present the basic information needed to deal with this aspect in an early stage of design. Typical scenarios, dimensions and ice loads are presented as an example. This section defines ice conditions while the assessment of the relevant ice load cases is presented in Section 5.2.4.

The Canadian *Code for offshore structures* (CSA-S471-92, 1992) requires that the expected physical environmental conditions are studied throughout all phases of the structure design life. The specific environmental effects and loads (wind, waves, currents, ice) resulting from the environment should be determined in accordance with that standard.

During the past decades the study of ice mechanics has been stimulated by the need to operate systems in cold offshore regions where ice is an important and sometimes the dominant factor. Most of the ice and structures involved are situated offshore. Thus, the focus of this section is primarily on sea ice and secondarily on lake and river ice.

4.5.2 Ice growth

The ice polymorph formed at atmospheric conditions is lighter than water (unlike most solids), which results in ice floating on water. The cover of floating ice acts as an insulating layer so that ice growth slows down as it gets thicker. Annual sheet ice (the ice that grows in a single winter) rarely grows thicker than about 2.5 m even in the high Arctic (Croasdale, 1984).

Ordinary ice, ie sea, lake or river ice, has a hexagonal crystallographic symmetry. Ice crystals or grains can vary in shape and typical dimensions are in the range of 1 mm to several centimetres. The structure of ice is further complicated by the presence of impurities in the form of salts, air or gases. At the usual temperature of sea ice in nature, the brine inclusions remain unfrozen and create additional weakness. Multi-year ice is stronger than first-year ice because of the cycles of warming and cooling and consolidation. The mechanical properties of sea ice are dependent on many factors:

- its crystalline structure
- temperature
- brine volume
- strain rate.

Ice growth can be estimated from temperatures, usually referred to as the *freezing degree day method*. This approach requires local calibration and has proven very useful in generating ice thickness statistics from historical temperature data.

4.5.3 Ice formations

Ice can be present as *sheet ice*, *ridges* and *rubble fields*, *landfast*, *iceberg* as described below.

- *Sheet ice* can be level ice or rafted ice that occurs when ice sheets shift over each other and freeze together. Rafted ice can be two or more times thicker than level ice.
- *Ice ridges* are formed by ice pressure induced by wind and current drag forces acting on the mobile ice sheets. Where ice sheets meet, ridges occur. Ridges are generally considered to be linear features. The accumulated ice blocks form a ridge with a sail of loosely consolidated blocks and a keel composed of both consolidated and unconsolidated blocks. The ratio of sail-height to keel-depth of a ridge is typically 1:3 to 1:4.5 (Machemehl, 1990). When ridges expand to all sides, they are generally referred to as *ice rubble fields*.

- In addition to the above, *ice rubble fields* may form around grounded objects, often referred to as shore pile-ups. The forces, formation and grounding of rubble fields are discussed in Kry (1980).
- Ice close to the shore can become connected to shore or *landfast*. Although landfast ice is essentially immobile, cyclic movements of several metres per day often occur; occasionally, as a result of storms, large movements of hundred of metres per hour have been recorded (Spedding, 1983). Between the landfast and mobile ice is a transition zone with extensive pressure ridging. Some of the ridges may become grounded and even scour the sea floor. Depending on the soil properties, ice scours of the sea floor can be considerable.
- The major source of *icebergs* is the Greenland ice cap. Icebergs can have a mass of millions of tons and are driven primarily by current (Gerwick, 1990). Movements up to 20 km per day are typical. Ice islands are tabular icebergs that have dropped from the main ice cap.

Ice encroachment is the term given to ice moving on to the surface of an island or top of a breakwater. It takes two forms: *ice over-ride* (see Figure 4.95) and *ice pile-up*.

- *Ice over-ride*, sometime called *ride-up*, is a rare phenomenon that only occurs with thick ice, smooth surfaces, low freeboards and gentle slopes. Ice over-ride may be avoided by increasing the height of freeboards, steepening slopes, roughening surfaces and other means that cause ice to jam and trigger ice pile-up.
- *Ice pile-up* may be triggered by all beach geometries except flat and smooth ones, massive concrete blocks and sheet pile walls. Steeper sloped islands, including those constructed from rock, favour ice pile-up rather than over-ride. In this case, an ice encroachment perimeter should be installed. No facilities should be placed within this perimeter.

Kovacs and Sodhi (1980) present extensive observations on shore ice pile-up and over-ride features in the Beaufort Sea. They identified shores with ice pile-ups extending as much as 40 m inland, but typically about 10 m from the sea. The pile-ups had sloping surfaces with angles from 30° to 45°. Pile-ups with an elevation of 10 m are considered high, although some have been recorded up to 20 m high. The ice blocks found in pile-ups have a length of one to five times the ice thickness and are generally composed of ice less than 1 m thick. For shore ice over-ride to occur, the driving forces (wind, current or thermal expansion) also need to be sufficient to overcome frictional, ploughing and jamming resistance. The forces required to initiate onshore ice movement are much reduced if a rise in water level occurs. Ice over-ride of more than 100 m has been reported.

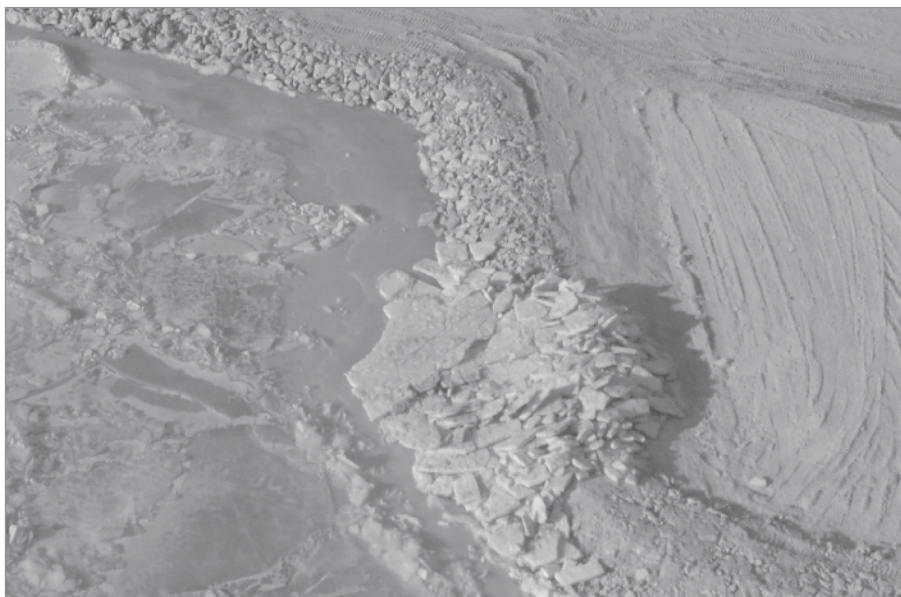


Figure 4.95 Typical ice over-ride observed in the Caspian Sea (courtesy H Lengkeek)

4.5.4 Typical winter ice action

Interactions of early winter ice with rock slopes impose quite moderate global ice loads at the ice line (see Figure 4.96A). Effectively, the thin ice has no bending capacity.

Then, after movements of thin ice against the *bare* structure, grounded ice rubble forms on the *upstream* side (see Figure 4.96B). Experience and calculations show that grounded ice rubble usually displays such sliding resistance on a sloping berm that the potential failure planes of the structure are driven down where the strength of the slope is greater. Effectively, the rubble generates a vertical load and the resulting force is a combination of both horizontal and vertical load. Thus, the failure plane has a different geometry and is deeper than for a purely horizontal load. As the rubble field grows and is more heavily grounded, it alone can resist a large proportion of the ice forces. Rubble ice in front of a structure increases the total sliding resistance as a consequence of the additional weight and resisting area (see Figure 4.96C). In rare situations, the refrozen layer can extend from its outside edge to the island. At this moment, as depicted in Figure 4.96D, the movement of the thick ice against the refrozen rubble can lead to crushing failure in the active zone. If new rubble is always being added to the rubble field, then the active zone is not frozen and load transmission is different.

Once ice rubble forms around structures, experience shows that ice over-ride across the rubble to the structure is not likely. During spring break-up, large sheets of thick ice are moved around by wind and currents. In rare situations, if no rubble existed around an island, an ice over-ride might occur.

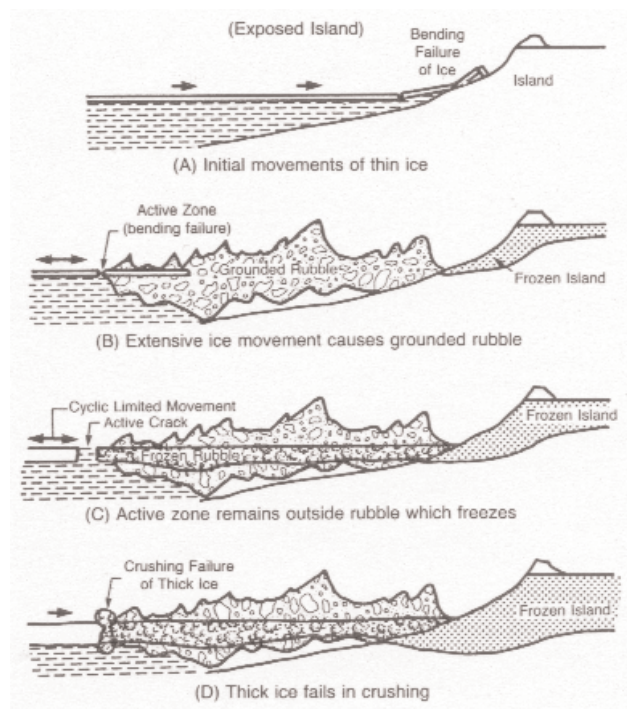


Figure 4.96 Typical winter ice action on sloping beaches (after Croasdale and Marcellus, 1978)

4.5.5 Data collection

Appropriate data collection is essential for safe and cost-effective construction in offshore cold regions. All environmental parameters that influence the design of structures in cold offshore regions should be identified and considered, which includes:

- *meteorology*: wind, air and sea temperature, precipitation, visibility
- *oceanography*: waves, currents, tide and storm surges, water level. Effectively, currents and wind determine the ice-load direction; the tide and water levels control the location of ice attack on the structure
- *ice conditions*: ice coverage, ice movement, ice features, ice geometry, ice properties, ice strength
- *geotechnical conditions*: foundation materials, seabed topography, ice gouging, permafrost. Ice will drift not only at the waterline but also on the structure and under water. The sea bed can thus be exposed to severe load, at the bottom of the ice pile, especially when the pile-up is moving due to a storm and when the sea bed is gouged by the ice. Pipeline, toe protection, geotextiles and berms can be severely damaged.

The sources of ice parameters needed for design are usually specifically designed ice field research programmes, which take into account the ice conditions in the region as well as the types of structure being considered. Some data (temperature, wind speed etc) can be obtained from regional sources and literature. Some ice parameters, eg thickness and drift, may be derived indirectly from historical data such as temperature and winds gathered at weather stations, although regional calibration is usually desirable. It is important to gather data over several years so that probabilistic distributions can be derived. Since most codes require a risk-based approach it requires design events to be specified at an appropriate level of probability by (eg the 100-year event). Typical ice-specific field measurements are presented below:

- *ice growth* can be monitored by measurement of level ice thickness with auger and correlated with temperature data
- *ice drift* can be determined by transmitting GPS devices mounted on the ice. GPS position is transmitted via satellite to a receiving station. Ice movement can also be assessed from sequential satellite images
- *occurrence of rafted and level ice* can be investigated by ice surveys using ground penetration radar (GPR) deployed from helicopter and on-ice measurement for calibration
- *full-scale ice strength* can be determined by full-thickness indentation tests and flexural tests. These may need expert interpretation. Index tests may also be used, eg small-scale compressive tests and borehole jack tests, which also require expert evaluation
- *ice temperature* profiles through an ice cover together with salinity profiles may also be used to assess ice strength using standard algorithms available from the literature (Thomas and Dieckmann, 2003)
- *ice interaction* mechanisms and characteristics of ice failure against slopes can be monitored by remote video camera
- *individual armourstone movement* can be determined by marking of individual stones and surveying before and after ice interaction
- *pits and gouges* in the sea floor are best measured using side-scan sonar and profilometers deployed from survey vessels in the spring immediately after ice break-up. Pits and gouges may also be measured from the ice during the winter. It is important to develop statistics on ice gouge and pit depths and frequencies (especially if considering buried pipelines as they approach rock structures). In very shallow water, gouges may be seen visually from a low-flying helicopter.

4.6 REFERENCES

- Abraham, G, Karelse, M and Van Os, A G (1979). "On the magnitude of interfacial shear of sub-critical stratified flows in relation to interfacial stability". *J Hydraulic Research*, vol 17, no 4, pp 273–284
- Ackers, P (1958). *Resistance of fluids flowing in channel and pipes*. Hydraulics Research Paper no 1, HMSO, London
- Ackers, P (1982). "Meandering channels and the influence of bed materials". In: R D Hey, J C Bathurst and C R Thorne (eds), *Gravel river beds*. John Wiley & Sons, Chichester, pp 389–414
- Ackers, P and Charlton, F G (1970). "Meander geometry arising from varying flows". *J Hydrology*, vol 11, no 3, pp 230–252
- Ackers, P, White, W R, Perkins, J A and Harrison, A J M (1978). *Weirs and flumes for flow measurement*. John Wiley & Sons, Chichester (ISBN 0 47199 637 8)
- Alves, J H G M, Banner, M L and Young, I R (2003). "Revisiting the Pierson-Moskowitz asymptotic limits for fully developed wind waves". *J Phys Oceanogr*, vol 33, pp 1301–1323
- American Petroleum Institute (1993). *Recommended practice for planning, designing and constructing fixed offshore platforms – load and resistance factor design*, 1st edn. RP2A-LRFD, API, Washington DC
- Andrews, E D (1980). "Effective and bankfull discharges of streams in the Yampa river basin, Colorado and Wyoming". *J Hydrology*, no 46, pp 311–330
- Aono, T and Goto, C (1995). "On the characteristics of one-dimensional spectra and non-dimensional parameters of wind waves". In: B L Edge (ed), *Proc 24th int conf coastal engg, Kobe, 23–28 Oct 1994*. ASCE, New York, vol 2, pp 12–26
- Aristaghes, C and Aristaghes, P (1985). *Théories de la houle, houle réelle, propagation de la houle*. STCPM no 85.1, STCPMVN, Compiègne, France, 175 pp
- ASTM (2002). "Soil and rock" (1). In: *Annual book of ASTM*. ASTM, vol 04.08, D420–D5779
- Banner, M L (1990). "Equilibrium spectra of wind waves". *J Phys Oceanogr*, vol 20, pp 966–984
- Battjes, J A (1974). *Computation of set-up, longshore currents, run-up and overtopping due to wind generated waves*. Report 74-2, Comm on Hydraulics, Dept of Civil Engrs, Univ of Technology, Delft
- Battjes, J A and Groenendijk, H W (2000). "Wave height distributions on shallow foreshores". *Coastal Engg*, vol 40, no 3, pp 161–182
- Battjes, J A, Zitman and T J, Holthuijsen, L H (1987). "A re-analysis of the spectra observed in JONSWAP". *J Phys Oceanogr*, vol 17, pp 1288–1295
- Benoit, M, Luck, M, Chevalier, C and Bélorgey, M (2003). "Near-bottom kinematics of shoaling and breaking waves: experimental investigation and numerical prediction". In: J McKee-Smith (ed), *Proc 28th int conf coastal engg, Cardiff, 7–12 Jul 2002*. World Scientific, pp 306–318
- Benoit, M, Marcos, F and Becq, F (1997a). "Development of a third generation shallow water wave model with unstructured spatial meshing". In: B L Edge (ed), *Proc 25th int conf coastal engg, Orlando, FL, 2–6 Sep 1996*. ASCE, New York, pp 465–478
- Benoit, M, Frigaard, P and Schäffer, H A (1997b). "Analyzing multidirectional wave spectra: a tentative classification of available methods". In: *Proc IAHR seminar on multidirectional waves and their interactions with structures, San Francisco*, pp 131–158
- Berkhoff, J C W (1972). "Computation of combined refraction-diffraction". In: *Proc 13th int conf coastal engg, Vancouver*. ASCE, New York, pp 471–490
- Bishop, C T and Donelan, M A (1989). "Wave prediction models". In: V C Lakhan and A S Trenhaile (eds), *Applications in coastal modelling*. Elsevier, Amsterdam (ISBN 0 4447 452 6), pp 75–106

- Bishop, C T, Donelan, M A and Kahma, K K (1992). “Shore Protection Manual’s wave prediction reviewed”. *Coastal Engg*, vol 17, no 1, pp 25–48
- Blaauw, H G and Van der Kaa, E J (1978). “Erosion of bottom and sloping banks caused by the screw-race of manoeuvring ships”. In: *Proc 11th int harbour congress, Antwerp*, 22–26 May
- Blackman, D L (1985). “New estimates of annual sea level maxima in the Bristol Channel”. *Estuarine, Coastal and Shelf Science*, vol 20, pp 229–232
- Blokland, T and Smedes, R H (1996). “In situ tests of current velocities and stone movements caused by a propeller jet against a vertical quay wall”. In: *Proc 11th int harbour congress, Antwerp*, 22–26 May
- Bonnefille, R (1992). *Cours d’hydraulique maritime*, 3rd edn. Masson, Paris, 208 pp
- Booij, N, Ris, R C and Holthuijsen, L H (1999). “A third generation model for coastal regions. I. Model description and validation”. *J Geophys Res*, vol 104, no C4, pp 7649–7666
- Borsboom, M, Doorn, N, Groeneweg, J and van Gent, M (2001). “A Boussinesq-type wave model that conserves both mass and momentum”. In: B L Edge (ed), *Proc 27th int conf coastal engg, Sydney, 16–21 Jul 2000*. ASCE, Reston, VA, pp 148–161
- Bouws, E, Gunther, H, Rosenthal, W and Vincent C L (1985). “Similarity of the wind wave spectrum in finite depth water. Part I: spectral form”. *J Geophys Res*, vol 90, no C1, pp 975–986
- Bowen, A J (1969). “The generation of longshore currents on a plane beach”. *J Marine Res*, vol 27
- Bowen, A J D, Inman, D L and Simons, V P (1968). “Wave ‘set-down’ and ‘set-up’”. *J Geophys Res*, vol 73, pp 2569–2577
- Bowers, E C (1993). “Low frequency waves in intermediate water depths”. In: B L Edge (ed), *Proc 23rd int conf coastal engg, Venice, 4–9 Sep 1992*. ASCE, New York, vol 1, pp 832–845
- Bravard, J P and Petit, F (2000). *Les cours d’eau – dynamique du système fluvial*. Armand Colin, Paris, p 222
- Bretschneider, C L (1954). *Generation of wind waves over a shallow bottom*. Tech Memo no 51, Beach Erosion Board, Office of the Chief of Engineer
- Bretschneider, C L (1970). “Wave forecasting relations for wave generation”. *Look Lab, Hawaii*, vol 1, no 3
- Brice, J C (1964). *Channel patterns and terraces of the Loup River in Nebraska*. Prof Paper 422D, US Geological Survey, p 41
- Brocard, D N and Harleman, D R F (1980). “Two-layer model for shallow horizontal convective circulation”. *J Fluid Mech*, vol 100, pp 129–146
- Brookes, A (1988). *Channelized rivers*. J Wiley & Sons, Chichester, p 326
- Carlier, M (1972). *Hydraulique générale et appliquée*. Eyrolles, Paris, 565 pp
- Carling, P A (1988). “The concept of dominant discharge applied to two gravel-bed streams in relation to channel stability thresholds”. *Earth Surface Processes and Landforms*, no 13, pp 355–367
- Carlston, C W (1965). “The relation of free meandering geometry to stream discharge and its geomorphic implications”. In: R J Chorley (ed), *Spatial analysis in geomorphology*. Methuen, London, pp 197–218
- Carr, J H (1952). *Wave protection aspects of harbor design*. Report E-11, Hydrodynamics Laboratory, California Institute of Technology
- Cavanié, A, Arhan, A and Ezraty, R (1976). “A statistical relationship between individual heights and periods of sea waves”. In: *Proc BOSS ’76 conf*, pp 354–360
- CERC (1977). *Shore protection manual [SPM]*. Coastal Engineering Research Center (CERC), USACE, Vicksburg, MS

- CERC (1977). *Shore protection manual [SPM], 3rd edn.* Coastal Engineering Research Center, US Army Corps of Engineers, Vicksburg, MS
- CETE Méditerranée (2003). “Propagation des crues en rivière”. In: *De la goutte de pluie à la mer*, 32 pp
- Chang, H H (1988). *Fluvial processes in river engineering.* J Wiley & Sons, New York
- Chitale, S V (1966). “Design of alluvial channels”. In: *Proc 6th congress of int com on irrigation and drainage (ICID)*. New Delhi, India. Report 17, Question 20
- Chow, V T (1959). *Open-channel hydraulics*, intl student edn. McGraw Hill, New York, 680 pp
- Christensen, B A (1972). “Incipient motion on cohesionless channel banks”. In: Hsieh Wen Shen (ed), *Sedimentation*. Fort Collins, CO, USA
- Coles, S G and Tawn, J A (1990). “Statistics of coastal flood prevention”. *Phil Trans Royal Soc London*, Series A, no 332, pp 457–476
- Corbett, D M (ed) (1945). *Stream-gaging procedure*. Water Supply Paper 888, US Geological Society, Washington DC
- Cowan, W L (1956). “Estimating hydraulic roughness coefficient”. *Agricultural Engineering*, vol 37, no 7, pp 473–475
- Croasdale, K R (1984). “Sea ice mechanics: a general overview”. *Marine Technology Soc J, Arctic Engg*, vol 18, no 1
- Croasdale, K R and Marcellus, R W (1978). “Ice and wave action on artificial islands in the Beaufort Sea”. *Can J Civ Engrs*, vol 5, no 1, pp 98–113
- Dean, R G (1965). “Stream function representation of nonlinear ocean waves”. *J Geophys Res*, vol 70, no 18, pp 4561–4572
- Dean, R G and Dalrymple, R A (1991). *Water wave mechanics for engineers and scientists*, 2nd edn. Advanced Series on Ocean Engineering, vol 2, World Scientific, Singapore
- Dean, R G and Dalrymple, R A (2004). *Coastal processes with engineering applications*. Cambridge University Press, 487 pp
- Degoutte, G (2001). *Cours d'hydraulique, dynamique et morphologie fluviale*. DEA hydrologie, hydrogéologie, géostatistique et géochimie, ENGREF, Paris. Available from <www.engref.fr/coursenligne/Hydraulique/hydraulique.html>
- de Jong, M (2004). “Origin and prediction of seiches in Rotterdam harbour basins”. In: *Comm on Hydraulic and Geotechnical Engg Report 04-02*. Dept of Civil Eng, Univ of Technology, Delft
- Dingemans, M (1987). *Verification of numerical wave propagation models with laboratory measurements, HISWA verification in the directional wave basin*. Technical Report H228, Part 1B, Appendices A–G. Delft Hydraulics, Delft
- Dingemans, M W (1997). *Water wave propagation over uneven bottoms. Part 2: Non-linear wave propagation*. Advanced Series on Ocean Engg, vol 13, World Scientific, Singapore, 970 pp
- Donelan, M A (1980). “Similarity theory applied to the sea forecasting of wave heights, periods and directions”. In: *Proc Canadian coastal conf*, pp 47–61
- Donelan, M A, Hamilton, J and Hui, W H (1985). “Directional spectra of wind generated waves”. *Phil Trans Royal Soc*, London, vol A315, pp 509–562
- Donelan, M A, Skafel, M, Graber, H, Liu, P, Schwab, D and Venkatesh, S (1992). “On the growth rate of wind-generated waves”. *Atmos-Ocean*, vol 30, pp 457–478
- Donnars, P and Benoit, M (1997). “Interactions in the stability of toe-berm and main-armour for rubble mound breakwaters: an experimental study”. In: B L Edge (ed), *Proc 25th int conf coastal engg, Orlando, FL, 2–6 Sep 1996*. ASCE, New York, pp 1617–1630

- Dunncliff, J (1994). *Geotechnical instrumentation for monitoring field performance*. John Wiley & Sons Inc, New York, 608 pp
- Dury, G H (1955). "Bedwidth and wave-length in meandering valleys". *Nature*, no 176, p 31
- Dury, G H (1969). "Relation of morphometry to runoff frequency". In: R J Chorley (ed), *Water, earth and man*. Methuen, London, p 419–430
- Dury, G H (1976). "Discharge prediction, present and former, from channel dimensions". *J Hydrology*, no 30, pp 219–245
- EAU (1996). *Recommendations of the committee for waterfront structures, harbours and waterways*, 7th English edn. Ernst & Sohn, Berlin
- EAU (2004). "Empfehlungen des Arbeitsausschusses 'Uferneufassungen' Häfen und Wasserstrassen", 10. Auflage
- Eckart, C (1952). "The propagation of gravity waves from deep to shallow-water". *Circular* no 521, National Bureau of Standards, Washington DC, pp 165–173
- EDF, SOGREAH, GRADIENT, LHF, STCPMVN (1992). *Projet Sisyphe. Phase 1: charriage ou transport total de sédiments à granulométrie uniforme – rapport no 5: rassemblement des connaissances et choix des formulations*, 108 pp
- Einstein, H A (1934). "Der Hydraulische oder Profil-Radius" [The hydraulic or cross-section radius]. *Schweizerische Bauzeitung*, Zürich, vol 103, no 8, 24 Feb, pp 89–91
- Einstein, H A and Banks, R B (1950). "Fluid resistance of composite roughness". *Trans Am Geophysical Union*, vol 31, no 4, Aug, pp 603–610
- Escarameia, M (1998). *River and channel revetments: a design manual*. Thomas Telford, London
- Fauchard, C and Meriaux, P (2004). *Méthodes géophysiques et géotechniques pour le diagnostic des digues de protection contre les crues*. Cemagref editions, Paris
- Fauchard, C and Potherat, P (2004). *Détection de cavités souterraines par méthodes géophysiques. Guide technique. Collection techniques et méthodes des laboratoires des ponts et chaussées*
- Fenton, J D (1988). "The numerical solution of steady water wave problems". *Computers and Geosciences*, vol 14, pp 357–368
- Fenton, J D (1990). "Nonlinear wave theories". In: Le Méhauté et Hanes (eds), *The sea*, vol 9, Part A, Wiley InterScience, Chichester, pp 3–25
- Fenton J D (1999). "Numerical methods for nonlinear waves". In: P L-F Liu (ed), *Advances in coastal and ocean engineering*, vol 5, World Scientific, Singapore, pp 241–324
- Fenton, J D and McKee, W D (1990). "On calculating the lengths of water-waves". *Coastal Engg*, vol 14, no 6, pp 499–513
- Friedrichs, C T and Aubrey, D G (1994). "Tidal propagation in strongly convergent channels". *J Geophys Res*, vol 99, pp 3321–3336
- Fuehrer, M, Pohl, H and Römisch, K (1987). "Propeller jet erosion and stability criteria for bottom protections of various constructions". *Bulletin*, no 58, PIANC, Brussels
- Funke, E R and Mansard, E P D (1981). "On the synthesis of realistic sea-states". In: *Proc 17th int conf coastal engg, Sydney, 1980*. ASCE, Reston, VA, pp 2974–2991
- Galland, J-C (1995). "Rubble-mound breakwater stability under oblique waves: an experimental study". In: B L Edge (ed), *Proc 24th int conf coastal engg, Kobe, 23–28 Oct 1994*. ASCE, New York, vol 2, pp 1061–1074
- Galland, J-C and Manoha, B (1991). "Influence of wave grouping on the stability of rubble mound breakwaters". In: *Proc XXIVth cong Int Assoc Hydraulic Research, Madrid*
- Gerwick, B C Jr (1990). "Ice forces on structures". *Ocean Engineering Science – The Sea*, vol 9, Part B, pp 1263–1301
- Glukhovskiy, B K (1966). *Investigation of sea wind waves*. Gidrometo-izdat, Leningrad, 283 pp

- Goda, Y (1970a). "Numerical experiments on wave statistics with spectral simulations". *Report*, Port and Harbour Res Inst (PHRI), Japan, vol 9, no 3
- Goda, Y (1970b). "A synthesis of breaker indices". *Trans Japan Soc Civil Engrs*, vol 2, pp 227–230
- Goda, Y (1978). "The observed joint distribution of periods and heights of sea waves". In: *Proc 16th int conf coastal engg, Hamburg*. ASCE, New York, pp 227–246
- Goda, Y (1988). "Statistical variability of sea-state parameters as a function of a wave spectrum". *Coastal engg in Japan*, vol 31, no 1, pp 39–52
- Goda, Y (1997). "Directional wave spectrum and its engineering applications". In: P L-F Liu (ed), *Advanced Series on Ocean Engineering*, vol 3. World Scientific, Singapore, pp 67–102
- Goda, Y (2000). "Random seas and design of maritime structures". In: P L-F Liu (ed) *Advanced Series on Ocean Engineering*, vol 15, World Scientific, Singapore, 444 pp
- Goda, Y (2003). "Revisiting Wilson's formulas for simplified wind-wave prediction". *J Waterway, Port, Coastal and Ocean Engg*, vol 129, no 2, pp 93–95
- Graf and Altinakar (1993). *Hydraulique fluviale*, vol 3. Presses Polytechniques et Universitaires Romandes
- Graff, J (1981). "An investigation of the frequency distributions of annual sea level maxima at ports around Great Britain". *Estuarine, Coastal and Shelf Science*, vol 12, pp 389–449
- Gregory, K J and Walling, D E (1985). *Drainage basin form and process. A geomorphological approach*. Edward Arnold, London, 458 pp
- Guo, J (2002). "Simple and explicit solution of wave dispersion equation". *Coastal Engg*, vol 45, no 2, pp 71–74
- Hamill, G A, Qurrain, H T and Johnston (1996). "The influence of a revetment on diffusion of a propeller wash". *Bulletin*, no 91, PIANC, Brussels
- Hamm, L (1995). "Modélisation numérique bidimensionnelle de la propagation de la houle dans la zone de déferlement". Ph Thesis Report, Université Joseph Fourier, Grenoble
- Hamm, L (2001). "Depth-limited wave breaking for the design of nearshore structures". In: *Proc 4th int symp ocean wave measurement and analysis, San-Francisco, 2–6 Sep*
- Hamm, L, Madsen, P A and Peregrine, D H (1993). "Wave transformation in the nearshore zone: a review". *Coastal Engg*, vol 21, no 1, pp 5–39
- Hanslow, D J and Nielsen, P (1992). "Wave setup on beaches and in river entrances". In: B L Edge (ed), *Proc 23rd int conf coastal engg, Venice, 4–9 Sep 1992*. ASCE, New York, vol 1, pp 240–252
- Hasselmann, K, Barnett, T P, Bouws, E, Carlson, H, Cartwright, D E, Enke, K, Ewing, J A, Gienapp, H, Hasselmann, D E, Kruseman, P, Meerburg, A, Müller, P, Olbers, D J, Richter, K, Sell, W and Walden, H (1973). "Measurements of wind-wave growth and swell decay during the Joint North Sea Wave Project (JONSWAP)". *Deutschen Hydrographischen Zeitschrift, Reihe A* (8°), no 12
- Hawkes, P J and Hague, R C (1994). *Validation of joint probability methods for large waves and high water levels*. Report SR 318, HR Wallingford, Wallingford
- Hawkes, P J, Gouldby, B P, Tawn, J A and Owen, M W (2002). "The joint probability of waves and water levels on coastal engineering design". *J Hydraulic Res*, vol 40, no 3, pp 241–251
- Hawkins, A B *et al* (eds) (1985). "Site investigations practice". In: *Proc 20th reg mtg Eng Group Geol Soc*
- Hedges, T S (1990). "Geogrids and geotextiles in the maritime and waterways environment". At: The hydraulic climate design workshop, Liverpool, 26–27 Sep
- Henderson, F M (1966). *Open channel flow*. Macmillan Press

- Herschey, R W (1999). *Hydrometry: principles and practice*, 2nd edn. John Wiley & Sons, Chichester (ISBN 0-47197350-5)
- Hey, R D (1982). "Design equations for mobile gravel-bed rivers". In: R D Hey, J C Bathurst and C R Thorne (eds), *Gravel-bed rivers*. John Wiley & Sons, Chichester, pp 553–574
- Hey, R D and Heritage, G L (1988). "Dimensional and dimensionless regime equations for gravel-bed rivers". In: W R White (ed), *Proc int conf river regime, Wallingford*. John Wiley & Sons, Chichester
- Hjulström, F (1935). "Studies of the morphological activity of rivers". *Bull Geol Inst Upsala*, vol XXV
- Hoffmans, G J C M and Verheij, H J (1997). *Scour manual*. AA Balkema, Rotterdam
- Holland, G J (1980). "An analytic model of the wind and pressure profiles in hurricanes". *Monthly Weather Review*, vol 108, pp 1212–1218
- Holthuijsen, L H, Booij, N and Herbers, T H C (1989). "A prediction model for stationary, short crested waves in shallow water with ambient currents". *Coastal Engg*, vol 13, no 1, pp 23–54
- Hooke, J M (1987). "Changes in meander morphology". In: V Gardiner (ed), *International geomorphology 1986*, Part I. John Wiley & Sons, New York, pp 591–609
- Horton (1933). "Separate roughness coefficients for channel bottom and sides". *Engineering News-record*, vol 111, no 22, 30 Nov, pp 652–653
- HR Wallingford (2005). *Joint probability: dependence mapping and best practice*. Technical report on dependence mapping. R&D Technical Report FD2308/TR1 (also HR Wallingford Report SR 623), Defra, London
- HR Wallingford (2005). *Use of joint probability methods for flood and coastal defence in England and Wales. A guide to best practice*. R&D Technical Report FD2308/TR2 (also HR Wallingford Report SR 653), Defra, London
- HR Wallingford and Lancaster University (1998). *The joint probability of waves and water levels. JOIN-SEA: a rigorous but practical new approach*. Report SR 537, as amended 2000, HR Wallingford, Wallingford
- Hughes, S A (1984). *The TMA shallow-water spectrum. Description and applications*. Technical Report CERC-84-7, US Army Engineer Waterways Experiment Station, Vicksburg, MS, USA, 42 pp
- Hughes, S A and Borgman, L E (1987). "Beta-Rayleigh distribution for shallow-water wave heights". In: R Dalrymple (ed), *Proc int conf coastal hydrodynamics, Delaware, USA*, pp 17–31
- Hunt, J N (1979). "Direct solution of wave dispersion equation". *J Waterway, Port, Coastal Engg Div*, ASCE WW-105, Nov, pp 457–459
- IAHR and PIANC (1986). *Sea state parameters*. Supplement to *Bulletin* no 52 of the Permanent International Association of Navigation Congresses, Brussels, 25 pp
- Intergovernmental Panel on Climate Change (2001). *Technical summary. Climate change 2001: impacts, adaptation and vulnerability*. IPCC, <www.ipcc.ch/pub/wg2TARtechsum.pdf>
- Isobe, M and Horikawa, K (1982). "Study on water particle velocities of shoaling and breaking waves". *Coastal Engg in Japan*, vol 25, pp 109–123
- ISSMGE-TC1 (2005). "Geotechnical investigations for offshore and nearshore developments". In: ISSMGE Technical Committee 1, *Soil investigation report*
- Izumiya, T and Horikawa, K (1984). "Wave energy equation applicable in and outside the surf zone". *Coastal Engg in Japan*, vol 27, pp 119–137
- James, C S (1994). "Evaluation of methods for predicting bend losses in meandering channels". *J Hyd Engg*, ASCE, vol 120, no 2, pp 245–253
- James, C S and Wark, J B (1992). *Conveyance estimation for meandering channels*. Report SR 329, HR Wallingford, Wallingford

- Jansen, P PH (ed) (1979). *Principles of river engineering*. Pitman, London
- Kahma, K K and Calkoen, C J (1992). "Reconciling discrepancies in the observed growth of wind-generated waves". *J Phys Oceanogr*, vol 22, pp 1389–1405
- Kalinkse, A A (1943). "The role of turbulence in river hydraulics". *Bull Univ Iowa, Studies in Engg*, vol 27, pp 266–279
- Kamphuis, J W (2001). "Designing for low frequency waves". In: B L Edge (ed), *Proc 27th int conf coastal engg, Sydney, 16–21 Jul 2000*. ASCE, Reston, VA, pp 1434–1447
- Kimura, A (1981). "Statistical properties of random waves". In: *Proc 17th int conf coastal engg, Sydney, 1980*. ASCE, Reston, VA, pp 2955–2973
- Kirkgöz, M S (1986). "Particle velocity prediction at the transformation point of plunging breakers". *Coastal Engg*, vol 10, no 2, pp 139–147
- Komar, P D and Miller, M C (1974). "Sediment transport threshold under oscillatory waves". In: *Proc 14th int conf coastal engg, Copenhagen*. ASCE New York, pp 756–775
- Kovacs, A and Sodhi, D S (1980). "Shore ice pile-up and ride-up: field observations, models, theoretical analyses". *Cold regions science and technology*, vol 2, pp 209–298
- Kry, P R (1980). "Third Canadian geotechnical colloquium: ice forces on wide structures". *Can Geotech J*, vol 17, pp 97–113
- Lacey, J (1930). "Stable channels in alluvium". *Proc Inst Civ Engrs*, vol 229, pp 259–384
- Leopold, L B, Wolman, M G and Miller, J D (1964). *Fluvial processes in geomorphology*. Freeman & Co, San Francisco, 522 pp
- Leopold, L B and Wolman, M G (1957). *River channel patterns-braided, meandering and straight*. Professional Paper 282B, US Geological Survey, pp 39–85
- Lino, M, Meriaux, P and Royet, P (2000). *Méthodologie de diagnostic des digues appliquée aux levées de la Loire moyenne*. Cemagref editions, Paris, 224 pp
- Liu, P L-F, Cho, Y-S, Briggs, M J, Kanoglu, U and Synolakis, C E (1995). "Run-up of solitary waves on a circular island". *J Fluid Mech*, vol 302, pp 259–285
- Longuet-Higgins, M S (1975). "On the joint distribution of wave periods and amplitudes of sea waves". *J Geophys Res*, vol 80, no 18, pp 2688–2694
- Longuet-Higgins, M S (1983). "On the joint distribution of the periods and amplitudes in a random wave field". *Proc Royal Soc London, Ser A*, pp 241–258
- Lotter, G K (1933). "Soobrazheniia k gidravlicheskomu rashetu rusels razlichnoi sherokhovatostii stenok" (Considerations on hydraulic design of channels with different roughness of walls). *Izvestiia Vsesoiuznogo Nauchno-Issledovatel'skogo Instituta Gidrotekhniki* [Trans All-Union Scientific Res Inst Engg], Leningrad, vol 9, pp 238–241
- Machemehl, J L (1990). "Wave and ice forces on artificial islands and Arctic structures". In: *Handbook of coastal and ocean engineering, vol I: wave phenomena and coastal structures*. Houston
- Ministry of Agriculture, Fisheries and Food (1999). *Flood and coastal defence project appraisal guidance: economic appraisal*. Report PB4650, MAFF, London
- Mahmood, K (1974). "Variation of regime coefficients in Pakistan canals". *J Waterways, Harbors and Coastal Engg Div*, vol 100, no 2, May, pp 85–104
- Mahmood, K and Shen, H W (1971). "The regime concept of sediment-transporting canals and rivers". In: H W Shen (ed), *River mechanics*. Water Resources Publications, Ft Collins, CO, pp 30.1–30.39
- Mathiesen, M, Goda, Y, Hawkes, P J, Mansard, E, Martin, M J, Peltier, E, Thompson, E F, and van Vledder, G P (1994). "Recommended practice for extreme wave analysis". *J Hydraulic Res*, vol 32, no 6, pp 803–814
- May, R, Ackers, J and Kirby, A (2002). *Manual on scour at bridges and other hydraulic structures*. C551, CIRIA, London

- McCowan (1894). "On the highest wave of permanent type". *Philosophical Magazine*, vol 38, Ser 5, pp 351–358
- McGahey, C and Samuels, P G (2003). "Methodology for conveyance estimation in two-stage straight, skewed and meandering channels". In: *Proc XXX IAHR congress, Thessaloniki*, vol C1. IAHR
- McKee Smith, J and Vincent, C L (2003). "Equilibrium ranges in surf zone wave spectra". *J Geophys Res*, vol 108, no C11, p 30-1 to p 30-11
- MEDD and METATLM (2005). "Thème 3: données hydrologiques". In: *Guide méthodologique de pilotage des études hydrauliques*, 39 pp. Available at <www.cetmef.equipement.gouv.fr> (club cours d'eau et environnement)
- Mehta, A J and Joshi, P B (1986). "Tidal inlet hydraulics". *J Hyd Engg*, ASCE, vol 114, no 11, pp 1321–1337
- Melville, B W and Coleman S E (2000). *Bridge scour*. Water Resources Publications, LLC, Colorado
- Mendez, F J, Losada, I J and Medina, R (2004). "Transformation model of wave height distribution on planar beaches". *Coastal Engg*, vol 50, no 3, pp 97–115
- Miche, R (1944). "Mouvements ondulatoires des mers en profondeur constante ou décroissante". *Annales des Ponts et Chaussées*, Chap 114, pp 131–164, 270–292 and 369–406
- Mitsuyasu, H, Tasai, F, Suhara, T, Mizuno, S, Ohkuso, M, Honda, T and Rikishi, K (1975). "Observations of the directional spectrum of ocean waves using a cloverleaf buoy". *J Phys Oceanogr*, vol 5, no 2, pp 750–760
- Morisawa, M (1985). *Rivers: form and process*. Longman, New York
- Mülhofer, L (1933). "Rauhigkeitsuntersuchungen in einem Stollen mit betonierter Sohle und unverkleideten Wänden" (Roughness investigations in a shaft with concrete bottom and unlined walls). *Wasserkraft und Wasserwirtschaft*, Munich, vol 28, no 8, pp 85–88
- Nixon, M (1959). "A study of the bankfull discharges of river in England and Wales". *Proc Inst Civ Engrs*, vol 93, pp 149–165
- Owen, N W (1988). *Wave prediction in reservoirs: comparison of available methods*. Report no EX-1809, HR Wallingford Ltd, Wallingford
- Pavolvski, N N (1931). *Uchebny Gidravlicheski Spravochnik* (for schools), 2nd edn. Kubuch, Leningrad, 168 pp
- Petit, F, Pauquet, A, Mabille, G and Franchimont, C (1994). "Variations de la récurrence du débit à pleins bords des rivières en relation avec la lithologie de leur bassin versant et les caractéristiques de leur lit". *Rev Géogr Alpine*, vol 12, pp 157–161
- Petts, G (1977). "Channel response to flow regulation: the case of the river Derwent, Derbyshire". In: K J Gregory (ed), *River channel changes*. J Wiley & Sons, Chichester, pp 145–164
- PIANC (1987). "Guidelines for the design and construction of flexible revetments incorporating geotextiles for inland waterways". Supplement to *Bulletin* no 57, report of InCom WG04, PIANC, Brussels
- PIANC (1997). "Guidelines for the design of armoured slopes under open piled quay walls". Supplement to *Bulletin* no 96, report of MarCom WG22, PIANC, Brussels
- PIANC (in preparation). *Guidelines for port constructions, related to bowthrusters*. Report of MarCom WG48, PIANC, Brussels
- Pierson, W J and Moskowitz, L (1964). "A proposed spectral form for fully developed wind seas based on the similarity law of S.A. Kitaigorodskii". *J Geophys Res*, vol 69, no 24
- Power, P T and Paysly, J M (1986). "The collection, interpretation and presentation of geotechnical data for marine pipeline projects". *Oceanology*, 301–4, Graham and Tratman, London

- Prandtl, L (1925). "Bericht ueber Untersuchungen zur ausgebildeten Turbulenz". *ZAMM*, vol 3, pp 136–139
- Proudman Oceanographic Laboratory (1995). *Extreme sea-levels at the UK A-class sites: optimal site-by-site analyses and spatial analyses for the east coast*. Internal Document no 72, POL, Liverpool
- Proudman Oceanographic Laboratory (1997). *Estimates of extreme sea conditions: spatial analyses for the UK coast*. Internal Document no 112, POL, Liverpool
- Przedwojski, B, Blazejewski, R and Pilarczyk, K W (1995). *River training techniques. Fundamentals, design and applications*. AA Balkema, Rotterdam
- Pugh, D T (1987). *Tides, surges and mean sea-level*. John Wiley & Sons, Chichester
- Rattanapitikon, W and Shibayama, T (2000). "Verification and modification of breaker height formulas". *Coastal Engg J*, vol 42, no 4, pp 389–406
- Rattanapitikon, W, Vivattanasirisak, T and Shibayama, T (2003). "A proposal of new breaker height formula". *Coastal Engg J*, vol 45, no 1, pp 29–48
- Richards, K (1982). *Rivers. Form and process in alluvial channels*. Methuen, London, p 357
- Rienecker, M M and Fenton, J D (1981). "A Fourier approximation for steady water waves". *J Fluid Mech*, vol 104, pp 119–137
- Ris, R C, Holthuijsen, L H and Booij, N (1999). "A third generation model for coastal regions. II. Verification". *J Geophys Res*, vol 104, no C4, pp 7667–7681
- Römish, K (1993) "Propellerstrahlinduzierte Erosionserscheinungen in Häfen". *HANSA*, no 8
- Rust, B R (1978) "Depositional models for braided alluvium". In: A D Miall (ed), *Fluvial sedimentology*. Mem Canadian Soc of Petrol Geol, Calgary, memoir 5, pp 602–625
- Savenije, H H G (1998). "Analytical expression for tidal damping in alluvial estuaries". *J Hyd Engg*, ASCE, vol 124, no 6, pp 615–618
- Saville, T, McClendon, E W and Cochran, A L (1962). "Freeboard allowance for waves in inland reservoirs". *Proc Am Soc Civ Engrs*, vol 18, no WW2
- Schumm, S A (1963). "Sinuosity of alluvial rivers in the Great Plains". *Bull Geol Soc America*, no 74, pp 1089–1100
- Schumm, S A (1968). "Speculations concerning palaeohydrologic control of terrestrial sedimentation". *Bull Geol Soc America*, vol 79, pp 1573–1588
- Schumm, S A (1977). *The fluvial system*. Wiley-Interscience, New York, p 338
- Seddon, J A (1900). "River hydraulics". *Trans Am Soc Civ Engrs*, vol 43, pp 179–229
- Sellin, R M J (1969). *Flow in channels*. Macmillan, London and St Martin's Press, New York, 194 pp
- Shahin, M (1985). *Hydrology of the Nile Basin*. Elsevier, Amsterdam
- Shi, F, Dalrymple, R A, Kirby, J T, Chen, Q and Kennedy, A B (2001). "A fully nonlinear Boussinesq model in generalized curvilinear coordinates". *Coastal Engg*, vol 42, pp 337–358
- Shields, A (1936). "Use of similarity mechanics of turbulence to shear movement (in German)". *Mitt. der Preuss Versuchanst Für Wasserbau und Schiffbau*, Helf 26, Inst of Hydraulics and Ship Building, Berlin
- Shuto, N (1974). "Non-linear long waves in a channel of variable section". *Coastal engg in Japan*, vol 17, pp 1–12
- Shuto, N (1991). "Numerical simulation of tsunamis". In: E Bernard (ed), *Tsunami hazard*. Kluwer Academic Publishers, Dordrecht, The Netherlands, pp 171–191
- Simm, J D, Brampton, A H, Beech, N W *et al* (1996). *Beach management manual*. Report 153, CIRIA, London

- Simon, B (1994). *Statistique des niveaux marins extremes le long des côtes de France* [in French]. Rapport d'étude no 001/94, Service Hydrographique et Océanographique de la Marine (SHOM), Brest, France
- Simons, D B and Albertson, M L (1960). "Uniform water conveyance channels in alluvial material". *Trans Am Soc Civ Engrs*, vol 128, Part I, pp 65–167
- Simons, D B and Senturk, F (1977). *Sediment transport technology*. Water Resources Publications, Fort Collins, CO, USA, 807 pp
- Sobey, R J, Goodwin, P, Thieke, R J and Westberg, R J (1987). "Application of Stokes, cnoidal and Fourier wave theories". *J Waterway, Port, Coastal and Ocean Engg*, vol 113, pp 565–587
- Sommerfeld, A (1896). "Mathematische Theorie der Diffraction" [in German]. *Matematische Annalen*, vol 47, pp 317–374
- Sørensen, O R and Sørensen, L S (2001). "Boussinesq type modelling using unstructured finite element technique". In: B L Edge (ed), *Proc 27th int conf coastal engg, Sydney, 16–21 Jul 2000*. ASCE, Reston, VA, pp 190–202
- Soulsby, R L (1987). "Calculating bottom orbital velocity beneath waves". *Coastal Engg*, vol 11, no 4, pp 371–380
- Spedding, L G (1983). *A large landfast ice movement*. POAC, Technical Research Centre of Finland, Helsinki
- Stive, M J F (1985). "A scale comparison of waves breaking on a beach". *Coastal Engg*, vol 9, no 2, pp 151–158
- Stive, M J F and Dingemans, M W (1984). *Calibration and verification of a one-dimensional wave decay model*. Technical report M1882, Delft Hydraulics, Delft
- Struiksmā, N and Klaassen, G J (1988). "On the threshold between meandering and braiding". In: W R White (ed), *Proc int conf river regime, Wallingford*. John Wiley & Sons, Chichester
- Svendsen, I A, Madsen, P A and Buhr-Hansen, J (1979). "Wave characteristics in the surf zone". In: *Proc 16th int conf coastal engg, Hamburg*. ASCE, New York, pp 520–539
- Sverdrup, H U and Munk, W H (1947). *Wind, sea and swell: theory of relations for forecasting*. HO pub no 601, US Navy Hydrographic Office
- Swart, D H and Crowley, J B (1988). "Generalized wave theory for a sloping bottom". In: *Proc 21st int conf coastal engg, Malaga*. ASCE, New York, pp 181–203
- Tadepalli, S and Synolakis, C E (1996). "Model for the leading waves of tsunamis". *Phys Rev Letters*, vol 77, no 10, pp 2141–2144
- Tang, X-N, Knight, D W and Samuels, P G (2001). "Wave-speed-discharge relationship from cross section survey". *J water and maritime engg, Proc Instn Civ Engrs*, vol 148, pt 2, pp 81–96
- Thomas, D N and Dieckmann, G S (2003). *Sea ice. An introduction to its physics, chemistry, biology and geology*. Blackwell Science, Oxford
- Thompson, E F and Vincent, L C (1985). "Significant wave height for shallow water design". *J Waterway, Port, Coastal and Ocean Engg*, vol 111, no 5, ASCE, pp 828–842
- Toba, Y (1973). "Local balance in the air-sea boundary layer". *J Oceanogr Soc Japan*, vol 29, pp 209–220
- Toba, Y (1997). "The 3/2 power law for ocean wind waves and its applications". In: P L F Liu (ed), *Advances in coastal and ocean engg*, vol 3. World Scientific, Singapore, pp 31–65
- Tolman, H L and Chalikov, D (1996). "Source terms in a third generation wind wave model". *J Phys Oceanogr*, vol 26, pp 2497–2518
- Tolman, H L (1991). "A third-generation model for wind waves on slowly varying unsteady and inhomogeneous depths and currents". *J Phys Oceanogr*, vol 21, pp 782–797
- Transport Association of Canada (2001). *Guide to bridge hydraulics*, 2nd edn. TAC, Ottawa

- Tricart, J (1977). "Types de lits fluviaux en Amazonie brésilienne". *Annales de Géographie*, no 473, pp 1–54
- Tucker, M J and Pitt, E G (2001). *Waves in ocean engineering*. Ocean Engg Book Series, vol 5, Elsevier, Oxford (ISBN 0-08-043566-1), 522 pp
- United Kingdom Climate Impacts Programme (2002). *Climate change scenarios for the United Kingdom. The UKCIP02 scientific report*. Tyndall Centre, University of East Anglia, Norwich
- USACE (1993). *River hydraulics, engineering and design*. EM 1110-2-1416, USACE, 70 pp
- USACE, *Engineer Manuals (EM)*:
- EM 1110-1-1804 *Geotechnical investigation* ENG 1836 ENG 1836 A (2001)
 - EM 1110-1-1802 *Geophysical exploration for engineering and environmental investigations* (1995)
 - EM 1110-2-1906 *Laboratory soils testing* (1986)
 - EM 1110-2-1907 *Soil sampling* (1972)
- USACE (2003). *Coastal engineering manual [CEM]* Engineer Manual 1110-2-1100, US Army Corps of Engineers, CHL-ERDC, WES, Vicksburg, MS
- Van den Berg, H J (1987a). "In-situ testing of soils". In: F G Bell (ed), *Ground engineer's reference book*. Ch 25, Butterworth-Heinemann, London
- Van den Berg, H J (1987b). "Laboratory testing of soils". In: F G Bell (ed), *Ground engineer's reference book*. Ch 20, Butterworth-Heinemann, London
- Van den Berg, J H (1995). "Prediction of alluvial channel pattern of perennial streams". *Geomorphology*, vol 12, pp 259–279
- Van den Brink, M (1998). *Prediction of sand wave occurrence*. Alkyon Hydraulic Consultancy & Research Report no B006, University of Twente
- Van der Meer, J W (1990). *Extreme shallow water wave conditions*. Report H198, Delft Hydraulics, Delft
- Van der Meer, J W, Langenberg, J W, Klein Breteler, M, Hurdle, D P and den Heijer, F (2003). "Wave boundary conditions and overtopping in complex areas". In: J McKee-Smith (ed), *Proc 28th int conf coastal engg, Cardiff, 7–12 Jul 2002*. World Scientific, pp 2092–2104
- Van der Wal, M (1989). *Cross-sections of navigation canals with berms* [in Dutch]. Report Q903, WL|Delft Hydraulics, Delft
- Van Gent, M R A (2001). "Wave run-up on dykes with shallow foreshores". *J Waterway, Port, Coastal and Ocean Engg*, vol 127, no 5, pp 254–262
- Van Rijn, L C (1982). "Equivalent roughness of alluvial bed". *Proc Am Soc Civ Eng J Hydr Div*, vol 108, no HY10
- Van Rijn, L C (1989). *Handbook of sediment transport by currents and waves*. Internal Report H461, Delft Hydraulics, Delft
- Van Vledder, G P (1993). "Statistics of wave group parameters". In: B L Edge (ed), *Proc 23rd int conf coastal engg, Venice, 4–9 Sep 1992*. ASCE, New York, vol 1, pp 946–959
- Van Vledder, G P and Battjes, J A (1992). "Discussion of 'List of sea-state parameters'". *J Waterway, Port, Coastal and Ocean Engg*, vol 118, no 2, pp 226–230
- Vreugdenhil, C B and Wijnbenga, J H A (1982). "Computation of flow patterns in rivers". *Proc Am Soc Civ Eng J Hydr Div*, vol 108, no HY11, pp 1296–1309
- WAMDI Group (1988). "The WAM-model. A third generation ocean wave prediction model". *J Phys Oceanogr*, vol 18, Dec, pp 1775–1810
- Weggel, J R (1972). "Maximum breaker height". *J Waterways, Harbors and Coastal Engg Div*, vol 98, no WW4, pp 529–548
- Wei, G, Kirby, J T, Grilli, S T and Subramanya, R (1995). "A fully nonlinear Boussinesq model for surface waves. Part 1. Highly nonlinear unsteady waves". *J Fluid Mech*, vol 294, pp 71–92

- Wilson, B W (1955). *Graphical approach to the forecasting of waves in moving fetches*. Tech Memo 73, Beach Erosion Board, US Army Corps of Engineers
- Wilson, B W (1963). *Generation and dispersion characteristics of tsunamis*. NESCO
- Wilson, B W (1965). "Numerical prediction of ocean waves in the North Atlantic for December 1959". *Deutsche Hydrographische Zeitschrift*, vol 18, no 3, pp 114–130
- Wilson, B W (1972). "Seiches". In: V T Chow (ed), *Advances in hydrosience*, vol 8. Academic Press, New York, pp 1–94
- Wilson, E M (1990). *Engineering hydrology*. Macmillan Press, London (ISBN 0-333-51717-2)
- Wu, J (1980). "Wind stress coefficients over the sea surface near neutral conditions. A revisit". *J Phys Oceanogr*, vol 10, pp 727–740
- Wu, C S and Thornton, E B (1986). "Wave numbers of linear progressive waves". *J Waterway, Port, Coastal and Ocean Engg*, vol 112, no 4, pp 536–540
- Yalin, M S (1992). *River mechanics*. Pergamon Press, Oxford
- Yassin, Ahmed M (1954). "Mean roughness coefficient in open channels with different roughness of bed and side walls". *Eidgenössische technische Hochschule Zürich, Mitteilungen aus der Versuchsanstalt für Wasserbau and Erdbau*, no 27, Verlag Leemann, Zürich
- Yeh, H, Liu, P L-F, Briggs, M and Synolakis, C E (1994). "Propagation and amplification of tsunamis at coastal boundaries". *Nature*, vol 372, pp 353–355
- Yoo, D, O'Conner, B A and McDowell, D M (1989). "Mathematical models of wave climate for port design". *Proc Inst Civ Engrs*, Part ii, vol 86, 513–30
- Young, I R (1988). "Parametric hurricane wave prediction model". *J Waterway, Port, Coastal and Ocean Engg*, vol 114, no 5, pp 639–652
- Young, I R (1992). "The determination of spectral parameters from significant wave height and peak period". *Ocean Engg*, vol 19, pp 497–508
- Young, I R (1995). "The determination of confidence limits associated with estimates of the spectral peak frequency". *Ocean Engg*, vol 22, no 7, pp 669–686
- Young, I R (1997). "The growth rate of finite depth wind-generated waves". *Coastal Engg*, vol 32, no 2-3, pp 181–195
- Young, I R and Verhagen, L A (1996). "The growth of fetch-limited waves in water of finite depth. Part I: total energy and peak frequency". *Coastal Engg*, vol 28, pp 47–78
- Zakharov, V (1999). "Statistical theory of gravity and capillary waves on the surface of a finite-depth fluid". *Eur J Mech B Fluids*, vol 18, pp 327–344

